

## DISSERTATION

### Mathematical Multiscale Modeling and Stability Analysis of Cancer Genesis

Ausgeführt zum Zwecke der Erlangung des akademischen Grades  
Doktor-Ingenieur (Dr.-Ing.)

unter der Leitung von  
Prof. Dr.-Ing. Naim Bajcinca  
Lehrstuhl für Mechatronik in Maschinenbau und Fahrzeugtechnik

genehmigt vom  
Fachbereich Maschinenbau und Verfahrenstechnik  
der  
Rheinland-Pfälzischen Technischen Universität Kaiserslautern-Landau

Vorgelegt von  
Frau  
M.Sc. Iqra Batool  
aus Jhelum, Pakistan

Kaiserslautern, Oktober 2023



Tag der Disputation:

22.12.2023

Promotionskommission

Vorsitzender:

Prof. Dr.-Ing. Sergiy Antonyuk

Erster Berichterstatter:

Prof. Dr.-Ing. Naim Bajcinca

Zweiter Berichterstatter:

Prof. Dr.habil. Shamsul Qamar



To my mother, Zahra!



---

## Acknowledgments

---

First and foremost, I am immensely grateful to ALLAH, the Most Gracious and Merciful, for all the wisdom, strength, and opportunities He has bestowed upon me.

I am deeply thankful to my supervisor, Prof. Dr.-Ing. Naim Bajcinca for his guidance, support, and invaluable insights throughout my journey of Ph.D. Your expertise and encouragement have been pivotal in shaping the direction of this work. I would also like to extend my sincere thanks to Prof. Dr. Habil. Shamsul Qamar for his support, constructive feedback, and being part of the thesis committee.

I would like to express my deepest gratitude to a very important person in my life, my mother, Ghulam Zahra. I owe my success to her unconditional support, endless love, and steadfast belief in my abilities. Your words of wisdom and encouragement have always provided me the strength to persevere. This accomplishment is as much yours as it is mine, and for that I am eternally grateful.

As I move forward, there is something that I would like to express - a profound gratitude to my siblings, Muneeb, Mujeeb, Haseeb, Kaiynat, and Danyal. However, my elder brother Muneeb deserves special mention as he has been a pillar of strength for our family. Over the years, he has provided a sense of security and continuity that has been invaluable to all of us. I am deeply thankful for his sacrifices, love, and enduring support, which have been the bedrock of our shared journey.

Special thanks are reserved for my life partner, my husband, Bilal. Your dedicated support, encouragement, and love have been an anchor in my academic journey. Your sacrifices and understanding have made this endeavor a shared triumph. I am grateful for the warmth of your presence and the strength of our partnership.

To my best friend, Saima, I want you to know that your friendship has been a true treasure to me. Your presence and encouragement have been a source of inspiration, strength, and solace. Thank you for being an integral part of my life.

Lastly, I want to thank the people who became my 'home away from home.' Yes, I am talking about you, Maham and Darrak. Your friendship, warmth, and support have made this place into a comforting sanctuary. Maham, I will always cherish the journey we shared together, and Darrak, my office mate and chatter extraordinaire; your words have been the true MVPs of this academic adventure!

Kaiserslautern, Oktober 2023





---

## Abstract

---

Cancer, a complex and multifaceted disease, continues to challenge the boundaries of biomedical research. In this dissertation, we explore the complexity of cancer genesis, employing multiscale modeling, abstract mathematical concepts such as stability analysis, and numerical simulations as powerful tools to decipher its underlying mechanisms. Through a series of comprehensive studies, we mainly investigate the cell cycle dynamics, the delicate balance between quiescence and proliferation, the impact of mutations, and the co-evolution of healthy and cancer stem cell lineages. The introductory chapter provides a comprehensive overview of cancer and the critical importance of understanding its underlying mechanisms. Additionally, it establishes the foundation by elucidating key definitions and presenting various modeling perspectives to address the cancer genesis. Next, cell cycle dynamics have been explored, revealing the temporal oscillatory dynamics that govern the progression of cells through the cell cycle.

The first half of the thesis investigates the cell cycle dynamics and evolution of cancer stem cell lineages by incorporating feedback regulation mechanisms. Thereby, the pivotal role of feedback loops in driving the expansion of cancer stem cells has been thoroughly studied, offering new perspectives on cancer progression. Furthermore, the mathematical rigor of the model has been addressed by deriving wellposedness conditions, thereby strengthening the reliability of our findings and conclusions. Then, expanding our modeling scope, we explore the interplay between quiescent and proliferating cell populations, shedding light on the importance of their equilibrium in cancer biology. The models developed in this context offer potential avenues for targeted cancer therapies, addressing perspective cell populations critical for cancer progression. The second half of the thesis focuses on multiscale modeling of proliferating and quiescent cell populations incorporating cell cycle dynamics and the extension thereof with mutation acquisition. Following rigorous mathematical analysis, the wellposedness of the proposed modeling frameworks have been studied along with steady-state solutions and stability criteria.

In a nutshell, this thesis represents a significant stride in our understanding of cancer genesis, providing a comprehensive view of the complex interplay between cell cycle dynamics, quiescence, proliferation, mutation acquisition, and cancer stem cells. The journey towards conquering cancer is far from over. However, this research provides valuable insights and directions for future investigation, bringing us closer to the ultimate goal of mitigating the impact of this formidable disease.



---

## Kurzfassung

---

Krebs ist eine komplexe und vielschichtige Krankheit, die die Grenzen der biomedizinischen Forschung immer wieder in Frage stellt. In dieser Dissertation erforschen wir die Komplexität der Krebsentstehung, indem wir die Multiskalenmodellierung, abstrakte mathematische Konzepte wie die Stabilitätsanalyse und numerische Simulationen als leistungsstarke Werkzeuge zur Entschlüsselung der zugrunde liegenden Mechanismen einsetzen. In einer Reihe umfassender Studien untersuchen wir vor allem die Dynamik des Zellzyklus, das empfindliche Gleichgewicht zwischen Ruhe und Proliferation, die Auswirkungen von Mutationen und die Koevolution von gesunden und Krebsstammzellen. Das Einführungskapitel bietet einen umfassenden Überblick über Krebs und die entscheidende Bedeutung des Verständnisses der ihm zugrunde liegenden Mechanismen. Darüber hinaus wird die Grundlage geschaffen, indem die wichtigsten Definitionen erläutert und verschiedene Modellierungsperspektiven vorgestellt werden, um die allgegenwärtige Krebsentstehung anzugehen. Als Nächstes wurde die Zellzyklusdynamik erforscht, wobei die zeitliche oszillierende Dynamik, die das Fortschreiten der Zellen durch den Zellzyklus bestimmt, aufgedeckt wurde.

In der ersten Hälfte der Arbeit werden die Zellzyklusdynamik und die Evolution von Krebsstammzelllinien unter Einbeziehung von Rückkopplungsregulationsmechanismen untersucht. Dabei wurde die zentrale Rolle von Rückkopplungsschleifen bei der Ausbreitung von Krebsstammzellen gründlich untersucht, was neue Perspektiven für die Krebsentstehung eröffnet. Dann erweitern wir unseren Modellierungsbereich und untersuchen das Zusammenspiel zwischen ruhenden und wuchernden Zellpopulationen, um die Bedeutung ihres Gleichgewichts in der Krebsbiologie zu beleuchten. Die in diesem Zusammenhang entwickelten Modelle bieten potenzielle Möglichkeiten für gezielte Krebstherapien, die auf perspektivische Zellpopulationen abzielen, die für das Fortschreiten von Krebs entscheidend sind. Die zweite Hälfte der Arbeit befasst sich mit der Multiskalenmodellierung von proliferierenden und ruhenden Zellpopulationen unter Einbeziehung der Zellzyklusdynamik und deren Erweiterung durch Mutationserwerb. Nach einer strengen mathematischen Analyse wurden die Existenz und Einzigartigkeit der vorgeschlagenen Modellierungsrahmen zusammen mit stationären Lösungen und Stabilitätskriterien untersucht.

Zusammenfassend lässt sich sagen, dass diese Arbeit einen bedeutenden Fortschritt in unserem Verständnis der Krebsentstehung darstellt, da sie einen umfassenden Überblick über das komplexe Zusammenspiel zwischen Zellzyklusdynamik, Ruhe, Proliferation, Mutationserwerb und Krebsstammzellen bietet. Der Weg zur Überwindung von Krebs ist noch lange nicht zu Ende. Diese Forschung liefert jedoch wertvolle Erkenntnisse und Hinweise für künftige Untersuchungen, die uns dem Ziel näher bringen, die Auswirkungen dieser schrecklichen Krankheit zu lindern.



---

# Contents

---

<b>1</b>	<b>Cancer: A biological perspective</b>	<b>1</b>
1.1	Introduction to cancer . . . . .	1
1.2	Key definitions . . . . .	3
1.2.1	Cell division . . . . .	3
1.2.2	Cell differentiation . . . . .	3
1.2.3	Self-renewal . . . . .	3
1.2.4	Cell age . . . . .	4
1.2.5	Cell maturity . . . . .	4
1.2.6	Pseudotime . . . . .	4
1.2.7	Proliferation . . . . .	4
1.2.8	Quiescence . . . . .	4
1.3	Cell lineages . . . . .	4
1.4	Mutations in cell lineages . . . . .	5
1.4.1	Types of mutations . . . . .	6
1.4.1.1	Point mutations . . . . .	7
1.4.1.2	Insertions and deletions (Indels) . . . . .	7
1.4.1.3	Silent mutations . . . . .	7
1.4.1.4	Inversions and translocations . . . . .	7
1.4.1.5	Repeat expansions . . . . .	7
1.4.1.6	Spontaneous and induced mutations . . . . .	7
1.4.2	Mutation rate . . . . .	7
1.5	Multiscales in cancer . . . . .	8
1.6	Modeling Techniques: Discrete, Continuum, Hybrid . . . . .	11
1.6.1	Discrete modeling . . . . .	11
1.6.2	Continuum modeling . . . . .	11
1.6.3	Hybrid modeling . . . . .	11
1.7	A brief review of cell population models . . . . .	12
1.7.1	Population growth models . . . . .	12
1.7.1.1	Exponential growth . . . . .	12
1.7.1.2	Logistic growth . . . . .	12
1.7.1.3	Monod kinetics . . . . .	13
1.7.1.4	Allee effect . . . . .	13
1.7.1.5	Baranyi model . . . . .	14
1.7.2	Markov chain models . . . . .	14
1.7.3	Agent-based models . . . . .	15
1.7.4	Physiologically structured population models . . . . .	15
1.7.4.1	McKendrick–von Foerster model . . . . .	15

1.7.4.2	Gurtin-MacCamy model . . . . .	16
1.7.4.3	Nonlinear Webb model . . . . .	16
<b>2</b>	<b>Cell cycle: Biological insights and mathematical abstractions</b>	<b>19</b>
2.1	Cell cycle: Molecular interactions . . . . .	20
2.2	Mathematical formulation . . . . .	22
2.2.1	Kinetic equations . . . . .	22
2.3	Numerical simulations . . . . .	26
<b>3</b>	<b>Mathematical model: Stem cell lineage</b>	<b>31</b>
3.1	Biological problem formulation . . . . .	31
3.2	Mathematical modeling . . . . .	33
3.2.1	Stem cell population . . . . .	35
3.2.2	Progenitor cell population . . . . .	36
3.2.3	Mature cell population . . . . .	38
3.2.4	Feedback regulation . . . . .	38
3.3	Steady-state solutions . . . . .	39
3.4	Numerical solution and simulation results . . . . .	41
3.4.1	Finite volume method . . . . .	41
3.4.2	Simulation results . . . . .	42
3.4.2.1	Case study: Evolution for different initial conditions . . . . .	47
3.4.2.2	Case study: Feedback signal as Hill function . . . . .	47
3.5	Model validation . . . . .	49
3.6	Discussion and conclusion . . . . .	51
<b>4</b>	<b>Mathematical analysis: Wellposedness of stem cell lineage model</b>	<b>53</b>
4.1	Banach fixed point theory: A brief overview . . . . .	53
4.1.1	Cauchy sequence . . . . .	54
4.1.2	Metric space . . . . .	54
4.1.3	Complete metric space . . . . .	54
4.1.4	Fixed point . . . . .	54
4.1.5	Contraction mapping . . . . .	54
4.1.6	Banach fixed point theorem . . . . .	54
4.2	Mathematical model . . . . .	55
4.2.1	Assumption and simplification . . . . .	55
4.3	Solution operator $S^\theta$ . . . . .	56
4.4	Fixed point of the solution operator $S^\theta$ . . . . .	60
4.5	Boundedness of solution . . . . .	69
4.6	Wellposedness results . . . . .	80
4.6.1	Existence and uniqueness of the solution . . . . .	80
4.6.2	Continuous dependence on problem data . . . . .	82
<b>5</b>	<b>Multiscale mathematical model: Proliferating and quiescent cell populations</b>	<b>83</b>
5.1	Biological problem formulation . . . . .	83
5.2	Mathematical modeling . . . . .	86
5.2.1	Age-structured model . . . . .	86
5.2.2	Cell cycle model . . . . .	88

5.3	Numerical solution and simulation results . . . . .	90
5.3.1	Simulation results . . . . .	92
5.4	Discussion and conclusion . . . . .	97
<b>6</b>	<b>Mathematical analysis: Wellposedness and stability properties of multiscale model</b>	<b>99</b>
6.1	Semigroup theory: A brief overview . . . . .	99
6.2	Existence and uniqueness of non-negative solution . . . . .	100
6.3	Existence and stability of steady-state solutions . . . . .	106
6.3.1	Existence of steady-state solutions . . . . .	107
6.3.2	Stability of steady-state solutions . . . . .	108
<b>7</b>	<b>Multiscale mathematical model: Healthy and cancerous proliferating and quiescent cell populations</b>	<b>115</b>
7.1	Biological problem formulation . . . . .	115
7.2	Mathematical modeling . . . . .	118
7.2.1	Age-structured model . . . . .	118
7.2.2	Cell cycle model . . . . .	120
7.3	Numerical solution and simulation results . . . . .	122
7.4	Discussion and conclusion . . . . .	127
<b>8</b>	<b>Mathematical analysis: Wellposedness and stability properties of multiscale model of healthy and cancer cell populations</b>	<b>129</b>
8.1	Existence and uniqueness of non-negative solution . . . . .	129
8.2	Existence and stability of steady-state . . . . .	135
8.2.1	Existence of steady-states . . . . .	135
8.2.2	Stability analysis of steady-state solutions . . . . .	137
<b>9</b>	<b>Conclusion and future outlooks</b>	<b>147</b>





---

## List of Figures

---

1.1	Symmetric and asymmetric stem cell divisions. . . . .	3
1.2	Stem cell lineage of blood-forming hematopoietic stem cells. . . . .	5
1.3	Different types of mutations. . . . .	6
1.4	Illustrative multiscale map of cancer. . . . .	10
1.5	Behavior of exponential and logistic growth models. . . . .	13
2.1	Key regulatory protein interactions in cell cycle phases. . . . .	20
2.2	Numerical simulations of the cell cycle model. . . . .	27
2.3	Cellular concentrations of different cell cycle regulators. . . . .	27
2.4	Cellular concentrations in the presence of full growth factors. . . . .	28
2.5	Cellular concentrations in the presence of different growth factors. . . . .	28
3.1	Model schematics: Co-evolution of healthy and mutated cell lineages. . . . .	34
3.2	Birth, death and differentiation functions for progenitor cells. . . . .	37
3.3	Behavior of cytokine feedback signal with respect to total population. . . . .	43
3.4	Cell density of healthy and mutated stem and mature cells. . . . .	44
3.5	Density distribution of healthy and mutated progenitor cells. . . . .	45
3.6	Cell density of healthy and mutated stem and mature cells. . . . .	45
3.7	Cell density of healthy and mutated stem and mature cells for various ICs. . . . .	46
3.8	Model behavior for a Hill feedback function with different coefficients. . . . .	48
3.9	Model fitting to the experimental data: Breast, prostate and colon cancers. . . . .	49
3.10	Model fitting to the experimental data: TUBO cancer cell line. . . . .	50
5.1	Model schematics of proliferating and quiescent cell populations coupled with cell cycle dynamics. . . . .	84
5.2	Evolution of microscale states (proteins) from the cell-cycle. . . . .	89
5.3	Computational mesh illustrating finite volume scheme. . . . .	91
5.4	Cell density distribution of quiescent and proliferating cell populations. . . . .	94
5.5	Non-trivial steady-state: Behavior of $N(t)$ , $g_f$ and $\gamma(t)$ . . . . .	94
5.6	Trivial steady-state: Behavior of $N(t)$ , $g_f$ and $\gamma(t)$ . . . . .	95
5.7	Exponential growth: Behavior of $N(t)$ , $g_f$ and $\gamma(t)$ . . . . .	95
7.1	Multiscale model schematics of proliferating and mutated populations in both healthy and mutated cell lines coupled with cell cycle. . . . .	117
7.2	Evolution of microscale states (proteins) from the cell-cycle. . . . .	121
7.3	Initial conditions of healthy and mutated proliferating and quiescent cells. . . . .	123
7.4	Behavior of proliferation rate $\beta_i(a)$ and transition rate $\alpha_i(a)$ of cells from proliferating to quiescent phase. . . . .	123

7.5	Steady state scenario of cell density distribution of different cell populations in macroscale. . . . .	124
7.6	Steady-state: Dynamics of the combined cell population, transition function $\gamma_i$ , and growth factors. . . . .	125
7.7	Behavior of proliferation rate $\beta_i(a)$ and transition rate $\alpha_i(a)$ of cells from proliferating to quiescent phase. . . . .	125
7.8	Exponential tumor growth scenario of cell density distribution of different cell populations in macroscale. . . . .	126
7.9	Exponential growth: Dynamics of the combined cell population, growth factors, and transition function $\gamma_i$ . . . . .	127

---

## List of Tables

---

2.1	Description of variables in cell cycle model. . . . .	23
2.2	Parameters of the cell cycle model. . . . .	26
2.3	Initial conditions used in cell cycle simulations. . . . .	26
3.1	Parameters and ICs of the model for healthy and mutated cell lineages. . . . .	43
3.2	Parameters used for model validation in Fig. 3.9. . . . .	51
3.3	Parameters used for model validation in Fig. 3.10. . . . .	51
5.1	Description of the cell states at the microscale. . . . .	88
5.2	Parameters used in the simulations of multiscale model of proliferating and quiescent cell populations. . . . .	93
5.3	Parameters used in the simulations of cell-cycle model. . . . .	96
7.1	Description of the cell states at the microscale. . . . .	120
7.2	Parameters used in the simulations of multiscale model of healthy and mutated proliferating and quiescent cell populations. . . . .	122



---

## List of Acronyms

---

A	adenine
ABM	agent-based model
BALB-neuT	mouse model of mammary carcinogenesis
C	cytosine
CDK	cyclin-dependent kinase
DNA	deoxyribonucleic acid
ECM	extracellular matrix
EGF	epidermal growth factor
EMT	epithelial-mesenchymal transition
FXS	Fragile X syndrome
G	guanine
KRAS	kirsten rat sarcoma virus
MD	molecular dynamics
mRNA	messenger ribonucleic acid
ODE	ordinary differential equation
PDE	partial differential equation
PDGF	platelet-derived growth factor
RB	retinoblastoma protein
T	thymine
TME	tumor microenvironment
TP53	tumor protein p53
TUBO	Turin-Bologna cell line
VEGF	vascular endothelial growth factor



---

## Cancer: A biological perspective

---

### 1.1 Introduction to cancer

Cancer, a complex and devastating disease, arises from the uncontrolled growth and division of cells within the human body. It is characterized by the accumulation of genetic mutations that disrupt the normal regulatory mechanisms governing cell growth and division. These mutations can occur in various genes responsible for controlling cell cycle progression, DNA repair, and apoptosis. Commonly mutated genes in cancer include tumor suppressor genes (e.g., TP53) and oncogenes (e.g., KRAS). Mutations can result from a wide range of factors, including exposure to carcinogens, genetic predisposition, or random errors in DNA replication. The accumulation of mutations leads to the transformation of normal cells into cancerous cells, which can evade the body's immune system and proliferate uncontrollably. In order to understand cancer from a biological perspective, it is essential to delve into the fundamental processes that govern normal cellular behavior. The human body consists of trillions of cells, each carrying out specific functions for maintaining tissue homeostasis and overall health of an organism. Cell division, the process by which a parent cell divides into two daughter cells, plays a vital role in growth, development, and tissue repair. Under normal circumstances, cell division is tightly regulated by a complex network of signaling pathways, ensuring that cells divide only when necessary and rectify any potential errors or abnormalities. However, the balance between cell growth and cell death is disrupted when mutations occur in critical genes involved in these regulatory mechanisms. Consequently, cells acquire the ability to divide uncontrollably, leading to the formation of tumors.

Cancer cells possess several distinct hallmarks that differentiate them from their healthy counterparts. The “hallmarks of cancer” is a conceptual framework that was proposed initially by Douglas Hanahan and Robert Weinberg in a seminal paper published in the journal *Cell* in 2000, titled “The Hallmarks of Cancer”, [1]. This framework outlines several fundamental characteristics or traits shared by most, if not all, human cancers as they progress and develop into malignant tumors. Over time, this framework has been expanded to include additional hallmarks and enabling characteristics, [2]. In addition, they introduced the concept of “enabling characteristics,” or means that enable premalignant cells to acquire the six hallmarks of cancer. Recently, authors further revisited the list, proposing one new emerging hallmark and two additional enabling characteristics, [3]. In the sequel, we discuss some of these cancer hallmarks.

First and foremost, cancer cells exhibit sustained proliferative signaling [4], meaning they continually receive and respond to signals that promote cell division, even without external stimuli. Additionally, cancer cells can evade programmed cell death, or apoptosis, which serves as a safeguard mechanism to eliminate damaged or abnormal cells [5]. Besides the essential ability of cancer cells to generate and maintain growth-promoting signals, they must also find ways to evade powerful mechanisms that restrain cell proliferation. Among these tumor suppressors, two stand out as prototypes: the RB (retinoblastoma-associated) and TP53 proteins, [6, 7]. These proteins are central hubs in two interconnected cellular regulatory networks that play pivotal roles in determining whether cells should proceed with proliferation or trigger programs leading to cellular senescence or apoptosis. Another hallmark of cancer is the ability to sustain angiogenesis, [4, 8], the process by which new blood vessels are formed to supply oxygen and nutrients to the growing tumor mass. It ensures the tumor's survival and facilitates its growth and metastatic potential, enabling cancer cells to invade and colonize other organs. Furthermore, cancer cells exhibit limitless replicative potential, achieved through the activation of an enzyme called telomerase, which prevents the shortening of telomeres (protective caps at the ends of chromosomes) that usually occurs with each round of cell division, [9, 10]. By maintaining the integrity of their telomeres, cancer cells can continue to divide indefinitely. In addition to these core hallmarks, cancer cells also display a remarkable ability to invade surrounding tissues and metastasize to distant sites. This invasive and metastatic behavior is driven by the acquisition of genetic alterations that enable cancer cells to detach from the primary tumor, invade the surrounding extracellular matrix, enter the bloodstream or lymphatic system, and establish secondary tumors in distant organs, [11, 12].

Developing effective therapeutic strategies for cancer requires a comprehensive understanding of the biological mechanisms that drive its initiation and progression. Multiscale mathematical modeling is a powerful tool to investigate the dynamic interplay between healthy and cancerous cellular populations, the impact of genetic mutations on tumor cell proliferation, the evolution of distinct cellular subpopulations, and the role of cell cycle dynamics in these processes. To ensure that mathematical models accurately represent the behavior of biological systems, it is essential to establish the uniqueness of solutions. Additionally, stability analysis helps to evaluate the long-term behavior of these solutions and distinguish whether a particular system tends to approach a steady state or exhibits fluctuations that may signify the onset or critical transition in cancer progression. By integrating mathematical models with experimental data, researchers can unravel the complex dynamics of cancer, explore new interventions, and refine treatment modalities. This interdisciplinary approach holds great promise for advancing our understanding of cancer biology and improving patient outcomes.

To conclude, cancer is a complex disease characterized by the accumulation of genetic mutations that disrupt normal cellular processes. These mutations confer cancer cells with distinct hallmarks, including uncontrolled proliferation, evasion of cell death, angiogenesis, limitless replicative potential, and invasive and metastatic behavior. To gain a better understanding of these processes, multiscale mathematical modeling proves to be an invaluable tool, allowing for the examination of cellular behavior at various levels, from molecular mutations to the broader spectrum of evolutionary changes. By employing such approach, we can gain valuable insights into the dynamics of both healthy and cancerous cell populations, which, in turn, can significantly contribute to the development of more efficacious therapeutic strategies.



## 1.2 Key definitions

### 1.2.1 Cell division

Cell division is a crucial biological process where a single parent cell divides into two or more daughter cells. This process is vital for the growth, development, tissue repair, and maintenance of multicellular organisms. The two main types of cell division are mitosis and meiosis.

- **Mitosis** is responsible for the growth and repair of tissues, resulting in two daughter cells with the same genetic information as the parent cell.
- **Meiosis** is a specialized cell division that occurs in germ cells and leads to the formation of cells with half the genetic material necessary for sexual reproduction.

### 1.2.2 Cell differentiation

The process of cell differentiation involves the specialization of undifferentiated or unspecialized stem cells to develop specific functions and structures. This transformation leads to the acquisition of unique characteristics, gene expression patterns, and functionalities that enable cells to perform specific roles within the body. The significance of this process lies in its crucial role in the development and maintenance of multicellular organisms.

### 1.2.3 Self-renewal

Self-renewal is a property of stem cells, that allows them to divide and generate daughter cells that are similar to the parent cell. It means that a stem cell can produce one or more daughter cells that retain the same stem cell properties, such as the ability to differentiate into specialized cell types. Self-renewal is essential for maintaining a pool of undifferentiated cells in tissues and organs, ensuring their long-term function and repair capabilities. Self-renewal can take place in two ways, as shown in Figure 1.1:

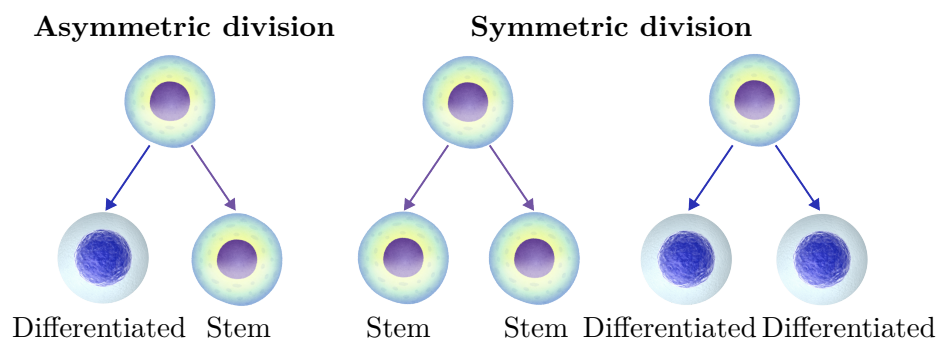


Figure 1.1: Symmetric and asymmetric stem cell divisions.

- *Symmetric self-renewal*: a stem cell divides to produce two daughter cells that are identical to the parent cell. Both daughter cells have the same stem cell properties and differentiation potential.
- *Asymmetric self-renewal*: a stem cell divides to produce two daughter cells, but they are not identical. One daughter cell retains the stem cell properties and maintains

stemness, while the other daughter cell undergoes differentiation and takes on a more specialized role.

#### 1.2.4 Cell age

Cell age refers to the biological or chronological age of individual cells within a population. It represents how long a cell has existed or its position in a developmental timeline based on biological features or markers.

#### 1.2.5 Cell maturity

Cell maturity represents the state of development or differentiation of a cell. It reflects how specialized or differentiated a cell has become in carrying out its specific functions within an organism.

#### 1.2.6 Pseudotime

Pseudotime is a computational concept used to order individual cells along a continuous trajectory or timeline based on their gene expression profiles. It represents the inferred developmental progression of cells within a biological system.

#### 1.2.7 Proliferation

Proliferation is a process of cell division and reproduction, resulting in the generation of new daughter cells from a single parent cell. It is a part of the cell cycle, which consists of phases such as  $G_1$  (gap 1), S (synthesis),  $G_2$  (gap 2), and M (mitosis). During the cell cycle, cells duplicate their genetic material (DNA replication) and then divide into two daughter cells.

#### 1.2.8 Quiescence

Quiescence, also known as the  $G_0$  phase of the cell cycle, is a state in which cells temporarily exit the active cell cycle and become non-dividing and non-proliferating. Cells in quiescence are in a resting phase. Cells enter quiescence such as lack of appropriate growth signals or response to stress. In this state, cells remain metabolically active but do not actively divide.

### 1.3 Cell lineages

A cell's lineage refers to the complete developmental history of a tissue or organ, starting from the initial stages in the fertilized embryo and proceeding through a series of divisions and differentiations until it reaches a specific cell type, known as its "cell fate." This lineage is established by tracing the cellular ancestry of an organism over time, starting from the original cells and concluding with a fully mature cell that can no longer undergo division. The life of an individual cell commences with a cell division event and culminates with either a second division, resulting in two offspring cells, or with cell death and no further offspring. Cells are the fundamental entities in cell lineages, and a *stem cell lineage* represents a unique lineage that originates from a stem cell or a population of stem cells, for instance, see Figure 1.2, which shows a stem cell lineage of blood-forming hematopoietic

stem cells that give rise to all blood and immune cell types, [13]. Stem cells are crucial in

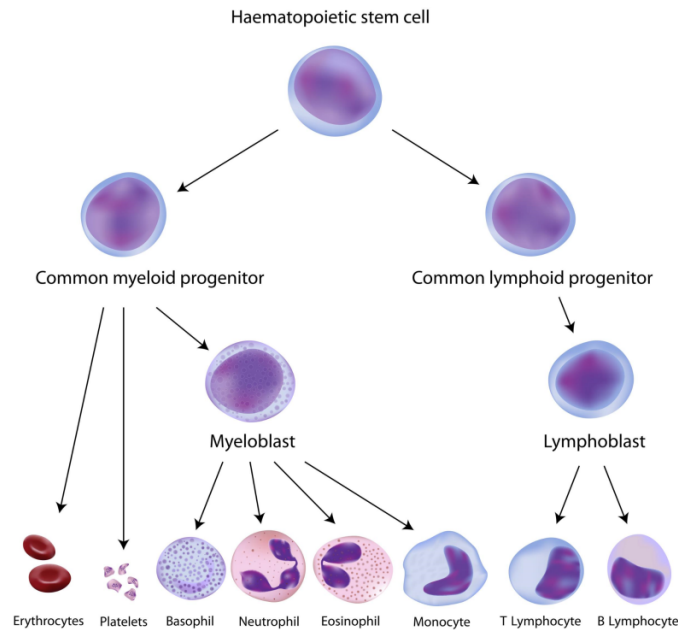


Figure 1.2: Stem cell lineage of blood-forming hematopoietic stem cells give rise to all blood and immune cell types [13].

development, tissue repair, and maintenance of organisms. They are classified based on their differentiation potential, including totipotent, pluripotent, multipotent, oligopotent, and unipotent stem cells, each with varying levels of developmental potential. The concept of stem cells encompasses multiple generations, as they possess the ability to *self-renew*, thus producing one or two cells resembling the parent, which ceases to exist upon splitting. Each type of stem cell exhibits a characteristic level of *potency*, which refers to the range of cell types they can develop into. The categorization of stem cells based on their potency is:

- *Totipotent*: Stem cells that can give rise to an entire organism and extra-embryonic tissues.
- *Pluripotent*: Stem cells that can develop into all cell types in an adult organism.
- *Multipotent*: Stem cells that can generate only a limited set of mature cell types.
- *Oligopotent*: Stem cells restricted to producing a few mature cell types.
- *Unipotent*: Stem cells with the ability to produce only one specific cell type.

## 1.4 Mutations in cell lineages

Over time, the human body's trillions of cells experience a gradual accumulation of inheritable changes. These changes manifest in a patchwork pattern across tissues, with some areas showing more advanced alterations that could potentially lead to disease. In contrast, other tissue regions may appear outwardly normal but subtly progress toward malfunction. Cancer, as a disease, advances through heritable changes in cells, which

are then passed down through cell lineages. To gain a comprehensive understanding of cancer progression, it is essential to delve into the history of cell lineages and how different lineages interact with each other. Inheritance relies on genes faithfully passed from one generation to the next in all living organisms, including microorganisms. While biochemical mechanisms are in place to ensure the accurate transmission of genes, *mutations* - sudden alterations in the sequence of nucleotide bases A, C, G, T - can and do occur, [14]. These mutations introduce variability into the gene pool and are also heritable. Therefore, a mutation can be defined as an “abrupt and heritable modification in the nucleotide sequence of a gene.” Mutations inevitably modify the genotype, which is the genetic makeup of a cell, consequently impacting the phenotype - the observable traits arising from that genotype’s expression in an organism.

Mutation stands as a critical phenomenon because it serves as the ultimate source of genetic diversity, [15]. Without mutations, all genes would remain unchanged, and the emergence of new variants or mutants (alleles) would be impossible. Hence, mutations play a pivotal role in providing the essential genetic variability that allows microorganisms to evolve and adapt effectively to environmental changes. However, it is crucial to strike a balance, as an excess of mutations occurring too frequently could disrupt the transmission of genetic information across generations significantly, [16].

### 1.4.1 Types of mutations

There are numerous mechanisms by which a DNA can be changed, leading to a variety of mutation types. A concise overview of some of these is given below:

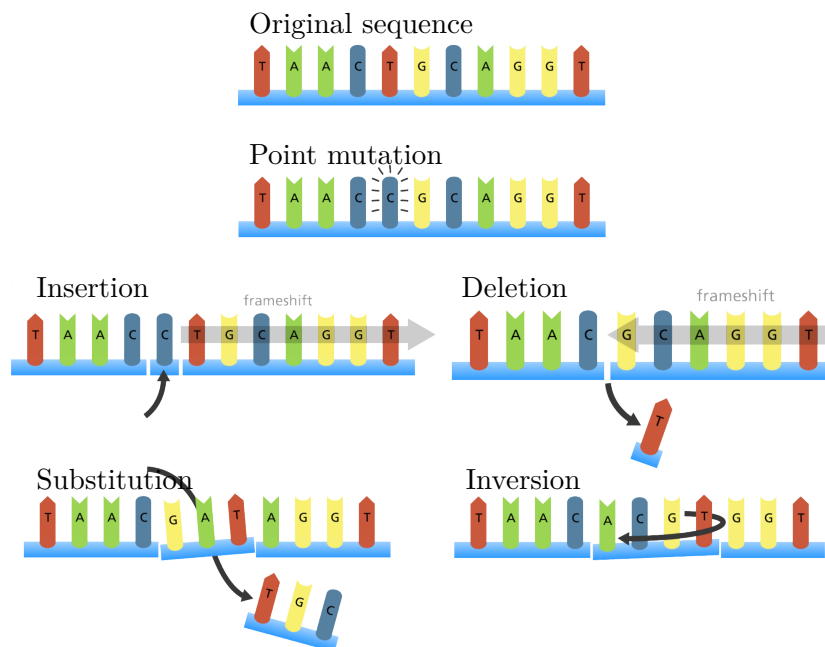


Figure 1.3: Different types of mutations, adapted from [17].

#### 1.4.1.1 Point mutations

Point mutations involve the substitution of one nucleotide base with another in the DNA sequence, [18]. There are two main subtypes:

- **Missense mutations:** In this type, a single nucleotide change leads to the substitution of one amino acid in a protein with another. Depending on the specific change, it can have either mild or severe effects on protein function.
- **Nonsense mutations** These mutations introduce a premature stop codon in the DNA sequence, leading to the production of a truncated, nonfunctional protein.

#### 1.4.1.2 Insertions and deletions (Indels)

Indels involve the addition (insertion) or removal (deletion) of one or more nucleotide bases from the DNA sequence. These mutations can lead to frameshifts, where the reading frame of the gene is altered, often resulting in nonfunctional proteins.

#### 1.4.1.3 Silent mutations

Silent mutations are point mutations that do not alter the amino acid sequence of a protein. They occur in non-coding regions of genes or in regions where multiple codons code for the same amino acid. While they do not change the protein's structure, they can still affect gene regulation and mRNA stability.

#### 1.4.1.4 Inversions and translocations

Inversions involve the reversal of a segment of DNA within a chromosome, while translocations involve the exchange of genetic material between non-homologous chromosomes. Both of these structural mutations can lead to disruptions in gene expression and potentially cause genetic disorders.

#### 1.4.1.5 Repeat expansions

Repeat expansion mutations involve the lengthening of repetitive DNA sequences within the genome. These mutations are associated with various genetic disorders, including Huntington's disease and fragile X syndrome (FXS).

#### 1.4.1.6 Spontaneous and induced mutations

Mutations can occur spontaneously due to errors in DNA replication or environmental factors. Induced mutations result from exposure to mutagens such as radiation, chemicals, or UV light.

### 1.4.2 Mutation rate

Mutation rate refers to the frequency at which genetic alterations occur in the DNA of an organism. Understanding the mutation rate is pivotal in comprehending the dynamics of genetic diversity, evolution, and the development of diseases, as it influences the emergence of new genetic variants within a population, which ultimately can lead to

cancer.

From the mathematical modeling perspective, *mutation rate* is typically defined as the probability of a cell undergoing a genetic mutation within a given unit of time. This probability can be represented mathematically as a rate constant denoted by the symbol  $m$ . The mutation rate is often expressed as mutations per cell division or mutations per cell per generation. Here is a simple mathematical representation of the mutation rate  $m$  in the context of a basic birth-death process:

$$P(\text{mutation in a given time interval}) = m \cdot \Delta t,$$

where  $P(\text{mutation in a given time interval})$  is the probability of a mutation occurring in a small time interval  $\Delta t$ . This equation provides a simple way to incorporate the mutation rate into mathematical models of cell populations.

## 1.5 Multiscales in cancer

Cancer is a multifaceted disease that involves various biological scales. It encompasses genetic changes that affect intracellular processes and tissue-level dynamics governing tumor growth and metastasis. These different biological scales correspond to different physical scales in length and time. For instance, intracellular biochemical reactions occur on timescales of seconds or less and often involve gradients over micrometer distances. Phenomena at the cellular and cell-to-cell level typically occur on length scales of tens of micrometers and timescales spanning seconds to minutes. At the tissue level, relevant scales are even more prominent. To bridge these scales, multiscale computational models can help us predict how perturbations at one scale can impact processes at other scales.

As cancer is inherently multiscale, different approaches are required to describe its variables in research. One such approach is the use of continuum descriptions which utilize differential equation-based models. Another approach involves the utilization of agent-based or stochastic models to describe discrete entities or events within cells and tissues. Hybrid models, which are a combination of both, are also used. These approaches are necessary as critical processes unfold at intracellular, cell-to-cell, and tissue levels in cancer. Understanding the characteristics and requirements of different modeling methods is crucial for accurately simulating various biological processes. Continuum models are ideal for predicting the spatiotemporal progression of intracellular signaling pathways, provided that a sufficient amount of protein and rate expressions are known. On the other hand, discrete models are better suited for processes that rely on cell-to-cell interactions, resulting in spatial variations. In some cases, hybrid models are necessary to simulate processes with spatial heterogeneity that are influenced by a field, like a chemokine gradient, which can be accurately described using continuum methods.

The term “multiscale” itself refers to the various levels or dimensions at which cancer can be studied and analyzed, see Figure 1.4. These scales offer unique perspectives on various aspects of cancer biology and its intricacies. Below are some of the primary multiscales utilized in cancer research:

- **Atomic scale:** The atomic scale is utilized to analyze the structural and dynamic characteristics of proteins, peptides, and lipids, and to investigate how these properties are impacted by environmental factors or interactions with ligands. At this scale, molecular dynamics (MD) simulations are the leading modeling approach, which involve the interaction of atoms and molecules over a specific

duration. Atomic-scale models operate within nanometer-length scales and deal with timescales in the order of nanoseconds.

- **Molecular scale:** Models that operate at the molecular level do not depict the individual molecular dynamics of proteins. Instead, they offer an average representation of properties across a population of proteins. This scale is primarily used to investigate cell signaling mechanisms, which serve as natural regulators in biological, [19]. Biomedicine is actively involved in analyzing this scale, and it holds the potential to reveal new therapeutic targets for combating diseases. The process of signal transduction begins with the binding of extracellular molecules (known as ligands) to receptors on the cell surface, ultimately leading to changes in cell function. Present modeling endeavors primarily focus on this scale, contributing valuable insights into quantifying relationships between signals and responses, and deciphering the signaling events governing cellular reactions, see [20]. Biochemical reactions involved in signaling pathways are often represented by ordinary differential equations (ODEs). Molecular-scale models encompass length scales ranging from nanometers to micrometers and timescales from microseconds to seconds.
- **Microscopic scale:** The microscopic scale also referred to as the tissue or multicellular scale, also encompasses the cellular scale, which includes the behaviors and properties of individual cells. A selectively permeable cell membrane encloses each cell, [21]. Models operating at this scale must effectively depict the transformation of normal cells into malignant ones, the associated changes in cell-cell and cell-matrix interactions, the complex and diverse tumor environment, and the presence of tumor heterogeneity. Typically, these models employ partial differential equations (PDEs) or agent-based modeling (ABM) to simulate these factors and processes, rather than ordinary differential equations (ODEs). It is worth noting that the simulation duration can significantly increase when examining individual cell behaviors in fine detail. Tissue-scale models encompass length scales ranging from micrometers to millimeters and timescales ranging from minutes to hours.
- **Macroscopic scale:** Macroscopic scale models focus on studying the overall behavior of the tumor, including its shape, morphology, level of vascularization, and invasiveness under different environmental conditions, [22]. To describe tissue properties at the macroscopic level, microscopic details of tissue structure are averaged over short spatial scales. This allows for the modeling of cell and substrate transport using conservation laws for spatiotemporally varying densities like partial differential equations (PDEs), instead of tracking individual cell activities. In these models, cells are generally treated as a single continuum, which is sometimes necessary because of the large number of cells involved. Macroscopic models consider how cells respond to gradient fields originating from various sources, including concentration gradients of diffusible or non-diffusible molecules, as well as strain and stress gradients produced by the growing tumor mass. These models operate within length scales ranging from millimeters to centimeters and timescales spanning from days to years.

Since molecular-level processes occur significantly faster, it is reasonable to posit that they reach a quasi-equilibrium state with the slower, higher-level processes. In other words, we can incorporate lower-level processes into the higher level using methods like constitutive equations or force fields. For instance, when a reaction unfolds at a rapid

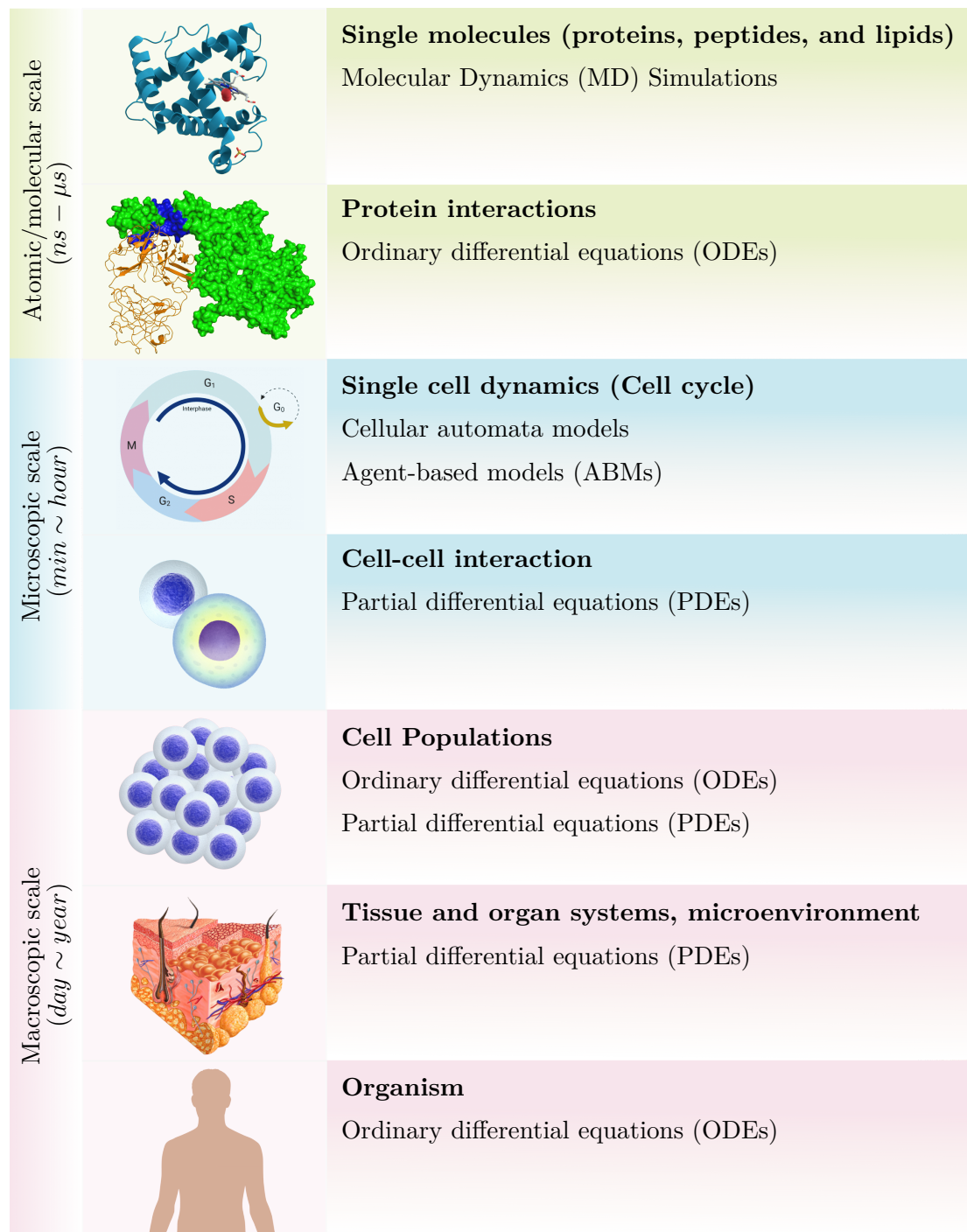


Figure 1.4: An illustration of multiscale map in cancer consisting of the DNA, proteins, cellular, subcellular interactions and tissue scales.

timescale, we can assume that the chemicals involved are in equilibrium. This assumption simplifies the integrated system by removing one of the differential equations, streamlining the solution process, and reducing computational demands, all while preserving model accuracy. This type of multiscale modeling, where lower-level processes (characterized by small spatial scales and fast dynamics) are integrated with higher-level processes



(involving large spatial scales and slower dynamics), has garnered significant attention in contemporary quantitative cancer research. It proves particularly valuable in developing multiscale models because the system of governing equations typically becomes extensive and complex.

## 1.6 Modeling Techniques: Discrete, Continuum, Hybrid

In this section, we delve into three main modeling techniques commonly used in cancer research to model various aspects of cancer dynamics and behavior.

### 1.6.1 Discrete modeling

Discrete modeling involves explicitly representing individual cells in both space and time, with their internal states updated based on predefined biological and biophysical rules. This method is particularly valuable for studying various aspects, including carcinogenesis, genetic instability, natural selection, and mechanisms of cell-cell and cell-matrix interactions. The dynamics of discrete cancer cells can be explored through lattice-based or lattice-free methods: the former employs a grid system in which cells reside, while the latter allows cells to operate in arbitrary locations and interact in various directions. Discrete modeling's strength lies in translating detailed biological findings into model rules, [23]. However, as the number of cells in the model increases, the computational demands escalate rapidly, limiting the spatial and temporal scales these models can effectively represent.

### 1.6.2 Continuum modeling

Continuum modeling, on the other hand, characterizes tumor tissue as a continuous medium, preceding the need to explicitly model individual cells. Instead, it operates at a larger scale and employs principles from continuum mechanics, typically employing partial differential equations (PDEs) or integro-differential equations to describe continuous fields for model variables. Standard variables in continuum models, such as cell volume fractions, density, and concentrations of substances like nutrients, oxygen, and growth factors, are more accessible for analysis and control compared to discrete modeling, [24]. While continuum models can capture global tumor growth and invasion properties at tissue scales, they cannot examine individual cell dynamics and discrete events, like epithelial-mesenchymal transition (EMT). This limitation is essential when studying the impact of genetic, cellular, and microenvironment factors on overall tumor behavior.

### 1.6.3 Hybrid modeling

Hybrid modeling aims to harness the strengths of both continuum and discrete modeling approaches. These models can be categorized into composite hybrid modeling and adaptive hybrid modeling, [25, 26]. In composite hybrid models, individual cells are treated discretely while interacting with chemical and mechanical continuum fields. These models facilitate the coupling of different scales influenced by the growth process, incorporating biophysical, biochemical, and biomechanical information between scales. In adaptive hybrid models, discrete and continuum representations of cells are chosen dynamically, with discrete modeling applied when necessary, such as for EMT, and

continuum modeling used for the tumor bulk. Adaptive hybrid modeling provides high resolution where needed while optimizing computational efficiency to support scalability for clinical applications. While both continuum and discrete approaches have provided valuable insights into cancer-related processes at specific spatial and temporal scales, the complexity of cancer and its intricate interactions demand a multiscale continuum-discrete (hybrid) approach. Hybrid models have the potential to bridge biological phenomena from molecular and cellular scales to the tumor scale, offering a comprehensive understanding of cancer dynamics.

## 1.7 A brief review of cell population models

In this section, we present a review of the models that can be employed to quantitatively model and simulate cell population dynamics.

### 1.7.1 Population growth models

#### 1.7.1.1 Exponential growth

Exponential growth can be described as follows:

$$\frac{dN}{dt} = rN, \quad N(0) = N_0,$$

where  $N$  is the number of cells and  $r$  is the population growth rate. This model assumes that the population rate of change is proportional to the population size  $N$ . By integration we can obtain an analytic solution that describes the number of cells in the population as a function of time  $t$  and growth rate

$$N(t) = N_0 \exp^{rt},$$

where  $N_0$  is the initial number of cells in the population. The major limitation of modeling growth as an exponential process is that the exponential phase of growth is short-lived in biologically realistic scenarios, Figure 1.5. It is only one phase of growth for cell populations when infinite natural resources are available.

#### 1.7.1.2 Logistic growth

In the real world, characterized by finite resources, exponential growth cannot be sustained indefinitely. Exponential growth might be observed in environments with a low number of individuals and abundant resources. However, as the population size increases, the availability of resources diminishes, leading to a deceleration in the growth rate. Ultimately, this growth rate reaches a point where it plateaus or stabilizes (as illustrated in Figure 1.5). This maximum population size, which denotes the highest population that a specific environment can sustain, is referred to as the carrying capacity, denoted as  $K$ . The logistic model describes changes in population size with time as

$$\frac{dN}{dt} = rN \left(1 - \frac{N}{K}\right), \quad N(0) = N_0.$$

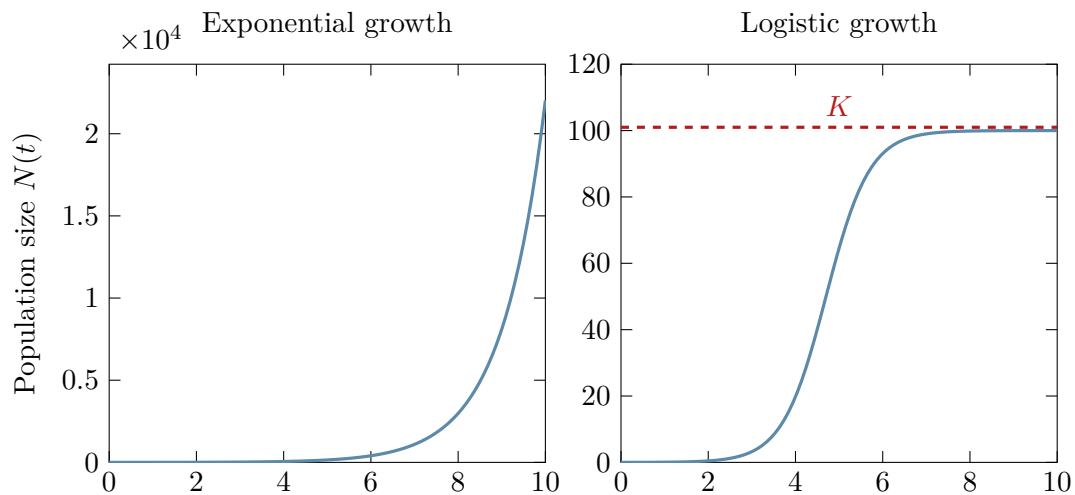


Figure 1.5: Behavior of exponential and logistic growth models.

Notice that when  $N$  is very small,  $1 - N/K$  becomes close 1, and the right side of the equation reduces to  $rN$ , which means the population is growing exponentially and is not influenced by carrying capacity. On the other hand, when  $N$  is large,  $1 - N/K$  becomes close to zero, which means that population growth will be slowed greatly or even stopped. Therefore, population growth is greatly slowed in large populations by the carrying capacity  $K$ . This model also allows for the population of a negative population growth, or a population decline.

### 1.7.1.3 Monod kinetics

The Monod model is a commonly employed mathematical model that links the rate of population growth, denoted as  $r$  to the concentration of a limiting resource, [27]. The Monod equation is as follows:

$$r = r_{\max} \frac{S}{K_s + S},$$

where  $r_{\max}$  represents the maximum growth rate achievable by microorganisms,  $S$  denotes the concentration of the essential substrate necessary for growth, and  $K_s$  signifies the value of  $S$  at which the growth rate reaches half of its maximum potential. It's important to note that both  $r_{\max}$  and  $K_s$  are empirical coefficients, and their specific values depend on the species and environmental conditions under consideration.

### 1.7.1.4 Allee effect

The Allee effect is a biological phenomenon in which the size of a population influences individual growth, deviating from the typical pattern of logistic growth, [28]. While Allee effects are commonly studied in ecology, particularly in the context of mating populations, they have also been integrated into models that describe populations of cancerous cells, [29]. The strong Allee effect where growth rate is negative at small  $N$  is described by the following ODE

$$\frac{dN}{dt} = rN \left(1 - \frac{N}{K}\right) \left(\frac{N}{N_c} - 1\right), \quad N(0) = N_0.$$

where  $N_c$  is the critical population size (threshold) required for growth. This model has stable fixed points at 0 and  $K$  and an unstable fixed point at  $N_c$ . The population has a negative growth rate when  $0 < N < N_c$  and a positive growth rate when  $N_c < N < K$ .

### 1.7.1.5 Baranyi model

The growth curve's lag-time or adaptation time is a crucial aspect that previous models do not adequately account for. The Baranyi model, on the other hand, accurately characterizes the lag phase and the transition to the exponential phase, and it is represented by the following form, [30]:

$$\frac{dN}{dt} = (\mu_{\max}\alpha(t)f(N) + \xi(t))N,$$

where  $\mu_{\max}$  is the maximum growth rate,  $\alpha(t)$  is an adjustment function, and  $f(N)$  is an inhibition function describing end-of-growth inhibition and finally,  $\xi(t)$  is a Gaussian white noise term to model stochastic fluctuations in population size.

The Baranyi model can be employed in conjunction with any of the models discussed before to depict the transition period that occurs before exponential growth or decay. The physiological state of individual cells is influenced by their prior growth environment and exposure to stressful conditions. This influence can lead to an extension of the lag phase and an increase in the variability of lag times between individual cells.

## 1.7.2 Markov chain models

Markov chain models are frequently used in cell population dynamics to describe and analyze the stochastic behavior of cell populations over time and to annotate morphological state and multiphenotype properties from experimental data, [31]. These models are particularly valuable when individual cells undergo discrete, probabilistic transitions between different states or phenotypes. In cell biology, individual cells can exist in various states or phenotypes, such as stem cells differentiating into specialized cell types or cancer cells transitioning between different stages of malignancy. Markov chain models capture these transitions as probabilistic events. Each state represents a specific cell condition, and the transitions between states occur with defined probabilities. At each time step, Markov chain models calculate the probabilities of cells transitioning from one state to another based on the current state distribution and transition probabilities. The core of a Markov chain model is the transition probability matrix. This matrix outlines the probabilities of transitioning from one state to another. It is a square matrix, and its elements represent the probabilities of transitioning from one state to another within a single time step. Additionally, cell-to-cell variability within a population can be accounted in Markov chain model. This is crucial when dealing with heterogeneous cell populations, as they allow for the modeling of stochastic behaviors and transitions between different subpopulations of cells. Estimating transition probabilities and other parameters of the Markov chain model often involves statistical methods and experimental data. Model parameters can be estimated through techniques like maximum likelihood estimation or Bayesian inference.

### 1.7.3 Agent-based models

Agent-based models (ABMs) simulate individual cells as autonomous agents with specific behaviors and rules. They are used to study cell-cell interactions, cell migration, and the emergence of complex behaviors in cell populations. Since cancer is known for heterogeneity, where cells within a tumor exhibit diverse behaviors and characteristics. ABMs excel in capturing this heterogeneity by representing individual cancer cells as agents with their unique attributes, including growth rates, mutations, and motility. Moreover, ABMs can simulate cell-cell interactions, including competition for resources, signaling, and genetic mutations. Agents interact based on proximity and can influence each other's behaviors. They can also incorporate the tumor microenvironment, including blood vessels, immune cells, and extracellular matrix components. These elements play crucial roles in tumor growth and response to therapy.

Agent-based models require data for parameterization, which can be challenging to obtain. However, advances in high-throughput technologies and patient-specific data collection have improved parameter estimation. Complex agent-based models can also be computationally intensive. There is always a trade-off between accuracy and computational complexity. However, techniques like parallel computing and optimization approaches help address this challenge. Finally, for agent-based models it is essential to ensure that model predictions align with experimental observations. Model validation often involves comparing simulation results to *in vitro* and *in vivo* data.

### 1.7.4 Physiologically structured population models

Structured population models used in ecology and population biology to describe and analyze populations that can be subdivided into distinct classes or categories based on specific characteristics or attributes. In other words, in these models size is viewed as a continuum variable specific to individuals, such as mass, volume, length, maturity, bacterial or viral load, or other physiologic or demographic property. These models are particularly valuable when studying populations with age, size, or other structured components that influence population dynamics. They describe how individual cells move between different states over time. Transition dynamics include birth, death, growth, and other processes specific to each state. The earliest models of age-structured populations, pioneered by Sharpe and Lotka in 1911, [32] and later by McKendrick in 1926, [33], laid the groundwork for utilizing partial differential equations in the modeling of continuous age structure within evolving populations.

#### 1.7.4.1 McKendrick–von Foerster model

The McKendrick–von Foerster equation is a linear first-order partial differential equation encountered in several areas of mathematical biology – for example, demography and cell proliferation modeling; it is applied when age structure is an important feature in the mathematical model. The model reads as, [33]:

$$\frac{\partial N}{\partial t} + \frac{\partial N}{\partial a} = -\mu(a)N, \quad N(0, a) = N_0(a),$$

where the population density  $N(a, t)$  is a function of age  $a$  and time  $t$ , and  $\mu(a)$  is the death function and  $N_0(a)$  is initial distribution. The boundary condition is

$$N(t, 0) = \int_0^{\infty} \beta(a)N(t, a)da,$$

where  $\beta(a)$  is birth function.

#### 1.7.4.2 Gurtin-MacCamy model

A significant resurgence of interest in age-structured models was sparked by the groundbreaking research of Gurtin and MacCamy in 1974, [34], particularly in the realm of nonlinear age-structured models. Their innovative approach, employing nonlinear Volterra integral equations, not only demonstrated the existence, uniqueness, and convergence to equilibrium of solutions but also applied these principles to nonlinear adaptations of the Sharpe-Lotka-McKendrick model. This work, known as Gurtin-MacCamy model, represented a pivotal advancement in the field of age-structured population modeling. The model can be expressed as

$$\frac{\partial N}{\partial t} + \frac{\partial N}{\partial a} = -\mu(N(t), a)N,$$

with the initial condition  $N(0, a) = N_0(a) \geq 0$  and non-local boundary condition

$$N(t, 0) = \int_0^{\infty} \beta(N(t), a)N(t, a)da \geq 0.$$

Here  $N(t, a)$  is the size (density) of a certain population of a given age  $a \geq 0$  at time  $t \geq 0$ ,  $\mu(N(t), a)$  is the per capita mortality rate and  $N(t, 0)$  is the birth function that depends on the age-structured size of the population and the per capita birth rate  $\beta(N(t), a)$ . The primary distinction arises from how birth and mortality rates are influenced by population density.

#### 1.7.4.3 Nonlinear Webb model

A nonlinear model of age and size structured population dynamics described by a density function  $N(t, a, x)$ , where  $t$  is time,  $a$  is age of individuals, and  $x$  is the size of individuals. The prototype model of this kind involves a growing population of cells characterized by varying cycle lengths (indicated by cell age) and diverse development stages (indicated by cell size). The initial size of the two daughter cells born from a dividing mother cell is governed by the division function  $k$ . The probability that a daughter cell born from a mother cell of size  $x$  has birth size between  $y_1$ , and  $y_2$  is  $\int_{y_1}^{y_2} k(y, x)dy$ . For all  $x$ ,  $k(y, x) = 0$  for  $y > x$  and  $\int_0^{\infty} k(y, x)dy = 1$ . The cell density  $N(t, a, x)$  satisfies the equation, [35]:

$$\frac{\partial}{\partial t}N(t, a, x) + \frac{\partial}{\partial a}N(t, a, x) + \frac{\partial}{\partial x}g(x)N(t, a, x) = -(\beta(a, x) + \mu(a, x))N(t, a, x),$$

with the initial condition  $N(0, a, x) = N_0(a, x) \geq 0$ , and boundary condition

$$N(t, 0, x) = 2 \int_0^{\infty} \int_0^{\infty} k(x, u)\beta(a, u)N(t, a, u)dudx \text{ (Asymmetric division),}$$

$$N(t, 0, x) = 4 \int_0^{\infty} \beta(a, 2x)N(t, a, 2x)da \text{ (Symmetric division).}$$

Here,  $g$  is the growth function which governs the growth of individual cells. If  $g(x) = c$ , where  $c$  is a constant, then individual cells have *linear growth*. The function  $\beta(a, x)$  is division rate for cells of age  $a$  and size  $x$  and finally  $\mu(a, x)$  represents the death rate of cells. The total population  $N_T(t)$  at any time  $t$  is

$$N_T(t) = \int_0^{a_{\max}} \int_0^{x_{\max}} N(t, a, x) dx da,$$

where  $a_{\max}$  and  $x_{\max}$  are maximum values of age and size, respectively.





---

### Cell cycle: Biological insights and mathematical abstractions

---

The cell cycle, an intricate sequence of molecular events, lies at the basis of life itself. It is the fundamental process by which cells grow, divide, and ultimately contribute to the growth, development, and maintenance of multicellular organisms, [36]. Furthermore, the cell cycle is the mechanism that allows multicellular organisms to grow, repair damaged tissues, and maintain their structural integrity. In embryonic development, the cell cycle is responsible for the formation of the body's various tissues and organs. Throughout an organism's life, the cell cycle continues to play a pivotal role in tissue renewal and repair.

At its core, the cell cycle is a highly regulated and sequential process that governs the duplication and division of a single parent cell into two identical daughter cells, [37]. This remarkable journey progresses through various distinct phases, each characterized by a series of events that guarantee the accurate transmission of genetic information from one generation to the next.

- **Interphase:** The journey commences during interphase, where the cell prepares itself for division. This phase encompasses three distinct subphases:  $G_1$  (Gap 1),  $S$  (Synthesis), and  $G_2$  (Gap 2). In  $G_1$ , the cell accumulates the necessary energy and resources for DNA replication. Subsequently, during the  $S$  phase, the cell replicates its DNA, ensuring that each daughter cell will receive a complete set of genetic instructions. Lastly,  $G_2$  serves as a checkpoint phase during which the cell evaluates if it is ready for division.
- **Mitosis:** Following interphase, the cell enters the phase known as mitosis. Here, the nucleus divides, and the cell's genetic material is apportioned into two separate daughter nuclei. Mitosis consists of a series of stages: prophase, metaphase, anaphase, and telophase, each with distinct cellular events and precise control mechanisms.
- **Cytokinesis:** After mitosis, the physical division of the cell takes place during cytokinesis. This process divides the cell's cytoplasm and organelles, ultimately yielding two distinct and genetically identical daughter cells.

Understanding the cell cycle is not only crucial for deciphering the essence of life but also for gaining insights into one of the most relentless foes of human health—cancer. Although the cell cycle represents an extraordinary feat of biological regulation, it is not immune to vulnerabilities. Among its most significant challenges is the emergence

of cancer. Cancer arises when the cell cycle's intricate control mechanisms break down, leading to uncontrolled cell growth and division. Mutations in genes that regulate the cell cycle, such as tumor suppressor genes and oncogenes, can disrupt the delicate balance between cell proliferation and cell death, [1]. Understanding the significance of the cell cycle's role in cancer is of paramount importance in the field of oncology. It has paved the path for advancement of the targeted therapies that aim to restore normal cell cycle control in cancer cells, offering hope in the ongoing battle against this devastating disease.

In the sequel, we delve into the molecular interactions of cell cycle in all four phases which play substantial role in the progression of cell cycle.

## 2.1 Cell cycle: Molecular interactions

A cell cycle encompasses of four different phases of growth and development that successively bring about the cell division. This division process can lead to either cell differentiation, which can occur symmetrically or asymmetrically, or cell proliferation. Notably, stem cells tend to differentiate more prominently than subsequent cell generations, which may progressively lose their differentiation potential over time. Here, we provide an in-depth explanation of the cell cycle process, which relies on intricate biochemical interactions as depicted in Figure 2.1.

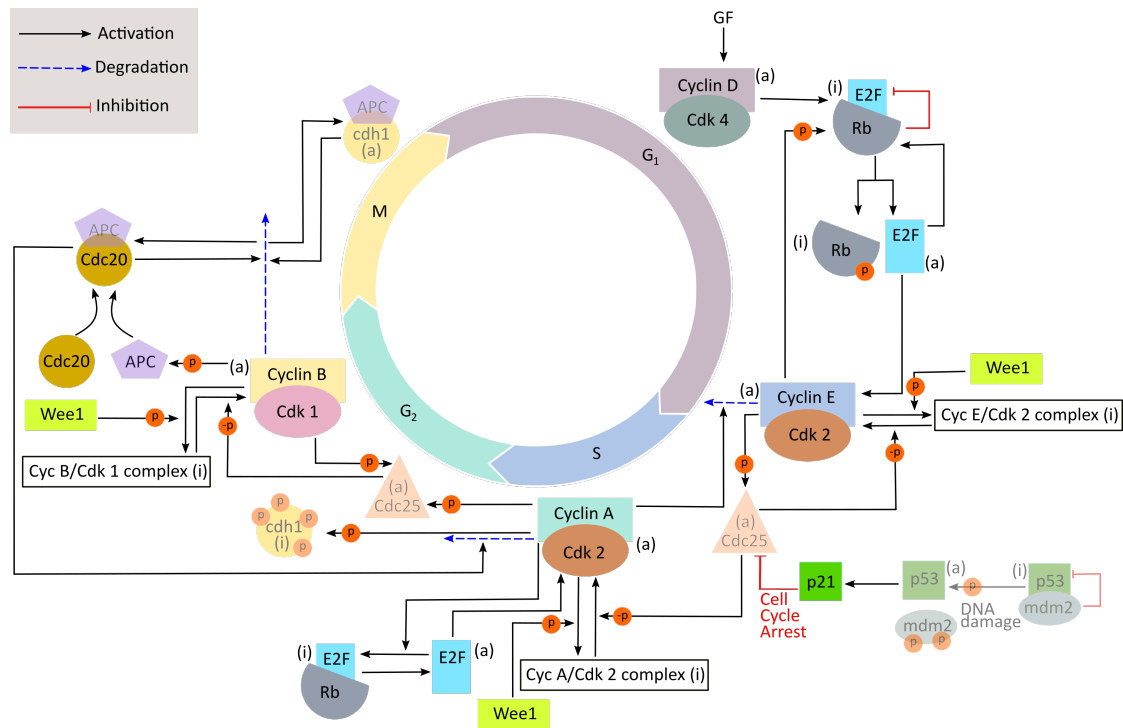


Figure 2.1: Protein Interactions during the cell cycle: Key regulatory events in each phase.

- **G<sub>0</sub> Phase:** The G<sub>0</sub> phase (G-zero phase) is a resting or quiescent phase of the cell cycle. Cells in the G<sub>0</sub> phase are not actively preparing to divide or undergoing the processes of the traditional cell cycle stages (G<sub>1</sub>, S, G<sub>2</sub>, and M phases). Instead,

they have temporarily exited the cell cycle and are in a non-dividing, resting state. However, the cells can re-enter the active cell cycle ( $G_1$  phase) when prompted by appropriate signals or changes in their environment. This transition from  $G_0$  to an active phase is often regulated by specific growth factors and signaling pathways.

- **$G_1$  Phase (Gap 1):** In the course of phase  $G_1$ , when the cell perceives enough amount of growth signals from the environment, it induces synthesis of Cyclin D to make an active complex with Cdk4/6. This complex can then trigger the activation of transcription factor E2F by phosphorylating its inhibitor retinoblastoma protein Rb. Resultantly, the transcription factor E2F is accumulated and activates the other important Cyclins, i.e., Cyclin D, E and A. Cyclin E and Cdk2 make an active complex and deactivates Rb by phosphorylation and thus cell transits to S phase.
- **S Phase (Synthesis):** The synthesis of Cyclin E by transcription factor E2F enables progression in S phase. The regulation of Cyclin E – Cdk2 complex is also performed by phosphorylation and dephosphorylation from Cyclin dependent kinase inhibitor Wee1 and phosphatase Cdc25. Further regulation is achieved by reversible association with tumor suppressor gene p21 followed from the pathway of p53, which inhibits the Cdk activity in case of DNA damage in the cell. After making an active complex, Cyclin A – Cdk2 triggers the degradation of Cyclin E – Cdk2 and inactivates the transcription factor E2F by phosphorylation to exit S phase.
- **$G_2$  Phase (Gap 2):** Cyclin A – Cdk2 complex accumulates, thus preparing the cell for mitosis and ensuring proper DNA replication.  $G_2$  serves as a checkpoint phase where the cell evaluates whether DNA replication in the S phase occurred correctly and if the cell is ready for mitosis. Accumulation of Cyclin B – Cdk1 occurs in  $G_2$  phase which also brought about the transition to M phase. Additional regulation of Cyclin A – Cdk2 and Cyclin B – Cdk2 complexes are also performed by phosphorylation and dephosphorylation from Cyclin dependent kinase inhibitor Wee1 and phosphatase Cdc25.
- **M Phase (Mitosis):** The M phase includes the stages of mitosis, where the nucleus divides, and cytokinesis, where the cell physically splits into two daughter cells. Cyclin B – Cdk1 complex is critical for the progression of mitosis. It triggers various events, including chromosome condensation, alignment, and separation. Additionally, it activates the protein Cdc20 by phosphorylation, that triggers the degradation of Cyclin A and also of Cyclin B. After mitosis, the cell undergoes cytokinesis, leading to the division of the cytoplasm and organelles, resulting in two separate daughter cells. The negative feedback reduces the Cdk activity to lowest level and cell exit the cell cycle to start over if the growth factors are available in sufficient amount.

The cell cycle can vary among different cell types and is tightly regulated to suit their specific functions and requirements. Variations in the cell cycle may involve differences in the duration of each phase or even the presence of specific checkpoints. Some of the examples include:

- In some cell types, like skin cells and gut epithelial cells, the cell cycle proceeds rapidly. These cells are often exposed to mechanical wear and tear and require continuous replacement. The  $G_1$  phase may be shorter or virtually absent in these

cells, allowing them to quickly enter the S phase for DNA replication and progress through the cell cycle. Checkpoints may be less stringent, as these cells prioritize rapid proliferation over meticulous error-checking, [38].

- Certain cell types, like neurons and muscle cells, can exit the cell cycle and become quiescent or non-dividing after reaching a specific stage of differentiation. These cells often spend a significant portion of their lifecycle in the  $G_0$  phase, where they do not actively participate in the cell cycle, [39].
- Stem cells are unique in that they can either undergo symmetric division (producing two identical stem cells) or asymmetric division (generating one stem cell and one differentiated cell). The balance between self-renewal and differentiation depends on the specific stem cell type and the tissue it resides in, [40].
- Cancer cells often exhibit uncontrolled cell cycle progression. They bypass checkpoints and rapidly divide, leading to tumor formation, [1]. Mutations in cell cycle regulatory genes, such as TP53 (p53) or RB1 (Rb), can disrupt the normal control mechanisms, allowing cancer cells to evade regulation, [41].

## 2.2 Mathematical formulation

### 2.2.1 Kinetic equations

Cell cycle regulation has been modeled using ordinary differential equations, representing the reaction rate kinetics of key cellular proteins. Modeling the dynamics of the cell cycle, particularly its temporal oscillatory behavior, is essential to strike a balance between complexity and simplicity. We focus on a subset of main proteins, referred to as core regulatory proteins, allowing for a more interpretable model while capturing the fundamental dynamics of the cell cycle. However, it is essential to recognize that these simplified models are abstractions of the complex biological reality. They capture the essential features of the cell cycle; however, they may not account for all possible regulatory mechanisms and interactions. In the sequel, we explain some critical proteins in our modeling framework. Cyclin complexes that are main functioning proteins, i.e., Cyclin D – Cdk4/6, Cyclin E – Cdk2, Cyclin A – Cdk2 and Cyclin B – Cdk1, are represented here by Md, Me, Ma and Mb, respectively. E2F is a transcription factor that plays a crucial role in the initiation of the cell cycle, and Cdc20 is an important component that, along with Anaphase promoting complex, degrades the Cyclin A and B in order for mitotic exit. Rb is a tumor suppressor protein critical in regulating the cell cycle and preventing uncontrolled cell proliferation. p21, also known as cyclin-dependent kinase inhibitor 1 (CDKN1A), plays a crucial role in cell cycle regulation and cell proliferation control. It is a well-known cell cycle inhibitor and tumor suppressor protein that is an important checkpoint regulator. Finally, Wee1 kinase plays a pivotal role in cell cycle regulation, specifically in controlling the progression of the cell cycle through phosphorylation of Cyclin-dependent kinases.

Our model consist of nine sates (proteins) that are sufficient to describe the cell cycle mechanism, see Eqs. (2.1)-(2.9). The proposed variables of the model are also listed in Table 2.1. The oscillatory dynamics of these proteins depicts the cell cycle exit and re-entry into another cell cycle. Following Michaelis–Menten kinetics, the system of ordinary differential equations can be expressed as follows:

## 2.2 Mathematical formulation

Variables	Definition
Md	Cyclin D – Cdk4/6 complex
E2F	Transcription factor E2F
Rb	Unphosphorylated Retinoblastoma protein
Wee1	Active, dephosphorylated form of kinase Wee1
Me	Cyclin E – Cdk2 complex
Ma	Cyclin A – Cdk2 complex
Mb	Cyclin B – Cdk1 complex
Cdc20	Protein that belongs to the anaphase-promoting complex (APC)
p21	Cyclin-dependent kinase inhibitor p21

Table 2.1: Description of variables in cell cycle model.

$$\frac{dM_d}{dt} = K_{sd} \left( \frac{GF}{K_{gf} + GF} \right) - K_{maxmdin} \left( \frac{M_d}{K_{md} + M_d} \right) - K_{p21md} M_d p21 \quad (2.1)$$

$$\begin{aligned} \frac{dE2F}{dt} = & K_{se2f} + K_{1e2f} \left( \frac{(E2F_{tot} - E2F)}{K_{e2f} + (E2F_{tot} - E2F)} \right) (M_d + M_e) - K_{rbe2f} R_b E2F \\ & - K_{e2fma} M_a \left( \frac{E2F}{K_{2e2f} + E2F} \right) - K_{de2f} E2F \end{aligned} \quad (2.2)$$

$$\frac{dR_b}{dt} = K_{srb} - K_{rbe2f} R_b E2F - K_{rbmd} M_d \left( \frac{R_b}{K_{rb} + R_b} \right) - K_{drb} R_b \quad (2.3)$$

$$\frac{dWee1}{dt} = K_{swee1} - K_{mdwee1} M_b \left( \frac{Wee1}{K_{wee1} + Wee1} \right) - K_{dwee1} Wee1 \quad (2.4)$$

$$\begin{aligned} \frac{dM_e}{dt} = & K_{sme} E2F - K_{wee1me} \left( \frac{M_e}{K_{me} + M_e} \right) Wee1 - K_{p21me} M_e p21 \\ & - K_{dme} M_a \left( \frac{M_e}{K_{1me} + M_e} \right) \end{aligned} \quad (2.5)$$

$$\begin{aligned} \frac{dM_a}{dt} = & K_{sma} E2F - K_{wee1ma} \left( \frac{M_a}{K_{ma} + M_a} \right) Wee1 - K_{p21ma} M_a p21 \\ & - K_{dma} Cdc20 \left( \frac{M_a}{K_{1ma} + M_a} \right) \end{aligned} \quad (2.6)$$

$$\begin{aligned} \frac{dM_b}{dt} = & K_{smb} M_a - K_{wee1mb} \left( \frac{M_b}{K_{mb} + M_b} \right) Wee1 - K_{p21mb} M_b p21 \\ & - K_{dmb} Cdc20 \left( \frac{M_b}{K_{1mb} + M_b} \right) \end{aligned} \quad (2.7)$$

$$\begin{aligned} \frac{dCdc20}{dt} = & K_{scdc20} M_b \left( \frac{(Cdc20_{tot} - Cdc20)}{K_{1cdc20} + (Cdc20_{tot} - Cdc20)} \right) \\ & - K_{maxcdc20ph} \left( \frac{Cdc20}{K_{cdc20} + Cdc20} \right) - K_{dcdc20} Cdc20 \end{aligned} \quad (2.8)$$

$$\begin{aligned} \frac{dp21}{dt} = & K_{1sp21} - K_{2sp21} E2F \left( \frac{K_{p21rb}}{K_{p21rb} + R_b} \right) - K_{p21md} M_d p21 - K_{p21me} M_e p21 \\ & - K_{p21ma} M_a p21 - K_{p21mb} M_b p21 - K_{1p21} M_e \left( \frac{p21}{K_{p21} + p21} \right) \\ & - K_{dp21} p21 \end{aligned} \quad (2.9)$$

Hereby, we observe the temporal oscillatory behavior of proteins which play an important role in determining the cell cycle varying dynamics. In stem cell lineage, each cell population has varying rates of molecular interactions and hence these parameters vary for every cell type. In the sequel, we present a detailed description of the parameters involved in the model given in the Table 2.2 in the same order as they are appearing in the equations.

Parameter	Description	Value
$K_{sd}$	Rate constant for synthesis of Cyclin D – Cdk4/6 induced by growth factors	$0.175h^{-1}$
$K_{gf}$	Michaelis constant for synthesis of the Cyclin D – Cdk4/6 complex induced by growth factors	$0.1\mu M$
$K_{maxmdin}$	Maximum degradation rate of Cyclin D – Cdk4/6 complex	$0.245\mu Mh^{-1}$
$K_{md}$	Michaelis constant for the degradation of Cyclin D – Cdk4/6	$0.1\mu M$
$K_{p21md}$	Bimolecular rate constant for binding of Cyclin D – Cdk4/6 to p21	$0.15\mu M^{-1}h^{-1}$
$K_{se2f}$	Basal rate of synthesis of E2F	$0.15\mu Mh^{-1}$
$K_{1e2f}$	Rate constant for activation of E2F by Cyclin D – Cdk4/6 and Cyclin E – Cdk2 complexes	$0.805h^{-1}$
$E2F_{tot}$	Total concentration of the transcription factor E2F	$2\mu M$
$K_{e2f}$	Michaelis constant for E2F activation by Cyclin D – Cdk4/6 and Cyclin E – Cdk2 complexes	$0.01\mu M$
$K_{rbe2f}$	Bimolecular rate constant for binding of Rb to E2F	$0.05\mu M^{-1}h^{-1}$
$K_{e2fma}$	Rate constant for phosphorylation of E2F by Cyclin A – Cdk2	$4h^{-1}$
$K_{2e2f}$	Michaelis constant for E2F phosphorylation by Cyclin A – Cdk2	$5\mu M$
$K_{de2f}$	Apparent first-order rate constant for non-specific E2F degradation	$0.002h^{-1}$
$K_{srb}$	Basal rate of synthesis of Rb	$0.8\mu Mh^{-1}$
$K_{rbmd}$	Rate constant for phosphorylation of Rb	$2.2h^{-1}$
$K_{rb}$	Michaelis constant for Rb phosphorylation	$0.1\mu M$
$K_{drb}$	Apparent first-order rate constant for Rb degradation	$0.01h^{-1}$
$K_{swee1}$	Rate of synthesis of kinase Wee1	$0.06\mu Mh^{-1}$
$K_{mdwee1}$	Rate constant for inactivation of kinase Wee1 through phosphorylation by Cyclin B – Cdk1	$1.2h^{-1}$
$K_{wee1}$	Michaelis constant for Wee1 inactivation through phosphorylation by Cyclin B – Cdk1	$0.1\mu M$
$K_{dwee1}$	Apparent first-order rate constant for degradation of active kinase Wee1	$0.1h^{-1}$
$K_{sme}$	Rate constant for synthesis of Cyclin E – Cdk2 induced by the transcription factor E2F	$0.21h^{-1}$
$K_{wee1me}$	Rate constant for inactivation of Cyclin E – Cdk2 through phosphorylation by kinases Wee1	$1.4h^{-1}$
$K_{me}$	Michaelis constant for Cyclin E – Cdk2 inactivation through phosphorylation by kinases Wee1	$0.1\mu M$

## 2.2 Mathematical formulation

$K_{p21me}$	Bimolecular rate constant for binding of Cyclin E – Cdk2 to p21	$0.2\mu M^{-1}h^{-1}$
$K_{dme}$	Rate constant for the degradation of Cyclin E – Cdk2 by Cyclin A – Cdk2	$0.35h^{-1}$
$K_{1me}$	Michaelis constant for the degradation of Cyclin E – Cdk2	$0.1\mu M$
$K_{sma}$	Rate constant for synthesis of Cyclin A – Cdk2 induced by the transcription factor E2F	$0.175h^{-1}$
$K_{wee1ma}$	Rate constant for inactivation of Cyclin A – Cdk2 through phosphorylation by kinases Wee1	$1.85h^{-1}$
$K_{ma}$	Michaelis constant for Cyclin A – Cdk2 inactivation through phosphorylation by kinases Wee1	$0.1\mu M$
$K_{p21ma}$	Bimolecular rate constant for binding of active Cyclin A – Cdk2 to p21	$0.15\mu M^{-1}h^{-1}$
$K_{dma}$	Rate constant for the degradation of the Cyclin A – Cdk2 complex by the protein Cdc20	$0.245h^{-1}$
$K_{1ma}$	Michaelis constant for the degradation, activated by Cdc20, of Cyclin A – Cdk2	$0.1\mu M$
$K_{smb}$	Rate constant for synthesis of Cyclin B – Cdk1 induced by Cyclin A – Cdk2	$0.21h^{-1}$
$K_{wee1mb}$	Rate constant for inactivation of Cyclin B – Cdk1 through phosphorylation by kinases Wee1	$2.1h^{-1}$
$K_{mb}$	Michaelis constant for Cyclin B – Cdk1 inactivation through phosphorylation by kinases Wee1	$0.1\mu M$
$K_{p21mb}$	Bimolecular rate constant for binding of Cyclin B – Cdk1 to p21	$0.12\mu M^{-1}h^{-1}$
$K_{dmb}$	Rate constant for the degradation of the Cyclin B – Cdk1 complex by the protein Cdc20	$0.28h^{-1}$
$K_{1mb}$	Michaelis constant for the degradation, activated by Cdc20, of Cyclin B – Cdk1	$0.005\mu M$
$K_{scdc20}$	Rate constant for activation of Cdc20 through phosphorylation by Cyclin B – Cdk1	$8h^{-1}$
$Cdc20_{tot}$	Total concentration of the protein Cdc20	$5\mu M$
$K_{1cdc20}$	Michaelis constant for Cdc20 activation through phosphorylation by Cyclin B – Cdk1	$0.1\mu M$
$K_{maxcdc20dph}$	Maximum rate of Cdc20 inactivation through dephosphorylation	$0.7\mu Mh^{-1}$
$K_{cdc20}$	Michaelis constant for Cdc20 inactivation through dephosphorylation	$0.1\mu M$
$K_{dcdc20}$	Apparent first-order rate constant for degradation of active Cdc20	$0.05h^{-1}$
$K_{1sp21}$	Basal, E2F-independent rate of synthesis of p21	$0.8\mu Mh^{-1}$
$K_{2sp21}$	Rate constant for synthesis of p21 induced by E2F	$0.1h^{-1}$
$K_{p21rb}$	Constant of inhibition by pRB of p21 synthesis	$0.1\mu M$
$K_{1p21}$	Rate constant for inactivation of p21 through phosphorylation by Cyclin E – Cdk2	$50h^{-1}$

$K_{p21}$	Michaelis constant for p21 phosphorylation by Cyclin E – Cdk2	$0.5\mu M$
$K_{dp21}$	Apparent first-order rate constant for non-specific p21 degradation	$0.06h^{-1}$

Table 2.2: Parameters of the cell cycle model.

## 2.3 Numerical simulations

In this section, the numerical solution of the cell cycle model, consisting of nine ordinary differential equations (ODEs), is presented. The model Eqs. (2.1)-(2.9) describes the dynamics of cell cycle protein concentrations, and the kinetic parameters used for the simulations are detailed in Table 2.2. The ODE solver ode45 is used for numerical solutions. The initial conditions used are given in Table 2.3.

Variables	Initial conditions
Md	0.01 mg/ml
Me	0.0148 mg/ml
Ma	0.77 mg/ml
Mb	0.15 mg/ml
p21	0.12 mg/ml
E2F	0.01 mg/ml
Rb	0.01 mg/ml
Wee1	0.01 mg/ml
Cdc20	0.01 mg/ml

Table 2.3: Initial conditions used in cell cycle simulations.

The model is simulated for a time interval of 0 to 100 hours. We observe oscillations in the concentrations of Cyclin complexes (Md, Me, Ma, Mb) and p21, in the presence of growth factor, as the cell cycle progresses through its all four phases, see Figure 2.2. There are approximately four to five cell cycles shown in this figure. On average, the cell cycle in mammalian cells can typically last around 18 to 24 hours. These oscillations of cell cycle proteins are crucial for regulating the progression of the cell division cycle. The Cyclin D – Cdk4/6 complex synthesizes and accumulates in the presence of maximum growth factors and therefore, its concentration increases, which symbolizes progression in  $G_1$  phase and then decreases, which depicts the transition from  $G_1$  to S phase. Consequently, following a series of molecular interactions, all cyclin complexes oscillate. These oscillations are tightly linked to the progression and regulation of the cell cycle. For instance, the presence of p21 inhibits the activity of cyclin-dependent kinase complexes if DNA damage is detected, thus preventing the cell from advancing through the  $G_1/S$  and S phases of the cell cycle by binding to CDKs, see Figure 2.2. Other cell cycle regulators from our model (E2F, Wee1, Cdc20, Rb) are plotted in Figure 2.3. These proteins are essential players in the control of the cell cycle, and their oscillatory behavior is tightly linked to the orderly progression of the cycle. The transcription factors E2F are kept in check by phosphorylation by Cyclin – Cdk complexes during the  $G_1$  phase. As cells progress through  $G_1$  into the S phase, these complexes become active



and phosphorylate Rb (which is initially active in  $G_1$  phase), leading to the release of E2F. Released E2F then triggers the transcription of genes necessary for DNA replication. Afterward, E2F levels decrease as cells exit the S phase, setting the stage for the next cell cycle.

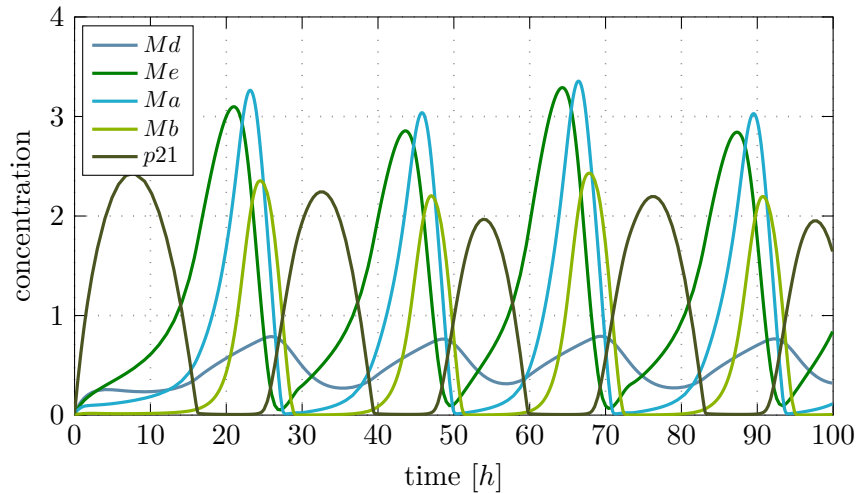


Figure 2.2: Numerical simulations of the cell cycle model. Almost four full cycles are shown. The curves represent the cellular concentrations of different Cyclin complexes (Cyclin D – Cdk4/6, Cyclin E – Cdk2, Cyclin A – Cdk2, and Cyclin B – Cdk1) and tumors suppressor protein (p21) in the presence of maximum growth factors.

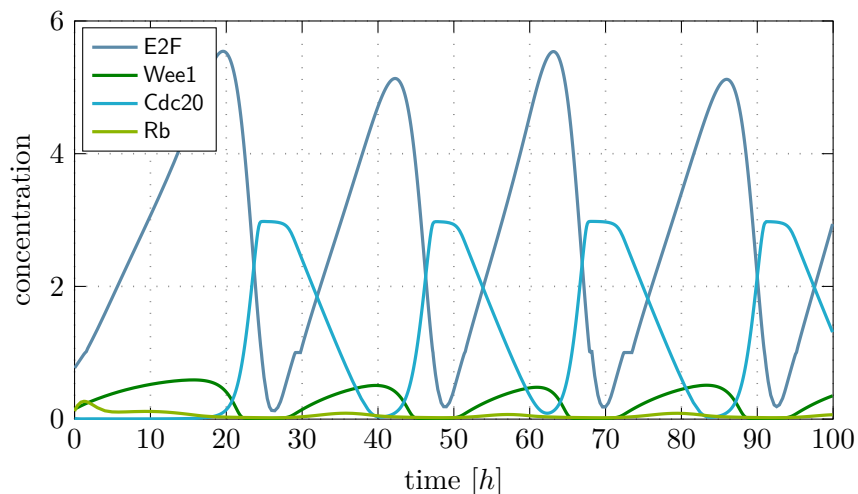


Figure 2.3: Numerical simulations of other cell cycle regulators including concentration of transcription factors (E2F), kinases (Wee1), anaphase promoting complex (Cdc20) and retinoblastoma protein (Rb) in the presence of maximum growth factors.

Wee1 activity peaks during the  $G_2$  phase. It phosphorylates and inhibits Cdk1, preventing premature entry into mitosis (M phase). As cells progress through  $G_2$ , Wee1 activity decreases, allowing Cdk1 to become active and initiate mitosis. This oscillation ensures that mitosis occurs only when conditions are suitable. Finally, Cdc20 binds to and

activates the Anaphase-Promoting Complex/Cyclosome APC/C during the M phase, leading to the degradation of Cyclin B and other proteins. This degradation is essential for exit from mitosis. After mitosis, Cdc20 levels decrease, ensuring that the APC/C is inactive during other cell cycle phases. In summary, the oscillations are essential for controlling the timing of critical cell cycle events, ensuring the duration of the cell cycle, and that cell division occurs accurately and with proper checkpoints. Any disturbances or abnormalities in cell cycle regulation can significantly affect cellular health and contribute to diseases, including cancer.

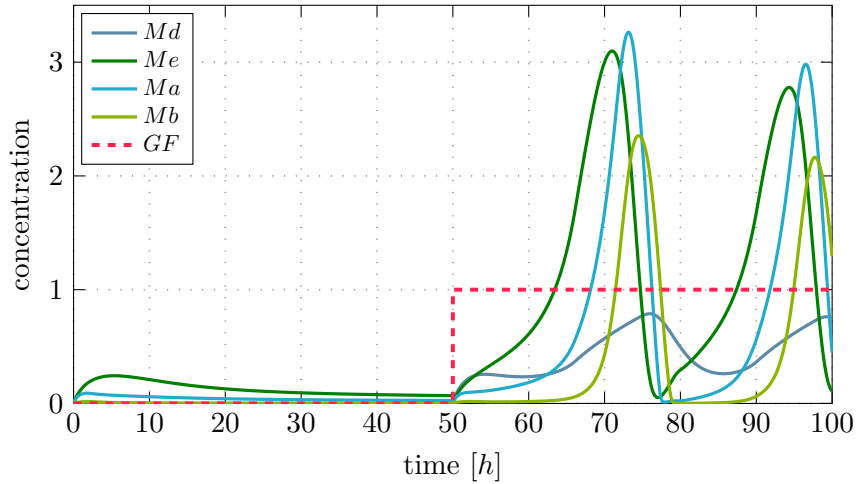


Figure 2.4: Numerical simulations of the cell cycle model. The curves represent the cellular concentrations of different Cyclin complexes (Cyclin D – Cdk4/6, Cyclin E – Cdk2, Cyclin A – Cdk2, and Cyclin B – Cdk1) in the presence of different growth factors. Initially, there are no growth factors and cell division cycle is not taking place. However from hour 50, growth factors are maximum and hence the cells are dividing.

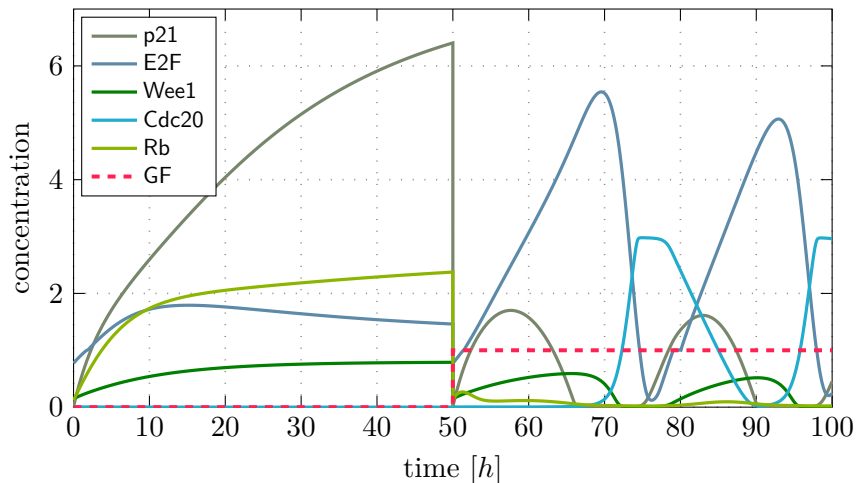


Figure 2.5: Cellular concentrations of tumor suppressor protein (p21), transcription factors (E2F), kinases (Wee1), anaphase promoting complex (Cdc20) and retinoblastoma protein (Rb) in the presence of different growth factors.

Next, we plotted another scenario where growth factors are kept equal to zero (i.e.,  $g_f = 0$ ) for the first  $50h$ , and then their value is set to maximum (i.e.,  $g_f = 1$ ) for the remaining time used in the simulations. It is important to note that growth factors are signaling molecules that play a pivotal role in regulating cell cycle progression by modulating the activity of Cyclin-dependent kinases (CDKs) and other crucial proteins. In the absence of growth factors, the oscillatory dynamics of the cell cycle are disrupted, resulting in a lack of cell division, as illustrated in Figure 2.4 and 2.5. The cell cycle dynamics are driven by a series of tightly interconnected and interrelated events. The absence of specific steps within this process can lead to the complete cessation of the entire cycle. Cyclin complexes are maintained at lower concentrations in Figure 2.4, while regulatory proteins in Figure 2.5 gradually increase in the absence of Cyclin complexes. Over time, they reach an equilibrium state. Growth factors, such as Epidermal Growth Factor (EGF) or Platelet-Derived Growth Factor (PDGF), can bind to their respective cell surface receptors, initiating intracellular signaling pathways. These pathways can then stimulate the synthesis of Cyclins (e.g., Cyclin D, Cyclin E) and only increased Cyclin levels promote the formation of active Cyclin – Cdk complexes, driving the cell cycle forward. Furthermore, fluctuations in the concentration of growth factors can impact the duration of oscillations in Cyclin levels and Cdk activity. Increased levels of growth factors tend to extend the duration of these oscillations, resulting in a faster progression of the cell cycle. In contrast, lower levels of growth factors have the opposite effect, leading to slower cell cycle progression. For instance, if we observe the duration of two cell cycle oscillations immediately following the maximization of growth factors in Figures 2.4 and 2.5, we can see that the first cell cycle has a longer duration compared to the second one.

In summary, variations in growth factors influence the oscillatory dynamics of the cell cycle by regulating the activity of Cyclin/Cdk complexes, regulating checkpoint control proteins, and impacting cell fate decisions. The precise timing and magnitude of growth factor signals are crucial for the orderly progression of the cell cycle, ensuring that cell division occurs in response to the appropriate external and internal signaling cues.



---

### Mathematical model: Stem cell lineage

---

Tumor emergence and progression is a complex phenomenon that assumes special molecular and cellular interactions. The hierarchical structuring and communication via feedback signaling of different cell types, which are categorized as the stem, progenitor, and differentiated cells in dependence of their maturity level, plays an important role. Under healthy conditions, these cells build a dynamical system that is responsible for facilitating the homeostatic regulation of the tissue. Generally, in this hierarchical setting, stem and progenitor cells are yet likely to undergo a mutation, when a cell divides into two daughter cells. This may lead to the development of abnormal characteristics in the cell, yielding an unrestrained number of cells. Therefore, the regulation of a stem cell's proliferation and differentiation rate is crucial for maintaining the balance in the overall cell population. In this chapter, a maturity based mathematical model with feedback regulation is formulated for healthy and mutated cell lineages. It is given in the form of coupled ordinary and partial differential equations. The focus is laid on the dynamical effects resulting from acquiring a mutation in the hierarchical structure of stem, progenitor and fully differentiated cells. Additionally, the effects of nonlinear feedback regulation from mature cells into both stem and progenitor cell populations have been inspected. The steady-state solutions of the model are derived analytically. Numerical simulations and results based on a finite volume scheme underpin various expected behavioral patterns of the homeostatic regulation and cancer evolution.

#### 3.1 Biological problem formulation

A tissue structure is comprised of various cell types arranged in a hierarchy according to specific characteristics, properties and functionalities. Typically, stem cells have the inherent property of indefinite self-renewal and differentiation into specialized cells [42]. Self-renewal in stem cells results in the production of the cells identical to the parent, [43]. As sources of a lineage structure, stem cells produce progenitor cells via differentiation and their properties vary accordingly. For a given cell type, cell lineage has to undergo a fixed number of maturity levels between the stem and differentiated cells. At the end of a cell line, the progenitor cells give rise to a mature cell population which does not possess the power to proliferate anymore, but can only experience apoptosis (the programmed cell death, [44]). The specialised functions in the tissue are performed by mature cells, while the tissue homeostasis is preserved by regulating the ratio of stem cells' self-renewal rate to differentiation. According to tumor stem cell hypothesis [45], cancer invasion and maintenance is driven by a small number of cells possessing the

properties of stem cells. It has been observed that cancer initiating cells are characterized by high proliferative potential, capability to differentiate into diverse phenotypes and strength to escape apoptosis [1, 45]. In fact, these so-called “tumor-initiating cells” are stem cells that have acquired mutations [45], while the rest of the tumor cells are either mutated progenitor or differentiated cells. The latter can undergo apoptosis and are less likely responsible to invade and persist the tumor [46]. Therefore, it has been suggested to eradicate the cancer stem cells by treatment to completely eliminate the cancer [47]. This motivates particularly the study of stem cell dynamics and their role in the cancer evolution. In this sense, the present paper tends to develop a mathematical modeling framework, which is useful to predict the observed behavioral patterns of cancer evolution and, additionally, help in a purposeful impact by means of external inputs (e.g. radiation) which leads to mutation acquisition.

Tumor development results from acquiring mutations and escaping the enzyme-coded fixation process, [48]. After acquiring a nonsense mutation, it can increase in number via cell division. Although not all mutations are harmful, certain mutations can contribute to malignant cell growth when acquired successively. While there exist various types of mutations, the ones which are crucial to cancer are characterized by enhanced proliferative potential, reduced apoptosis, genetic instability and reduced tumor suppression, [1]. It has also been observed that typically one to ten mutations are required in a cell to revamp into a malignant one, [1, 49, 50]. The mutated cells also possess a progeny, because these cells not only proliferate, but can also differentiate to successive cell types. In other words, there exists another hierarchical structure of mutated (i.e. cancer) cells besides the healthy one. Herein, the interesting aspect to study is the joint evolution of both progenies sharing the same environment.

The functionality of any multi-cellular organism as a whole depends greatly on the active feedback regulation process [51]. The loss of this homeostatic control escalates the growth of cells in the tissue which culminate in the advent of cancer. The precise nature of this feedback is not known [51]. In the literature, it is assumed that the mature cells secrete feedback signals which manipulate the stem cell’s division strength in order to maintain the balance between its self-renewal and differentiation rate [51]. The escalating growth of the cell population may approach the steady-state due to the effects induced by the feedback [52]. Various cell lineage frameworks have been introduced in the literature to investigate the dynamics of tissue regulation via feedback loop [51–53]. For a structural inspection of the feedback in a system consisting of two different cell lines with distinct properties, it is necessary to consider a model of each sub-population. The latter is based on the assumption that in every lineage, there exist a discrete chain of maturation stages, which is sequentially arranged [54, 55]. This will additionally help to understand the evolution of each sub-population individually, as well as the interaction with other sub-populations.

A variety of mathematical models have been formulated for explicitly modeling each of the cell subpopulations in a tissue using either discrete [51, 52, 56–62] or continuous [63, 64] cell maturity representations. The analysis in the present paper strongly relies on the latter two references. In [63], a continuous maturity structured model of granulopoiesis has been developed using partial differential equations (PDEs) for bone marrow granulocyte precursors and ordinary differential equation (ODE) for the blood granulocytes. The population of stem cells is assumed to be constant. The proliferation and mobilization rates along with apoptosis were modeled as functions of cell maturity. The scaled maturity

level lies between zero and one. While the authors focused on the identification of the fastest mutation sequences leading to emergence of the cancer, the feedback regulation from the mature cells was entirely neglected. Due to the lack of regulation, such structures produce unbounded growth of cell populations only, and in particular can not predict steady-state evolution. On the other hand, in [64], the authors have used a similar maturity based continuous model along with additional stem cell dynamics in the form of an ODE model. The model is rather general and supports hierarchical structures of cell lineage. As opposed to [64], we assign a separate sub-population to mature cells and introduce the feedback homeostatic regulation therefrom, which has been neglected in both, [64] and [63]. Our model provides a generic framework to investigate the dynamics involved in the evolution of both normal and mutated cell populations under continuous maturation process and feedback regulation. The main motivation behind this model is to develop an insight into the process, while taking into account most relevant features of this multi-step process.

In the present paper, we consider the dynamical interaction of three different sub-populations: (i) the stem, (ii) progenitor and (iii) differentiated cells, while highlighting the effects of feedback regulation from the mature cell population. More specifically, we analyze the coupling of two progenies consisting of healthy and mutated cells, while our main interest lies in investigating the feedback regulation from the separately modeled dynamics of mature cell population into the stem and maturity structured progenitor cell populations. In our framework, the stem and differentiated cells are modeled using ODEs, assuming minimum and maximum maturity, respectively, while PDEs with continuous maturity distributions are used to predict the evolution of the progenitor cells. In particular, the differentiation rate is not assumed to be constant as in [64], it is rather considered to be a function of maturity. Although there exist several models with feedback regulation in the literature, to our best knowledge, this is a first attempt to cover the feedback regulation in a more generic framework of stem cell lineage with continuous maturity distribution along with the mutated cell lineage resulting from the mutation acquisition in healthy cells. Finally, it is also interesting to highlight that our mathematical model can predict the stem cell hypothesis, claiming that even a small number of mutated stem cells can invade the overall cell population.

## 3.2 Mathematical modeling

The mathematical model of the stem cell line is rather complex as the cells vary continuously in course of maturation with time. In this work, instead of considering the evolution of net cell population, we split it into different sub-populations to account for their specific dynamics. The very initial cell state, i.e., stem cells, has the potential to stay undifferentiated and not to divide frequently under the conditions of homeostatic regulation [42, 65, 66]. As a middle stage in the cell evolution from stem cells all the way to full differentiation, we discriminate the progenitor cells, which undergo proliferation at relatively high rates and give rise to the population of fully mature cells. In the process of maturation, the proliferative potential and mortality rate of progenitor cells vary drastically until the terminal differentiation. To capture these dynamical effects, it is necessary to consider the maturity distribution of progenitor cells, which is mathematically described by means of PDEs. The last transition stage in the cell line from progenitor cells refers to fully mature cells that are specialized to perform their functions

in the respective tissue without further division, and undergo apoptosis after a short span of life.

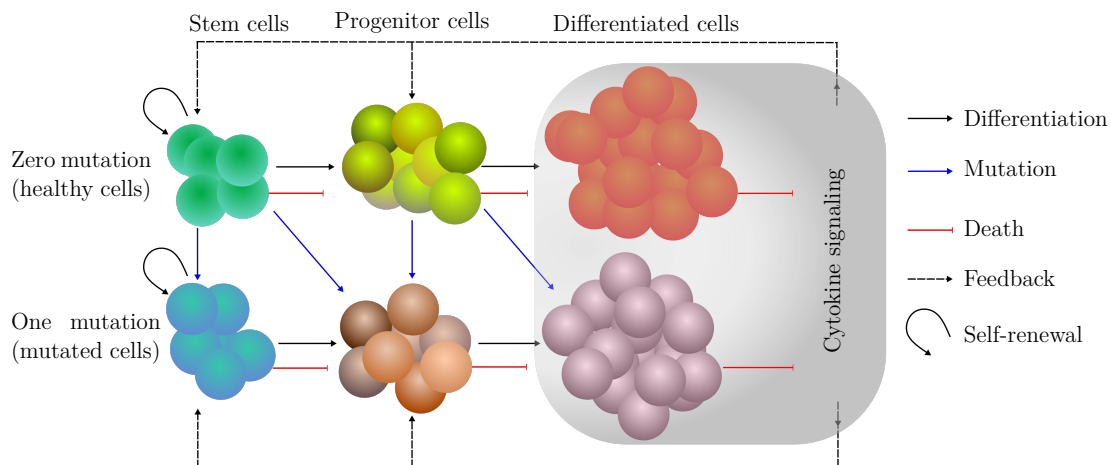


Figure 3.1: Schematics of the model. Co-evolution of normal and mutated cells in the presence of feedback regulation. The model captures the evolution of stem cell lineages with zero and one mutation. Stem cells can self-renew, differentiate and undergo apoptosis. The resulting progeny continues to proliferate until terminally differentiates into mature cells. Note that, during the division of a cell, there is a probability of getting a mutation. The feedback originates from the mature cells and thus regulates the self-renewal and proliferation rate of stem and progenitor cells, respectively.

The schematics of our model in Fig. 3.1 depicts the possible interactions between subsequent cell types ensuing from symmetric/asymmetric self-renewal, mutation, differentiation and apoptosis. The two parallel cell lines refer to the healthy and mutated cells (perhaps cancer, if cells acquire a lethal mutation) with zero and one mutation, respectively. Notice that, we consider only one mutation to keep the model simple for investigation. The model can be scaled up easily to the acquisition of multiple mutations. The potential for self-renewal is labeled as the property only for the stem cells in both healthy and mutated states, while the differentiation of cells is undertaken by both stem cell and progenitor cell populations. However, apoptosis can occur at all transition states with a certain rate. Since the number of cells increases with each step of maturation [67], the evolution scheme of all cell states as described above may lead to abnormal growth tending towards an unbounded number of cells. To avoid such unrestrained behavior of cell growth, one has to introduce feedback regulation. This modeling scheme enables investigation of the dynamical behavior (i.e., evolution and control) of the overall cell population with and without feedback homeostatic regulation. The discrete compartmental setting of the model facilitates the implementation and withdrawal of the feedback signals into and from the different transition states, respectively.

In the sequel, we explain the governing model equations for the cell lineage dynamics of healthy and mutated cells. Thereby,  $C_0(t)$  and  $C_1(t)$  refer to the number of stem cells with zero and one mutation, respectively. Similarly,  $P_0(x, t)$  and  $P_1(x, t)$  correspond to the progenitor cells with zero and one mutation, respectively, while  $M_0(t)$  and  $M_1(t)$  refer to the number of fully differentiated healthy and mutated cell populations. As the cells in the compartment of the stem and mature cells are assumed to behave alike, one can infer



a modeling scheme in the form of ODEs. On the other hand, the healthy and mutated progenitor cells require a property space, with cell maturity as a property variable. Since all the intermediate transitioning cell states between stem and fully differentiated cells are modeled as progenitor cells, the cells therein continuously differentiate to higher maturity states. Thus, the progenitor cells in both healthy and mutated states require partial differential equations.

### 3.2.1 Stem cell population

Stem cells are assumed to possess zero maturity level and they define the boundary conditions for the progenitor cell population at minimum maturity. The primary characteristics of stem cells responsible for their evolution are self-renewal and differentiation. The self-renewal can occur in two different ways, symmetrically or asymmetrically. Either way, there is a probability of acquiring a mutation during the division process, this yields an influx into the mutated stem cell population. On the other hand, differentiation of stem cells without mutation acquisition results in healthy progenitor cells, and those with a mutation influence to mutated progenitor cells. The stem cell population increases by symmetric self-renewal only, whereas the other mechanisms, e.g., mutation acquisition and differentiation, cause a decrement. The dynamical behavior of the stem cells is then described by the following mathematical expressions

$$\frac{d}{dt}C_0(t) = [(1 - 2m)\alpha_{S_0}(s) - m\alpha_{A_0}(s) - \alpha_{D_0}(s) - \delta_{C_0}]k_0C_0(t), \quad (3.1)$$

$$\frac{d}{dt}C_1(t) = [\alpha_{S_1}(s) - \alpha_{D_1}(s) - \delta_{C_1}]k_1C_1(t) + [2m\alpha_{S_0}(s) + m\alpha_{A_0}(s)]k_0C_0(t). \quad (3.2)$$

The initial conditions of healthy and mutated stems cells are  $C_0(0) = c_0$  and  $C_1(0) = c_1$ , respectively. In the above equations,  $k_0$  and  $k_1$  are the proliferation rates of stem cell with zero and one mutation, respectively. The first term on the right-hand side in Eq. (3.1) refers to symmetric self-renewal with probability  $\alpha_{S_0}$ , which results either in a decrement in the stem cell population by one, if the stem cells acquire a mutation with rate  $m$ , i.e.  $-\alpha_{S_0}(s)mk_0C_0$ , or increase the pool by one in case of no mutation, i.e.  $(1 - m)\alpha_{S_0}(s)k_0C_0$ . The second term represents an asymmetric self-renewal of stem cells with probability  $\alpha_{A_0}$  in which the stem cells decrease by one, while asymmetrically self-renewing and acquiring a mutation. The third term represents the differentiation of stem cells with probability  $\alpha_{D_0}$ , which is always followed by a decrement in stem cell population by one. The resulting progeny from the differentiation of cells will influx into the progenitor cell population. Note that the feedback signal  $s$  has been introduced into the stem cell probability of self-renewal (symmetric/asymmetric) and differentiation to maintain tissue homeostasis. This feedback signal is determined by the mature cell population, as shown below in Eq. (3.12). Finally, the fourth term describes the death of stem cells with a rate of  $\delta_{C_0}$ , which reduces the stem cell population by one.

In Eq. (3.2), the first three terms in a square bracket on the right-hand side describe the symmetric self-renewal, differentiation and death of mutated stem cells  $C_1$  with the probability of  $\alpha_{S_1}$ ,  $\alpha_{D_1}$ , and  $\delta_{C_1}$ , respectively. The last two terms (in the second square bracket) correspond to the influx from healthy stem cell population  $C_0$  as a consequence of mutations acquired during symmetric and asymmetric self-renewal, Eq. (3.1).

### 3.2.2 Progenitor cell population

The maturity distribution of progenitor cells represented by  $P_0(x, t)$  and  $P_1(x, t)$  constitutes of all maturity stages between stem and mature cell populations with  $x$  as maturity variable. Obviously,  $\int_{x_1}^{x_2} P_i(x, t) dx$ ,  $i = 0, 1$ , is equal to the number of cells between maturity  $x_1$  and  $x_2$ . The maturity is defined by a continuous variable which stands for the remaining proliferative potential of the cell and its capability to perform cellular functions. The governing equations and the initial conditions for normal and mutated progenitor cells read:

$$\partial_t P_0(x, t) + \partial_x [g_0(x) P_0(x, t)] = [(1 - 2m')\beta_0(x, s) - \mu_0(x)] P_0(x, t), \quad (3.3)$$

$$\partial_t P_1(x, t) + \partial_x [g_1(x) P_1(x, t)] = [\beta_1(x, s) - \mu_1(x)] P_1(x, t) + 2m'\beta_0(x, s) P_0(x, t), \quad (3.4)$$

with initial conditions  $P_0(x, 0) = p_0(x)$ ,  $P_1(x, 0) = p_1(x)$  and boundary conditions

$$g_0(0)P_0(0, t) = [2(1 - m)\alpha_{D_0}(s) + (1 - m)\alpha_{A_0}(s)]k_0C_0(t), \quad (3.5)$$

$$g_1(0)P_1(0, t) = [2\alpha_{D_1}(s) + \alpha_{A_1}(s)]k_1C_1(t) + [2m\alpha_{D_0}(s) + m\alpha_{A_0}(s)]k_0C_0(t), \quad (3.6)$$

for  $t > 0$ .

The functions  $g_0(x)$  and  $g_1(x)$  stand for the differentiation rate of progenitor cells with zero and one mutation, respectively. On the right-hand side of Eq. (3.3), the first and second terms in the square bracket represent the birth and loss of progenitor cells due to a mutation with the rate  $m'$ . The progenitor cells are assumed to acquire one mutation at a time. The proliferation rates  $\beta_0(x, s)$  and  $\beta_1(x, s)$  of healthy and mutated progenitor cells depend on the maturity level and tend to zero as the cells achieve the higher maturity level [68]. The third term describes the apoptosis of progenitor cells  $P_0(x, t)$  with maturity dependent death rate  $\mu_0(x)$  and generally it gets higher as the cell matures. On the right-hand side of Eq. (3.4), the first two terms in a square bracket represent the proliferation and death of the mutated progenitor cells with the rate  $\beta_1(x, s)$  and  $\mu_1(x)$ , respectively. The last term represents the influx from the healthy progenitor cells via mutation. Note that, the proliferation potential and rate of apoptosis for the progenitor cells is defined as function of maturity. The early progenitor cells have higher proliferation potential as compared to the late progenitor cells. On the other hand, as mentioned earlier the death rate of progenitor cells is meager for early progenitor cells and increases after differentiating to a certain maturity level [69, 70], see Fig. 3.2 (a). Although this does not hold for all cell types but true for of haemopoietic cells. There are many choices which can be suitable for proliferation and death rates of progenitor cells. Here, we borrow from [64] the following functional forms for  $\beta_i$  and  $\mu_i$ ,

$$\beta_i(x, s) = -\frac{1}{2}b_i(s) \tanh(\rho_{\beta_i}(x - \omega_{\beta_i})) + \frac{1}{2}b_i(s), \quad (3.7)$$

$$\mu_i(x) = \frac{1}{2}d_i \tanh(\rho_{\mu_i}(x - \omega_{\mu_i})) + \frac{1}{2}d_i, \quad (3.8)$$

where  $i = 0, 1$ , and  $b_i$  and  $d_i$  represent the maximum rate of proliferation and apoptosis, respectively. Furthermore,  $\omega_{\beta_i}$  represent the maturity level at which the progenitor cells proliferate at half of the maximum rate and  $\rho_{\beta_i}$  refers to the steepness of the proliferation switch. Similarly, the maturity at which progenitor cells die at half of the maximum rate is  $\omega_{\mu_i}$  and the steepness of the switch is  $\rho_{\mu_i}$ . Here, the feedback signal  $s$  is introduced in

the proliferation rate of progenitor cells. The behavior of the functional forms of  $\beta_i$  (for a fixed value of feedback, i.e.,  $s = 1$ ) and  $\mu_i$  are depicted in Fig. 3.2 (a).

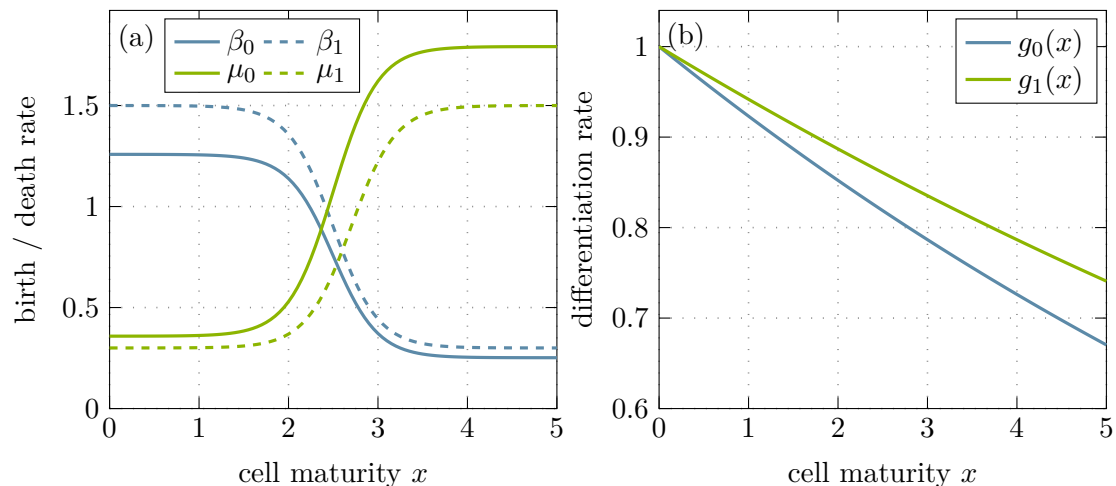


Figure 3.2: Birth, death and differentiation functions for progenitor cells. (a) Birth and death functions for both, healthy and mutated progenitor cell populations. The solid black and red lines represent the birth and death rate of healthy progenitor cell population, respectively, whereas the dotted black and red lines depict the birth and death rate of mutated progenitor cells. (b) Differentiation function of healthy and mutated progenitor cell populations represented by black and red line, respectively.

Next, we introduce the differentiation function  $g_i(x)$  which describes the rate at which the cells mature. It is a strictly positive and continuously differentiable function. In the pool of progenitor cells, continuous differentiation takes place alongside cellular division (maturation process). In maturity-time representation, mitosis takes place at same maturity levels [71]. From the modeling viewpoint, it means that in an infinitesimal time interval  $(t, t + dt)$ , a cell with maturity  $x$  either matures to level  $x + dx$  with probability  $g(x)dt$  or divides into two daughter cells with probability  $\beta(x, s)dt$ .

The progenitor cell population is heterogeneous with respect to cell maturation velocities [71] and typically, the maturity rate decreases along with an increasing maturity level. In order to define  $g(x)$ , we fix the maximum maturation velocity equal to one then we use a monotonically decreasing function of the following functional form  $g_i(x) = \exp(-h_i x)$ ,  $i = 0, 1$  in our model. Here, the differentiation functions  $g_i(x)$  are bounded between 0 and 1, thus the parameters  $h_i$  are to be selected in such a way that  $g_i(x)$  should not get near zero within the specified range of maturity variable, i.e.,  $x_{\min} \leq x \leq x_{\max}$ , see Fig. 3.2 (b). We assume lower differentiation potential for mutated cells because poor cellular differentiation is one of the important traits of cancer [72, 73].

During a division process, progenitor cells can also undergo a mutation. In this model, the healthy progenitor cells  $P_0(x, t)$  acquire a mutation with a mutation rate  $m'$  to either proliferate into a mutated progenitor cell population  $P_1(x, t)$  or to differentiate into a mutated differentiated cell population  $M_1(x, t)$ .

### 3.2.3 Mature cell population

The mature cell population is constituted by all the cells that attain the maximum maturity level, i.e.  $x^*$ . These cells do not possess any proliferating potential and only undergo apoptosis after a particular time. Therefore, mature cells cannot acquire any additional mutation and are specialized to perform their assigned functions in the tissue. The following equations describe the healthy and mutated density of mature cells represented by  $M_0(t)$  and  $M_1(t)$ , respectively:

$$\frac{dM_0}{dt} = g_0(x^*)P_0(x^*, t) - \delta_{M_0}M_0, \quad M_0(0) = m_0, \quad (3.9)$$

$$\frac{dM_1}{dt} = g_1(x^*)P_1(x^*, t) + 2m'\beta_0(x^*, s)P_0(x^*, t) - \delta_{M_1}M_1, \quad M_1(0) = m_1. \quad (3.10)$$

In Eq. (3.9), the first term on the right-hand side describes the inflow into healthy mature cells via terminal differentiation of progenitor cells with maturity rate  $g_0(x^*)$ , while the second term defines the apoptosis of the mature cells with a rate of  $\delta_{M_0}$ . The first term on the right-hand side of Eq. (3.10) is the influx from fully differentiated mutated progenitor cells, and the second term represents the influx from healthy progenitor cells due to an acquired mutation. The last term involving the rate  $\delta_{M_1}$  refers to the death of mutated mature cell population.

### 3.2.4 Feedback regulation

In the signaling mechanism among the cells, the growth response is modulated by cytokine proteins along with other proliferation regulating factors, [51]. Cytokines bind to their specific membrane-associated receptors which results in the activation of signal transduction pathways, [74]. Studies have shown that in order to maintain the number of cells in balance, these signals have to depend on the mature cell population [75, 76]. The dynamics of cytokine signaling molecules  $\zeta$  can be described by an ODE as:  $\dot{\zeta} = v - \delta_\zeta\zeta - \gamma\zeta M$ , where  $v$  is the maximum secretion rate of cytokine signals,  $\delta_\zeta$  represents the natural decrement of the signals  $\zeta$ , and  $\gamma$  is the rate by which the total mature cell population  $M = M_0 + M_1$  (consisting of both healthy and mutated mature cells) regulate the cytokine signals. Substituting  $s = (\delta_\zeta/v)\zeta$  and  $k_\zeta = \gamma/\delta_\zeta$ , the above equation turns into

$$\dot{s} = \delta_\zeta(1 - s - k_\zeta s M). \quad (3.11)$$

Since the cytokine signals are typically secreted at a higher rate than that of proliferation and differentiation of the cells, these drift quickly to a steady state. Hence, using quasi-steady state approximation, the equilibrium state for the feedback signal intensity

$$s = \frac{1}{1 + k_\zeta M} \quad (3.12)$$

follows from Eq. (3.11). This shows that in the absence of mature cell population, the signal intensity is maximal, i.e.,  $s = 1$ , and it drops to a minimum with a significant increase in the mature cell population. The probabilities  $\alpha_{S_i}(s)$ ,  $\alpha_{A_i}(s)$  and  $\alpha_{D_i}(s)$  in Eq. (3.1)–(3.2) and the maximum birth rates  $b_i(s)$  in the birth functions  $\beta_i(x, s)$  of progenitor cells in Eq. (3.3)–(3.4) are assumed to change linearly in  $s$ , cf. Eq. (3.7), given that

slopes are positive which leads to the following linear forms  $\alpha_{S_i}(s) = \bar{\alpha}_{S_i}s$ ,  $\alpha_{A_i}(s) = \bar{\alpha}_{A_i}s$ ,  $\alpha_{D_i}(s) = \bar{\alpha}_{D_i}s$  and  $b_i(s) = \bar{b}_i s$ , where  $\bar{\alpha}_{S_i}$ ,  $\bar{\alpha}_{A_i}$ ,  $\bar{\alpha}_{D_i}$  and  $\bar{b}_i$  represent maximum symmetric self-renewal, maximum asymmetric self-renewal, maximum differentiation of stem cell and maximum birth rate of progenitor cells, respectively.

### 3.3 Steady-state solutions

In this section, we derive the steady-state solutions of our governing equations (3.1)–(3.10). For the sake of convenience, we hereby simplify the notation, reading

$$\frac{d}{dt}C_0(t) = \gamma_{00}(s)C_0(t), \quad C_0(0) = c_0 \quad (3.13)$$

$$\frac{d}{dt}C_1(t) = \gamma_{10}(s)C_1(t) + \gamma_{11}(s)C_0(t), \quad C_1(0) = c_1, \quad (3.14)$$

for the populations of healthy and mutated cells, respectively, with  $\gamma_{00}$ ,  $\gamma_{10}$  and  $\gamma_{11}$  defined as

$$\gamma_{00}(s) := [(1 - 2m)\alpha_{S_0}(s) - m\alpha_{A_0}(s) - \alpha_{D_0}(s) - \delta_{C_0}]k_0 \quad (3.15)$$

$$\gamma_{10}(s) := [\alpha_{S_1}(s) - \alpha_{D_1}(s) - \delta_{C_1}]k_1, \quad \gamma_{11}(s) = [2m\alpha_{S_0}(s) + m\alpha_{A_0}(s)]k_0. \quad (3.16)$$

In a similar manner, the PDEs that describe the progenitor cells read:

$$\partial_t P_0(x, t) + \partial_x [g_0(x)P_0(x, t)] = \gamma_0(x, s)P_0(x, t), \quad (3.17)$$

$$\partial_t P_1(x, t) + \partial_x [g_1(x)P_1(x, t)] = \gamma_1(x, s)P_1(x, t) + 2m'\beta_0(x, s)P_0(x, t), \quad (3.18)$$

where  $\gamma_0(x, s)$  and  $\gamma_1(x, s)$  are given by

$$\gamma_0(x, s) := (1 - 2m')\beta_0(x, s) - \mu_0(x), \quad \gamma_1(x, s) := \beta_1(x, s) - \mu_1(x). \quad (3.19)$$

Finally, the equations of mature cell population stay same as before in Fig.s. (3.9) and (3.10). In the sequel, we assume the following conditions:

$$\left. \begin{aligned} c_0, c_1, m_0, m_1 &\in \mathbb{R}_{\geq 0}, \quad p_0, p_1 : [0, x^*] \rightarrow \mathbb{R}_{\geq 0} \\ g_{0x}, g_{1x} &\in \mathbb{L}^\infty([0, x^*]) \\ \beta_0(x, s), \beta_1(x, s) &\in \mathbb{L}^\infty([0, x^*] \times \mathbb{R}), \quad \mu_0(x), \mu_1(x) \in \mathbb{L}^\infty([0, x^*]) \\ \gamma_{00}(s) &:= \gamma_{00}(M) \text{ is a decreasing function, i.e., } \gamma_{00}(+\infty) < 0. \end{aligned} \right\} \quad (3.20)$$

To address the question of the existence of any steady-state under a homeostatic regulation, we need to solve the following system of equations, for the steady-state unknowns  $\bar{C}_0$ ,  $\bar{C}_1$ ,  $\bar{P}_0$ ,  $\bar{P}_1$ ,  $\bar{M}_0$  and  $\bar{M}_1$ :

$$\gamma_{00}(\bar{M})\bar{C}_0 = 0 \quad (3.21)$$

$$\gamma_{10}(\bar{M})\bar{C}_1 + \gamma_{11}(\bar{M})\bar{C}_0 = 0 \quad (3.22)$$

$$\frac{d}{dx}[g_0(x)\bar{P}_0(x)] = \bar{\gamma}_0(x)\bar{P}_0(x) \quad (3.23)$$

$$\frac{d}{dx}[g_1(x)\bar{P}_1(x)] = \bar{\gamma}_1(x)\bar{P}_1(x) + 2m'\bar{\beta}_0(x^*)\bar{P}_0(x) \quad (3.24)$$

$$g_0(x^*)\bar{P}_0(x^*) - \delta_{M_0}\bar{M}_0 = 0 \quad (3.25)$$

$$g_1(x^*)\bar{P}_1(x^*) + 2m'\bar{\beta}_0(x^*)\bar{P}_0(x^*) - \delta_{M_1}\bar{M}_1 = 0, \quad (3.26)$$

with  $\bar{\gamma}_0(x) := \gamma_0(x, \bar{M})$ ,  $\bar{\gamma}_1(x) := \gamma_1(x, \bar{M})$  and  $\bar{\beta}_0(x^*) = \beta_0(x^*, \bar{M})$  and the boundary conditions given as

$$g_0(0)\bar{P}_0(0) = (1 - m)[2\alpha_{D_0}(\bar{M}) + \alpha_{A_0}(\bar{M})]k_0\bar{C}_0 \quad (3.27)$$

$$g_1(0)\bar{P}_1(0) = [2\alpha_{D_1}(\bar{M}) + \alpha_{A_1}(\bar{M})]k_1\bar{C}_1 + m[2\alpha_{D_0}(\bar{M}) + \alpha_{A_0}(\bar{M})]k_0\bar{C}_0. \quad (3.28)$$

The trivial steady-state, i.e.,  $\bar{C}_0 = 0$ ,  $\bar{C}_1 = 0$ ,  $\bar{P}_0 = 0$ ,  $\bar{P}_1 = 0$ ,  $\bar{M}_0 = 0$ ,  $\bar{M}_1 = 0$  is evident from Eqs. (3.21)–(3.26). However, the system also admits a non-trivial steady-state under the assumption  $\gamma_{00}(0) > 0$ . In this case, from Eq. (3.21) we get immediately

$$\gamma_{00}(\bar{M}) = 0. \quad (3.29)$$

Now, using Eq. (3.15) in the above relation, we obtain:

$$[(1 - 2m)\alpha_{S_0}(\bar{M}) - m\alpha_{A_0}(\bar{M}) - \alpha_{D_0}(\bar{M}) - \delta_{C_0}]k_0 = 0, \quad (3.30)$$

where the probabilities  $\alpha_{S_0}(\bar{M})$ ,  $\alpha_{A_0}(\bar{M})$ , and  $\alpha_{D_0}(\bar{M})$  are defined as

$$\alpha_{S_0}(\bar{M}) = \frac{\alpha_{S_0}}{1 + k_\zeta \bar{M}}, \quad \alpha_{A_0}(\bar{M}) = \frac{\alpha_{A_0}}{1 + k_\zeta \bar{M}}, \quad \alpha_{D_0}(\bar{M}) = \frac{\alpha_{D_0}}{1 + k_\zeta \bar{M}}, \quad (3.31)$$

and  $\alpha_{S_0}, \alpha_{A_0}, \alpha_{D_0} \in \mathbb{R}_{>0}$ . By employing the above relations in Eq. (3.30), we derive the relation for  $\bar{M}$ , which is:

$$\bar{M} = \frac{1}{k_\zeta \delta_{C_0}} [(1 - 2m)\alpha_{S_0} - m\alpha_{A_0} - \alpha_{D_0} - \delta_{C_0}]. \quad (3.32)$$

Next, to solve the ODEs (3.23) and (3.24) for progenitor cells, we compute the boundary conditions at the final maturity, i.e.,  $x = x^*$  from the Fig.s. (3.25) and (3.26)

$$\bar{P}_0(x^*) = \frac{\delta_{M_0} \bar{M}_0}{g_0(x^*)}, \quad \bar{P}_1(x^*) = -\frac{2m' \bar{\beta}_0(x^*) \delta_{M_0} \bar{M}_0}{g_0(x^*) g_1(x^*)} + \frac{\delta_{M_1} \bar{M}_1}{g_1(x^*)}. \quad (3.33)$$

The steady-state boundary values result by solving the ODEs (3.23) and (3.24) for the healthy and mutated progenitor cells  $\bar{P}_0(x)$  and  $\bar{P}_1(x)$ :

$$\bar{P}_0(x) = \frac{\delta_{M_0} \bar{M}_0}{g_0(x)} e^{f_0(x)}, \quad (3.34)$$

$$\bar{P}_1(x) = \frac{e^{f_1(x)}}{g_1(x)} \left[ 2m' \int_x^{x^*} e^{-f_1(x)} \bar{\beta}_0(x) \bar{P}_0(x) dx + g_1(x^*) \bar{P}_1(x^*) \right], \quad (3.35)$$

with

$$f_0(x) := \int_x^{x^*} \frac{\bar{\gamma}_0(\xi)}{g_0(\xi)} d\xi, \quad f_1(x) := \int_x^{x^*} \frac{\bar{\gamma}_1(\xi)}{g_1(\xi)} d\xi. \quad (3.36)$$

Further, we use the boundary conditions given in Fig.s. (3.27) and (3.28) to compute the steady-state values of healthy and mutated stem cells, respectively

$$\bar{C}_0 = \frac{\delta_{M_0} \bar{M}_0 (1 + k_\zeta \bar{M})}{k_0 (1 - m) [2\alpha_{D_0} + \alpha_{A_0}]} e^{f_0(0)} \quad (3.37)$$

$$\bar{C}_1 = \frac{1 + k_\zeta \bar{M}}{k_1 [2\alpha_{D_1} + \alpha_{A_1}]} \left[ \lambda_1 e^{f_1(0)} - \frac{m \delta_{M_0} \bar{M}_0}{1 - m} e^{f_0(0)} \right], \quad (3.38)$$

where  $\lambda_1 := 2m' \bar{\beta}_0(0) \bar{P}_0(0) \int_0^{x^*} e^{f_1(0)} dx + g_1(x^*) \bar{P}_1(x^*)$ . Eventually, we derive the steady-state relation for healthy mature cells  $\bar{M}_0$  from Eq. (3.22):

$$\bar{M}_0 = \frac{e^{f_1(0)} (1 - m) (2\alpha_{D_0} + \alpha_{A_0}) \lambda_1 \lambda_2}{m \delta_{M_0} e^{f_0(0)} [(2\alpha_{S_0} + \alpha_{A_0}) (2\alpha_{D_1} + \alpha_{A_1}) + (2\alpha_{D_0} + \alpha_{A_0}) \lambda_2]}, \quad (3.39)$$

where  $\lambda_2 = \alpha_{S_1} - \alpha_{D_1} - \delta_{C_1} (1 + k_\zeta \bar{M})$ . Note that, the steady-state relation for healthy mature cells  $\bar{M}_1$  can be easily determined utilizing Eqs. (3.32) and (3.39).

From the above derivation of steady-states, we can summarise the following observations. The steady-states of our coupled nonlinear model cannot be defined explicitly, but the sum of the steady-states of healthy and mutated mature cells, used to compute feedback can be represented by an explicit relation. Moreover, the steady-states of stem and progenitor cells highly depend on the steady-state of mature cells due to the feedback inclusion.

## 3.4 Numerical solution and simulation results

### 3.4.1 Finite volume method

In this section, the numerical method used to solve the governing nonlinear Eqs. (3.1)–(3.10) is presented. We apply already developed finite volume method (FVM) with central upwind scheme for the flux approximation on hyperbolic partial differential equations in MATLAB. The domain of the problem has been discretized in both, space and time. The timeline is discretized into  $N_t$  steps with equidistant interval  $\Delta t = t^{k+1} - t^k$ . The spatial stepsize is given by  $\Delta x = x^*/N_x$ , where  $N_x$  is the maximum number of spatial nodes given by  $x_j = j\Delta x$ ,  $0 \leq j \leq N_x$ . The discretized progenitor cell density associated with the  $j^{\text{th}}$  spatial interval at time  $k$  reads

$$P_{i,j}^k = \frac{1}{\Delta x} \int_{x_{j-\frac{1}{2}}}^{x_{j+\frac{1}{2}}} P_i(y, t^k) dy, \quad \text{where } i = 0, 1.$$

The necessary Courant-Friedrichs-Lewy (CFL) condition for convergence of the solution requires  $\max_{x \in \{x_j\}} g_i(x) \frac{\Delta t}{\Delta x} \leq 1$ . The PDEs (3.3)–(3.4) are hyperbolic in nature and with the discretization defined above, we can implement the following algorithm to solve the coupled differential equations.

First, the initial conditions are given as

$$C_i^0 = c_i, \quad P_{i,j}^0 = \frac{1}{\Delta x} \int_{x_{j-\frac{1}{2}}}^{x_{j+\frac{1}{2}}} p_i(y) dy, \quad M_i^0 = m_i, \quad \text{for } i = 0, 1.$$

For each time step  $k$ , the feedback from mature cells is calculated as

$$s^k = \frac{1}{1 + k_\zeta (M_0^k + M_1^k)}.$$

Then, the stem cell population at time  $t^{k+1}$  can be discretized as follows

$$C_i^{k+1} \approx C_i^k + \Delta t \left( \frac{d}{dt} C_i^k \right), \quad i = 0, 1, \quad (3.40)$$

and the following relation result for healthy and mutated stem cells, respectively

$$\begin{aligned} C_0^{k+1} &= \left( 1 + \Delta t \left( (1 - 2m)\alpha_{S_0}(s^k) - m\alpha_{A_0}(s^k) - \alpha_{D_0}(s^k) - \delta_{S_0} \right) k_0 \right) C_0^k \\ C_1^{k+1} &= \left( 1 + \Delta t \left( \alpha_{S_1}(s^k) - \alpha_{D_1}(s^k) - \delta_{S_1} \right) k_1 \right) C_1^k \\ &\quad + \Delta t m \left( 2\alpha_{S_0}(s^k) - \alpha_{A_0}(s^k) \right) k_0 C_0^k. \end{aligned}$$

The boundary conditions for progenitor cells at  $j = 0$  are given as

$$\begin{aligned} P_{0,0}^{k+1} &= (1 - m)(2\alpha_{D_0}(s^k) + \alpha_{A_0}(s^k))k_0 C_0^k \\ P_{1,0}^{k+1} &= (2\alpha_{D_1}(s^k) + \alpha_{A_1}(s^k))k_1 C_1^k + (2\alpha_{D_0}(s^k) + \alpha_{A_0}(s^k))mk_0 C_0^k. \end{aligned}$$

The discretization of the PDEs concerning the density of the progenitor cell populations is given in accordance with the central upwinding scheme as follows

$$\begin{aligned} P_{0,j}^{k+1} &= P_{0,j}^k - \frac{\Delta t}{\Delta x} \left( g_0(x_j)P_{0,j}^k - g_0(x_{j-1})P_{0,j-1}^k \right) \\ &\quad + \Delta t \left( (1 - 2m')\beta_0(x_j, s^k) - \mu_0(x_j) \right) P_{0,j}^k \\ P_{1,j}^{k+1} &= P_{1,j}^k - \frac{\Delta t}{\Delta x} \left( g_1(x_j)P_{1,j}^k - g_1(x_{j-1})P_{1,j-1}^k \right) \\ &\quad + \Delta t \left( (\beta_1(x_j, s^k) - \mu_1(x_j)) P_{1,j}^k + 2m'\beta_0(x_j, s^k)P_{0,j}^k \right). \end{aligned}$$

Finally, the discretized ODEs for mature cells are given as following

$$\begin{aligned} M_0^{k+1} &= M_0^k + \Delta t \left( g_0(x_{N_x})P_{0,N_x}^k - \delta_{M_0}M_0^k \right) \\ M_1^{k+1} &= M_1^k + \Delta t \left( g_1(x_{N_x})P_{1,N_x}^k + 2m'\beta_0(x_{N_x}, s^k)P_{0,N_x}^k - \delta_{M_1}M_1^k \right), \end{aligned}$$

which also involves the influx from progenitor cells  $P_0^k$  and  $P_1^k$  at the maximum maturity  $x = x^*$ . The mature cell populations  $M_0$  and  $M_1$  will manipulate the feedback in the next time step and consequently, feedback will alter the dynamics of stem, progenitor or both cell populations to stabilize the exponential growth.

### 3.4.2 Simulation results

In this section, we present the model simulations for illustration purposes. The initial states and the used parameters are given in Table 3.1. The forthcoming results are computed by the numerical scheme given at the end of this section. The maturity variable  $x$  belongs to  $[0, 5]$  with the value of maximum maturity  $x^*$  set to be 5. The step sizes for time  $\Delta t$  and maturity  $\Delta x$  used in simulations are 0.01 and 0.05, respectively. The behavioral patterns of the model are investigated hereby with the objective to observe the evolution of all six sub-populations with the feedback regulation, which is determined from the total number of both healthy and mutated mature cells. In general, after acquiring a mutation, the mutated cell gains fitness and thus differ considerably from healthy cells, [57]. Therefore, the probability of mutated stem cells to self-renew is greater



### 3.4 Numerical solution and simulation results

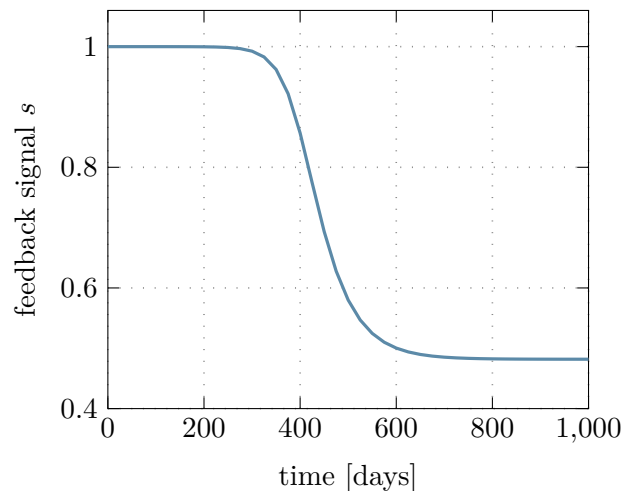


Figure 3.3: The cytokine feedback signal reduces over time with the increasing number of mature healthy and mutated cells.

Param.	Description	Parameter values		Units
		$i = 0$	$i = 1$	
$c_i$	Initial stem cell density	18000 [59, 77]	0	$mL^{-1}$
$m_i$	Initial mature cell density	0	0	$mL^{-1}$
$\bar{\alpha}_{S_i}$	Maximum symmetric self-renew probability	0.176 [78]	0.25	-
$\bar{\alpha}_{A_i}$	Maximum asymmetric self-renew probability	0.60 [78]	0.60	-
$\bar{\alpha}_{D_i}$	Maximum differentiation probability	0.15 [78]	0.15	-
$\delta_{C_i}$	Stem cells' death rate	0.0125 [59]	0.053[70]	$day^{-1}$
$\delta_{M_i}$	Mature cells' death rate	1.8 [70]	1.9[70]	$day^{-1}$
$m$	Mutation rate of stem cells	$10^{-4}$ [79, 80]	-	-
$m'$	Mutation rate of progenitor cells	$10^{-6}$ [81]	-	-
$k_i$	Stem cell proliferation rate	0.47[65]	0.60	$day^{-1}$
$\omega_{\beta_i}$	Maturity at proliferation switch	2.50	2.50	days
$\rho_{\beta_i}$	Steepness of progenitor cells proliferation switch	2	2	-
$\omega_{\mu_i}$	Maturity at death switch	2.50	2.70	days
$\rho_{\mu_i}$	Steepness of progenitor cells death switch	2	2	-
$b_i$	Max. progenitor cells proliferation rate	1.51 [82]	1.8[82]	$day^{-1}$
$d_i$	Max. progenitor cells death rate	2.15	1.8	$day^{-1}$
$k_{\zeta}$	Ratio of $\gamma$ to $\delta_S$	$1.85 \times 10^{-9}$	$1.85 \times 10^{-9}$	-

Table 3.1: Initial values and parameters of the model for both, healthy and mutated cell lineages, where  $i = 0$  stands for the parameters of healthy cell line with zero mutation and  $i = 1$  represents the parameters of mutated cell lineage with one mutation.

in simulations relative to the healthy ones, while the death rate is reduced, see Table

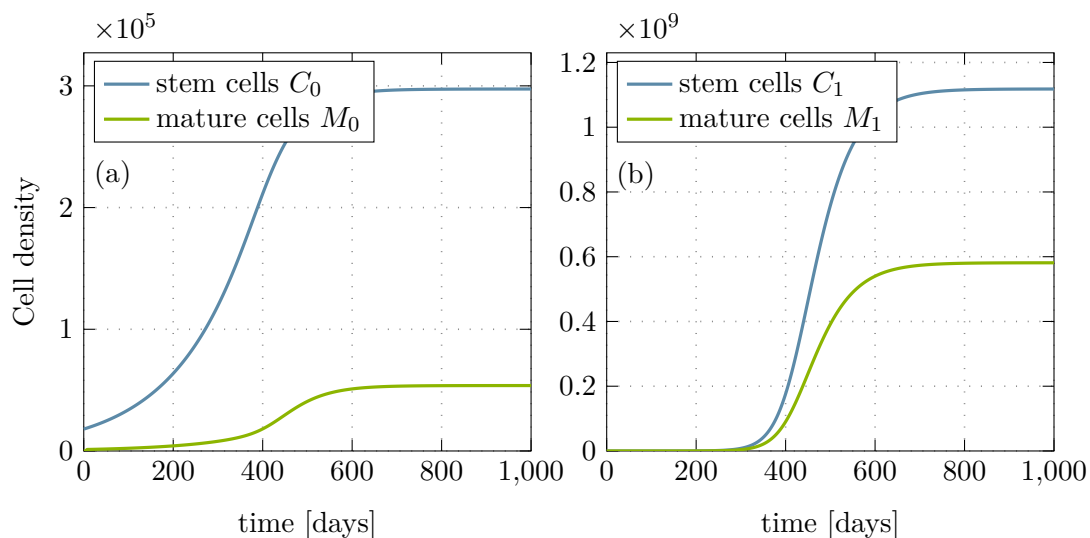


Figure 3.4: Healthy and mutated stem and mature cells are shown. (a) Healthy stem cells with initial value of  $18000 \text{ mL}^{-1}$  grow exponentially and converge to a steady-state. Healthy mature cells depict a similar behavior with initial condition equal to zero. (b) Mutated stem cells with initial condition equal to zero, increase exponentially and attain a steady-state at relatively large value while mutated mature cells depict a similar behavior with initial condition equal to zero.

3.1. The feedback influences the the probabilities of symmetric/asymmetric self-renewal and differentiation in stem cells whereas in progenitor cells, the feedback is influencing the maximum proliferation rate  $b_i$  in the birth function  $\beta(x, s)$ . The simulations are initialized with healthy stem cells as  $c_0 := C_0(0) = 18000 \text{ mL}^{-1}$ , while all the rest of the sub-populations have been set to zero. Initially, the feedback signal is maximum, i.e., equal to one, because no differentiated cells exist, while over the course of time, the increase in the healthy and mutated mature cell population leads to a reduction of the feedback signal, as shown in Fig. 3.3. The parameters used in Fig. 3.3-3.4 are given in Table 3.1. The exponential growth in healthy stem cell population results in the increase of all healthy and mutated cell types Fig. 3.4. A steady-state is achieved in healthy stem cells and consequently in all other sub-populations, see Fig. 3.4 and 3.4. The achieved steady-states coincide with the analytically calculated steady states of all cell states in Eqs. (3.35-3.39). The feedback signal plays the central role in the stabilization of the model states. In the absence of this feedback signal, the exponential growth continues and thus results in an unnatural number of cells.

Fig. 3.6 depicts another behavior of the model in which all the parameters used are same as in Table 3.1 but the symmetric self-renewal rate of stem cells  $\bar{\alpha}_{S_0} = 0.175$  and their death rate  $\delta_{C_0} = 0.016 \text{ day}^{-1}$ . Contrary to Fig. 3.4, the healthy stem cells  $C_0$  in Fig. 3.6(a) start decreasing after a gradual increase for a while and eventually land to a very low number. Indeed, similar behavior has been shown by the healthy mature cells in Fig. 3.6(a), whereas the mutated stem and mature cells still attain their respective steady-states, as shown in Fig. 3.6(b).

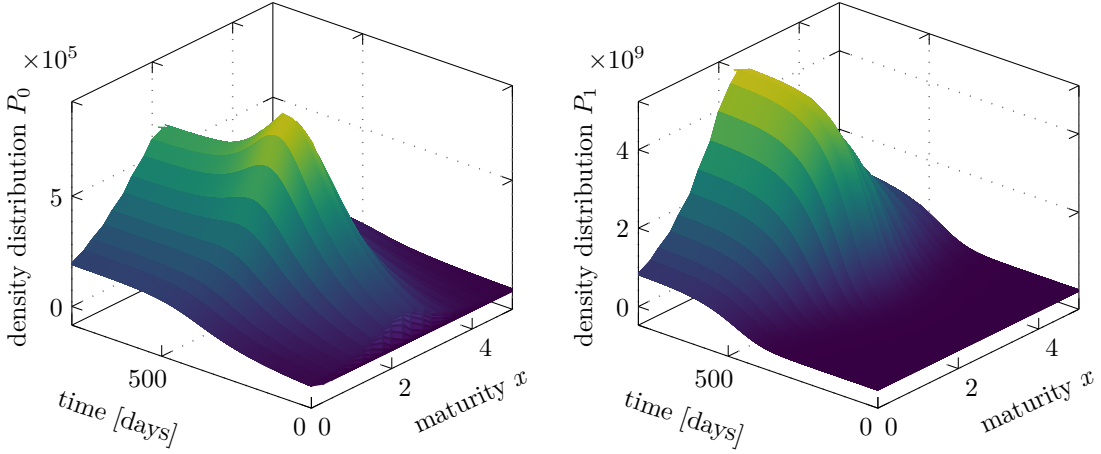


Figure 3.5: Density distribution of progenitor cells. Left: Distribution of healthy progenitor cells  $P_0(t, x)$ . Right: Distribution of mutated progenitor cells  $P_1(t, x)$ . It continues to grow a higher number and approach a steady-state.

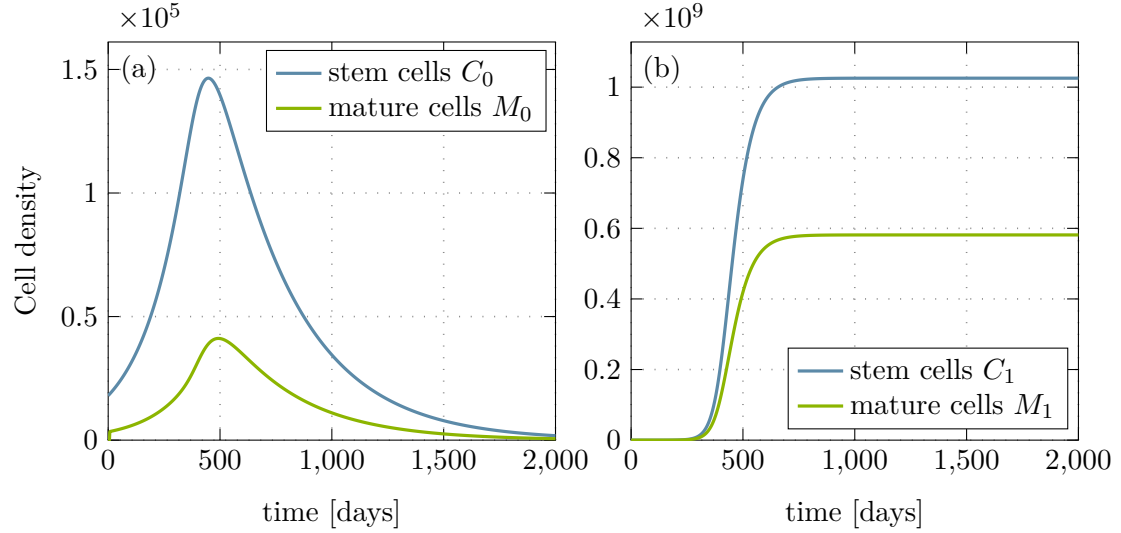


Figure 3.6: Cell density of healthy and mutated stem and mature cells are shown. (a) Healthy stem cells with initial value of  $18000 \text{ mL}^{-1}$  grow exponentially and start decreasing in number and mutated stem cells with initial condition equal to zero, increase exponentially until attain a steady-state at relatively large value. (b) Healthy mature cells with initial condition equal to zero, depict the same behavior as healthy stem cells while mutated mature cells depict a similar behavior as mutated stem cells with initial condition equal to zero.

In accordance with the dynamics of healthy and mutated stem cell populations described in Eq. (3.1) and (3.2), respectively, the probabilities of symmetric/asymmetric self-renewal and differentiation rates are influenced by the feedback signal. The rapidly increasing healthy and mutated mature cell number in Fig. 3.6(c and d) tends to abate the value of cytokine feedback signals pursuant to the relation in Eq. (3.12). It can be easily observed from Eq. (3.1) that, as the feedback signal drops, the probabilities

of symmetric/asymmetric stem cell self-renewal  $\alpha_{S_0}/\alpha_{A_0}$  and differentiation  $\alpha_{D_0}$  also decrease. Note that these probabilities vary linearly with feedback signal  $s$  having a positive slope. As a consequence, with the temporal evolution of healthy stem cells, death rate dominates over self-renewal, and healthy stem cells start declining in number, cf. Fig. (3.1). In Eq. (3.2) for mutated stem cells, the decline in feedback signal reduces the probability of self-renewal and differentiation in mutated stem cells. Nevertheless, the mutated cells still manage to grow in a higher number due to the increased fitness as stated before and thus approaching a steady-state. This scenario, in which the healthy cell line deteriorates and only mutated cells prevail over time, could also be called ‘pure cancerous steady-state’.

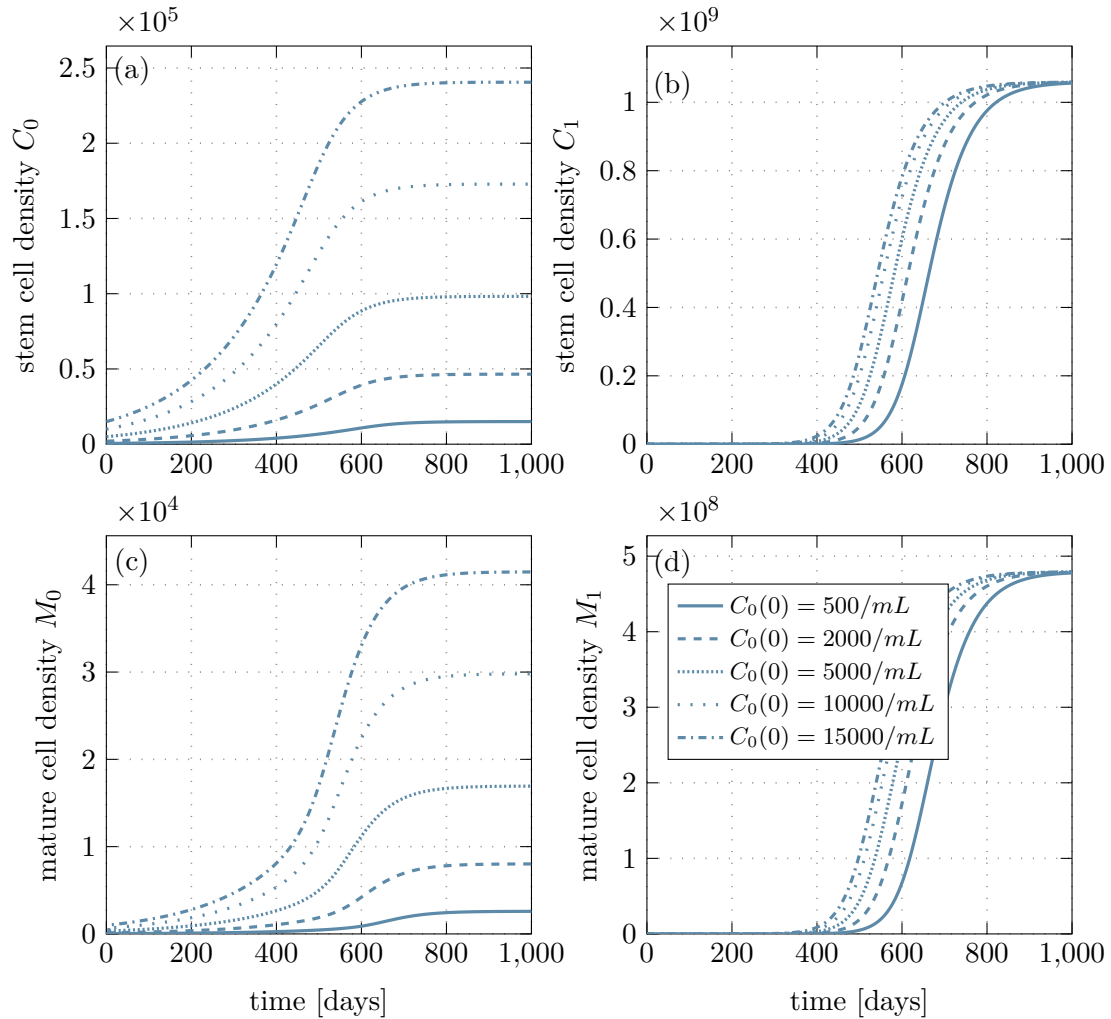


Figure 3.7: Number of healthy and mutated stem and mature cells with different initial conditions of healthy stem cells. The rest of the states have initial conditions equal to zero. (a) Healthy stem cells achieve a respective steady state for a corresponding initial value. (b) Mutated stem cells with initial condition equal to zero, attain a same steady-state at all initial values of  $C_0(t)$ . (c) Healthy mature cells with initial condition equal to zero, depict the same behavior as healthy stem cells. (d) Mutated mature cells depict a similar behavior as mutated stem cells with initial condition equal to zero.

The establishment of the steady-state via feedback regulation has already been suggested in the literature [51], where the authors have considered ODE settings for the discrete cell populations of the stem cells all the way to the differentiated cells. Moreover, it is mentioned that the whole dynamics of stem cell lineages can be controlled by a single negative feedback loop, i.e., cytokine signaling.

It is important to mention that in our model feedback is only effecting the birth rates, but the results can also be achieved by influencing the death rates via feedback signal [83]. Moreover, in our model, the division rates of stem cell populations  $\{k_i, i = 0, 1\}$ , are not depending on feedback signal because it has been validated in [84] and [51] that an efficient control mechanism underlies the modulation of self-renewal and differentiation rates as compared to the maintenance of proliferation rates in stem cells. It is evident from the simulation results as well that even without feedback regulation in division rates, the mutated stem cell population does achieve a steady-state.

#### 3.4.2.1 Case study: Evolution for different initial conditions

Fig. 3.7 demonstrates the behavior of the model concerning different initial values of the stem cell population. All other cell population states (mutated stem cells, healthy and mutated progenitor cells, and mature cells) are initialized with zero number of cells. The parameter values used are similar as in Table 3.1. It can be seen that with any number of initial healthy stem cells  $C_0(0)$ , the steady states are achieved at the same time in healthy stem  $C_0(t)$  and mature  $M_0(t)$  cells, Fig. 3.7 (a) and (c); however, the magnitudes of the steady states are different. On the other hand, in mutated cell populations, the effect of different initial conditions is reflected only in the rates at which the steady states are achieved, while the magnitude of steady-state is the same for all initial values, see Fig. 3.7 (b) and (d). It implies that no matter how many healthy stem cells are there at any particular age, the subsequent mutations can lead to a substantial amount of mutated cell populations.

#### 3.4.2.2 Case study: Feedback signal as Hill function

Here we want to analyse the model behavior when we define the relation between feedback signal  $s$  and total number of mature cells  $M$  using Hill function as compared to the behavior produced by the relation in Eq. (3.12). Since increase in the concentration of mature cells represses the feedback signal, we define their relation using the Hill function as follows:

$$s = \frac{1}{1 + \left(\frac{M}{K_M}\right)^n}, \quad (3.41)$$

where  $K_M$  is the mature cell concentration ( $2.6 \times 10^6 mL^{-1}$ ) at which feedback signal is half a maximum and  $n$  is the Hill coefficient. Note that the Eq. (3.41) coincides with Eq. (3.12) when  $n = 1$  and  $K_M = 1/k_\zeta$ . The simulations have been performed using Hill feedback function in Eq. (3.41) and it turns out that the model depicts the similar behavior to the previous case, compare Fig. 3.8 with 3.4 and 3.6. In Fig. 3.8 (a)-(d), the model parameters used are similar as in Table 3.1, whereas in Fig. 3.8 (e)-(h) the parameter values which have been varied are symmetric and asymmetric self renewal rate of stem cells as  $\bar{\alpha}_{S0} = 0.175$  and  $\bar{\alpha}_{A0} = 0.6650$ , respectively.

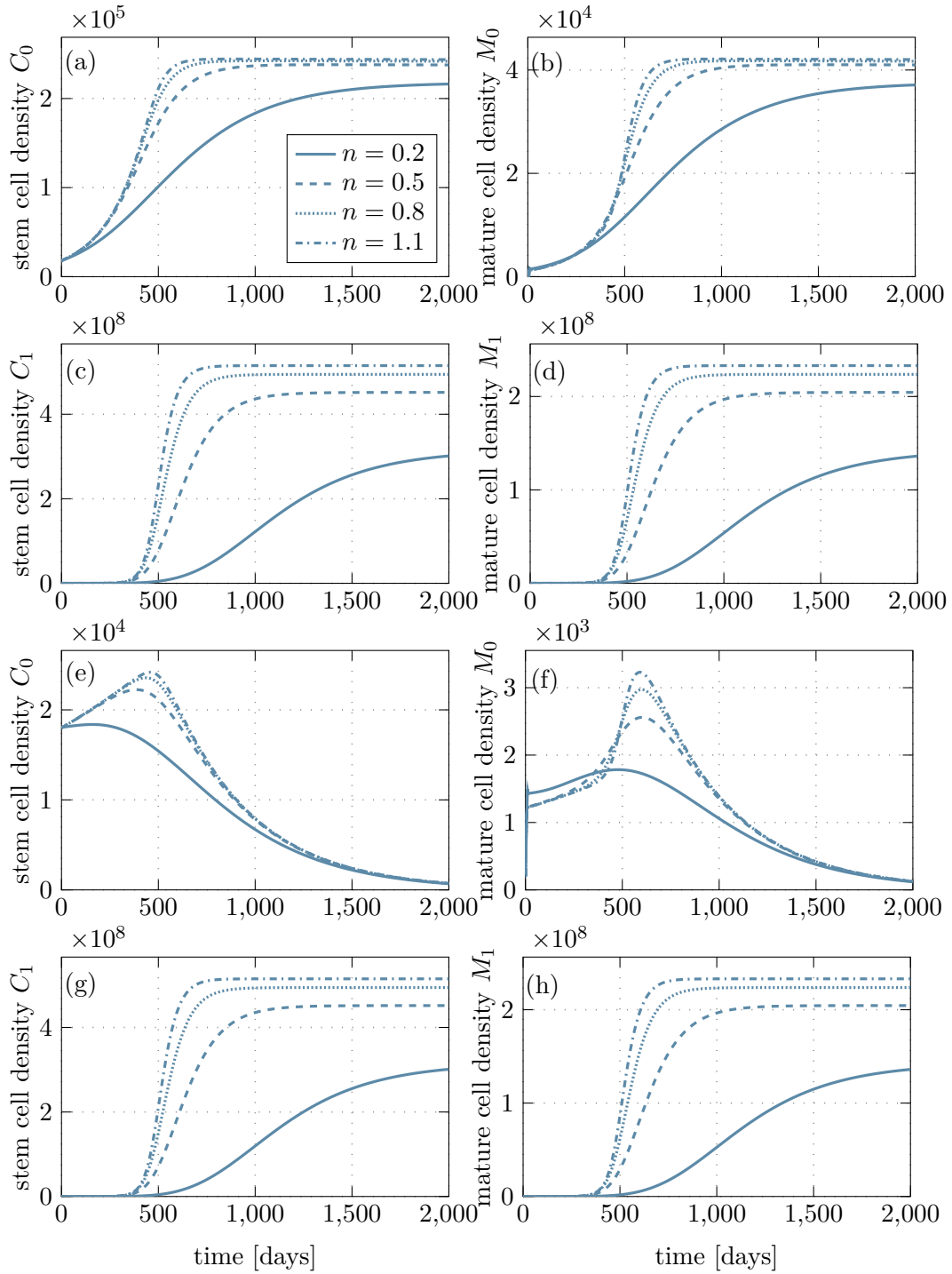


Figure 3.8: Model behavior by using Hill feedback function for various Hill coefficient values. All cell states achieve non-trivial steady-states (a)-(d). Pure cancerous steady-states where healthy cells decline with time (e)-(h) .

It is to be noted that the dynamics of the stem and progenitor cells are maintained in homeostasis by inducing feedback only in the self-renewal rates. One can also achieve homeostasis by inducing the feedback in the death rates [83]. However, death rates are

kept constant in the current paper; see Table 3.1. Moreover, in our model, the division rates of stem cell populations  $\{k_i, i = 0, 1\}$ , are not depending on feedback signal because it has been validated in [84] and [51] that an efficient control mechanism underlies the modulation of self-renewal and differentiation rates as compared to the maintenance of proliferation rates in stem cells. It is evident from the simulation results as well that even without feedback regulation in division rates, the mutated stem cell population does achieve a steady-state.

### 3.5 Model validation

In this section, we validate the behavior of our model with different experimental measurements taken from the literature. In Fig. 3.9, we use the tumor volume measurements for three different cancers, namely prostate, breast and colon for validation purpose. The experimental data sets are taken from [85–87]. These data sets are obtained by establishing human tumor xenografts in mice. The measurements of tumor volume are available from the day of implantation and during exponential growth. To compare our model behavior with the tumor volume, we first compute the total number of mutated cells  $N(t)$ , which is the sum of mutated stem, progenitor, and mature cells, as

$$N(t) := C_1(t) + \int_{x_0}^{x_1} P_1(x, t) dx + M_1(t).$$

Then, considering the effective volume of a cell in the tumor to be  $4.18 \times 10^{-6} \text{ mm}^3$  [88], the whole tumor volume  $V(t)$  is computed as [89]

$$V(t) = 4.18 \times 10^{-6} N(t) \text{ mm}^3.$$

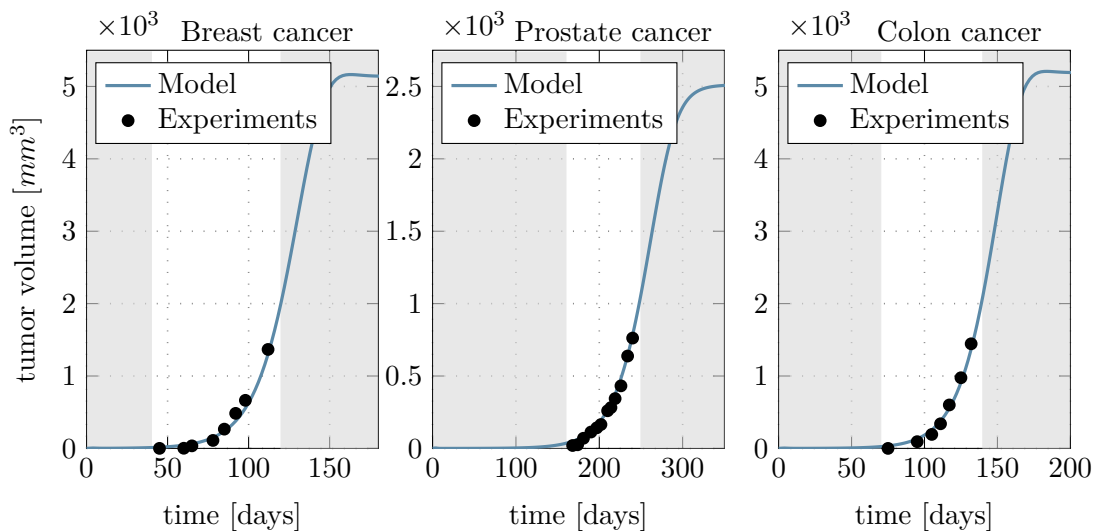


Figure 3.9: Model fitting to the experimental data. Validation of the model using different experimental data for breast, prostate and colon cancer cells. The data are available only during the exponential growth and the model (blue line) fits the data (black dots) for the given values. The grey shaded regions are the model predictions before and after the available experimental measurements and a steady-state is achieved under cytokine feedback signaling.

The tumor volume calculated from the cell count of the proposed model (blue lines) fits very well to the experimental data (black marks) in all three scenarios, see Fig. 3.9. The grey shaded regions depict the predicted model behavior before and after the available experimental values. Our model attains a steady-state in all three simulations due to the feedback via cytokine signals. Note that, the steady-states may vary in reality for different cancer types and also individually but the proposed model is flexible enough to depict various steady-state scenarios. The healthy cell lineage is considered to be initially at a steady-state. The parameters used in Fig. 3.9 are given in Table 3.2.

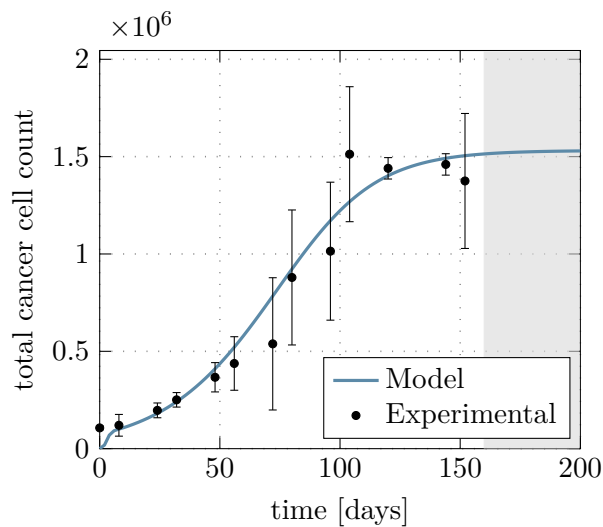


Figure 3.10: Model fitting to the experimental data. The model has been validated with the data set derived by TUBO Cancer cell line [90]. The experimental data are represented by black error bars representing mean  $\pm$  standard deviation. The blue line is the model fit to the experimental measurements. Our proposed model predicts an establishment of the steady-state in grey shaded area where no measurements of cell count were available.

The model has been further validated by using another experimental data set generated in vitro experiments on TUBO cancer cells and is reported in [90], see Fig. 3.10. TUBO cancer cells are a cloned line derived in vitro from a BALB-neuT mouse mammary carcinoma. The data set consists of mean  $\pm$  standard deviation for total cell count. The model fits to the mean values for more than 65 percent of the data set. The initial conditions for healthy cell line are equal to their respective steady-state values. The initial condition of mutated stem cells is equal to  $2 \times 10^4 \text{ mL}^{-1}$  and for mutated progenitor and mature cells are equal to zero. The parameter values used in the Fig. 3.10 are given in Table 3.3. The mutation rates for healthy stem and progenitor cells are  $10^{-4}$  and  $10^{-6}$  [81], respectively. The exponential growth and achievement of the steady-state requires enhanced proliferation and self-renewal rates of stem cells. Thereby, the maximum self-renewal probability of healthy and mutated stem cells represented by  $\bar{\alpha}_{S0}$  and  $\bar{\alpha}_{S1}$  are used as 0.35 and 0.40, respectively. The sum of the probabilities for symmetric self-renewal, asymmetric self-renewal and differentiation is still kept equal to 1.



Parameters	Values		
	Breast	Prostate	Colon
$c_1$	$2.5 \times 10^5 mL^{-1}$	$3 \times 10^4 mL^{-1}$	$0.7 \times 10^5 mL^{-1}$
$k_\zeta$	$12.8 \times 10^{-10}$	$12.8 \times 10^{-10}$	$12.8 \times 10^{-10}$
$m_1$	$0 mL^{-1}$	$0 mL^{-1}$	$0 mL^{-1}$
$d_1$	$1.36 \text{ day}^{-1}$	$1.36 \text{ day}^{-1}$	$1.36 \text{ day}^{-1}$
$\bar{\alpha}_{S_0}$	0.36 [78]	0.31 [78]	0.36 [78]
$d_0$	$1.67 \text{ day}^{-1}$ [70]	$1.67 \text{ day}^{-1}$ [70]	$1.67 \text{ day}^{-1}$
$\bar{\alpha}_{S_1}$	0.40	0.30	0.40
$b_1$	$1.09 \text{ day}^{-1}$ [82]	$1.09 \text{ day}^{-1}$	$1.09 \text{ day}^{-1}$
$\bar{\alpha}_{A_0}$	0.80 [78]	0.70 [78]	0.80 [78]
$b_0$	$1.23 \text{ day}^{-1}$ [82]	$1.23 \text{ day}^{-1}$	$1.23 \text{ day}^{-1}$
$\bar{\alpha}_{A_1}$	0.50	0.50	0.50
$\rho_{\mu_1}$	8	8	8
$\delta_{C_0}$	$0.24 \text{ day}^{-1}$	$0.17 \text{ day}^{-1}$ [70]	$0.24 \text{ day}^{-1}$
$\rho_{\mu_0}$	8	8	8
$\delta_{C_1}$	$1.0 \text{ day}^{-1}$ [91]	$1.6 \text{ day}^{-1}$	$1.0 \text{ day}^{-1}$ [91]
$\omega_{\mu_1}$	2.95 days	2.95 days	2.95 days
$\delta_{M_0}$	$2.1 \text{ day}^{-1}$ [70]	$2.1 \text{ day}^{-1}$ [70]	$2.1 \text{ day}^{-1}$ [70]
$\omega_{\mu_0}$	2.80 days [70]	2.80 days	2.80 days
$\delta_{M_1}$	$0.3 \text{ day}^{-1}$	$0.5 \text{ day}^{-1}$	$0.3 \text{ day}^{-1}$
$\rho_{\beta_1}$	2	2	2
$m$	$10^{-4}$ [79, 80]	$10^{-4}$	$10^{-4}$
$\rho_{\beta_0}$	2	2	2
$m'$	$10^{-6}$ [81]	$10^{-6}$	$10^{-6}$
$\omega_{\beta_1}$	1.80 days	1.80 days	1.80 days
$k_1$	$0.60 \text{ day}^{-1}$ [65]	$0.60 \text{ day}^{-1}$	$0.60 \text{ day}^{-1}$
$\omega_{\beta_0}$	1.45 days	1.45 days	1.45 days

Table 3.2: The values of the parameters used in the simulations of Fig. 3.9 are presented for all three cancer types.

Parameter	Value	Parameter	Value
$m$	$10^{-4}$	$m'$	$10^{-6}$ [81]
$\bar{\alpha}_{S_0}$	0.35	$\bar{\alpha}_{S_1}$	0.40
$\delta_{C_0}$	$1.40 \text{ day}^{-1}$	$\delta_{C_1}$	$2.20 \text{ day}^{-1}$
$\delta_{M_0}$	$2.10 \text{ day}^{-1}$	$\delta_{M_1}$	$0.50 \text{ day}^{-1}$
$k_0$	$1 \text{ day}^{-1}$	$k_1$	$1 \text{ day}^{-1}$
$k_\zeta$	$1.42 \times 10^{-7}$		

Table 3.3: Parameters used for model validation in Fig. 3.10.

### 3.6 Discussion and conclusion

According to the stem cell hypothesis, the persistence of cancer is regulated by a small number of cancer cells which share the same biological properties as the stem cells, [45].

The results of this model are in accordance with the stem cell hypothesis because the mutated stem cells are responsible for the evolution and persistence of the whole mutated cell lineage due to their elevated self-renewal and differentiation potential, see Fig. 3.4–3.5. An efficient feedback mechanism must exist with heavy cross-talks between the cells themselves and the extracellular environment to robustly regulate the system comprising of cell lineages with various cell types. In the proposed model, the feedback in both, the stem and progenitor cell populations allows mimicking the intercellular interactions among the cells. Moreover, the model provides an insight that the self-renewal rate of stem cells turns out to be very critical for persistence and maintenance of healthy cell line. As shown in the Fig. 3.6, the influence of the feedback lead to the extinction of healthy cell line because the self-renewal rate of stem cells was reduced. Thus leading to the fact that to maintain the healthy cell population, the critical ratio of stem cell's self-renewal to differentiation rate should be maintained.

The proposed model have some drawbacks too. First, the model assumes a single mutation leading to cancer evolution, which might not be true in many cases but the model structure is flexible to incorporate more mutations and to predict the evolution of cancer depending on their individual effects. Secondly, the model assumes only cytokines feedback signaling but of course there exist several feedback mechanisms, for instance, chalone [51], mechanosensing [92] etc. Furthermore, the simulations are performed assuming linear dependence on feedback signal which might not be very realistic, however, the precise nature of this feedback is still unknown.

We propose a generic modeling framework to investigate the coupled dynamics of the healthy and mutated cell lineages, entailing homeostatic regulation. We show that the model predicts familiar behaviour and evolutionary patterns of cancer. For instance, the small number of mutated stem cells are responsible for the evolution of whole mutated cell lineage. Moreover, the healthy cell line significantly declines in number due to the sensitivity of symmetric self renewal rate of stem cell. Thus, the symmetric and asymmetric self-renewal rates of stem cells are crucial for the persistence and maintenance of both cell lines. The model is also validated with different experimental measurements of the tumor available in the literature. With regard to future work, it is possible to extend our model to include additional phenomena, e.g. cell de-differentiation and other feedback mechanisms. Its architecture also enables heterogeneous type mutations to be introduced, which can be of interest to gain additional insights in the development of cancer and, additionally in the faster emergence of cancer. A future appealing step concerns the stability analysis of the dynamical behavior and sensitivity analysis with respect to the process parameters.

### Mathematical analysis: Wellposedness of stem cell lineage model

---

In the realm of mathematical analysis and its applications, the existence and uniqueness of solutions are fundamental questions. According to Hadamard, a problem is considered well-posed when it has a unique solution that continuously depends on the initial data [93]. The property of wellposedness is crucial, especially when making predictions based on the given problem data. Analyzing structured population models for cell differentiation through mathematical means is relatively rare in the literature. While techniques for proving the existence of a unique solution for coupled nonlinear ODE-PDE models exist, each physical problem's mathematical framework requires its unique approach to identify the conditions for a unique solution. Some of the approaches studied for problems of our class include semigroup theory [94, 95], Banach fixed point theory [96, 97], and iterative methods (based on induction) [98, 99], among others.

This chapter aims to establish the wellposedness of the nonlinear coupled ODE-PDE model introduced in Chapter 3. The motivation behind this analysis is to demonstrate the mathematical rigor of the proposed model. We establish the existence of a globally unique solution for our mathematical model of stem cell lineages utilizing the well-established Banach fixed point theory within our problem settings, defining solution bounds and making assumptions about the function spaces concerning the given data and solution variables.

#### 4.1 Banach fixed point theory: A brief overview

Banach fixed point theory, named after the renowned Polish mathematician Stefan Banach, constitutes a branch of functional analysis dedicated to studying fixed points of specific mappings in metric spaces. One of the most celebrated outcomes of fixed point theory is the Banach contraction mapping principle, used in studying nonlinear equations. It establishes conditions under which a mapping in a complete metric space possesses a unique fixed point. It provides a systematic framework for investigating the existence and uniqueness of fixed points of certain self maps of metric space, and provides a contractive method to find those fixed points. In the sequel, an introduction to Banach fixed point theory along with some related definitions is presented.

### 4.1.1 Cauchy sequence

A sequence  $\{x_n\}$  is called a *Cauchy sequence* if for any given  $\epsilon > 0$ , there exists  $N \in \mathbb{N}$  such that for all  $n, m \geq N$  implies

$$|x_n - x_m| < \epsilon.$$

### 4.1.2 Metric space

A metric space is a set equipped with a distance function (metric) that quantifies the distance between any two points in the set. Formally, a *metric space* is defined as a pair  $(X, d)$ , where  $X$  is the set of elements, and  $d : X \times X \rightarrow \mathbb{R}$  is a function that satisfies the following properties for all  $x, y$ , and  $z$  in  $X$ :

- Non-negativity:  $d(x, y) \geq 0$ ;
- Identity of indiscernibles:  $d(x, y) = 0$  if and only if  $x = y$ ;
- Symmetry:  $d(x, y) = d(y, x)$ ;
- Triangle inequality:  $d(x, y) + d(y, z) \geq d(x, z)$ .

### 4.1.3 Complete metric space

A metric space  $(X, d)$  is called complete if every Cauchy sequence in  $X$  converges to a limit within  $X$ . A Cauchy sequence is a sequence of elements  $\{x_n\}$  such that for any  $\epsilon > 0$ , there exists an  $N$  such that  $d(x_n, x_m) < \epsilon$  for all  $n, m \geq N$ .

### 4.1.4 Fixed point

A *fixed point* on a mapping  $T : X \rightarrow X$  of a set  $X$  into itself is an  $x \in X$  which is mapped onto itself, that is

$$Tx = x.$$

For example, the mapping  $x \rightarrow x^2$  on  $\mathbb{R}$  has two fixed points; 0 and 1.

### 4.1.5 Contraction mapping

Let  $(X, d)$  be a metric space. A mapping  $T : X \rightarrow X$  is called a *contraction mapping* on  $X$  if there exists a constant  $k$  ( $0 \leq k < 1$ ) such that

$$d(T(x), T(y)) \leq k * d(x, y) \text{ for all } x, y \in X.$$

This condition ensures that the mapping “contracts” distances, meaning that the images ( $T(x)$  and  $T(y)$ ) of points under  $T$  are closer together than the original points.

### 4.1.6 Banach fixed point theorem

Let  $(X, d)$  be a complete metric space and let  $T : X \rightarrow X$  be a contraction mapping on  $X$ , then  $T$  has a unique fixed point, i.e.,  $x^* \in X$  such that

$$T(x^*) = x^*.$$

In this chapter, we investigate the model wellposedness utilizing Banach fixed point theory. The general approach in this work involves defining a solution operator for the decoupled dynamics of the model and demonstrating that it acts as a contraction mapping. We then prove that the fixed point of this contraction mapping corresponds to the solution of the original problem. Finally, by applying the Banach fixed point argument, we affirm our results.

## 4.2 Mathematical model

In the sequel, we write the governing model equations for the cell lineage dynamics of healthy and mutated cells together from Chapter 3 as:

$$\frac{d}{dt}C_0(t) = [(1 - 2m)\alpha_{S_0}(s) - m\alpha_{A_0}(s) - \alpha_{D_0}(s) - \delta_{C_0}]k_0C_0(t), \quad (4.1)$$

$$\frac{d}{dt}C_1(t) = [\alpha_{S_1}(s) - \alpha_{D_1}(s) - \delta_{C_1}]k_1C_1(t) + [2m\alpha_{S_0}(s) + m\alpha_{A_0}(s)]k_0C_0(t), \quad (4.2)$$

$$\partial_t P_0(x, t) + \partial_x [g_0(x)P_0(x, t)] = [(1 - 2m')\beta_0(x, s) - \mu_0(x)]P_0(x, t), \quad (4.3)$$

$$\partial_t P_1(x, t) + \partial_x [g_1(x)P_1(x, t)] = [\beta_1(x, s) - \mu_1(x)]P_1(x, t) + 2m'\beta_0(x, s)P_0(x, t), \quad (4.4)$$

with boundary conditions for  $t > 0$

$$g_0(x_0)P_0(x_0, t) = [2(1 - m)\alpha_{D_0}(s) + (1 - m)\alpha_{A_0}(s)]k_0C_0(t), \quad (4.5)$$

$$g_1(x_0)P_1(x_0, t) = [2\alpha_{D_1}(s) + \alpha_{A_1}(s)]k_1C_1(t) + [2m\alpha_{D_0}(s) + m\alpha_{A_0}(s)]k_0C_0(t), \quad (4.6)$$

$$\frac{dM_0}{dt} = g_0(x^*)P_0(x^*, t) - \delta_{M_0}M_0, \quad (4.7)$$

$$\frac{dM_1}{dt} = g_1(x^*)P_1(x^*, t) + 2m'\beta_0(x^*, s)P_0(x^*, t) - \delta_{M_1}M_1, \quad M_1(0) = m_1. \quad (4.8)$$

The initial conditions are  $C_0(0) = c_0$ ,  $C_1(0) = c_1$ ,  $P_0(x, 0) = f_0(x)$ ,  $P_1(x, 0) = f_1(x)$ ,  $M_0(0) = m_0$ ,  $M_1(0) = m_1$ . Finally, the dynamics of cytokine feedback signaling molecules  $\zeta$  can be described by an ODE [100] as:

$$\frac{d\zeta}{dt} = v - (\delta_\zeta + \gamma M)\zeta, \quad (4.9)$$

where  $v$  is the maximum secretion rate of cytokine signals,  $\delta_\zeta$  represents the natural decrement of the signals  $\zeta$ , and  $\gamma$  is the rate by which the total mature cell population  $M = M_0 + M_1$  (consisting of both healthy and mutated mature cells) regulate the cytokine signals. Substituting  $s = (\delta_\zeta/v)\zeta$  and  $k_\zeta = \gamma/\delta_\zeta$ , the above equation turns into

$$\dot{s} = \delta_\zeta(1 - s - k_\zeta s M), \quad s(0) = s_0. \quad (4.10)$$

### 4.2.1 Assumption and simplification

Hereby, we invoke a strong assumption in the model that the auxiliary functions and parameters depend linearly on the feedback signal concentration  $s$ . Thus, we get

$$\begin{aligned} \alpha_{S_0}(s) &= \alpha_{S_0}s, \alpha_{A_0}(s) = \alpha_{A_0}s, \alpha_{D_0}(s) = \alpha_{D_0}s, \alpha_{S_1}(s) = \alpha_{S_1}s, \alpha_{D_1}(s) = \alpha_{D_1}s \\ \text{and } \beta_0(x, s) &= \beta_0(x)s, \beta_1(x, s) = \beta_1(x)s, \end{aligned} \quad (4.11)$$

where  $\alpha_{S_0}, \alpha_{A_0}, \alpha_{D_0}, \alpha_{S_1}, \alpha_{D_1} \in \mathbb{R}_{\geq 0}$ . Using (4.11), the model equations (4.1)-(4.10) can be re-written as

$$\frac{d}{dt}C_0(t) = k_0 (((1 - 2m)\alpha_{S_0} - m\alpha_{A_0} - \alpha_{D_0})s - \delta_{C_0}) C_0(t), \quad C_0(0) = c_0, \quad (4.12)$$

$$\frac{d}{dt}C_1(t) = k_1 ((\alpha_{S_1} - \alpha_{D_1})s - \delta_{C_1}) C_1(t) + mk_0 (2\alpha_{S_0} + \alpha_{A_0}) sC_0(t), \quad C_1(0) = c_1, \quad (4.13)$$

$$\partial_t P_0(x, t) + \partial_x [g_0(x)P_0(x, t)] = (((1 - 2m')\beta_0(x))s - \mu_0(x)) P_0(x, t), \quad (4.14)$$

$$\partial_t P_1(x, t) + \partial_x [g_1(x)P_1(x, t)] = (\beta_1(x)s - \mu_1(x)) P_1(x, t) + 2m'\beta_0(x)sP_0(x, t), \quad (4.15)$$

with the initial conditions  $P_0(x, 0) = f_0(x)$ ,  $P_1(x, 0) = f_1(x)$  and boundary conditions for  $t > 0$

$$g_0(x_0)P_0(x_0, t) = k_0 (2(1 - m)\alpha_{D_0} + (1 - m)\alpha_{A_0}) sC_0(t) := h_0(t), \quad (4.16)$$

$$g_1(x_0)P_1(x_0, t) = k_1 (2\alpha_{D_1} + \alpha_{A_1}) sC_1(t) + k_0 (2m\alpha_{D_0} + m\alpha_{A_0}) sC_0(t) := h_1(t). \quad (4.17)$$

Finally, the equations for healthy and mutated mature cells and the feedback signal concentration are

$$\frac{dM_0}{dt} = g_0(x^*)P_0(x^*, t) - \delta_{M_0}M_0, \quad M_0(0) = m_0, \quad (4.18)$$

$$\frac{dM_1}{dt} = g_1(x^*)P_1(x^*, t) + 2m'\beta_0(x^*)sP_0(x^*, t) - \delta_{M_1}M_1, \quad M_1(0) = m_1, \quad (4.19)$$

$$\frac{ds}{dt} = \delta_\zeta(1 - s - k_\zeta sM), \quad s(0) = s_0. \quad (4.20)$$

Next, we employ the above model to prove the existence of a unique solution under the assumption introduced in this section.

### 4.3 Solution operator $S^\theta$

Consider the initial data satisfying

$$c_0, c_1, m_0, m_1, s_0 \in \mathbb{R}_{\geq 0}, \text{ and } f_0(x), f_1(x) : [x_0, x^*] \rightarrow \mathbb{R}_{\geq 0}, h_0(t), h_1(t) : [0, T] \rightarrow \mathbb{R}_{\geq 0},$$

with continuously differentiable auxiliary functions

$$\begin{aligned} g_0, g_1, \beta_0, \beta_1, \mu_0, \mu_1 : [x_0, x^*] \rightarrow \mathbb{R}_{\geq 0} \text{ and } g_0, g_1, \beta_0, \beta_1, \mu_0, \mu_1 \in C^1([x_0, x^*]), \\ g_0(x), g_1(x) > 0, \forall x \in [x_0, x^*) \text{ and } s : [0, T] \rightarrow [0, 1]. \end{aligned} \quad (4.21)$$

Moreover, we assume that the parameters involved in the model fulfill

$$x_0, x^*, T, m, m', \alpha_{S_0}, \alpha_{A_0}, \alpha_{D_0}, \alpha_{S_1}, \alpha_{A_1}, \alpha_{D_1} \in \mathbb{R}_{\geq 0}, \text{ and}$$

$$k_0, k_1, \delta_{C_0}, \delta_{C_1}, \delta_{M_0}, \delta_{M_0}, \delta_{M_1}, k_\zeta, \delta_\zeta \in \mathbb{R}_{\geq 0}.$$

Meeting the requirements for auxiliary functions set out above in (4.21) and the following restriction on the specified data space will ensure the wellposedness of model.

**Definition 4.3.1** (Problem data space). We define a space for the given data as

$$\Theta := \left\{ (c_0, c_1, m_0, m_1, f_0, f_1, h_0, h_1, s_0) \mid f_0, f_1 \in C^1([x_0, x^*]) \text{ with } \int_{x_0}^{x^*} \frac{P_0(x)}{g_0(x)} dx < \infty, \right. \\ \left. \int_{x_0}^{x^*} \frac{P_1(x)}{g_1(x)} dx < \infty, m_0 \geq 0, m_1 \geq 0, c_0 \geq 0, c_1 \geq 0, s_0 \geq 0, h_0, h_1 \in C^1([0, T]) \right. \\ \left. \text{with } h_0(0) = f_0(x_0), h_1(0) = f_1(x^*) \right\}.$$

For each  $\theta = (c_0, c_1, m_0, m_1, f_0, f_1, h_0, h_1, s_0) \in \Theta$ , the norm of the function space  $\Theta$  is defined as

$$\|\theta\|_\Theta := |c_0| + |c_1| + |m_0| + |m_1| + |s_0| + \|f_0\|_\infty + \|f_1\|_\infty + \|h_0\|_\infty + \|h_1\|_\infty,$$

where  $|\cdot|$  and  $\|\cdot\|_\infty$  denote the absolute value and  $L^\infty$  norm, respectively.

**Definition 4.3.2** (Solution Bounds). For  $\theta = (c_0, c_1, m_0, m_1, f_0, f_1, h_0, h_1, s_0) \in \Theta$ , define the following upper bounds

$$\bar{g}_0 := \max_{x \in [x_0, x^*]} g_0(x), \bar{g}_1 := \max_{x \in [x_0, x^*]} g_1(x), \bar{h}_0 := \max_{t \in [0, T]} h_0(t), \bar{h}_1 := \max_{t \in [0, T]} h_1(t), \\ \bar{\mu}_0 := \max_{x \in [x_0, x^*]} \mu_0(x), \bar{\mu}_1 := \max_{x \in [x_0, x^*]} \mu_1(x), \bar{\beta}_0 := \max_{x \in [x_0, x^*]} \beta_0(x), \bar{\beta}_1 := \max_{x \in [x_0, x^*]} \beta_1(x).$$

Furthermore, the functions that serve as bound for solution variables are

$$\bar{C}_0 := \Theta \times [0, T] \rightarrow \mathbb{R}, \bar{C}_0(\theta, t) := c_0 \exp(k_0((1 - 2m)\bar{\alpha}_{S_0} - m\bar{\alpha}_{A_0} - \bar{\alpha}_{D_0} - \delta)t), \\ \bar{C}_1 := \Theta \times [0, T] \rightarrow \mathbb{R}, \bar{C}_1(\theta, t) := \frac{m(2\alpha_{S_0} + \alpha_{A_0})k_0\bar{C}_0(\theta, t)}{(\delta_{C_1} - \alpha_{S_1})k_1}, \\ \bar{P}_0 := \Theta \times [0, T] \rightarrow \mathbb{R}, \bar{P}_0(\theta, t) := \exp(((1 - 2m')\bar{\beta}_0 - \bar{\mu}_0)t) (((1 - 2m')\bar{\beta}_0 - \bar{\mu}_0)\bar{h}_0 g_0(x_0) \\ + \|f_0\|_1), \\ \bar{P}_1 := \Theta \times [0, T] \rightarrow \mathbb{R}, \bar{P}_1(\theta, t) := (\bar{\mu}_1 - \bar{\beta}_1)(2m'\bar{\beta}_0\bar{P}_0(\theta, t))\bar{g}_1\bar{x}^* + \exp((\bar{\beta}_1 - \bar{\mu}_1)t) \\ ((\bar{\beta}_1 - \bar{\mu}_1)\bar{h}_1 g_1(x_0) + \|f_1\|_1), \\ \bar{M}_0 := \Theta \times [0, T] \rightarrow \mathbb{R}, \bar{M}_0(\theta, t) := \frac{g_0(x^*)\bar{P}_0(\theta, t)}{\delta_{M_0}}, \\ \bar{M}_1 := \Theta \times [0, T] \rightarrow \mathbb{R}, \bar{M}_1(\theta, t) := \frac{g_1(x^*)\bar{P}_1(\theta, t) + 2m'\beta_0(x^*)\bar{P}_0(\theta, t)}{\delta_{M_1}}, \\ \bar{s} := \Theta \times [0, T] \rightarrow \mathbb{R}, \bar{s}(\theta, t) := 1.$$

Next, we simplify the PDEs (4.14) and (4.15) for the sake of analysis. Thereby, we define a parameter transform for  $x$  by which we drop the maturity rates  $g_0(x)$  and  $g_1(x)$  from the convective terms of the PDEs (4.14) and (4.15), respectively.

**Lemma 4.3.1** (Parameter transform for  $x$ ). Let  $g(x) > 0, \forall x \in [x_0, x^*]$ . Then, there exists a number  $\bar{x}^* \in (0, \infty]$  and a function  $x : [0, \bar{x}^*) \rightarrow [x_0, x^*)$  satisfying the following conditions:

1.  $\frac{dx}{d\bar{x}} = g(x(\bar{x}))$  for all  $\bar{x} \in (0, \bar{x}^*)$

2.  $x(0) = x_0$
3.  $\lim_{\bar{x} \rightarrow \bar{x}^*} x(\bar{x}) = x^*$ .

*Proof.* For the proof, see [97]. □

We define  $T' \in (0, T]$  to restrict our problem to a shorter time interval in order to guarantee that the solution operator is contractive.

**Definition 4.3.3** (Variable space). We define  $X_{T'} := L^1([0, T']) \times L^1([0, T']) \times L^1([0, T'] \times [x_0, x^*)) \times L^1([0, T'] \times [x_0, x^*)) \times L^1([0, T']) \times L^1([0, T']) \times L^1([0, T'])$ . For any  $\theta \in \Theta$  define the following associated function spaces

$$Y_{T'}^{\theta,1} := \{y_1 \in L^1([0, T']) \mid 0 \leq y_1(t) \leq \overline{C_0}(\theta, t) \text{ for almost all } t \in [0, T']\},$$

$$Y_{T'}^{\theta,2} := \{y_2 \in L^1([0, T']) \mid 0 \leq y_2(t) \leq \overline{C_1}(\theta, t) \text{ for almost all } t \in [0, T']\},$$

$$Y_{T'}^{\theta,3} := \left\{ y_3 \in L^1([0, T'] \times [x_0, x^*)) \mid \int_{x_0}^{x^*} y_3(x, t) dx \leq \overline{P_0}(\theta, t) \text{ for almost all } t \in [0, T'] \text{ and } y_3(x, t) \geq 0 \text{ for almost all } t \in [0, T'], x \in [x_0, x^*) \right\},$$

$$Y_{T'}^{\theta,4} := \left\{ y_4 \in L^1([0, T'] \times [x_0, x^*)) \mid \int_{x_0}^{x^*} y_4(x, t) dx \leq \overline{P_1}(\theta, t) \text{ for almost all } t \in [0, T'] \text{ and } y_4(x, t) \geq 0 \text{ for almost all } t \in [0, T'], x \in [x_0, x^*) \right\},$$

$$Y_{T'}^{\theta,5} := \{y_5 \in L^1([0, T']) \mid 0 \leq y_5(t) \leq \overline{M_0}(\theta, t) \text{ for almost all } t \in [0, T']\},$$

$$Y_{T'}^{\theta,6} := \{y_6 \in L^1([0, T']) \mid 0 \leq y_6(t) \leq \overline{M_1}(\theta, t) \text{ for almost all } t \in [0, T']\},$$

$$Y_{T'}^{\theta,7} := \{y_7 \in L^1([0, T']) \mid 0 \leq y_7(t) \leq \overline{s}(\theta, t) \text{ for almost all } t \in [0, T']\},$$

$$Y_{T'}^\theta := Y_{T'}^{\theta,1} \times Y_{T'}^{\theta,2} \times Y_{T'}^{\theta,3} \times Y_{T'}^{\theta,4} \times Y_{T'}^{\theta,5} \times Y_{T'}^{\theta,6} \times Y_{T'}^{\theta,7} \subset X_{T'}.$$

For any  $\xi = (x_1, x_2, x_3, x_4, x_5, x_6, x_7) \in X_{T'}$  and  $t \in [0, T']$ , define the norm

$$\|\xi\|_X := \int_0^{T'} \|\xi\|_t dt,$$

with

$$\|\xi\|_t := |x_1(t)| + |x_2(t)| + \int_{x_0}^{x^*} |x_3(x, t)| dx + \int_{x_0}^{x^*} |x_4(x, t)| dx + |x_5(t)| + |x_6(t)| + |x_7(t)|.$$

Now, we are able to define a solution operator which consists of all the solution variables. It is to be noted that with reference to Lemma 4.3.1, we define the following transformations for the involved PDEs (4.14) and (4.15). For  $g_0(x), g_1(x) > 0$  and  $g_0(x), g_1(x) \in C^1([x_0, x^*])$  and  $\forall x \in [x_0, x^*]$ , there exist functions  $x(\bar{x}_0)$  and  $x(\bar{x}_1)$  such that

$$\frac{dx}{d\bar{x}_0} = g_0(x(\bar{x}_0)), x(0) = x_0 \text{ and } \frac{dx}{d\bar{x}_1} = g_1(x(\bar{x}_1)), x(0) = x_0$$

hold for all  $\bar{x}_0 \in (0, \bar{x}_0^*)$  and  $\bar{x}_1 \in (0, \bar{x}_1^*)$ , respectively. In the following definition, the solution operators for  $P_0^\theta$  and  $P_1^\theta$  are stemming from the transformed PDEs. The details of this can be found in Section 4.4.



**Definition 4.3.4** (Solution operator). For  $\theta \in \Theta$ , we define the solution operator  $S^\theta[y] := (C_0^\theta[y], C_1^\theta[y], P_0^\theta[y], P_1^\theta[y], M_0^\theta[y], M_1^\theta[y], s^\theta[y])$  as

$$S^\theta : Y_{T'}^\theta \rightarrow L^1([0, T']) \times L^1([0, T']) \times L^1([0, T'] \times [x_0, x^*]) \times L^1([0, T'] \times [x_0, x^*]) \\ \times L^1([0, T']) \times L^1([0, T']) \times L^1([0, T']),$$

with

$$\begin{aligned} C_0^\theta &: Y_{T'}^\theta \rightarrow L^1([0, T']), \\ C_1^\theta &: Y_{T'}^\theta \rightarrow L^1([0, T']), \\ P_0^\theta &: Y_{T'}^\theta \rightarrow L^1([0, T']) \times [x_0, x^*], \\ P_1^\theta &: Y_{T'}^\theta \rightarrow L^1([0, T']) \times [x_0, x^*], \\ M_0^\theta &: Y_{T'}^\theta \rightarrow L^1([0, T']), \\ M_1^\theta &: Y_{T'}^\theta \rightarrow L^1([0, T']), \\ s^\theta &: Y_{T'}^\theta \rightarrow L^1([0, T']), \end{aligned}$$

such that for all  $y = (y_1, y_2, y_3, y_4, y_5, y_6, y_7) \in Y_{T'}^\theta$  and almost all  $t \in [0, T']$  and  $\bar{x} \in [0, \bar{x}^*]$ :

$$\begin{aligned} C_0^\theta[y](t) &:= c_0 \exp \left( \int_0^t k_0 \left( (1 - 2m)\bar{\alpha}_{S_0} - m\bar{\alpha}_{A_0} - \bar{\alpha}_{D_0} \right) y_7(\lambda) - \delta_{C_0} \right) d\lambda, \\ C_1^\theta[y](t) &:= \exp \left( \int_0^t k_1 \left( (\bar{\alpha}_{S_1} - \bar{\alpha}_{D_1}) y_7(\lambda) - \delta_{C_1} \right) d\lambda \right) \left[ c_1 + \right. \\ &\quad \left. \int_0^t \exp \left( k_1 \int_0^\epsilon \left( -\bar{\alpha}_{S_1} + \bar{\alpha}_{D_1} \right) y_7(\lambda) + \delta_{C_1} \right) d\lambda \right] \times (m(2\bar{\alpha}_{S_0} + \bar{\alpha}_{A_0}) k_0 y_1(\epsilon) y_7(\epsilon)) d\epsilon, \end{aligned}$$

$$P_1^\theta[y](x(\bar{x}_1), t) := \frac{1}{g_1(x(\bar{x}_1))} \times \begin{cases} \exp \left( \int_0^t \beta_1(x(\lambda + \bar{x}_1 - t)) y_7(\lambda) - \mu_1(x(\lambda + \bar{x}_1 - t)) d\lambda \right) \\ \times \left[ \int_0^t \exp \left\{ - \int_0^\epsilon \beta_1(x(\lambda + \bar{x}_1 - t)) y_7(\lambda) - \mu_1(x(\lambda + \bar{x}_1 - t)) d\lambda \right\} \right. \\ \left. (2m' \beta_0(x(\epsilon + \bar{x}_1 - t)) y_3(x(\epsilon + \bar{x}_1 - t), \epsilon) y_7(\epsilon)) g_1(x(\epsilon + \bar{x}_1 - t)) d\epsilon \right. \\ \left. + f_1(x(\bar{x}_1 - t)) g_1(x(\bar{x}_1 - t)) \right], & \bar{x}_1 \geq t \\ \exp \left( \int_0^{\bar{x}_1} \beta_1(x(\lambda)) y_7(\lambda + t - \bar{x}_1) - \mu_1(x(\lambda)) d\lambda \right) \\ \times \left[ \int_0^{\bar{x}_1} \exp \left\{ - \int_0^\epsilon \beta_1(x(\lambda)) y_7(\lambda + t - \bar{x}_1) - \mu_1(x(\lambda)) d\lambda \right\} \right. \\ \left. (2m' \beta_0(x(\epsilon)) y_3(x(\epsilon), \epsilon + t - \bar{x}_1) y_7(\epsilon + t - \bar{x}_1)) g_1(x(\epsilon)) d\epsilon \right. \\ \left. + h_1(t - \bar{x}_1) g_1(x_0) \right], & \bar{x}_1 < t \end{cases}$$

$$P_0^\theta[y](x(\bar{x}_0), t) := \frac{1}{g_0(x(\bar{x}_0))} \times \begin{cases} \exp\left(\int_0^t (1-2m')\beta_0(x(\lambda + \bar{x}_0 - t))y_7(\lambda) - \mu_0(x(\lambda + \bar{x}_0 - t))d\lambda\right) \\ \times f_0(x(\bar{x}_0 - t))g_0(x(\bar{x}_0 - t)), & \bar{x}_0 \geq t \\ \exp\left(\int_0^{\bar{x}_0} (1-2m')\beta_0(x(\lambda))y_7(\lambda + t - \bar{x}_0) - \mu_0(x(\lambda))d\lambda\right) \\ \times h_0(t - \bar{x}_0)g_0(x_0), & \bar{x}_0 < t \end{cases}$$

$$M_0^\theta[y](t) := \exp(-\delta_{M_0}t) \left[ \int_0^t \exp(\delta_{M_0}\lambda)g_0(x^*)y_3(x^*, \lambda)d\lambda + m_0 \right],$$

$$M_1^\theta[y](t) := \exp(-\delta_{M_1}t) \left[ \int_0^t \exp(\delta_{M_1}\lambda)(g_1(x^*)y_4(x^*, \lambda) + 2m'\beta_0(x^*)y_3(x^*, \lambda)y_7(\lambda))d\lambda + m_1 \right],$$

$$s^\theta[y](t) := \exp\left(-\int_0^t \delta_\zeta(1 + k_\zeta(y_5(\lambda) + y_6(\lambda)))d\lambda\right) \times \left[ \int_0^t \exp\left(\int_0^\epsilon \delta_\zeta(1 + k_\zeta(y_5(\lambda) + y_6(\lambda)))d\lambda\right) \delta_\zeta d\epsilon + s_0 \right].$$

#### 4.4 Fixed point of the solution operator $S^\theta$

Note that the latter definition of the operator  $S^\theta$  is motivated by the solutions of the following decoupled ODE-PDE system. Thus, for any given functions  $\bar{y}_1, \bar{y}_2 \in C^0([0, T])$ ,  $\bar{y}_3, \bar{y}_4 \in C^0([x_0, x^*] \times [0, T])$ ,  $\bar{y}_5, \bar{y}_6, \bar{y}_7 \in C^0([0, T])$ , and  $\theta = (c_0, c_1, m_0, m_1, s_0, f_0, f_1, h_0, h_1) \in \Theta$ , the solution variables  $C_0, C_1, P_0, P_1, M_0, M_1, s$  can be found from the following decoupled ODE-PDE system:

$$\frac{d}{dt}C_0(t) = [((1-2m)\bar{\alpha}_{S_0} - m\bar{\alpha}_{A_0} - \bar{\alpha}_{D_0})\bar{y}_7(t) - \delta_{C_0}]k_0C_0(t),$$

$$\frac{d}{dt}C_1(t) = [(\bar{\alpha}_{S_1} - \bar{\alpha}_{D_1})\bar{y}_7(t) - \delta_{C_1}]k_1C_1(t) + m(2\bar{\alpha}_{S_0} + \bar{\alpha}_{A_0})\bar{y}_7(t)k_0\bar{y}_1(t),$$

$$\partial_t P_0(x, t) + \partial_x[g_0(x)P_0(x, t)] = [(1-2m')\beta_0(x)\bar{y}_7(t) - \mu_0(x)]P_0(x, t),$$

$$\partial_t P_1(x, t) + \partial_x[g_1(x)P_1(x, t)] = [\beta_1(x)\bar{y}_7(t) - \mu_1(x)]P_1(x, t) + 2m'\beta_0(x)\bar{y}_7(t)\bar{y}_3(x, t),$$

$$\frac{d}{dt}M_0(t) = g_0(x^*)\bar{y}_3(x^*, t) - \delta_{M_0}M_0,$$

$$\frac{d}{dt}M_1(t) = g_1(x^*)\bar{y}_4(x^*, t) + 2m'\beta_0(x^*)\bar{y}_3(x^*, t)\bar{y}_7(t) - \delta_{M_1}M_1,$$

$$\frac{d}{dt}s(t) = \delta_\zeta(1 - s - k_\zeta s(\bar{y}_5(t) + \bar{y}_6(t))),$$

with the initial conditions  $C_0(0) = c_0$ ,  $C_1(0) = c_1$ ,  $P_0(x, 0) = f_0(x)$ ,  $P_1(x, 0) = f_1(x)$ ,  $M_0(0) = m_0$ ,  $M_1(0) = m_1$ ,  $s(0) = s_0$ , and boundary conditions

$$g_0(0)P_0(0, t) = (1-m)[2\bar{\alpha}_{D_0} + \bar{\alpha}_{A_0}\bar{y}_7(t)]k_0\bar{y}_1(t) := h_0(t),$$

$$g_1(0)P_1(0, t) = [2\bar{\alpha}_{D_1} + \bar{\alpha}_{A_1}\bar{y}_7(t)]k_1\bar{y}_2(t) + m[2\bar{\alpha}_{D_0} + \bar{\alpha}_{A_0}\bar{y}_7(t)]k_0\bar{y}_1(t) := h_1(t),$$

for  $t > 0$ . Note that all representatives of  $S^\theta$  that operate on  $Y_{T'}^\theta$ , cannot solve the ODE-PDE system because all components of  $Y_{T'}^\theta$  are from the subspace of  $L^1$ , and for every differentiable function, there exists an equivalent function that is nowhere differentiable with respect to  $L^1$  norm. Therefore, we will consider one particular representative of  $S^\theta$ , which we call the unique continuous representative. Likewise, we can argue that since the fundamental theorem of analysis is only applicable to integrals over continuous functions, we choose the continuous equivalence classes of the functions on which  $S^\theta$  is applied.

**Lemma 4.4.1.** Let  $y = (y_1, y_2, y_3, y_4, y_5, y_6, y_7) \in Y_{T'}^\theta$  be such that there exists a continuous representative  $\bar{y} = (\bar{y}_1, \bar{y}_2, \bar{y}_3, \bar{y}_4, \bar{y}_5, \bar{y}_6, \bar{y}_7)$  of  $y$ . Then, the unique continuous representatives of  $C_0^\theta[y]$ ,  $C_1^\theta[y]$ ,  $P_0^\theta[y]$ ,  $P_1^\theta[y]$ ,  $M_0^\theta[y]$ ,  $M_1^\theta[y]$ , and  $s^\theta[y]$  solve the decoupled ODE-PDE system.

*Proof.* The claim for  $C_0^\theta[y]$ ,  $C_1^\theta[y]$ ,  $M_0^\theta[y]$ ,  $M_1^\theta[y]$ ,  $s^\theta[y]$  follows from the ODE theory, see Lemma 1 in appendix. Now, we need to prove that the continuous representatives of  $P_0^\theta[y]$ ,  $P_1^\theta[y]$  satisfy (4.14), (4.15), (4.16) and (4.17). It is easy to see that the initial and boundary conditions are satisfied at  $\bar{x}_0 = t$  and  $\bar{x}_1 = t$  by the continuous representatives of  $P_0^\theta[y]$  and  $P_1^\theta[y]$ , respectively. To show that (4.14) and (4.15) also satisfy the claim, assume that  $t \in (0, T)$ ,  $\bar{x}_0 \in (0, \bar{x}_0^*)$  and  $\bar{x}_1 \in (0, \bar{x}_1^*)$ . We denote the continuous representatives of  $P_0^\theta[y]$  and  $P_1^\theta[y]$  as  $P_0$  and  $P_1$ , respectively. Further, we introduce the notations  $\tilde{P}_0(x(\bar{x}_0), t) := g_0(x(\bar{x}_0))P_0(x(\bar{x}_0), t)$  and  $\tilde{P}_1(x(\bar{x}_1), t) := g_1(x(\bar{x}_1))P_1(x(\bar{x}_1), t)$ . We begin by proving the existence of a continuous representative for  $P_0^\theta[y]$  and thereby, we will compute  $\frac{\partial \tilde{P}_0(x(\bar{x}_0), t)}{\partial \bar{x}_0}$  and  $\frac{\partial \tilde{P}_0(x(\bar{x}_0), t)}{\partial t}$  using the definition of  $P_0^\theta$  and prove the continuity at  $\bar{x}_0 = t$  by showing that left and right limits exist and are equal to the value of function at  $\bar{x}_0 = t$ . The derivative  $\frac{\partial \tilde{P}_0(x(\bar{x}_0), t)}{\partial \bar{x}_0}$  for  $\bar{x}_0 \geq t$  results in

$$\begin{aligned} \frac{\partial \tilde{P}_0}{\partial \bar{x}_0} = & \exp\left(\int_0^t (1 - 2m')\beta_0(x(\lambda + \bar{x}_0 - t))y_7(\lambda) - \mu_0(x(\lambda + \bar{x}_0 - t))d\lambda\right) \left[ f_0'(x(\bar{x}_0 - t)) \right. \\ & g_0^2(x(\bar{x}_0 - t)) + f_0(x(\bar{x}_0 - t))g_0'(x(\bar{x}_0 - t))g_0(x(\bar{x}_0 - t)) + \frac{\partial}{\partial \bar{x}_0} \int_0^t (1 - 2m') \\ & \left. \beta_0(x(\lambda + \bar{x}_0 - t))y_7(\lambda) - \mu_0(x(\lambda + \bar{x}_0 - t))d\lambda f_0(x(\bar{x}_0 - t))g_0(x(\bar{x}_0 - t)) \right]. \end{aligned}$$

After simplification, we get

$$\begin{aligned} \frac{\partial \tilde{P}_0}{\partial \bar{x}_0} = & \tilde{P}_0(x(\bar{x}_0), t) \left( (1 - 2m')\beta_0(x(\bar{x}_0))y_7(t) - \mu_0(x(\bar{x}_0)) + \right. \\ & \left. \frac{\partial}{\partial \bar{x}_0} \int_0^t (1 - 2m')\beta_0(x(\lambda + \bar{x}_0 - t))y_7(\lambda) - \mu_0(x(\lambda + \bar{x}_0 - t))d\lambda \right) - \frac{\partial \tilde{P}_0(x(\bar{x}_0), t)}{\partial t}. \end{aligned}$$

Applying the limit  $\bar{x}_0 \rightarrow t^+$  on both sides of above equation yields

$$\lim_{\bar{x}_0 \rightarrow t^+} \frac{\partial \tilde{P}_0}{\partial \bar{x}_0} = \tilde{P}_0(x(t), t) 2((1 - 2m')\beta_0(x(t))y_7(t) - \mu_0(x(t))) - \frac{\partial \tilde{P}_0(x(t), t)}{\partial t}. \quad (4.22)$$

Next, we consider the other case, when  $\bar{x}_0 < t$ , the derivative  $\frac{\partial \tilde{P}_0(x(\bar{x}_0), t)}{\partial \bar{x}_0}$  results in

$$\begin{aligned} \frac{\partial \tilde{P}_0(x(\bar{x}_0), t)}{\partial \bar{x}_0} = & \tilde{P}_0(x(\bar{x}_0), t) \left( (1 - 2m')\beta_0(x(\bar{x}_0))y_7(t) - \mu_0(x(\bar{x}_0)) + \right. \\ & \left. \frac{\partial}{\partial t} \int_0^{\bar{x}_0} (1 - 2m')\beta_0(x(\lambda))y_7(\lambda + t - \bar{x}_0) - \mu_0(x(\lambda))d\lambda \right) - \frac{\partial \tilde{P}_0(x(\bar{x}_0), t)}{\partial t}. \end{aligned}$$

Then, applying the limit  $\bar{x}_0 \rightarrow t^-$  on the both sides of above equation, we have

$$\lim_{\bar{x}_0 \rightarrow t^-} \frac{\partial \tilde{P}_0(x(\bar{x}_0), t)}{\partial \bar{x}_0} = \tilde{P}_0(x(t), t) 2((1 - 2m')\beta_0(x(t))y_7(t) - \mu_0(x(t))) - \frac{\partial \tilde{P}_0(x(t), t)}{\partial t}. \quad (4.23)$$

From Eq. (4.22) and Eq. (4.23), it follows that

$$\lim_{\bar{x}_0 \rightarrow t^+} \frac{\partial \tilde{P}_0(x(\bar{x}_0), t)}{\partial \bar{x}_0} = \lim_{\bar{x}_0 \rightarrow t^-} \frac{\partial \tilde{P}_0(x(\bar{x}_0), t)}{\partial \bar{x}_0}.$$

Now, we can calculate the differential quotient at  $(t, x(t))$ . By mean value theorem, we can assign some  $\varrho_h \in (t, t+h)$  (or  $\varrho_h \in (t+h, t)$ ) to each  $h > 0$  or  $(h < 0)$  such that

$$\frac{\tilde{P}_0(x(t+h), t) - \tilde{P}_0(x(t), t)}{h} = \frac{\partial \tilde{P}_0(x(\varrho_h), t)}{\partial \bar{x}_0}.$$

We have that

$$\begin{aligned} \frac{\partial \tilde{P}_0(x(t), t)}{\partial \bar{x}_0} &= \lim_{h \rightarrow 0} \frac{\tilde{P}_0(x(t+h), t) - \tilde{P}_0(x(t), t)}{h} = \lim_{h \rightarrow 0} \frac{\partial \tilde{P}_0(x(\varrho_h), t)}{\partial \bar{x}_0} = \lim_{\bar{x}_0 \rightarrow t} \frac{\partial \tilde{P}_0(x(\bar{x}_0), t)}{\partial \bar{x}_0} \\ &= \tilde{P}_0(x(t), t) 2((1 - 2m')\beta_0(x(t))y_7(t) - \mu_0(x(t))) - \frac{\partial \tilde{P}_0(x(t), t)}{\partial t} \end{aligned}$$

exists at  $\bar{x}_0 = t$  and that the partial derivative is continuous in the direction of  $\bar{x}_0$ . Next, we consider  $\frac{\partial \tilde{P}_0(x(\bar{x}_0), t)}{\partial t}$  for  $\bar{x}_0 \geq t$ , which by using the definition of  $\tilde{P}_0$ , results in

$$\begin{aligned} \frac{\partial \tilde{P}_0(x(\bar{x}_0), t)}{\partial t} &= \tilde{P}_0(x(\bar{x}_0), t) \left( (1 - 2m')\beta_0(x(\bar{x}_0))y_7(t) - \mu_0(x(\bar{x}_0)) + \frac{\partial}{\partial \bar{x}_0} \int_0^t (1 - 2m') \right. \\ &\quad \left. \beta_0(x(\lambda + \bar{x}_0 - t))y_7(\lambda) - \mu_0(x(\lambda + \bar{x}_0 - t))d\lambda \right) - \frac{\partial \tilde{P}_0(x(\bar{x}_0), t)}{\partial \bar{x}_0}. \end{aligned}$$

Finally, applying the limit  $\bar{x}_0 \rightarrow t^+$ , yields

$$\lim_{\bar{x}_0 \rightarrow t^+} \frac{\partial \tilde{P}_0(x(\bar{x}_0), t)}{\partial t} = \tilde{P}_0(x(t), t) 2((1 - 2m')\beta_0(x(t))y_7(t) - \mu_0(x(t))) - \frac{\partial \tilde{P}_0(x(t), t)}{\partial t}.$$

Now, for  $\bar{x}_0 < t$ , the derivative  $\frac{\partial \tilde{P}_0(x(\bar{x}_0), t)}{\partial t}$  simplifies to

$$\begin{aligned} \frac{\partial \tilde{P}_0(x(\bar{x}_0), t)}{\partial t} &= \tilde{P}_0(x(\bar{x}_0), t) \left( (1 - 2m')\beta_0(x(\bar{x}_0))y_7(t) - \mu_0(x(\bar{x}_0)) + \right. \\ &\quad \left. \frac{\partial}{\partial t} \int_0^{\bar{x}_0} (1 - 2m')\beta_0(x(\lambda))y_7(\lambda + t - \bar{x}_0) - \mu_0(x(\lambda))d\lambda \right) - \frac{\partial \tilde{P}_0(x(\bar{x}_0), t)}{\partial \bar{x}_0}. \end{aligned}$$

Consequently, taking the limit  $\bar{x}_0 \rightarrow t^-$  results in

$$\lim_{\bar{x}_0 \rightarrow t^-} \frac{\partial \tilde{P}_0(x(\bar{x}_0), t)}{\partial t} = \tilde{P}_0(x(t), t) 2((1 - 2m')\beta_0(x(t))y_7(t) - \mu_0(x(t))) - \frac{\partial \tilde{P}_0(x(t), t)}{\partial \bar{x}_0}.$$

Therefore, it holds that

$$\lim_{\bar{x}_0 \rightarrow t^+} \frac{\partial \tilde{P}_0(x(\bar{x}_0), t)}{\partial t} = \lim_{\bar{x}_0 \rightarrow t^-} \frac{\partial \tilde{P}_0(x(\bar{x}_0), t)}{\partial t},$$

which gives the continuity of  $\tilde{P}_0$  and  $\frac{\partial \tilde{P}_0(x(\bar{x}_0), t)}{\partial \bar{x}_0}$ .

Now, we prove this claim for  $\tilde{P}_1$ . Consider  $\frac{\partial \tilde{P}_1(x(\bar{x}_1), t)}{\partial \bar{x}_1}$  for  $\bar{x}_1 \geq t$ , then by using the definition of  $P_1^\theta$  and simplifying, we have

$$\begin{aligned} \frac{\partial \tilde{P}_1}{\partial \bar{x}_1} = & \tilde{P}_1(x(\bar{x}_1), t) \left( \beta_1(x(\bar{x}_1)) y_7(t) - \mu_1(x(\bar{x}_1)) + \frac{\partial}{\partial \bar{x}_1} \int_0^t \beta_1(x(\bar{x}_1)) y_7(\lambda) - \mu_1(x(\bar{x}_1)) d\lambda \right) \\ & - \frac{\partial \tilde{P}_1(x(\bar{x}_1), t)}{\partial t} + \exp \left( \int_0^t \beta_1(x(\bar{x}_1)) y_7(\lambda) - \mu_1(x(\bar{x}_1)) d\lambda \right) \left[ \exp \left( - \int_0^t y_7(\lambda) \right. \right. \\ & \left. \left. \beta_1(x(\bar{x}_1)) - \mu_1(x(\bar{x}_1)) d\lambda \right) (2m' \beta_0(x(\bar{x}_1)) y_3(x(\bar{x}_1), t) y_7(t)) g_1(x(\bar{x}_1)) + \frac{\partial}{\partial \bar{x}_1} \right. \\ & \left. \int_0^t \exp \left( - \int_0^\epsilon \beta_1(x(\bar{x}_1)) y_7(\lambda) - \mu_1(x(\bar{x}_1)) d\lambda \right) (2m' \beta_0(x(\bar{x}_1)) y_3(x(\bar{x}_1), \epsilon) y_7(\epsilon)) \right. \\ & \left. \left. g_1(x(\bar{x}_1)) d\epsilon \right] \right]. \end{aligned}$$

After applying the limit  $\bar{x}_1 \rightarrow t^+$  on both sides of above equation yields

$$\begin{aligned} \lim_{\bar{x}_1 \rightarrow t^+} \frac{\partial \tilde{P}_1}{\partial \bar{x}_1} = & \tilde{P}_1(x(t), t) 2(\beta_1(x(t)) y_7(t) - \mu_1(x(t))) - \frac{\partial \tilde{P}_1(x(t), t)}{\partial t} \\ & + 4m' \beta_0(x(t)) y_3(x(t), t) y_7(t) g_1(x(t)). \end{aligned}$$

Consider the case when  $\bar{x}_1 < t$ , then the derivative takes the following form:

$$\begin{aligned} \frac{\partial \tilde{P}_1}{\partial \bar{x}_1} = & \tilde{P}_1(x(\bar{x}_1), t) \left( \beta_1(x(\bar{x}_1)) y_7(t) - \mu_1(x(\bar{x}_1)) + \frac{\partial}{\partial t} \int_0^{\bar{x}_1} \beta_1(x(\lambda)) y_7(t) - \mu_1(x(\lambda)) \right. \\ & \left. d\lambda \right) - \frac{\partial \tilde{P}_1(x(\bar{x}_1), t)}{\partial t} + \exp \left( \int_0^{\bar{x}_1} \beta_1(x(\lambda)) y_7(t) - \mu_1(x(\lambda)) d\lambda \right) \\ & \left[ \exp \left( - \int_0^{\bar{x}_1} \beta_1(x(\lambda)) y_7(t) - \mu_1(x(\lambda)) d\lambda \right) 2m' \beta_0(x(\bar{x}_1)) y_3(x(\bar{x}_1), t) y_7(t) \right. \\ & \left. g_1(x(\bar{x}_1)) + \frac{\partial}{\partial t} \int_0^{\bar{x}_1} \exp \left( - \int_0^\epsilon \beta_1(x(\lambda)) y_7(t) - \mu_1(x(\lambda)) d\lambda \right) 2m' \beta_0(x(\epsilon)) \right. \\ & \left. \left. y_3(x(\epsilon), t) y_7(t) g_1(x(\epsilon)) d\epsilon \right] \right], \end{aligned}$$

and, thus after applying limit  $\bar{x}_1 \rightarrow t^-$  on both sides of above equation yields

$$\begin{aligned} \lim_{\bar{x}_1 \rightarrow t^-} \frac{\partial \tilde{P}_1(x(\bar{x}_1), t)}{\partial \bar{x}_1} = & \tilde{P}_1(x(t), t) 2(\beta_1(x(t)) y_7(t) - \mu_1(x(t))) - \frac{\partial \tilde{P}_1(x(t), t)}{\partial t} \\ & + 4m' \beta_0(x(t)) y_3(x(t), t) y_7(t) g_1(x(t)). \end{aligned}$$

Ultimately, it holds that

$$\lim_{\bar{x}_1 \rightarrow t^+} \frac{\partial \tilde{P}_1(x(\bar{x}_1), t)}{\partial \bar{x}_1} = \lim_{\bar{x}_1 \rightarrow t^-} \frac{\partial \tilde{P}_1(x(\bar{x}_1), t)}{\partial \bar{x}_1}.$$

Next, we can calculate the differential quotient at  $(t, x(t))$ . By mean value theorem, we can assign some  $\varrho_h \in (t, t+h)$  (or  $\varrho_h \in (t+h, t)$ ) to each  $h > 0$  or  $(h < 0)$  such that

$$\frac{\tilde{P}_1(x(t+h), t) - \tilde{P}_1(x(t), t)}{h} = \frac{\partial \tilde{P}_1(x(\varrho_h), t)}{\partial \bar{x}_1}.$$

So, we get that

$$\begin{aligned} \frac{\partial \tilde{P}_1(x(t), t)}{\partial \bar{x}_1} &= \lim_{h \rightarrow 0} \frac{\tilde{P}_1(x(t+h), t) - \tilde{P}_1(x(t), t)}{h} = \lim_{h \rightarrow 0} \frac{\partial \tilde{P}_1(x(\varrho_h), t)}{\partial \bar{x}_1} = \lim_{\bar{x}_1 \rightarrow t} \frac{\partial \tilde{P}_1(x(\bar{x}_1), t)}{\partial \bar{x}_1} \\ &= \tilde{P}_1(x(t), t) 2(\beta_1(x(t))y_7(t) - \mu_1(x(t))) - \frac{\partial \tilde{P}_1(x(t), t)}{\partial t} \\ &\quad + 4m'\beta_0(x(t))y_3(x(t), t)y_7(t)g_1(x(t)), \end{aligned}$$

exists and that the partial derivative is continuous in the direction of  $\bar{x}_1$ . In the next step, we consider  $\frac{\partial \tilde{P}_1(x(\bar{x}_1), t)}{\partial t}$  for  $\bar{x}_1 \geq t$ , then by using the definition of  $P_1^\theta$  we have

$$\begin{aligned} \frac{\partial \tilde{P}_1(x(\bar{x}_1), t)}{\partial t} &= \tilde{P}_1(x(\bar{x}_1), t) \left( \beta_1(x(\bar{x}_1))y_7(t) - \mu_1(x(\bar{x}_1)) + \frac{\partial}{\partial \bar{x}_1} \int_0^t \beta_1(x(\bar{x}_1))y_7(\lambda) - \right. \\ &\quad \left. \mu_1(x(\bar{x}_1))d\lambda \right) - \frac{\partial \tilde{P}_1(x(\bar{x}_1), t)}{\partial \bar{x}_1} + \exp \left( \int_0^t \beta_1(x(\bar{x}_1))y_7(\lambda) - \mu_1(x(\bar{x}_1))d\lambda \right) \\ &\quad \left[ \exp \left( - \int_0^t y_7(\lambda)\beta_1(x(\bar{x}_1)) - \mu_1(x(\bar{x}_1))d\lambda \right) (2m'\beta_0(x(\bar{x}_1))y_3(x(\bar{x}_1), t) \right. \\ &\quad \left. y_7(t))g_1(x(\bar{x}_1)) + \frac{\partial}{\partial \bar{x}_1} \int_0^t \exp \left( - \int_0^\epsilon \beta_1(x(\bar{x}_1))y_7(\lambda) - \mu_1(x(\bar{x}_1))d\lambda \right) \right. \\ &\quad \left. (2m'\beta_0(x(\bar{x}_1))y_3(x(\bar{x}_1), \epsilon)y_7(\epsilon))g_1(x(\bar{x}_1))d\epsilon \right]. \end{aligned}$$

and, thus applying the limit  $\bar{x}_1 \rightarrow t^+$ , yields

$$\begin{aligned} \lim_{\bar{x}_1 \rightarrow t^+} \frac{\partial \tilde{P}_1(x(\bar{x}_1), t)}{\partial t} &= \tilde{P}_1(x(t), t) 2(\beta_1(x(t))y_7(t) - \mu_1(x(t))) - \frac{\partial \tilde{P}_1(x(t), t)}{\partial t} \\ &\quad + 4m'\beta_0(x(t))y_3(x(t), t)y_7(t)g_1(x(t)). \end{aligned}$$

If  $\bar{x}_1 < t$ , then  $\frac{\partial \tilde{P}_1(x(\bar{x}_1), t)}{\partial t}$  reads

$$\begin{aligned} \frac{\partial \tilde{P}_1}{\partial t} &= \tilde{P}_1(x(\bar{x}_1), t) \left( \beta_1(x(\bar{x}_1))y_7(t) - \mu_1(x(\bar{x}_1)) + \frac{\partial}{\partial t} \int_0^{\bar{x}_1} \beta_1(x(\lambda))y_7(t) - \mu_1(x(\lambda)) \right. \\ &\quad \left. d\lambda \right) - \frac{\partial \tilde{P}_1(x(\bar{x}_1), t)}{\partial \bar{x}_1} + \exp \left( \int_0^{\bar{x}_1} \beta_1(x(\lambda))y_7(t) - \mu_1(x(\lambda))d\lambda \right) \\ &\quad \left[ \exp \left( - \int_0^{\bar{x}_1} \beta_1(x(\lambda))y_7(t) - \mu_1(x(\lambda))d\lambda \right) 2m'\beta_0(x(\bar{x}_1))y_3(x(\bar{x}_1), t)y_7(t) \right. \\ &\quad \left. g_1(x(\bar{x}_1)) + \frac{\partial}{\partial t} \int_0^{\bar{x}_1} \exp \left( - \int_0^\epsilon \beta_1(x(\lambda))y_7(t) - \mu_1(x(\lambda))d\lambda \right) 2m'\beta_0(x(\epsilon)) \right. \\ &\quad \left. y_3(x(\epsilon), t)y_7(t)g_1(x(\epsilon))d\epsilon \right], \end{aligned}$$

which after applying limit,  $\bar{x}_1 \rightarrow t^-$ , reduces to

$$\begin{aligned} \lim_{\bar{x}_1 \rightarrow t^-} \frac{\partial \tilde{P}_1(x(\bar{x}_1), t)}{\partial t} &= \tilde{P}_1(x(t), t) 2(\beta_1(x(t))y_7(t) - \mu_1(x(t))) - \frac{\partial \tilde{P}_1(x(t), t)}{\partial t} \\ &\quad + 4m'\beta_0(x(t))y_3(x(t), t)y_7(t)g_1(x(t)). \end{aligned}$$

Thus, it holds that

$$\lim_{\bar{x}_1 \rightarrow t^+} \frac{\partial \tilde{P}_1(x(\bar{x}_1), t)}{\partial t} = \lim_{\bar{x}_1 \rightarrow t^-} \frac{\partial \tilde{P}_1(x(\bar{x}_1), t)}{\partial t}.$$

This gives the claim of continuity of  $\tilde{P}_1$  and  $\frac{\partial \tilde{P}_1(x(\bar{x}_1), t)}{\partial \bar{x}_1}$ .

This completes the proof.  $\square$

**Remark 4.4.1.** Note that not every equivalence class in  $L^1([0, T'])$  contains a continuous representative. However, for all  $y \in Y_{T'}^\theta$ , the classes  $C_0^\theta[y]$ ,  $C_1^\theta[y]$ ,  $P_0^\theta[y]$ ,  $P_1^\theta[y]$ ,  $M_0^\theta[y]$ ,  $M_1^\theta[y]$  and  $s^\theta[y]$  each contain a continuous representative. This has been shown in Lemma 4.4.1. Therefore, for each fixed point of  $S^\theta$  there exists a continuous representative.

**Lemma 4.4.2.** Let  $y = (y_1, y_2, y_3, y_4, y_5, y_6, y_7) \in Y_{T'}^\theta$  with continuous representative  $\bar{y} = (\bar{y}_1, \bar{y}_2, \bar{y}_3, \bar{y}_4, \bar{y}_5, \bar{y}_6, \bar{y}_7)$ . Then there exists a unique solution to the decoupled ODE-PDE system.

*Proof.* The claim for  $C_0^\theta[y]$ ,  $C_1^\theta[y]$ ,  $M_0^\theta[y]$ ,  $M_1^\theta[y]$ ,  $s^\theta[y]$  follows from ODE theory, see Lemma 1. To prove that the continuous representatives of  $P_0^\theta[y]$  and  $P_1^\theta[y]$  are unique, we need to derive the explicit relations for  $P_0$  and  $P_1$  and, therefore, we use the method of characteristics to solve both PDEs (4.14) and (4.15). We start with the transformation of the PDEs using previously defined  $\tilde{P}_0(x, t) := g_0(x)P_0(x, t)$  and  $\tilde{P}_1(x, t) := g_1(x)P_1(x, t)$  for  $t \in [0, T']$  and  $x \in [x_0, x_1]$ . Then for all  $t \in (0, T')$  and  $x \in (x_0, x_1)$ , we have from Eq. (4.14)

$$\frac{\partial}{\partial t} \left( \frac{\tilde{P}_0(x, t)}{g_0(x)} \right) + \frac{\partial}{\partial x} \left( \frac{g_0(x)\tilde{P}_0(x, t)}{g_0(x)} \right) = [(1 - 2m')\beta_0(x)\bar{y}_7(t) - \mu_0(x)] \left( \frac{\tilde{P}_0(x, t)}{g_0(x)} \right)$$

or equivalently

$$\frac{\partial}{\partial t} \tilde{P}_0(x, t) + g_0(x) \frac{\partial}{\partial x} \tilde{P}_0(x, t) = [(1 - 2m')\beta_0(x)\bar{y}_7(t) - \mu_0(x)] \tilde{P}_0(x, t). \quad (4.24)$$

Similarly, from Eq. (4.15), we have

$$\begin{aligned} \frac{\partial}{\partial t} \left( \frac{\tilde{P}_1(x, t)}{g_1(x)} \right) + \frac{\partial}{\partial x} \left( \frac{g_1(x)\tilde{P}_1(x, t)}{g_1(x)} \right) &= [\beta_1(x)\bar{y}_7(t) - \mu_1(x)] \left( \frac{\tilde{P}_1(x, t)}{g_1(x)} \right) \\ &\quad + 2m'\beta_0(x)\bar{y}_3(x, t)\bar{y}_7(t), \end{aligned}$$

equivalently

$$\begin{aligned} \frac{\partial}{\partial t} \tilde{P}_1(x, t) + g_1(x) \frac{\partial}{\partial x} \tilde{P}_1(x, t) &= [\beta_1(x)\bar{y}_7(t) - \mu_1(x)] \tilde{P}_1(x, t) \\ &\quad + (2m'\beta_0(x)\bar{y}_3(x, t)\bar{y}_7(t))g_1(x). \end{aligned} \quad (4.25)$$

Next, we use the parameter transform from Lemma 4.3.1 to drop the growth terms (i.e.,  $g_0(x)$  and  $g_1(x)$ ) and introduce  $\bar{x}_0$  and  $\bar{x}_1$  as new maturity variables for  $P_0$  and  $P_1$ , respectively. We obtain

$$\begin{aligned} \frac{\partial}{\partial \bar{x}_0} \tilde{P}_0(x(\bar{x}_0), t) &= \frac{dx}{d\bar{x}_0} \frac{\partial}{\partial x} \tilde{P}_0(x, t) = g_0(x(\bar{x}_0)) \frac{\partial}{\partial x} \tilde{P}_0(x, t), \\ \frac{\partial}{\partial \bar{x}_1} \tilde{P}_1(x(\bar{x}_1), t) &= \frac{dx}{d\bar{x}_1} \frac{\partial}{\partial x} \tilde{P}_1(x, t) = g_1(x(\bar{x}_1)) \frac{\partial}{\partial x} \tilde{P}_1(x, t). \end{aligned}$$

Therefore, from Eqs. (4.24) and (4.25) it follows that

$$\frac{\partial}{\partial t} \tilde{P}_0(x(\bar{x}_0), t) + \frac{\partial}{\partial \bar{x}_0} \tilde{P}_0(x(\bar{x}_0), t) = [(1 - 2m')\beta_0(x(\bar{x}_0))\bar{y}_7(t) - \mu_0(x(\bar{x}_0))] \tilde{P}_0(x(\bar{x}_0), t), \quad (4.26)$$

$$\begin{aligned} \frac{\partial}{\partial t} \tilde{P}_1(x(\bar{x}_1), t) + \frac{\partial}{\partial \bar{x}_1} \tilde{P}_1(x(\bar{x}_1), t) &= [\beta_1(x(\bar{x}_1))\bar{y}_7(t) - \mu_1(x(\bar{x}_1))] \tilde{P}_1(x(\bar{x}_1), t) \\ &+ (2m'\beta_0(x(\bar{x}_1))\bar{y}_3(x(\bar{x}_1), t)\bar{y}_7(t))g_1(x(\bar{x}_1)), \end{aligned} \quad (4.27)$$

respectively. Now, we use the method of characteristics (MOC) to find the explicit relations of both  $\tilde{P}_0(x(\bar{x}_0), t)$  and  $\tilde{P}_1(x(\bar{x}_1), t)$ . Starting with Eq. (4.26), we suppose that  $\tilde{P}_0(x(\bar{x}_0), t)$  can be described by an ODE along the curve  $(x(\phi_1(u)), \phi_2(u)) = \phi(u)$ , and we define

$$\begin{aligned} \dot{\phi}_1(u) &:= 1 \Rightarrow \phi_1(u) = u + c_1, \\ \dot{\phi}_2(u) &:= 1 \Rightarrow \phi_2(u) = u + c_2, \\ \text{and } z(u) &:= \tilde{P}_0(x(\phi_1(u)), \phi_2(u)), \end{aligned}$$

where  $c_1, c_2 \in \mathbb{R}$  are constants. Then, it holds that

$$\begin{aligned} \frac{dz}{du} &= \frac{d\tilde{P}_0(x(\phi_1(u)), \phi_2(u))}{du} \\ &= \frac{\partial \tilde{P}_0(x(\phi_1(u)), \phi_2(u))}{\partial x} \frac{dx(\phi_1(u))}{d\phi_1} \frac{d\phi_1(u)}{du} + \frac{\partial \tilde{P}_0(x(\phi_1(u)), \phi_2(u))}{\partial \phi_2} \frac{d\phi_2(u)}{du} \\ &= ((1 - 2m')\beta_0(x(\phi_1(u)))\bar{y}_7(\phi_2(u)) - \mu_0(x(\phi_1(u)))) \tilde{P}_0(x(\phi_1(u)), \phi_2(u)) \\ &= ((1 - 2m')\beta_0(x(\phi_1(u)))\bar{y}_7(\phi_2(u)) - \mu_0(x(\phi_1(u)))) z(u). \end{aligned} \quad (4.28)$$

We can describe  $\tilde{P}_0$  by ODE (4.28) such that

$$\begin{aligned} \tilde{P}_0(x(u + c_1), u + c_2) &= \tilde{P}_0(x(\phi_1(u)), \phi_2(u)) = z(u) \\ &= \exp \left\{ \int_0^u (1 - 2m')\beta_0(x(\phi_1(\tilde{u})))\bar{y}_7(\phi_2(\tilde{u})) - \mu_0(x(\phi_1(\tilde{u}))) d\tilde{u} \right\} z(0) \\ &= \exp \left\{ \int_0^u (1 - 2m')\beta_0(x(\phi_1(\tilde{u})))\bar{y}_7(\phi_2(\tilde{u})) - \mu_0(x(\phi_1(\tilde{u}))) d\tilde{u} \right\} \tilde{P}_0(x(\phi_1(0)), \phi_2(0)) \\ &= \exp \left\{ \int_0^u (1 - 2m')\beta_0(x(\tilde{u} + c_1))\bar{y}_7(\tilde{u} + c_2) - \mu_0(x(\tilde{u} + c_1)) d\tilde{u} \right\} \tilde{P}_0(x(c_1), c_2). \end{aligned}$$

Next, we define the boundary set  $\Gamma := \{[x_0, x^*] \times \{0\}\} \cup \{\{x_0\} \times [0, T']\}$ , such that if a curve  $(x(\phi_1(u)), \phi_2(u))$  starts in  $\Gamma$ , then we can use the boundary conditions to determine  $\tilde{P}_0(x(c_1), c_2)$ . For  $(x(u + c_1), u + c_2)$  to be in  $\Gamma$ , either  $c_1 = 0$  or  $c_2 = 0$ . This leads to the following two scenarios. In the first case, we consider  $c_1 = 0$  and  $c_2 \in [0, T')$  is arbitrary, then we have

$$\tilde{P}_0(x(u), u + c_2) = \exp \left\{ \int_0^u (1 - 2m')\beta_0(x(\tilde{u}))\bar{y}_7(\tilde{u} + c_2) - \mu_0(x(\tilde{u})) d\tilde{u} \right\} \tilde{P}_0(x(0), c_2).$$

We can now use the solution along these characteristics in order to get a solution in  $\{(x(\bar{x}_0), t) | t \in [0, T'], \bar{x}_0 \in [0, \min(\bar{x}_0^*, t)]\}$ :

$$\bar{x}_0 \stackrel{!}{=} \phi_1(u) = u + c_1 = u \Rightarrow u = \bar{x}_0 \text{ and } t \stackrel{!}{=} \phi_2(u) = u + c_2 \Rightarrow c_2 = t - u,$$



which implies

$$\tilde{P}_0(x(\bar{x}_0), t) = \exp \left\{ \int_0^{\bar{x}_0} (1 - 2m') \beta_0(x(\tilde{u})) \bar{y}_7(\tilde{u} + t - \bar{x}_0) - \mu_0(x(\tilde{u})) d\tilde{u} \right\} h_0(t - \bar{x}_0) g_0(x_0).$$

This proves the equation for  $g_0(x(\bar{x}_0))P_0(x(\bar{x}_0), t)$  in the case for  $\bar{x}_0 < t$ . Next, we consider  $c_1 \in [0, \bar{x}_0^*)$  is arbitrary and  $c_2 = 0$ , then we have

$$\tilde{P}_0(x(u + c_1), u) = \exp \left\{ \int_0^u (1 - 2m') \beta_0(x(\tilde{u} + c_1)) \bar{y}_7(\tilde{u}) - \mu_0(x(\tilde{u} + c_1)) d\tilde{u} \right\} \tilde{P}_0(x(c_1), 0).$$

In a similar way, we can now use the solution along these characteristics in order to get a solution in  $\{(x(\bar{x}_0), t) | t \in [0, T'], \bar{x} \in [t, \bar{x}_0^*)\}$ :

$$\bar{x}_0 \stackrel{!}{=} \phi_1(u) = u + c_1 \Rightarrow c_1 = \bar{x}_0 - u \text{ and } t \stackrel{!}{=} \phi_2(u) = u \Rightarrow t = u$$

and, thus

$$\begin{aligned} \tilde{P}_0(x(\bar{x}_0), t) &= \exp \left\{ \int_0^t (1 - 2m') \beta_0(x(\tilde{u} + \bar{x}_0 - t)) \bar{y}_7(\tilde{u}) - \mu_0(x(\tilde{u} + \bar{x}_0 - t)) d\tilde{u} \right\} \\ &\quad \times f_0(x(\bar{x}_0 - t)) g_0(x(\bar{x}_0 - t)). \end{aligned}$$

This proves the equation for  $g_0(x(\bar{x}_0))P_0(x(\bar{x}_0), t)$  in the case for  $\bar{x}_0 \geq t$ . Now, we find the explicit relation for  $\tilde{P}_1(x(\bar{x}_1), t)$  from Eq. (4.27). Following the similar way, we suppose that  $\tilde{P}_1(x(\bar{x}_1), t)$  can be described by an ODE along the curve  $(x(\varphi_1(u)), \varphi_2(u)) = \varphi(u)$  and we define

$$\begin{aligned} \dot{\varphi}_1(u) &:= 1 \Rightarrow \varphi_1(u) = u + k_1, \\ \dot{\varphi}_2(u) &:= 1 \Rightarrow \varphi_2(u) = u + k_2, \\ z(u) &:= \tilde{P}_1(x(\varphi_1(u)), \varphi_2(u)), \end{aligned}$$

where  $k_1, k_2 \in \mathbb{R}$  are constants. Then, proceeding in a similar manner as for  $P_0$ , it holds that

$$\begin{aligned} \frac{dz}{du} &= (\beta_1(x(\varphi_1(u))) \bar{y}_7(\varphi_2(u)) - \mu_1(x(\varphi_1(u)))) z(u) \\ &\quad + (2m' \beta_0(x(\varphi_1(u))) \bar{y}_3(x(\varphi_1(u)), \varphi_2(u)) \bar{y}_7(\varphi_2(u))) g_1(x(\varphi_1(u))). \end{aligned} \quad (4.29)$$

We can describe  $\tilde{P}_1$  by the ODE (4.29) such that

$$\begin{aligned} \tilde{P}_1(x(u+k_1), u+k_2) &= \tilde{P}_1(x(\varphi_1(u)), \varphi_2(u)) = z(u) \\ &= \exp \left\{ \int_0^u \beta_1(x(\varphi_1(\tilde{u}))) \bar{y}_7(\varphi_2(\tilde{u})) - \mu_1(x(\varphi_1(\tilde{u}))) d\tilde{u} \right\} \\ &\quad \times \left[ \int_0^u \exp \left\{ - \int_0^{\tilde{u}} \beta_1(x(\varphi_1(\tilde{v}))) \bar{y}_7(\varphi_2(\tilde{v})) - \mu_1(x(\varphi_1(\tilde{v}))) d\tilde{v} \right\} \right. \\ &\quad \left. (2m' \beta_0(x(\varphi_1(\tilde{u}))) \bar{y}_3(x(\varphi_1(\tilde{u})), \varphi_2(\tilde{u})) \bar{y}_7(\varphi_2(\tilde{u}))) g_1(x(\varphi_1(\tilde{u}))) d\tilde{u} + z(0) \right] \\ &= \exp \left\{ \int_0^u \beta_1(x(\tilde{u} + k_1)) \bar{y}_7(\tilde{u} + k_2) - \mu_1(x(\tilde{u} + k_1)) d\tilde{u} \right\} \\ &\quad \times \left[ \int_0^u \exp \left\{ - \int_0^{\tilde{u}} \beta_1(x(\tilde{v} + k_1)) \bar{y}_7(\tilde{v} + k_2) - \mu_1(x(\tilde{v} + k_1)) d\tilde{v} \right\} (2m' \right. \\ &\quad \left. \beta_0(x(\tilde{u} + k_1)) \bar{y}_3(x(\tilde{u} + k_1), \tilde{u} + k_2) \bar{y}_7(\tilde{u} + k_2)) g_1(x(\tilde{u} + k_1)) d\tilde{u} + \tilde{P}_0(x(k_1), k_2) \right], \end{aligned}$$

where we have used  $z(0) = \tilde{P}_1(x(\phi_1(0)), \phi_2(0))$  with  $\phi_1(0) = k_1$  and  $\phi_2(0) = k_2$ . Next, we define the boundary set  $\Gamma := \{[x_0, x_1] \times \{0\}\} \cup \{\{x_0\} \times [0, T']\}$  such that if a curve  $(x(\varphi_1(u)), \varphi_2(u))$  starts in  $\Gamma$ , then we can use boundary conditions to determine  $\tilde{P}_1(x(k_1), k_2)$ . If we want  $(x(u + k_1), u + k_2)$  to be in  $\Gamma$ , then either  $k_1 = 0$  or  $k_2 = 0$ . This leads to the following two cases. Firstly, we take  $k_1 = 0$  and  $k_2 \in [0, T')$  is arbitrary, then we have

$$\begin{aligned} \tilde{P}_1(x(u), u + k_2) &= \exp \left\{ \int_0^u \beta_1(x(\tilde{u})) \bar{y}_7(\tilde{u} + k_2) - \mu_1(x(\tilde{u})) d\tilde{u} \right\} \\ &\quad \times \left[ \int_0^u \exp \left\{ - \int_0^{\tilde{u}} \beta_1(x(\tilde{v})) \bar{y}_7(\tilde{v} + k_2) - \mu_1(x(\tilde{v})) d\tilde{v} \right\} \right. \\ &\quad \left. (2m' \beta_0(x(\tilde{u})) \bar{y}_3(x(\tilde{u}), \tilde{u} + k_2) \bar{y}_7(\tilde{u} + k_2)) g_1(x(\tilde{u})) d\tilde{u} + \tilde{P}_0(x(0), k_2)) \right]. \end{aligned}$$

We can now use the solution along these characteristics in order to get a solution in  $\{(x(\bar{x}_1), t) | t \in [0, T'], \bar{x}_1 \in [0, \min(\bar{x}_1^*, t))\}$ :

$$\bar{x}_1 \stackrel{!}{=} \varphi_1(u) = u + k_1 = u \Rightarrow u = \bar{x}_1 \text{ and } t \stackrel{!}{=} \varphi_2(u) = u + k_2 \Rightarrow k_2 = t - u.$$

Thus, it implies

$$\begin{aligned} \tilde{P}_1(x(\bar{x}_1), t) &= \exp \left\{ \int_0^{\bar{x}_1} \beta_1(x(\tilde{u})) \bar{y}_7(\tilde{u} + t - \bar{x}_1) - \mu_1(x(\tilde{u})) d\tilde{u} \right\} \\ &\quad \times \left[ \int_0^{\bar{x}_1} \exp \left\{ - \int_0^{\tilde{u}} \beta_1(x(\tilde{v})) \bar{y}_7(\tilde{v} + t - \bar{x}_1) - \mu_1(x(\tilde{v})) d\tilde{v} \right\} (2m' \beta_0(x(\tilde{u})) \right. \\ &\quad \left. \bar{y}_3(x(\tilde{u}), \tilde{u} + t - \bar{x}_1) \bar{y}_7(\tilde{u} + t - \bar{x}_1)) g_1(x(\tilde{u})) d\tilde{u} + h_1(t - \bar{x}_1) g_1(x_0) \right]. \end{aligned}$$

This proves the equation for  $g_1(x(\bar{x}_1)) P_1(x(\bar{x}_1), t)$  in the case for  $\bar{x}_1 < t$ . Secondly, we consider  $k_1 \in [0, \bar{x}_1^*)$  is arbitrary and  $k_2 = 0$ , then we have

$$\begin{aligned} \tilde{P}_1(x(u + k_1), u) &= \exp \left\{ \int_0^u \beta_1(x(\tilde{u} + k_1)) \bar{y}_7(\tilde{u}) - \mu_1(x(\tilde{u} + k_1)) d\tilde{u} \right\} \\ &\quad \times \left[ \int_0^u \exp \left\{ - \int_0^{\tilde{u}} \beta_1(x(\tilde{v} + k_1)) \bar{y}_7(\tilde{v}) - \mu_1(x(\tilde{v} + k_1)) d\tilde{v} \right\} (2m' \right. \\ &\quad \left. \beta_0(x(\tilde{u} + k_1)) \bar{y}_3(x(\tilde{u} + k_1), \tilde{u}) \bar{y}_7(\tilde{u})) g_1(x(\tilde{u} + k_1)) d\tilde{u} + \tilde{P}_0(x(k_1), 0) \right]. \end{aligned}$$

Similar to the last case, we can now use the solution along these characteristics in order to get a solution in  $\{(x(\bar{x}_1), t) | t \in [0, T'], \bar{x}_1 \in [t, \bar{x}_1^*)\}$ :

$$\bar{x}_1 \stackrel{!}{=} \varphi_1(u) = u + k_1 \Rightarrow k_1 = \bar{x}_1 - u \text{ and } t \stackrel{!}{=} \varphi_2(u) = u \Rightarrow t = u.$$

Finally, we have

$$\begin{aligned} \tilde{P}_1(x(\bar{x}_1), t) &= \exp \left\{ \int_0^t \beta_1(x(\tilde{u} + \bar{x}_1 - t)) \bar{y}_7(\tilde{u}) - \mu_1(x(\tilde{u} + \bar{x}_1 - t)) d\tilde{u} \right\} \\ &\quad \times \left[ \int_0^t \exp \left\{ - \int_0^{\tilde{u}} \beta_1(x(\tilde{v} + \bar{x}_1 - t)) \bar{y}_7(\tilde{v}) - \mu_1(x(\tilde{v} + \bar{x}_1 - t)) d\tilde{v} \right\} \right. \\ &\quad (2m' \beta_0(x(\tilde{u} + \bar{x}_1 - t)) \bar{y}_3(x(\tilde{u} + \bar{x}_1 - t, \tilde{u})) \bar{y}_7(\tilde{u})) g_1(x(\tilde{u} + \bar{x}_1 - t)) d\tilde{u} \\ &\quad \left. + f_1(x(\bar{x}_1 - t)) g_1(x(\bar{x}_1 - t)) \right]. \end{aligned}$$

This proves the equation for  $g_1(x(\bar{x}_1))P_1(x(\bar{x}_1), t)$  in the case for  $\bar{x}_1 \geq t$ .  $\square$

**Theorem 4.4.1.** Let  $y = (y_1, y_2, y_3, y_4, y_5, y_6, y_7) \in Y_{T'}^\theta$ . Then  $y$  is a fixed point of  $S^\theta$  if and only if its continuous representative solves the basic ODE-PDE system on  $[0, T']$ .

*Proof.* If  $y$  is a fixed point of  $S^\theta$ , then its continuous representative solves the basic PDE system on  $[0, T']$ . This follows from Lemma 4.4.1. For the other case, if continuous representative  $\bar{y}$  of  $y$  solves the basic ODE-PDE system on  $[0, T']$  then  $y$  is a fixed point of  $S^\theta$ . Here, we can argue that if  $\bar{y}$  solves the basic ODE-PDE system on  $[0, T']$  then it also solves the decoupled ODE-PDE system and since the solution to this system is unique (by Lemma 4.4.2) and equal to the continuous representative of

$$S^\theta := (C_0^\theta[y], C_1^\theta[y], P_0^\theta[y], P_1^\theta[y], M_0^\theta[y], M_1^\theta[y], s^\theta[y]),$$

(by Lemma 4.4.1), we get that  $y$  must coincide with  $S^\theta[y]$  almost everywhere, i.e.,  $y$  must be a fixed point of  $S^\theta$ .  $\square$

## 4.5 Boundedness of solution

**Proposition 4.5.1.** For all  $y = (y_1, y_2, y_3, y_4, y_5, y_6, y_7) \in Y_{T'}^\theta$  with a continuous representative, it holds that

$$\begin{aligned} C_i^\theta[y](t) &\in [0, \bar{C}_i(\theta, t)], \\ \int_{x_0}^{x^*} P_i^\theta[y](x, t) dx &\leq \bar{P}_i(\theta, t), \quad P_i^\theta[y](x, t) \geq 0, \\ M_i^\theta[y](t) &\in [0, \bar{M}_i(\theta, t)], \\ s^\theta[y](t) &\in [0, \bar{s}(\theta, t)], \end{aligned}$$

for almost all  $t \in [0, T']$  and  $x \in [x_0, x^*]$ , where  $i \in \{0, 1\}$ .

*Proof.* It is obvious (from the definition of operators) that  $C_0^\theta, C_1^\theta, P_0^\theta, P_1^\theta, M_0^\theta, M_1^\theta$ , and  $s^\theta$  are non-negative almost everywhere. To find the upper bounds, we let  $\bar{y} = (\bar{y}_1, \bar{y}_2, \bar{y}_3, \bar{y}_4, \bar{y}_5, \bar{y}_6, \bar{y}_7)$ , denote the continuous representative of  $y$  and use  $C_0, C_1, P_0, P_1, M_0, M_1$ , and  $s$  to refer to the continuous representative of  $C_0^\theta, C_1^\theta, P_0^\theta, P_1^\theta, M_0^\theta, M_1^\theta$  and  $s^\theta$ , respectively. We begin with finding the upper bound for  $C_0$  and by Lemma 4.4.1, for all  $t \in (0, T')$  we have

$$\begin{aligned} \frac{d}{dt} C_0(t) &= ((1 - 2m)\bar{\alpha}_{S_0} - m\bar{\alpha}_{A_0} - \bar{\alpha}_{D_0})\bar{y}_7(t) - \delta_{C_0} k_0 C_0(t) \\ &\leq ((1 - 2m)\bar{\alpha}_{S_0} - m\bar{\alpha}_{A_0} - \bar{\alpha}_{D_0})\bar{s}(t, \theta) - \delta_{C_0} k_0 C_0(t). \end{aligned}$$

Hence,

$$\bar{s}(t, \theta) = \frac{\delta_{C_0}}{(1 - 2m)\bar{\alpha}_{S_0} - m\bar{\alpha}_{A_0} - \bar{\alpha}_{D_0}} \Rightarrow \frac{d}{dt} C_0(t) \leq 0.$$

We get that  $C_0(t) \leq \bar{C}_0(t, \theta)$  for all  $t \in [0, T']$  together with  $\bar{C}_0(0, \theta) = c_0$ . Next, we consider  $C_1$  and for all  $t \in (0, T')$ , we have

$$\begin{aligned} \frac{d}{dt} C_1(t) &= ((\bar{\alpha}_{S_1} - \bar{\alpha}_{D_1})\bar{y}_7(t) - \delta_{C_1})k_1 C_1(t) + (2m\bar{\alpha}_{S_0} + m\bar{\alpha}_{A_0})\bar{y}_7(t)k_0 \bar{y}_1(t) \\ &\leq (\bar{\alpha}_{S_1} \bar{s}(t, \theta) - \delta_{C_1})k_1 C_1(t) + (2m\bar{\alpha}_{S_0} + m\bar{\alpha}_{A_0})\bar{s}(t, \theta)k_0 \bar{C}_0(t, \theta). \end{aligned}$$

Therefore,

$$C_1(t) = \overline{C}_1(t, \theta) \Rightarrow \frac{d}{dt} C_1(t) \leq 0.$$

This proves that  $C_1(t) \leq \overline{C}_1(t, \theta)$  for all  $t \in [0, T']$ . Now, we consider  $P_0$  and for  $t \in [0, T']$ , we have

$$\begin{aligned} \int_{x_0}^{x^*} P_0(t, x) dx &= \int_0^{\bar{x}_0^*} g_0(x(\bar{x}_0)) P_0(t, x(\bar{x}_0)) d\bar{x}_0 \\ &= \int_0^t g_0(x(\bar{x}_0)) P_0(t, x(\bar{x}_0)) d\bar{x}_0 + \int_t^{\bar{x}_0^*} g_0(x(\bar{x}_0)) P_0(t, x(\bar{x}_0)) d\bar{x}_0 \\ &= \int_0^t \exp \left( \int_0^{\bar{x}_0} (1 - 2m') \beta_0(x(\lambda)) y_7(\lambda + t - \bar{x}_0) - \mu_0(x(\lambda)) d\lambda \right) h_0(t - \bar{x}_0) \\ &\quad g_0(x_0) d\bar{x}_0 + \int_t^{\bar{x}_0^*} f_0(x(\bar{x}_0 - t)) \exp \left( \int_0^t (1 - 2m') \beta_0(x(\lambda + \bar{x}_0 - t)) y_7(\lambda) \right. \\ &\quad \left. - \mu_0(x(\lambda + \bar{x}_0 - t)) d\lambda \right) g_0(x(\bar{x}_0 - t)) d\bar{x}_0. \end{aligned}$$

Using Definition 4.3.2, we obtain:

$$\begin{aligned} \int_{x_0}^{x^*} P_0(t, x) dx &\leq \bar{h}_0 g_0(x_0) \int_0^t \exp \left( ((1 - 2m') \bar{\beta}_0 \bar{s}(\theta, t) - \bar{\mu}_0) \bar{x}_0 \right) d\bar{x}_0 + \int_t^{\bar{x}_0^*} f_0(x(\bar{x}_0 - t)) \\ &\quad \exp \left( ((1 - 2m') \bar{\beta}_0 \bar{s}(\theta, t) - \bar{\mu}_0) t \right) g_0(x(\bar{x}_0 - t)) d\bar{x}_0 \\ &= \exp \left( ((1 - 2m') \bar{\beta}_0 \bar{s}(\theta, t) - \bar{\mu}_0) t \right) \left( ((1 - 2m') \bar{\beta}_0 \bar{s}(\theta, t) - \bar{\mu}_0) \bar{h}_0 g_0(x_0) \right. \\ &\quad \left. + \|f_0\|_1 \right). \end{aligned}$$

Thus, when  $\bar{s}(\theta, t) = 1$ , we have

$$\int_{x_0}^{x^*} P_0(t, x) dx \leq \exp \left( ((1 - 2m') \bar{\beta}_0 - \bar{\mu}_0) t \right) \left( ((1 - 2m') \bar{\beta}_0 - \bar{\mu}_0) \bar{h}_0 g_0(x_0) + \|f_0\|_1 \right).$$

Next, we want to show the upper bound of  $P_1(t, x)$ . Considering  $P_1$  for  $t \in [0, T']$ , we have

$$\begin{aligned} \int_{x_0}^{x^*} P_1(t, x) dx &= \int_0^{\bar{x}_1^*} g_1(x(\bar{x}_1)) P_1(t, x(\bar{x}_1)) d\bar{x}_1 \\ &= \int_0^t g_1(x(\bar{x}_1)) P_1(t, x(\bar{x}_1)) d\bar{x}_1 + \int_t^{\bar{x}_1^*} g_1(x(\bar{x}_1)) P_1(t, x(\bar{x}_1)) d\bar{x}_1. \end{aligned}$$

Then, by using  $P_1(t, x(\bar{x}_1))$  and Definition 4.3.2, it reduces to

$$\begin{aligned} \int_{x_0}^{x^*} P_1(t, x) dx &\leq \int_0^t \exp \left( \int_0^{\bar{x}_1} (\bar{\beta}_1 \bar{s}(\theta, t) - \bar{\mu}_1) d\lambda \right) \left[ \int_0^{\bar{x}_1} \exp \left\{ - \int_0^\epsilon (\bar{\beta}_1 \bar{s}(\theta, t) - \bar{\mu}_1) d\lambda \right\} \right. \\ &\quad \left. (2m' \bar{\beta}_0 \bar{P}_0(\theta, t) \bar{s}(\theta, t)) \bar{g}_1 d\epsilon + \bar{h}_1 g_1(x_0) \right] d\bar{x}_1 + \int_t^{\bar{x}_1^*} \exp \left( \int_0^t (\bar{\beta}_1 \bar{s}(\theta, t) \right. \\ &\quad \left. - \bar{\mu}_1) d\lambda \right) \left[ \int_0^\epsilon \exp \left\{ - \int_0^\epsilon (\bar{\beta}_1 \bar{s}(\theta, t) - \bar{\mu}_1) d\lambda \right\} (2m' \bar{\beta}_0 \bar{P}_0(\theta, t) \bar{s}(\theta, t)) \bar{g}_1 d\epsilon \right. \\ &\quad \left. + f_1(x(\bar{x}_1 - t)) g_1(x(\bar{x}_1 - t)) \right] d\bar{x}_1 \\ &= (\bar{\mu}_1 - \bar{\beta}_1 \bar{s}(\theta, t)) (2m' \bar{\beta}_0 \bar{P}_0(\theta, t) \bar{s}(\theta, t)) \bar{g}_1 \bar{x}_1^* + \exp \left( (\bar{\beta}_1 \bar{s}(\theta, t) - \bar{\mu}_1) t \right) \\ &\quad (\bar{h}_1 g_1(x_0) (\bar{\beta}_1 \bar{s}(\theta, t) - \bar{\mu}_1) + \|f_1\|_1). \end{aligned}$$

Now, consider  $M_0$  and for all  $t \in (0, T')$ , we have

$$\frac{d}{dt}M_0(t) = g_0(x^*)\bar{y}_3(x^*, t) - \delta_{M_0}M_0 \leq g_0(x^*)\bar{P}_0(\theta, t) - \delta_{M_0}M_0.$$

Thus,

$$M_0(t) = \bar{M}_0(t, \theta) \Rightarrow \frac{d}{dt}M_0(t) \leq 0.$$

This proves that  $M_0(t) \leq \bar{M}_0(t, \theta)$  for all  $t \in [0, T']$ . Next, we take  $M_1$  and for all  $t \in (0, T')$ , it follows that

$$\begin{aligned} \frac{d}{dt}M_1(t) &= g_1(x^*)\bar{y}_4(x^*, t) + 2m'\beta_0(x^*)\bar{y}_3(x^*, t)\bar{y}_7(t) - \delta_{M_1}M_1 \\ &\leq g_1(x^*)\bar{P}_1(\theta, t) + 2m'\beta_0(x^*)\bar{P}_0(\theta, t)\bar{s}(\theta, t) - \delta_{M_1}M_1. \end{aligned}$$

Consequently,

$$M_1(t) = \bar{M}_1(t, \theta) \Rightarrow \frac{d}{dt}M_1(t) \leq 0.$$

This proves that  $M_1(t) \leq \bar{M}_1(t, \theta)$  for all  $t \in [0, T']$ . Finally, consider  $s$  and for all  $t \in (0, T')$ , it follows that

$$\frac{d}{dt}s(t) = \mu(1 - s - k_\zeta s(\bar{y}_5(t) + \bar{y}_6(t))) \leq \mu(1 - s).$$

Therefore,

$$s(t) = \bar{s}(t, \theta) \Rightarrow \frac{d}{dt}s(t) \leq 0.$$

This proves that  $s(t) \leq \bar{s}(t, \theta)$  for all  $t \in [0, T']$ . □

**Lemma 4.5.1.** Let  $\theta^a = (c_0^a, c_1^a, m_0^a, m_1^a, s_0^a, f_0^a, f_1^a, h_0^a, h_1^a) \in \Theta$  and  $\eta > 0$ , then for all  $\theta^b = (c_0^b, c_1^b, m_0^b, m_1^b, s_0^b, f_0^b, f_1^b, h_0^b, h_1^b) \in \Theta$  with  $\|\theta^a - \theta^b\|_\Theta < \eta$ , it holds that  $h_0^i(t)$ ,  $h_1^i(t)$ ,  $\bar{C}_0(\theta^i, t)$ ,  $\bar{C}_1(\theta^i, t)$ ,  $\bar{M}_0(\theta^i, t)$ ,  $\bar{M}_1(\theta^i, t)$ ,  $\bar{s}(\theta^i, t)$ ,  $\bar{P}_0(\theta^i, t)$ ,  $\bar{P}_1(\theta^i, t)$ ,  $f_0^i(x)$ ,  $f_1^i(x) \leq \text{const.}(\theta^a, \eta)$  for  $i = a, b$  and all  $t \in [0, T]$ ,  $x \in [x_0, x^*]$ .

*Proof.* The case  $i = a$  is trivial. For  $i = b$ , let  $t \in [0, T]$  and consider

$$\begin{aligned} |h_0^a(t) - h_0^b(t)| &\leq \|h_0^a - h_0^b\|_\infty \leq \|\theta^a - \theta^b\|_\Theta < \eta \implies h_0^b(t) \leq \text{const.}(\theta^a, \eta), \\ |f_0^a(t) - f_0^b(t)| &\leq \|f_0^a - f_0^b\|_\infty \leq \|\theta^a - \theta^b\|_\Theta < \eta \implies f_0^b(t) \leq \text{const.}(\theta^a, \eta). \end{aligned}$$

The proof for other solution variables follows in a similar manner using the definitions of bounds. □

Next, we will employ the general Lemma 2 to prove the boundedness of our solution variables.

**Lemma 4.5.2.** Let  $\theta^a \in \Theta$ ,  $\eta > 0$ . There exist non-negative constants  $C_{C_0}(\theta^a, \eta)$ ,  $C_{C_1}(\theta^a, \eta)$ ,  $C_{M_0}(\theta^a, \eta)$ ,  $C_{M_1}(\theta^a, \eta)$  and  $C_s(\theta^a, \eta)$  such that for all  $\theta^b \in \Theta$  with  $\|\theta^a - \theta^b\| < \eta$ , and  $y^a \in Y_{T'}^{\theta^a}$ ,  $y^b \in Y_{T'}^{\theta^b}$ , it holds that

$$\begin{aligned} |C_0^{\theta^a}[y^a](t) - C_0^{\theta^b}[y^b](t)| &\leq C_{C_0}(\theta^a, \eta) \left( \int_0^t \|y^a - y^b\|_\lambda d\lambda + \|\theta^a - \theta^b\|_\Theta \right), \\ |C_1^{\theta^a}[y^a](t) - C_1^{\theta^b}[y^b](t)| &\leq C_{C_1}(\theta^a, \eta) \left( \int_0^t \|y^a - y^b\|_\lambda d\lambda + \|\theta^a - \theta^b\|_\Theta \right), \\ |M_0^{\theta^a}[y^a](t) - M_0^{\theta^b}[y^b](t)| &\leq C_{M_0}(\theta^a, \eta) \left( \int_0^t \|y^a - y^b\|_\lambda d\lambda + \|\theta^a - \theta^b\|_\Theta \right), \\ |M_1^{\theta^a}[y^a](t) - M_1^{\theta^b}[y^b](t)| &\leq C_{M_1}(\theta^a, \eta) \left( \int_0^t \|y^a - y^b\|_\lambda d\lambda + \|\theta^a - \theta^b\|_\Theta \right), \\ |s^{\theta^a}[y^a](t) - s^{\theta^b}[y^b](t)| &\leq C_s(\theta^a, \eta) \left( \int_0^t \|y^a - y^b\|_\lambda d\lambda + \|\theta^a - \theta^b\|_\Theta \right), \end{aligned}$$

for almost all  $t \in [0, T']$ .

*Proof.* For  $t \in [0, T']$ ,  $x = (x_1, x_2, x_3, x_4, x_5, x_6, x_7) \in X_{T'}$ , and  $\theta \in \Theta$ , we prove the statement for each variable separately. Starting with  $C_0^\theta$ , we define  $p(t, x, \theta) := ((1 - 2m)\bar{\alpha}_{S_0} - m\bar{\alpha}_{A_0} - \bar{\alpha}_{D_0})k_0x_7(t) - \delta_{C_0}k_0$  and  $g(t, x, \theta) := 0$ . Now, let  $\theta^a, \theta^b \in \Theta$  with  $\|\theta^a - \theta^b\| < \eta$  and  $y^a \in Y_{T'}^{\theta^a}$ ,  $y^b \in Y_{T'}^{\theta^b}$ . For  $i = a, b$ , it holds that

$$\begin{aligned} p(t, y^i, \theta^i) &= ((1 - 2m)\bar{\alpha}_{S_0} - m\bar{\alpha}_{A_0} - \bar{\alpha}_{D_0})k_0y_7(\theta^i, t) - \delta_{C_0}k_0 \\ &\leq ((1 - 2m)\bar{\alpha}_{S_0})k_0s(\theta^i, t) \\ &\stackrel{\text{Lemma 4.5.1}}{\leq} \text{const.}(\theta^a, \eta), \\ g(t, y^i, \theta^i) &\leq \text{const.}(\theta^a, \eta), \end{aligned}$$

and

$$\begin{aligned} |p(t, y^a, \theta^a) - p(t, y^b, \theta^b)| &\leq ((1 - 2m)\bar{\alpha}_{S_0} - m\bar{\alpha}_{A_0} - \bar{\alpha}_{D_0})k_0|y_7^a(t) - y_7^b(t)| \\ &\leq \text{const.}(\theta^a, \eta)\|y^a - y^b\|_t, \\ |g(t, y^a, \theta^a) - g(t, y^b, \theta^b)| &\leq \text{const.}(\theta^a, \eta)\|y^a - y^b\|_t. \end{aligned}$$

By Lemma 2, the claim for  $C_0^\theta$ , i.e.,

$$|C_0^{\theta^a}[y^a](t) - C_0^{\theta^b}[y^b](t)| \leq C_{C_0}(\theta^a, \eta) \left( \int_0^t \|y^a - y^b\|_\lambda d\lambda + \|\theta^a - \theta^b\|_\Theta \right),$$

is proved. Further, we consider  $C_1^\theta$  and define  $p(t, x, \theta) := ((\bar{\alpha}_{S_1} - \bar{\alpha}_{D_1})x_7(t) - \delta_{C_1})k_1$  and  $g(t, x, \theta) := (2m\bar{\alpha}_{S_0} + m\bar{\alpha}_{A_0})x_7(t)k_0x_1(t)$ . For  $i = a, b$ , it holds that

$$\begin{aligned} p(t, y^i, \theta^i) &= ((\bar{\alpha}_{S_1} - \bar{\alpha}_{D_1})y_7(\theta^i, t) - \delta_{C_1})k_1 \leq (\bar{\alpha}_{S_1} - \bar{\alpha}_{D_1})k_1s(\theta^i, t) \\ &\stackrel{\text{Lemma 4.5.1}}{\leq} \text{const.}(\theta^a, \eta) \\ g(t, y^i, \theta^i) &= (2m\bar{\alpha}_{S_0} + m\bar{\alpha}_{A_0})y_7(\theta^i, t)k_0y_1(\theta^i, t) \leq (2m\bar{\alpha}_{S_0} + m\bar{\alpha}_{A_0})k_0s(\theta^i, t)C_0(\theta^i, t) \\ &\stackrel{\text{Lemma 4.5.1}}{\leq} \text{const.}(\theta^a, \eta), \end{aligned}$$

and

$$\begin{aligned}
 |p(t, y^a, \theta^a) - p(t, y^b, \theta^b)| &\leq (\bar{\alpha}_{S_1} - \bar{\alpha}_{D_1})k_1|y_7^a(t) - y_7^b(t)| \leq \text{const.}(\theta^a, \eta)\|y^a - y^b\|_t, \\
 |g(t, y^a, \theta^a) - g(t, y^b, \theta^b)| &\leq (2m\bar{\alpha}_{S_0} + m\bar{\alpha}_{A_0})k_0|y_7^a(t)y_1^a(t) - y_7^b(t)y_1^b(t)| \\
 &\leq (2m\bar{\alpha}_{S_0} + m\bar{\alpha}_{A_0})k_0|y_7^a(t)||y_1^a(t) - y_1^b(t)| + |y_1^b(t)||y_7^a(t) - y_7^b(t)| \\
 &\leq \text{const.}(\theta^a, \eta)\|y^a - y^b\|_t,
 \end{aligned}$$

where we used the inequality  $|x_1y_1 - x_2y_2| \leq |x_1| \cdot |y_1 - y_2| + |y_2| \cdot |x_1 - x_2|$ . This gives us the claim for  $C_1^\theta$ . Next, considering  $M_0^\theta$  and defining  $p(t, x, \theta) := -\delta_{M_0}$ , and  $g(t, x, \theta) := g_0(x^*)x_3(x^*, t)$ . For  $i = a, b$ , it holds that

$$\begin{aligned}
 p(t, y^i, \theta^i) &= -\delta_{M_0} \leq \text{const.}(\theta^a, \eta) \\
 g(t, y^i, \theta^i) &= g_0(x^*)y_3^i(x^*, t) \leq g_0(x^*)P_1^i(x^*, t) \\
 &\leq \text{const.}(\theta^a, \eta)
 \end{aligned}$$

and

$$\begin{aligned}
 |p(t, y^a, \theta^a) - p(t, y^b, \theta^b)| &= 0 \leq \text{const.}(\theta^a, \eta)\|y^a - y^b\|_t, \\
 |g(t, y^a, \theta^a) - g(t, y^b, \theta^b)| &\leq g_0(x^*)|y_3^a(x^*, t) - y_3^b(x^*, t)| \\
 &\leq \text{const.}(\theta^a, \eta)\|y^a - y^b\|_t.
 \end{aligned}$$

This gives the claim for  $M_0^\theta$ . Next, we consider  $M_1^\theta$  and define  $p(t, x, \theta) := -\delta_{M_1}$  and  $g(t, x, \theta) := g_1(x^*)x_4(x^*, t) + 2m'\beta_0(x^*)x_3(x^*, t)x_7(t)$ . For  $i = a, b$  it holds that

$$\begin{aligned}
 p(t, y^i, \theta^i) &= -\delta_{M_1} \leq \text{const.}(\theta^a, \eta) \\
 g(t, y^i, \theta^i) &= g_1(x^*)y_4^i(x^*, t) + 2m'\beta_0(x^*)y_3^i(x^*, t)y_7(\theta^i, t) \\
 &= g_1(x^*)P_1^i(x^*, t) + 2m'\beta_0(x^*)P_0^i(x^*, t)s(\theta^i, t) \\
 &\leq g_1(x^*)\bar{P}_1^i(x^*, t) + 2m'\beta_0(x^*)\bar{P}_0^i(x^*, t)\bar{s}(\theta^i, t) \\
 &\leq \text{const.}(\theta^a, \eta)
 \end{aligned}$$

and

$$\begin{aligned}
 |p(t, y^a, \theta^a) - p(t, y^b, \theta^b)| &= 0 \leq \text{const.}(\theta^a, \eta)\|y^a - y^b\|_t, \\
 |g(t, y^a, \theta^a) - g(t, y^b, \theta^b)| &\leq g_1(x^*)|y_4^a(x^*, t) - y_4^b(x^*, t)| + 2m'\beta_0(x^*) \\
 &\quad |y_3^a(x^*, t)y_7^a(t) - y_3^b(x^*, t)y_7^b(t)| \\
 &\leq g_1(x^*)|y_4^a(x^*, t) - y_4^b(x^*, t)| + 2m'\beta_0(x^*)|y_3^a(x^*, t)| \\
 &\quad |y_7^a(t) - y_7^b(t)| + 2m'\beta_0(x^*)|y_7^b(t)||y_3^a(x^*, t) - y_3^b(x^*, t)| \\
 &\leq \text{const.}(\theta^a, \eta)\|y^a - y^b\|_t.
 \end{aligned}$$

This gives the claim for  $M_1^\theta$ . Finally, consider  $s^\theta$  and define  $p(t, x, \theta) := -(\delta_\zeta + k_\zeta(x_5(t) + x_6(t)))$  and  $g(t, x, \theta) := \delta_\zeta$ . For  $i = a, b$  it holds that

$$\begin{aligned}
 p(t, y^i, \theta^i) &= -(\delta_\zeta + k_\zeta(y_5(\theta^i, t) + y_6(\theta^i, t))) \leq -(\delta_\zeta + k_\zeta(\bar{M}_0(\theta^i, t) + \bar{M}_1(\theta^i, t))) \\
 &\leq \text{const.}(\theta^a, \eta) \\
 g(t, y^i, \theta^i) &= \delta_\zeta \leq \text{const.}(\theta^a, \eta)
 \end{aligned}$$

and

$$\begin{aligned}
 |p(t, y^a, \theta^a) - p(t, y^b, \theta^b)| &= k_\zeta (|y_5^a(t) - y_5^b(t)| + |y_6^a(t) - y_6^b(t)|) \\
 &\leq \text{const.}(\theta^a, \eta) \|y^a - y^b\|_t, \\
 |g(t, y^a, \theta^a) - g(t, y^b, \theta^b)| &= 0 \leq \text{const.}(\theta^a, \eta) \|y^a - y^b\|_t.
 \end{aligned}$$

This gives the claim for  $s^\theta$ . □

**Lemma 4.5.3.** Let  $\theta^a \in \Theta$ ,  $\eta > 0$ . There exist non-negative constants  $C_{P_0}(\theta^a, \eta)$  and  $C_{P_1}(\theta^a, \eta)$  such that for all  $\theta^b \in \Theta$  with  $\|\theta^a - \theta^b\| < \eta$  and  $y^a \in Y_{T'}^{\theta^a}$ ,  $y^b \in Y_{T'}^{\theta^b}$ , then for almost all  $t \in [0, T']$ , it holds that

$$\begin{aligned}
 \int_{x_0}^{x^*} |P_0^{\theta^a}[y^a](x, t) - P_0^{\theta^b}[y^b](x, t)| dx &\leq C_{P_0}(\theta^a, \eta) \left( \int_0^t \|y^a - y^b\|_\lambda d\lambda + \|\theta^a - \theta^b\|_\Theta \right), \\
 \int_{x_0}^{x^*} |P_1^{\theta^a}[y^a](x, t) - P_1^{\theta^b}[y^b](x, t)| dx &\leq C_{P_1}(\theta^a, \eta) \left( \int_0^t \|y^a - y^b\|_\lambda d\lambda + \|\theta^a - \theta^b\|_\Theta \right).
 \end{aligned}$$

*Proof.* Let  $t \in [0, T']$ ,  $\theta^a \in \Theta$ ,  $\eta > 0$ ,  $\theta^b \in \Theta$  with  $\|\theta^a - \theta^b\| < \eta$  and  $y^a \in Y_{T'}^{\theta^a}$ ,  $y^b \in Y_{T'}^{\theta^b}$ . Throughout the proof,  $P_0^a$ ,  $P_0^b$ ,  $P_1^a$ , and  $P_1^b$  denote the continuous representatives of the equivalence classes of  $P_0^{\theta^a}[y^a]$ ,  $P_0^{\theta^b}[y^b]$ ,  $P_1^{\theta^a}[y^a]$ , and  $P_1^{\theta^b}[y^b]$ , respectively. Similar to the previous approach, the strategy is to show that the individual integrals are bounded and satisfy the claim and then to show it for the whole term. We start with the  $P_0(x, t)$ . We first consider the integral over the interval  $[t, x^*]$ . It holds that

$$\begin{aligned}
 \int_t^{x^*} |P_0^a(x, t) - P_0^b(x, t)| dx &\leq \int_t^{\bar{x}_0^*} g_0(x(\bar{x}_0 - t)) \left[ f_0^a(x(\bar{x}_0 - t)) \exp \left( \int_0^t (1 - 2m') \right. \right. \\
 &\quad \left. \left. \beta_0(x(\lambda + \bar{x}_0 - t)) y_7^a(\lambda) - \mu_0(x(\lambda + \bar{x}_0 - t)) d\lambda \right) \right. \\
 &\quad \left. - \exp \left( \int_0^t (1 - 2m') \beta_0(x(\lambda + \bar{x}_0 - t)) y_7^b(\lambda) \right. \right. \\
 &\quad \left. \left. - \mu_0(x(\lambda + \bar{x}_0 - t)) d\lambda \right) \right] + |f_0^a(x(\bar{x}_0 - t)) - f_0^b(x(\bar{x}_0 - t))| \\
 &\quad \times \exp \left( \int_0^t (1 - 2m') \beta_0(x(\lambda + \bar{x}_0 - t)) y_7^b(\lambda) \right. \\
 &\quad \left. - \mu_0(x(\lambda + \bar{x}_0 - t)) d\lambda \right) \Big] d\bar{x}_0,
 \end{aligned}$$

where we used the property of real numbers  $|x_1 y_1 - x_2 y_2| \leq |x_1| \cdot |y_1 - y_2| + |y_2| \cdot |x_1 - x_2|$



and Definition 4.3.2. Using  $|e^x - e^y| \leq \max\{e^x, e^y\}|x - y|$ , it follows that

$$\begin{aligned}
 \int_t^{x^*} |P_0^a(x, t) - P_0^b(x, t)| dx &\leq \int_t^{\bar{x}_0^*} g_0(x(\bar{x}_0 - t)) \left[ f_0^a(x(\bar{x}_0 - t))(1 - 2m')\beta_0(x(\lambda + \bar{x}_0 - t)) \right. \\
 &\quad \left. \int_0^t |y_7^a(\lambda) - y_7^b(\lambda)| d\lambda + |f_0^a(x(\bar{x}_0 - t)) - f_0^b(x(\bar{x}_0 - t))| \right. \\
 &\quad \left. \exp\left(\int_0^t (1 - 2m')\beta_0(x(\lambda + \bar{x}_0 - t))y_7^b(\lambda) \right. \right. \\
 &\quad \left. \left. - \mu_0(x(\lambda + \bar{x}_0 - t))d\lambda\right) \right] d\bar{x}_0 \\
 &\leq (1 - 2m')\bar{\beta}_0 \int_t^{\bar{x}_0^*} g_0(x(\bar{x}_0 - t))f_0^a(x(\bar{x}_0 - t)) \\
 &\quad \int_0^t |y_7^a(\lambda) - y_7^b(\lambda)| d\lambda d\bar{x}_0 + \exp\left(\left((1 - 2m')\bar{\beta}_0\bar{s}(\theta^b, T) - \bar{\mu}_0\right) \right. \\
 &\quad \left. T\right) \int_t^{\bar{x}_0^*} |f_0^a(x(\bar{x}_0 - t)) - f_0^b(x(\bar{x}_0 - t))| g_0(x(\bar{x}_0 - t)) d\bar{x}_0 \\
 &\leq (1 - 2m')\bar{\beta}_0 \int_0^{\bar{x}_0^*} g_0(x(\bar{x}_0))f_0^a(x(\bar{x}_0)) d\bar{x}_0 \int_0^t |y_7^a(\lambda) - y_7^b(\lambda)| \\
 &\quad d\lambda + \exp\left(\left((1 - 2m')\bar{\beta}_0\bar{s}(\theta^b, T) - \bar{\mu}_0\right)T\right) \int_0^{\bar{x}_0^*} g_0(x(\bar{x}_0)) \\
 &\quad |f_0^a(x(\bar{x}_0)) - f_0^b(x(\bar{x}_0))| d\bar{x}_0 \\
 &= (1 - 2m')\bar{\beta}_0 \|f_0^a\|_1 \int_0^t |y_7^a(\lambda) - y_7^b(\lambda)| d\lambda + \exp\left(\left((1 - 2m') \right. \right. \\
 &\quad \left. \left. \bar{\beta}_0\bar{s}(\theta^b, T) - \bar{\mu}_0\right)T\right) \int_{x_0}^{x_1} |f_0^a(x) - f_0^b(x)| dx,
 \end{aligned}$$

and, finally

$$\int_t^{x^*} |P_0^a(x, t) - P_0^b(x, t)| dx \leq \text{const.}(\theta^a, \eta) \left( \int_0^t \|y^a - y^b\|_\lambda d\lambda + \|\theta^a - \theta^b\|_\Theta \right).$$

Now, consider the integral over the rest of the interval  $[x_0, t)$ . We have

$$\begin{aligned}
 \int_{x_0}^t |P_0^a(x, t) - P_0^b(x, t)| dx &\leq \int_0^t g_0(x_0) \left[ \exp\left(\int_0^{\bar{x}_0} (1 - 2m')y_7^a(\lambda + t - \bar{x}_0)\beta_0(x(\lambda)) \right. \right. \\
 &\quad \left. \left. - \mu_0(x(\lambda))d\lambda\right) - \exp\left(\int_0^{\bar{x}_0} (1 - 2m')\beta_0(x(\lambda))y_7^b(\lambda + t - \bar{x}_0) \right. \right. \\
 &\quad \left. \left. - \mu_0(x(\lambda))d\lambda\right) \right] |h_0^a(t - \bar{x}_0) + \exp\left(\int_0^{\bar{x}_0} (1 - 2m')\beta_0(x(\lambda)) \right. \\
 &\quad \left. y_7^b(\lambda + t - \bar{x}_0) - \mu_0(x(\lambda))d\lambda\right) |h_0^a(t - \bar{x}_0) - h_0^b(t - \bar{x}_0)| \Big] d\bar{x}_0,
 \end{aligned}$$

where we have used the same property of real numbers  $|x_1y_1 - x_2y_2| \leq |x_1| \cdot |y_1 - y_2| + |y_2| \cdot |x_1 - x_2|$  and Definition 4.3.2. Then, by using  $|e^x - e^y| \leq \max\{e^x, e^y\}|x - y|$ , we

end up with

$$\begin{aligned}
 \int_{x_0}^t |P_0^a(x, t) - P_0^b(x, t)| dx &\leq \int_0^t g_0(x_0) \left[ h_0^a(t - \bar{x}_0) \left| \int_0^{\bar{x}_0} (1 - 2m') \beta_0(x(\lambda)) y_7^a(\lambda + t - \bar{x}_0) \right. \right. \\
 &\quad \left. \left. - \mu_0(x(\lambda)) d\lambda - \int_0^{\bar{x}_0} (1 - 2m') \beta_0(x(\lambda)) y_7^b(\lambda + t - \bar{x}_0) \right. \right. \\
 &\quad \left. \left. - \mu_0(x(\lambda)) d\lambda \right| + |h_0^a(t - \bar{x}_0) - h_0^b(t - \bar{x}_0)| \right. \\
 &\quad \left. \left| \exp \left( \int_0^{\bar{x}_0} (1 - 2m') \beta_0(x(\lambda)) y_7^b(\lambda + t - \bar{x}_0) \right. \right. \right. \\
 &\quad \left. \left. \left. - \mu_0(x(\lambda)) d\lambda \right) \right| \right] d\bar{x}_0 \\
 &\leq g_0(x_0) \bar{h}_0^a \bar{\beta}_0 (1 - 2m') \int_0^t \int_0^{\bar{x}_0} |y_7^a(\lambda + t - \bar{x}_0) - y_7^b(\lambda + t - \bar{x}_0)| \\
 &\quad d\lambda d\bar{x}_0 + \exp \left( ((1 - 2m') \bar{\beta}_0 \bar{s}(\theta, T) - \bar{\mu}_0) \bar{x}_0^* \right) \\
 &\quad \int_0^t |h_0^a(t - \bar{x}_0) - h_0^b(t - \bar{x}_0)| d\bar{x}_0 \\
 &\leq g_0(x_0) \bar{h}_0^a \bar{\beta}_0 (1 - 2m') \int_0^t \int_{t-\bar{x}_0}^t |y_7^a(\lambda) - y_7^b(\lambda)| \\
 &\quad d\lambda d\bar{x}_0 + \exp \left( ((1 - 2m') \bar{\beta}_0 \bar{s}(\theta, T) - \bar{\mu}_0) \bar{x}_0^* \right) \\
 &\quad \int_0^t |h_0^a(t) - h_0^b(t)| dt \\
 &\leq g_0(x_0) \bar{h}_0^a \bar{\beta}_0 (1 - 2m') T \int_0^t |y_7^a(\lambda) - y_7^b(\lambda)| d\lambda \\
 &\quad + \exp \left( ((1 - 2m') \bar{\beta}_0 \bar{s}(\theta, T) - \bar{\mu}_0) \bar{x}_0^* \right) \int_0^t |h_0^a(t) - h_0^b(t)| dt \\
 &\leq \text{const.}(\theta^a, \eta) \left( \int_0^t \|y^a - y^b\|_\lambda d\lambda + \|\theta^a - \theta^b\|_\Theta \right).
 \end{aligned}$$

Now, combining the intervals over the integral, we get the complete statement for  $P_0$

$$\begin{aligned}
 \int_{x_0}^{x_1} |P_0^a(x, t) - P_0^b(x, t)| dx &= \int_{x_0}^t |P_0^a(x, t) - P_0^b(x, t)| dx + \int_t^{x_1} |P_0^a(x, t) - P_0^b(x, t)| dx \\
 &\leq C_{P_0}(\theta^a, \eta) \left( \int_0^t \|y^a - y^b\|_\lambda d\lambda + \|\theta^a - \theta^b\|_\Theta \right).
 \end{aligned}$$

Finally, we get the claim for  $P_0$ .

Now, we prove the statement for  $P_1$  by first considering the integral over interval  $[t, x_1]$ :

$$\begin{aligned}
 \int_t^{x_1} |P_1^a(x, t) - P_1^b(x, t)| dx &= \int_t^{\bar{x}_1^*} g_1(x(\bar{x}_1)) |P_1^a(x(\bar{x}_1), t) - P_1^b(x(\bar{x}_1), t)| d\bar{x}_1 \\
 &\leq \int_t^{\bar{x}_1^*} \left[ \exp \left( \int_0^t \beta_1(x(\bar{x}_1)) y_7^a(\lambda) - \mu_1(x(\bar{x}_1)) d\lambda \right) \left| \int_0^t \exp \left( - \int_0^\epsilon \beta_1(x(\bar{x}_1)) y_7^a(\lambda) \right. \right. \right. \\
 &\quad \left. \left. \left. - \mu_1(x(\bar{x}_1)) d\lambda \right) (2m' \beta_0(x(\bar{x}_1)) y_3^a(x(\bar{x}_1), \epsilon) y_7^a(\epsilon)) g_1(x(\bar{x}_1)) d\epsilon + \right. \right. \\
 &\quad \left. \left. f_1^a(x(\bar{x}_1 - t)) g_1(x(\bar{x}_1 - t)) - \int_0^t \exp \left( - \int_0^\epsilon \beta_1(x(\bar{x}_1)) y_7^b(\lambda) - \mu_1(x(\bar{x}_1)) d\lambda \right) \right. \right. \\
 &\quad \left. \left. (2m' \beta_0(x(\bar{x}_1)) y_3^b(x(\bar{x}_1), \epsilon) y_7^b(\epsilon)) g_1(x(\bar{x}_1)) d\epsilon + f_1^b(x(\bar{x}_1 - t)) g_1(x(\bar{x}_1 - t)) \right| + \right. \\
 &\quad \left. \left\{ \int_0^t \exp \left( - \int_0^\epsilon \beta_1(x(\bar{x}_1)) y_7^b(\lambda) - \mu_1(x(\bar{x}_1)) d\lambda \right) (2m' \beta_0(x(\bar{x}_1)) y_3^b(x(\bar{x}_1), \epsilon) \right. \right. \\
 &\quad \left. \left. y_7^b(\epsilon)) g_1(x(\bar{x}_1)) d\epsilon + f_1^b(x(\bar{x}_1 - t)) g_1(x(\bar{x}_1 - t)) \right\} \left| \exp \left( \int_0^t \beta_1(x(\bar{x}_1)) y_7^a(\lambda) \right. \right. \right. \\
 &\quad \left. \left. \left. - \mu_1(x(\bar{x}_1)) d\lambda \right) - \exp \left( \int_0^t \beta_1(x(\bar{x}_1)) y_7^b(\lambda) - \mu_1(x(\bar{x}_1)) d\lambda \right) \right] d\bar{x}_1,
 \end{aligned}$$

where we used the property of real numbers  $|x_1 y_1 - x_2 y_2| \leq |x_1| \cdot |y_1 - y_2| + |y_2| \cdot |x_1 - x_2|$  and Definition 4.3.2. Simplifying above relation, we get

$$\begin{aligned}
 \int_t^{x_1} |P_1^a(x, t) - P_1^b(x, t)| dx &\leq \int_t^{\bar{x}_1^*} \exp \left( \int_0^t \beta_1(x(\bar{x}_1)) y_7^a(\lambda) - \mu_1(x(\bar{x}_1)) d\lambda \right) 2m' \beta_0(x(\bar{x}_1)) \\
 &\quad g_1(x(\bar{x}_1)) \int_0^t \left[ \exp \left( - \int_0^\epsilon \beta_1(x(\bar{x}_1)) y_7^a(\lambda) - \mu_1(x(\bar{x}_1)) d\lambda \right) |y_3^a(x(\bar{x}_1), \epsilon) y_7^a(\epsilon) \right. \\
 &\quad \left. - y_3^b(x(\bar{x}_1), \epsilon) y_7^b(\epsilon)| + \left| \exp \left( \int_0^t \beta_1(x(\bar{x}_1)) y_7^a(\lambda) - \mu_1(x(\bar{x}_1)) d\lambda \right) \right. \right. \\
 &\quad \left. \left. - \exp \left( \int_0^t \beta_1(x(\bar{x}_1)) y_7^b(\lambda) - \mu_1(x(\bar{x}_1)) d\lambda \right) \right| y_3^b(x(\bar{x}_1), \epsilon) y_7^b(\epsilon) \right] d\epsilon d\bar{x}_1 + \\
 &\quad \int_t^{\bar{x}_1^*} \exp \left( \int_0^t \beta_1(x(\bar{x}_1)) y_7^a(\lambda) - \mu_1(x(\bar{x}_1)) d\lambda \right) g_1(x(\bar{x}_1 - t)) (f_1^a(x(\bar{x}_1 - t)) \\
 &\quad - f_1^b(x(\bar{x}_1 - t))) d\bar{x}_1 + \left\{ \exp ((\bar{\mu}_1 - \bar{\beta}_1 \bar{s}(\theta, T)) T) (\bar{\mu}_1 - \bar{\beta}_1 \bar{s}(\theta, T)) \right. \\
 &\quad \left. (2m' \bar{\beta}_0 \bar{P}_0(\theta, T) \bar{s}(\theta, T)) \bar{g}_1(\bar{x}_1^* - T) + \int_{x_1}^{x_1} f_1^b(x) dx \right\} \bar{\beta}_1 \int_0^t |y_7^a(\lambda) - y_7^b(\lambda)| d\lambda.
 \end{aligned}$$

Using  $|e^x - e^y| \leq \max\{e^x, e^y\}|x - y|$ , it follows that

$$\begin{aligned}
 \int_t^{x_1} |P_1^a(x, t) - P_1^b(x, t)| dx &\leq \int_t^{\bar{x}_1^*} \exp((\bar{\beta}_1 \bar{s}(\theta, T) - \bar{\mu}_1)T) 2m' \bar{\beta}_0 \bar{g}_1 \\
 &\quad \int_0^t \left[ \exp((\bar{\mu}_1 - \bar{\beta}_1 \bar{s}(\theta, T))\epsilon) |y_3^a(x(\bar{x}_1), \epsilon) y_7^a(\epsilon) - y_3^b(x(\bar{x}_1), \epsilon) y_7^b(\epsilon)| \right. \\
 &\quad \left. + \left| \int_0^t \beta_1(x(\bar{x}_1)) y_7^a(\lambda) - \mu_1(x(\bar{x}_1)) d\lambda - \int_0^t \beta_1(x(\bar{x}_1)) y_7^b(\lambda) - \mu_1(x(\bar{x}_1)) d\lambda \right| \right. \\
 &\quad \left. \bar{P}_0(\theta, T) \bar{s}(\theta, T) \right] d\epsilon d\bar{x}_1 + \exp((\bar{\beta}_1 \bar{s}(\theta, T) - \bar{\mu}_1)T) \int_0^{\bar{x}_1^*} g_1(x(\bar{x}_1)) (f_1^a(x(\bar{x}_1)) - \\
 &\quad f_1^b(x(\bar{x}_1))) d\bar{x}_1 + \left\{ \exp((\bar{\mu}_1 - \bar{\beta}_1 \bar{s}(\theta, T))T) (\bar{\mu}_1 - \bar{\beta}_1 \bar{s}(\theta, T)) (2m' \bar{\beta}_0 \bar{P}_0(\theta, T) \right. \\
 &\quad \left. \bar{s}(\theta, T)) \bar{g}_1(\bar{x}_1^* - T) + \|f_1^b\| \right\} \bar{\beta}_1 \int_0^t |y_7^a(\lambda) - y_7^b(\lambda)| d\lambda \\
 &\leq \exp((\bar{\beta}_1 \bar{s}(\theta, T) - \bar{\mu}_1)T) 2m' \bar{\beta}_0 \bar{g}_1 \int_t^{\bar{x}_1^*} \int_0^t \left[ \exp((\bar{\mu}_1 - \bar{\beta}_1 \bar{s}(\theta, T))\epsilon) |y_3^a(x(\bar{x}_1), \epsilon) \right. \\
 &\quad \left. y_7^a(\epsilon) - y_3^b(x(\bar{x}_1), \epsilon) y_7^b(\epsilon)| + \bar{\beta}_1 \bar{P}_0(\theta, T) \bar{s}(\theta, T) \int_0^t |y_7^a(\lambda) - y_7^b(\lambda)| d\lambda \right] d\epsilon d\bar{x}_1 \\
 &\quad + \exp((\bar{\beta}_1 \bar{s}(\theta, T) - \bar{\mu}_1)T) \int_{x_0}^{x_1} (f_1^a(x) - f_1^b(x)) dx + \text{const.}(\theta^a, \eta) \\
 &\quad \int_0^t \|y^a - y^b\|_\lambda d\lambda \\
 &\leq \exp((\bar{\beta}_1 \bar{s}(\theta, T) - \bar{\mu}_1)T) 2m' \bar{\beta}_0 \bar{g}_1 \left[ \int_t^{\bar{x}_1^*} \int_0^t \exp((\bar{\mu}_1 - \bar{\beta}_1 \bar{s}(\theta, T))\epsilon) |y_3^a(x(\bar{x}_1), \epsilon) \right. \\
 &\quad \left. y_7^a(\epsilon) - y_3^b(x(\bar{x}_1), \epsilon) y_7^b(\epsilon)| d\epsilon d\bar{x}_1 + \bar{\beta}_1 \bar{P}_0(\theta, T) \bar{s}(\theta, T) (\bar{x}_1^* - T) \right. \\
 &\quad \left. \int_0^t |y_7^a(\lambda) - y_7^b(\lambda)| d\lambda \right] + \text{const.}(\theta^a, \eta) \|\theta^a - \theta^b\|_\Theta \\
 &\quad + \text{const.}(\theta^a, \eta) \int_0^t \|y^a - y^b\|_\lambda d\lambda \\
 &\leq \text{const.}(\theta^a, \eta) \left( \int_0^t \|y^a - y^b\|_\lambda d\lambda + \|\theta^a - \theta^b\|_\Theta \right).
 \end{aligned}$$

Eventually, we get

$$\int_t^{x_1} |P_1^a(x, t) - P_1^b(x, t)| dx \leq \text{const.}(\theta^a, \eta) \left( \int_0^t \|y^a - y^b\|_\lambda d\lambda + \|\theta^a - \theta^b\|_\Theta \right). \quad (4.30)$$

Now, consider the integral over the rest of the interval  $[x_0, t)$  and following similar lines

as before,

$$\begin{aligned}
 \int_{x_0}^t |P_1^a(x, t) - P_1^b(x, t)| dx &= \int_0^t g_1(x(\bar{x}_1)) |P_1^a(x(\bar{x}_1), t) - P_1^b(x(\bar{x}_1), t)| d\bar{x}_1 \\
 &= \int_0^t \left[ \exp \left( \int_0^{\bar{x}_1} \beta_1(x(\lambda)) y_7^a(t) - \mu_1(x(\lambda)) d\lambda \right) \left\{ \int_0^{\bar{x}_1} \exp \left( - \int_0^\epsilon \beta_1(x(\lambda)) y_7^a(t) \right. \right. \right. \\
 &\quad \left. \left. - \mu_1(x(\lambda)) d\lambda \right) (2m' \beta_0(x(\epsilon)) y_3^a(x(\epsilon), t) y_7^a(t)) g_1(x(\epsilon)) d\epsilon + h_1^a(t - \bar{x}_1) g_1(x_0) \right\} \\
 &\quad \left. - \exp \left( \int_0^{\bar{x}_1} \beta_1(x(\lambda)) y_7^b(t) - \mu_1(x(\lambda)) d\lambda \right) \left\{ \int_0^{\bar{x}_1} \exp \left( - \int_0^\epsilon \beta_1(x(\lambda)) y_7^b(t) - \right. \right. \right. \\
 &\quad \left. \left. \mu_1(x(\lambda)) d\lambda \right) (2m' \beta_0(x(\epsilon)) y_3^b(x(\epsilon), t) y_7^b(t)) g_1(x(\epsilon)) d\epsilon + h_1^b(t - \bar{x}_1) g_1(x_0) \right\} \right] d\bar{x}_1 \\
 &\leq \int_0^t \exp \left( \int_0^{\bar{x}_1} \beta_1(x(\lambda)) y_7^a(t) - \mu_1(x(\lambda)) d\lambda \right) \left| \int_0^{\bar{x}_1} 2m' \beta_0(x(\epsilon)) g_1(x(\epsilon)) \right. \\
 &\quad \left\{ \exp \left( - \int_0^\epsilon \beta_1(x(\lambda)) y_7^a(t) - \mu_1(x(\lambda)) d\lambda \right) y_3^a(x(\epsilon), t) y_7^a(t) - \right. \\
 &\quad \left. \exp \left( - \int_0^\epsilon \beta_1(x(\lambda)) y_7^b(t) - \mu_1(x(\lambda)) d\lambda \right) y_3^b(x(\epsilon), t) y_7^b(t) \right\} d\epsilon + \\
 &\quad g_1(x_0) (h_1^a(t - \bar{x}_1) - h_1^b(t - \bar{x}_1)) \left| d\bar{x}_1 + \int_0^t \left\{ \int_0^{\bar{x}_1} \exp ((\bar{\mu}_1 - \bar{\beta}_1 \bar{s}(\theta, T)) \epsilon) \right. \right. \\
 &\quad \left. \left. (2m' \bar{\beta}_0 \bar{P}_0(\theta, T) \bar{s}(\theta, T)) \bar{g}_1 d\epsilon + \bar{h}_1^b g_1(x_0) \right\} \right. \\
 &\quad \left. \left| \int_0^{\bar{x}_1} \beta_1(x(\lambda)) y_7^a(t) - \mu_1(x(\lambda)) d\lambda - \int_0^{\bar{x}_1} \beta_1(x(\lambda)) y_7^b(t) - \mu_1(x(\lambda)) d\lambda \right| d\bar{x}_1 \right. \\
 &\leq \exp ((\bar{\beta}_1 \bar{s}(\theta, T) - \bar{\mu}_1) \bar{x}_1^*) \left[ 2m' \bar{\beta}_0 \bar{g}_1 \int_0^t \int_0^{\bar{x}_1} \exp ((\bar{\mu}_1 - \bar{\beta}_1 \bar{s}(\theta, T)) \epsilon) |y_3^a(x(\epsilon), t) \right. \\
 &\quad \left. y_7^a(t) - y_3^b(x(\epsilon), t) y_7^b(t)| d\epsilon d\bar{x}_1 + \bar{P}_0(\theta, t) \bar{s}(\theta, t) \bar{\beta}_1 \int_0^t \int_0^{\bar{x}_1} \int_0^\epsilon |y_7^a(t) - y_7^b(t)| d\lambda \right. \\
 &\quad \left. d\epsilon d\bar{x}_1 + g_1(x_0) \int_0^t (h_1^a(t) - h_1^b(t)) dt \right] \\
 &\quad + \text{const.}(\theta^a, \eta) \int_0^t \|y^a - y^b\|_\lambda d\lambda \\
 &\leq \exp ((\bar{\beta}_1 \bar{s}(\theta, T) - \bar{\mu}_1) \bar{x}_1^*) \left[ 2m' \bar{\beta}_0 \bar{g}_1 \int_0^t \int_0^{\bar{x}_1} \exp ((\bar{\mu}_1 - \bar{\beta}_1 \bar{s}(\theta, T)) \epsilon) |y_3^a(x(\epsilon), t) \right. \\
 &\quad \left. y_7^a(t) - y_3^b(x(\epsilon), t) y_7^b(t)| d\epsilon d\bar{x}_1 + \frac{1}{2} \bar{P}_0(\theta, t) \bar{s}(\theta, t) \bar{\beta}_1 \bar{x}_1^{*2} \int_0^t |y_7^a(t) - y_7^b(t)| d\bar{x}_1 \right. \\
 &\quad \left. + g_1(x_0) \int_0^t (h_1^a(t) - h_1^b(t)) dt \right] + \text{const.}(\theta^a, \eta) \int_0^t \|y^a - y^b\|_\lambda d\lambda \\
 &\leq \text{const.}(\theta^a, \eta) \left( \int_0^t \|y^a - y^b\|_\lambda d\lambda + \|\theta^a - \theta^b\|_\Theta \right).
 \end{aligned}$$

As the end result, we obtain

$$\int_{x_0}^t |P_1^a(x, t) - P_1^b(x, t)| dx \leq \text{const.}(\theta^a, \eta) \left( \int_0^t \|y^a - y^b\|_\lambda d\lambda + \|\theta^a - \theta^b\|_\Theta \right). \quad (4.31)$$

Finally, (4.30) and (4.31) give the statement on the whole interval as

$$\int_{x_0}^{x_1} |P_1^a(x, t) - P_1^b(x, t)| dx \leq C_{P_1}(\theta^a, \eta) \left( \int_0^t \|y^a - y^b\|_\lambda d\lambda + \|\theta^a - \theta^b\|_\Theta \right).$$

This completes the proof.  $\square$

Now we are ready to state and prove the main statement of this section.

**Theorem 4.5.1.** Let  $\theta^a \in \Theta$ ,  $\eta > 0$ . There exist non-negative constants  $C_S(\theta^a, \eta)$  such that for all  $\theta^b \in \Theta$  with  $\|\theta^a - \theta^b\| < \eta$  and  $y^a \in Y_{T'}^{\theta^a}$ ,  $y^b \in Y_{T'}^{\theta^b}$ , it holds that

$$\|S^{\theta^a}[y^a] - S^{\theta^b}[y^b]\|_t \leq C_S(\theta^a, \eta) \left( \int_0^t \|y^a - y^b\|_\lambda d\lambda + \|\theta^a - \theta^b\|_\Theta \right),$$

for almost all  $t \in [0, T']$ .

*Proof.* The proof follows from the Lemma 4.5.2 and 4.5.3.  $\square$

## 4.6 Wellposedness results

In this section, we prove that there exists a unique solution of the model (4.12-4.20) for time  $t \in [0, T]$ . We also show that the solution of the model depends continuously on given problem data, which concludes that the proposed model is well-posed.

### 4.6.1 Existence and uniqueness of the solution

Let  $\theta \in \Theta$  be fixed, and  $\eta > 0$  be arbitrary. We choose  $T' \in (0, T]$  such that  $T' C_S(\theta, \eta) \leq q < 1$  and  $\frac{T}{T'} \in \mathbb{N}$ . We intend to show the existence of a unique solution to the original ODE-PDE system in  $Y_{nT'}^\theta$  for all  $n = 1, 2, \dots, \frac{T}{T'}$  by induction. Let us begin with  $n = 1$  then for all  $y^a, y^b \in Y_{T'}^\theta$  with continuous representatives, it holds that

$$\begin{aligned} \|S^\theta[y^a] - S^\theta[y^b]\|_X &= \int_0^{T'} \|S^\theta[y^a] - S^\theta[y^b]\|_t dt \\ &\leq T' C_S(\theta, \eta) \left( \int_0^t \|y^a - y^b\|_\lambda d\lambda + \|\theta - \theta\|_\Theta \right) \quad (\text{by Theorem 4.5.1}) \\ &\leq q \|y^a - y^b\|_X. \end{aligned}$$

Therefore,  $S^\theta$  is a contraction on the space  $\tilde{Y}_{T'}^\theta := \{y \in Y_{T'}^\theta \mid \exists \text{ cont. repr. of } y\}$ . Following the standard proof of Banach fixed point theorem, we get that applying  $S^\theta$  iteratively gives a Cauchy sequence in  $Y_{T'}^\theta$ , [101]. For any  $y^{(0)} \in Y_{T'}^\theta$  define the sequence  $(y^{(i)})_{i \in \mathbb{N}}$  by setting  $y^{(i+1)} := S^\theta[y^{(i)}] \in Y_{T'}^\theta$  for  $i = 0, 1, \dots$ . Then, we have that

$$\begin{aligned} \|S^\theta[y^{(i+1)}] - S^\theta[y^{(i)}]\|_X &\leq q \|y^{(i+1)} - y^{(i)}\|_X \\ &= q \|S^\theta[y^{(i)}] - S^\theta[y^{(i-1)}]\|_X \end{aligned}$$

and, so

$$\|S^\theta[y^{(i+1)}] - S^\theta[y^{(i)}]\|_X \leq q^i \|S^\theta[y^{(0)}] - y^{(0)}\|_X,$$

for all  $i = 1, 2, \dots$ . Consequently, for all  $j \geq i$

$$\begin{aligned} \|y^{(j)} - y^{(i)}\|_X &= \|S^\theta[y^{(j-1)}] - S^\theta[y^{(i-1)}]\|_X \\ &\leq \sum_{k=i-1}^{j-2} \|S^\theta[y^{(k+1)}] - S^\theta[y^{(k)}]\|_X \\ &\leq \|S^\theta[y^{(0)}] - y^{(0)}\|_X \sum_{k=i-1}^{j-2} q^k. \end{aligned}$$

Since  $Y_{T'}^\theta$  is a complete metric space and  $\tilde{Y}_{T'}^\theta \subset Y_{T'}^\theta$ , the limit of the above-mentioned Cauchy sequence exists in  $Y_{T'}^\theta$ . Moreover, we know that every fixed point of  $S^\theta$  must have a continuous representative, therefore, the sequence converges to a fixed point in  $\tilde{Y}_{T'}^\theta$ , which is unique because  $S^\theta$  is a contraction. Thus, by Theorem 4.4.1, we get the existence of a unique solution to the basic ODE-PDE system in  $Y_{T'}^\theta$ .

Next, we take  $1 < n \leq \frac{T}{T'}$ . By induction hypothesis, we know that there exists a unique solution  $\hat{y} = (\hat{y}_1, \hat{y}_2, \hat{y}_3, \hat{y}_4, \hat{y}_5, \hat{y}_6, \hat{y}_7)$  in  $Y_{(n-1)T'}^\theta$ . We define the restricted space

$$\begin{aligned} \tilde{Y}_{nT'}^\theta := & \{(y_1, y_2, y_3, y_4, y_5, y_6, y_7) \in Y_{nT'}^\theta \mid y_1(t) = \hat{y}_1(t), y_2(t) = \hat{y}_2(t), y_3(\cdot, t) \stackrel{!}{=} \hat{y}_3(\cdot, t), \\ & y_4(\cdot, t) \stackrel{!}{=} \hat{y}_4(\cdot, t), y_5(t) = \hat{y}_5(t), y_6(t) = \hat{y}_6(t), y_7(t) = \hat{y}_7(t) \text{ for almost all} \\ & t \in [0, (n-1)T']\}. \end{aligned}$$

$\tilde{Y}_{nT'}^\theta$  is a closed subset of  $Y_{nT'}^\theta$  and hence a complete metric space. Since  $\hat{y}$  is a fixed point of  $S^\theta$  on  $Y_{(n-1)T'}^\theta$ , therefore, the operator  $S^\theta$  when applied to any  $y \in \tilde{Y}_{nT'}^\theta$  with continuous representative returns an element of  $\tilde{Y}_{nT'}^\theta$  with continuous representative. Therefore, we get for all  $y^a, y^b \in \tilde{Y}_{nT'}^\theta$  with a continuous representative that

$$\begin{aligned} \|S^\theta[y^a] - S^\theta[y^b]\|_X &= \int_0^{nT'} \|S^\theta[y^a] - S^\theta[y^b]\|_t dt \\ &= \int_{(n-1)T'}^{nT'} \|S^\theta[y^a] - S^\theta[y^b]\|_t dt \\ &\leq \int_{(n-1)T'}^{nT'} C_S(\theta, \eta) \int_0^t \|y^a - y^b\|_\lambda d\lambda dt \\ &\leq C_S(\theta, \eta) \int_{(n-1)T'}^{nT'} \int_0^{nT'} \|y^a - y^b\|_\lambda d\lambda dt \\ &= (nT' - (n-1)T') C_S(\theta, \eta) \|y^a - y^b\|_X \\ &\leq q \|y^a - y^b\|_X. \end{aligned}$$

Utilizing the same argument as in the induction start (for  $n = 1$ ), we also get the existence of a unique fixed point in  $\tilde{Y}_{nT'}^\theta$ . This implies the existence and uniqueness of a solution in  $Y_{nT'}^\theta$ : Existence of the solution follows from Theorem 4.4.1. For uniqueness, let  $y \in Y_{nT'}^\theta$  be any solution to the original ODE-PDE system. By the induction hypothesis,  $y$  restricted to the time interval  $[0, (n-1)T']$  must be equal to  $\hat{y}$ . Hence  $y \in \tilde{Y}_{nT'}^\theta$  is the unique fixed point in  $\tilde{Y}_{nT'}^\theta$ .

Since,  $nT' = T$ , this concludes the results.

### 4.6.2 Continuous dependence on problem data

Let  $T' = T$ . For  $i = \{a, b\}$  let  $\theta^i = (c_0^i, c_1^i, m_0^i, m_1^i, f_0^i, f_1^i, h_0^i, h_1^i, s_0^i) \in \Theta$  and  $y^i = (C_0^i, C_1^i, P_0^i, P_1^i, M_0^i, M_1^i, s^i)$  be the unique solution of Eqs. (4.1-4.10) with

$$\begin{aligned} C_0^i(0) &:= c_0^i, & C_1^i(0) &:= c_1^i, \\ P_0^i(x, 0) &:= f_0^i(x), & P_1^i(x, 0) &:= f_1^i(x), & x_0 \leq x \leq x^* \\ P_0^i(x_0, t) &:= h_0^i(t), & P_1^i(x_0, t) &:= h_1^i(t), & 0 < t \leq T \\ M_0^i(0) &:= m_0^i, & M_1^i(0) &:= m_1^i \\ s^i(0) &:= s_0^i. \end{aligned}$$

Then by Theorem 4.4.1,  $y^a$  and  $y^b$  are fixed points of  $S^{\theta^a}$  and  $S^{\theta^b}$ , respectively. By Theorem 4.5.1, for almost all  $t \in [0, T]$  it holds that

$$\begin{aligned} \|y^a - y^b\|_t &= \|S^{\theta^a}[y^a] - S^{\theta^b}[y^b]\|_t \\ &\leq C_S(\theta^a, \eta) \left( \int_0^t \|y^a - y^b\|_\lambda d\lambda + \|\theta^a - \theta^b\|_\Theta \right) \\ &\leq C_S(\theta^a, \eta) \|\theta^a - \theta^b\|_\Theta (1 + C_S(\theta^a, \eta) t e^{C_S(\theta^a, \eta)t}) \quad (\text{Gronwall's inequality}) \\ &\leq C_S(\theta^a, \eta) (1 + C_S(\theta^a, \eta) T e^{C_S(\theta^a, \eta)T}) \|\theta^a - \theta^b\|_\Theta \\ &= \text{const.}(\theta^a, \eta) \|\theta^a - \theta^b\|_\Theta. \end{aligned}$$

This implies that

$$\|y^a - y^b\|_X \leq \text{const.}(\theta^a, \eta) \|\theta^a - \theta^b\|_\Theta.$$

Thus, it shows that the solution of the original ODE-PDE system continuously depends on the given problem data.

Hereby, we conclude that the proposed model is well-posed.



---

## Multiscale mathematical model: Proliferating and quiescent cell populations

---

In this chapter, we propose a nonlinear multiscale mathematical model for age-structured proliferating and quiescent cell populations (PDEs) coupled with cell cycle protein dynamics (ODEs). The model assumes a bidirectional transition between the proliferating and quiescent subpopulations. The coupling between the two scales is introduced based on biological findings inherited from the literature. Numerical simulations are performed using the finite volume method to examine the impact of parameters on the nonlinear dynamics of the model. Our model demonstrates the underlying impact of cell cycle dynamics on the evolution of cell population in a tissue. The main focus of this work is to investigate the balance between proliferating and quiescent cell populations, which play a crucial role in maintaining homeostasis in a cell population.

### 5.1 Biological problem formulation

One of the cornerstones in understanding human tumor growth is mammalian cell division patterns. Many researchers have been drawn to it, and it has been the subject of extensive research for decades. Most theoretical research works explore the life cycle by utilizing age-structured frameworks. Some examples of age-structured growth models include epidemic [102–104], microscopic virus [105, 106] and cell population [107–110] models. However, the underlying molecular intricacies of a tissue necessitate a more comprehensive modeling framework comprising special molecular and cellular interactions.

In any living tissue, the dividing cells can be classified into quiescent and proliferating compartments. Proliferating cells divide by going through various stages in cell-cycle ( $G_1, S, G_2, M$ ). Quiescent cells, on the other hand, do not grow or proliferate; instead, they move from the proliferative compartment to the  $G_0$  phase and remain there until differentiation or apoptosis. For tissue homeostasis to be preserved, cells must be able to switch between the quiescent and proliferative phases. However, the transitioning between the two compartments relies on signaling molecules, which are known as growth or anti-growth factors [111]. Proliferating cells grow within a tumor cell population until the tumor is active and malignant. Besides, the total number of cells, i.e., in both quiescent and proliferating cell populations, remains stable (on average) to preserve homeostasis; therefore, the size of the proliferative compartment in a healthy cell population remains confined. The schematics of a multiscale modeling framework employed in this paper is shown below in Figure 5.1. b

This work primarily focuses on formulating a model of the cell population (in both proliferative and quiescent compartments) and analyzing its dynamics concerning the behavior of cell-cycle proteins. Age-structured models, as previously indicated, have been widely employed in this direction. These include models investigating cell population only in quiescent phase [110], cell population only in proliferating phase [112, 113]. Finally, cell population dynamics involving both quiescent and proliferating phases [109, 114–118]. Nevertheless, the influence of molecular interactions at the subcellular level on balance between proliferative and quiescent phases has not been studied.

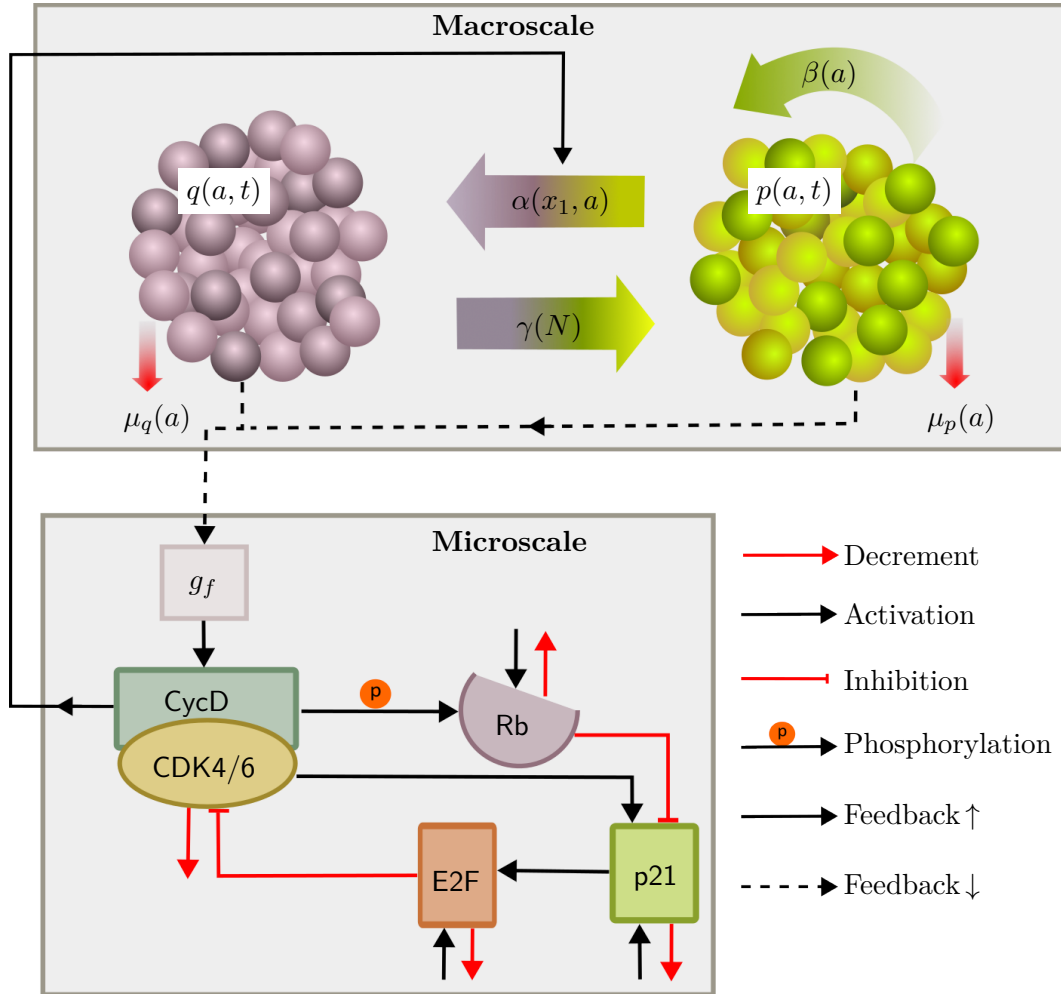


Figure 5.1: In the macro-scale, two populations of proliferating and quiescent cells are shown with various transition effects given by  $\alpha$ ,  $\beta$ ,  $\gamma$ , and  $\mu$  functions. At the bottom, the microscale is represented with all four protein states and their interactions which are explained using legends in the bottom left. The feedback from the macroscale, in the form of growth factors  $g_f$ , manipulates the cell-cycle (microscale). The feedback loop is closed by the rate  $\alpha$  (corresponds to the rate of cells transitioning from proliferating to quiescent phase), determined by the protein dynamics at the microscale.

Thereby, we formulate a multiscale model by employing mathematical tools which can also encompass the heterogeneity of a complex system lying at the sub-cellular level. We primarily focus on two predominant scales, i.e., macroscale (population dynamics) and

microscale (cell-cycle dynamics), and define the coupling between these two time and age varying scales. Age refers to the time elapsed since last division, [113, 119]. Note that in addition to the physical time variable (denoted by  $t$ ), age-structured models introduce the age variable (denoted as  $a$ ) which has rather a physiological character. The concept of “cell age” characterizes the biological variability within a proliferating cell population. Partial differential equations (PDEs) are used to simulate cell populations in the quiescent and proliferative stages at the macroscale. While ordinary differential equations are used to predict sub-cellular protein interactions related to cell-cycle dynamics (ODEs). Finally, through feedback in both directions, the two scales are connected. As mentioned earlier, proliferating cells represent a complete cycle of cell division ( $G_1, S, G_2, M$ ). Cells in the early proliferating phase, known as  $G_1$ , can transition to the quiescent phase till they reach the restriction point (R). However, depending on the concentration of  $G_1$  phase cyclin protein ( $x_1$ ), the cells transit to S phase from late  $G_1$  phase. It is also clear that restriction point (R) splits the cells in the  $G_1$ -phase in two parts such that the cells become quiescent before R but can no longer avoid division once R is passed, [120, 121]. In quiescent phase, cells do not divide or grow, but they continue to perform their other cellular functions. A bidirectional cell transitioning between quiescence and proliferation phases plays an essential role in tissue homeostasis, and it is regulated by extracellular environmental conditions [111]. In tumoral tissue, the balance in the bidirectional transition is disturbed, and cells may grow unconditionally [122]. Recent experiments have also revealed that cyclins are the most significant regulatory molecules for changes in cell-cycle phase, [123]. As a result, we use a crucial aspect in the dynamics of cell-cycle (i.e., from  $G_1 - S$  phase transition) to predict the evolution of a transitional balance between quiescent and proliferating subpopulations, that is essential to maintain homeostasis.

A variety of proteins are expressed at the microscale, which play an essential role in the sequential transition between different phases of cell-cycle. The complex network of protein interactions in the cell-cycle has been mathematically described using ODEs and simulated by several authors, including [124–129] and references therein. However, for simplicity, we consider only four proteins (i.e., Cyclin D – CDK4/6, p21, E2F, and Rb) from the network of proteins which participate in the cell-cycle dynamics, see Chapter 2. These proteins are chosen because they are primarily engaged in Cyclin D’s activity and the progression of cells to the S from  $G_1$  phase. The motivation stems from experimental results, which have shown that Cyclin D regulates the transition between the  $G_0$  and  $G_1$  phase, see [130–132]. Furthermore, when Cyclin D is over-expressed, cells in the proliferative phase commit to cell division, and when Cyclin D is under-expressed, cells enter a quiescent phase. It should be noted that these molecular interactions are assumed to occur in a fast growing population of cells and not in a single cell. Moreover, we assume averaged concentrations of these proteins in proliferating and quiescent cell subpopulations without considering cell to cell variability. In the sequel, we provide the biological relevance of cell-cycle proteins. The advancement in the cell-cycle is regulated by cyclin proteins (structural protein) and their cyclin-dependent kinase (CDK) inhibitors. There is a specific Cyclin – CDK complex for every phase in the cell-cycle. When micro-environment of a cell has enough growth signals, it initiates a cell-cycle that spans the activities of phase-specific complexes of cyclin protein and their catalytic partners CDK. Cyclin D activates during the  $G_1$  phase and is induced merely by growth factors, [133]. When there are no growth factors, the concentration of Cyclin D declines,

and the cell does not start the cycle. Growth-factors attach to particular receptors located on the external cytoplasmic membrane of the cell, which activates intra-cellular signaling pathways (i.e., Raf/Map/Ras kinase), which ultimately leads to the synthesis of Cyclin D (see [14, 134, 135], for more details). Cyclin D makes an active complex with CDK4/6 with a maximum synthesis rate. This complex can then trigger the activation of transcription factor E2F by phosphorylating its inhibitor retinoblastoma protein Rb. Resultantly, the transcription factor E2F is accumulated and activates the other essential cyclins involved in the cell-cycle.

To summarize, we develop a multiscale model to primarily address the concerns relevant to impairment in cell transitioning between quiescent and proliferating compartments, which results in unlimited tumor growth, and whether Cyclin D is responsible for the deregulation of cells transitioning between quiescent and proliferating compartments.

## 5.2 Mathematical modeling

### 5.2.1 Age-structured model

The cell populations in quiescent and proliferating compartments are described by transport PDEs (partial differential equations) of nonlinear hyperbolic type, which characterize the density distribution of the cells concerning physiological age  $a$  and time  $t$ . In the quiescent phase, the cell density  $q(a, t)$  is given by

$$\frac{\partial}{\partial t} q(a, t) = \alpha(a, x_1) p(a, t) - (\gamma(N) + \mu_q(a)) q(a, t), \quad (5.1)$$

where the first term  $\alpha(a, x_1) p(a, t)$  is the inflow from the proliferating cells at the rate  $\alpha(a, x_1)$ , which is further regulated by a microscale variable, namely the age-specific concentration of Cyclin complex  $x_1$ . The detail of the microscale variables is presented later in this section. The next term refers to the loss in quiescent cell density caused by either returning to cell division with the rate  $\gamma(N)$  in the proliferating phase or by cell death as a result of apoptosis (or necrosis), as depicted by death rate  $\mu_q(a)$ . The total number cell population in both phases is represented by  $N(t)$ , which is defined in Eq. (5.3). The cells in the quiescent phase do not age (or in other words, the cells halt their age), therefore in Eq. (5.1), the convection term concerning physiological age  $a$  is not present. In the proliferating phase, the cell number density represented by  $p(a, t)$  reads

$$\frac{\partial}{\partial t} p(a, t) + \frac{\partial}{\partial a} (g(a) p(a, t)) = \gamma(N) q(a, t) - (\beta(a) + \alpha(a, x_1) + \mu_p(a)) p(a, t), \quad (5.2)$$

where  $g(a)$  stands for the rate of evolution of a cell-cycle. The first term on the right  $\gamma(N) q(a, t)$  denotes the transition from the quiescent to the proliferating cells. The following term  $\beta(a) p(a, t)$  symbolizes the number of cells that complete cell division at some age of the proliferating phase, whereas the cells that are moving to the quiescent phase from proliferating phase without having undergone division are given by the term  $\alpha(a, x_1) p(a, t)$ . Finally, the decrement in proliferating cell density because of apoptosis/necrosis is described by the death rate  $\mu_p(a)$ . The cell population,  $N(t)$ , defined as the sum of all cells in the quiescent and proliferating phases across all ages, is given as:

$$N(t) = \int_0^{a^*} (q(a, t) + p(a, t)) da, \quad (5.3)$$

where  $a^*$  is the maximal age of the cells. The initial conditions are defined as:

$$p(a, 0) = p_0(a), \quad q(a, 0) = q_0(a), \quad \forall a \geq 0. \quad (5.4)$$

The boundary condition is given as follows:

$$g(0)p(0, t) = 2 \int_0^{a^*} \beta(a)p(a, t)da, \quad (5.5)$$

for  $t > 0$ , where the number 2 appears because of the two newborn cells, which begin in the proliferating phase with age 0. The function, which defines the number of cells switching from quiescent to proliferating phase,  $\gamma(N)$ , takes the form of monotone decreasing Hill function of  $N$ :

$$\gamma(N) = \frac{\nu\theta^\kappa}{\theta^\kappa + N^\kappa}, \quad (5.6)$$

where  $\nu$  defines the maximal rate of cell transitioning from quiescent to proliferating population (e.g., when there are no cells, i.e.,  $N = 0$ ),  $\kappa$  is the Hill coefficient and  $\theta$  characterises the entire cell population reaching the half maximum of  $\nu$ . It means that the percentage of quiescent cells which enter the proliferative phase again declines to zero when the cell population rises, thus depicting density inhibition. The usage of the Hill function is motivated here to describe nonlinear and saturable mechanisms between the total cell population and the transition rate, see [136]. The number of cells that complete the division at some age in the proliferation phase are represented by function  $\beta(a)$ . The age  $a$  regulates the function  $\beta(a)$  in such a way that it is almost zero until a minimum age of cells, and then it increases until the age  $a^*$ :

$$\beta(a) = \frac{\rho_1 a^{\gamma_1}}{\rho_2^{\gamma_1} + a^{\gamma_1}}, \quad (5.7)$$

where  $\rho_1$  is the maximum proliferation rate,  $\rho_2$  is the age at which the half-maximum effect is achieved, and the exponent  $\gamma_1$  is the Hill coefficient. Next we define the rate at which the cells leave the proliferating phase and become quiescent is given by the relation in (7.10). It depends on both age  $a$  and the amount of Cyclin D – CDK4/6 complex  $x_1$ :

$$\alpha(a, x_1) = \sigma_1 \frac{\sigma_2^{\gamma_2}}{(\sigma_2^{\gamma_2} + x_1^{\gamma_2})} \frac{\sigma_3^{\gamma_3}}{(\sigma_3^{\gamma_3} + a^{\gamma_3})}. \quad (5.8)$$

The function  $\alpha(a, x_1)$  determines the number of cells that do not divide because of growth-inhibiting factors. Age dependence in  $\alpha$  is motivated because the cells transit from the proliferating to quiescent phase only until a certain age that specifies a restriction point R in the cell-cycle ( $G_1 - S$  phase transition). However, until the restriction point, the concentration of Cyclin complex  $x_1$  must be under a certain threshold to allow cells to leave the proliferating phase. In Eq. (7.10),  $\gamma_2$  and  $\gamma_3$  are Hill coefficient,  $\sigma_2$  and  $\sigma_3$  represent the concentration of Cyclin D – CDK4/6 complex  $x_1$  and age  $a$ , respectively, and after  $\gamma_2$  and  $\gamma_3$ , the rate function  $\alpha$  asymptotically decreases to zero and thus avoiding transition of cells to quiescent phase. It indicates that at age  $\sigma_3$ , cells are inevitably devoted to entering the proliferation compartment. Lastly,  $\sigma_2$  is the limit for the concentration of Cyclin' complex, which determines R, the restriction point.

In the process of cell-signaling, cell growth is regulated by the proteins called cytokine and other proliferation governing factors, [137]. Cytokines proteins attach to their special

receptors, thus activating signal transduction pathways, [138]. As per different studies, it is evident that the number of cells can be kept in balance by cytokine signals, which depend on the total cell population [139]. For detailed explanation concerning the dynamics of cytokine signals, please see [140, 141]. After quasi-steady-state approximation, the number of growth factors  $g_f$  stemming from the total cell number  $N$  is given as,

$$g_f = \frac{1}{1 + k_t N}, \quad (5.9)$$

indicating maximum intensity, i.e.,  $g_f = 1$ , for small cell density and effectively zero intensity for large cell densities.

### 5.2.2 Cell cycle model

As previously stated, we consider only four microscale states (proteins) in the cell-cycle model, which are plausible enough to incorporate reversible transition between quiescent and proliferating phase. We utilise the kinetics of Michaelis-Menten to describe the chemical reactions with enzymes and substrates from the cell-cycle, which are briefly described in the sequel. Cyclin D protein makes a complex with its catalytic partner CDK4-6 when there are sufficient growth factors. After the formation of Cyclin D – CDK4/6 complex, it phosphorylates other proteins from the cell-cycle, which are critical to advancement in the first growth phase of the cell-cycle and crossing the restriction point R, [130, 142]. More precisely, the Cyclin D – CDK4/6 complex phosphorylates the retinoblastoma protein Rb to inactivate it and thus release the transcription factor E2F, which in result activates many growth promoting signals to progress the cell-cycle. p21, which inhibits CDK, regulates the cell-cycle by hindering the functions of the several CDK proteins. The description of proteins is given in the Table 5.1. We consider the evolution of cell-cycle proteins in a single-cell whose dynamics is representative of the behavior of all cells in a population. We consider that all cells behave identical and thus one ode model with similar parameters for all cells in a population represents the microscale of underlying cell-cycle dynamics. We further postulate that our representative cell in the microscale completes division at some age  $a^*$ , while, of course, our model accounts for the cells with shorter cycles at the macroscale via function  $\beta(a)$ . The following ODE system describes the cell-cycle dynamics, [143]:

$$\frac{dx_1}{da} = k_{1s} \left( \frac{g_f}{k_{gf} + g_f} \right) - k_{14} x_4 x_1 - k_{1d} \left( \frac{x_1}{k_1 + x_1} \right), \quad (5.10a)$$

$$\frac{dx_2}{da} = k_{21} \left( \frac{x_{2t} - x_2}{k_2 + (x_{2t} - x_2)} \right) x_1 - k_{32} x_2 x_3 - k_{2d} x_2, \quad (5.10b)$$

$$\frac{dx_3}{da} = k_{3s} - k_{32} x_2 x_3 - k_{31} \left( \frac{x_3}{k_3 + x_3} \right) x_1 - k_{3d} x_3, \quad (5.10c)$$

$$\frac{dx_4}{da} = k_{4s} + k_{42} \left( \frac{k_{34}}{k_{34} + x_3} \right) x_2 - k_{41} \left( \frac{x_4}{k_4 + x_4} \right) x_1 - k_{4d} x_4. \quad (5.10d)$$

In Eq.(5.10a), the first term on the right-hand side describes the synthesis of Cyclin D – CDK4/6 complex induced by the growth factors  $g_f$ . The last two terms

Description	State
Cyclin D – CDK4/6	$x_1$
E2F	$x_2$
Rb	$x_3$
p21	$x_4$

Table 5.1: Description of the cell states at the microscale.

describe the binding of Cyclin D – CDK4/6 complex with tumor suppressor protein p21 and the degradation rate of Cyclin D – CDK4/6 complex, which is induced by other cell cycle proteins, for example, Cyclin D, respectively. In Eq.(5.10b), the first term on the right-hand side describes the synthesis of transcription factors E2F induced by Cyclin D – CDK4/6 complex. The second term denotes the decrement of E2F due to inhibition by retinoblastoma protein Rb, while the last term depicts a constant inactivation rate of E2F induced by other cell cycle proteins, for instance, Cyclin A. In the third equation (5.10c), the first term on the right-hand side represents the synthesis of free un-phosphorylated retinoblastoma protein Rb. The second term denotes the decline in Rb by making a complex with E2F to inhibit it. The third term refers to the deactivation of Rb by phosphorylation from Cyclin D – CDK4/6 complex and the last one to the degradation of Rb. In Eq. (5.10d), the first and second terms represent the synthesis of p21 by ATM/ATR, TGF $\beta$  pathways and induced by E2F, respectively. The third term represents the decrement in p21 due to inhibition of Cyclin D – CDK4/6 complex, and the last term stands for the degradation of p21. The description of the parameters involved in the cell cycle model (5.10a)-(5.10d) is described below in the Table 5.3. The detailed derivation of the microscale model equations is not given here; however, we suggest the interested readers to read [143] for more details. For understanding, the model simulations of above mentioned four microscale states are shown in Figure 5.2.

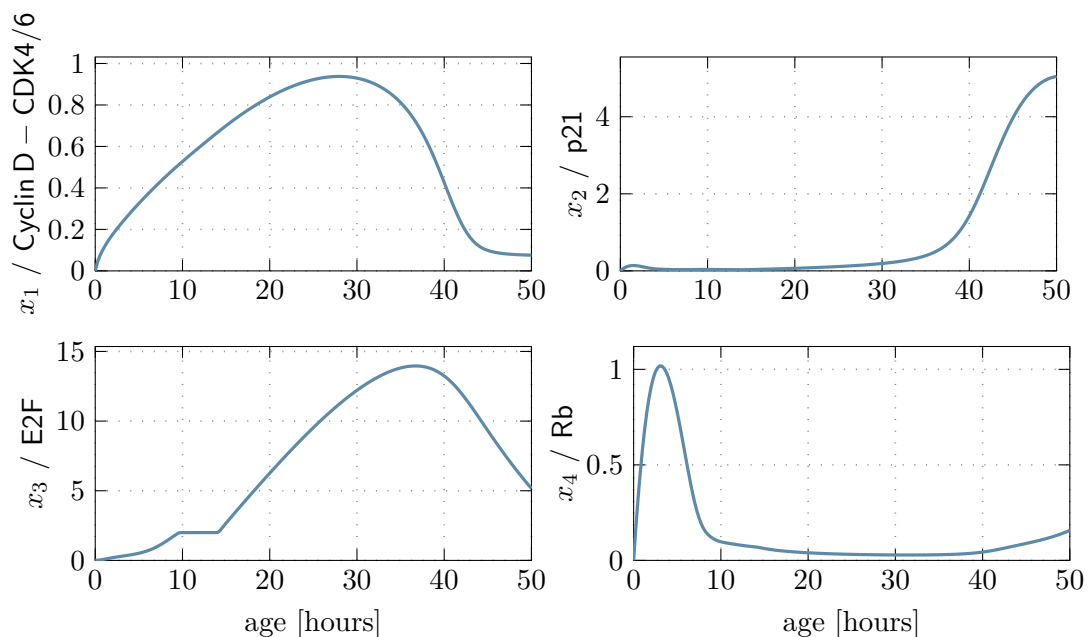


Figure 5.2: Evolution of microscale proteins from the cell-cycle. Cyclin D – CDK4/6 shows a complete activation and degradation within a full cycle. The concentration of transcription factor E2F is elevated since Retinoblastoma protein Rb is inactivated with the rise in Cyclin D – CDK4/6 complex. Similarly, protein p21 elevates near the end of the cell-cycle to help in the degradation of the Cyclin’ complex.

### 5.3 Numerical solution and simulation results

In this section, we present the numerical method used to solve the system (5.1)-(5.2) and (5.10a)-(5.10d) in MATLAB. Finite volume method (FVM) is implemented using central upwind discretization scheme for flux approximation of hyperbolic transport type PDEs, [144]. FVM is a well-established numerical simulation approach and its details can be found in [145, 146]. Hereby, we introduce the following notations:

- $\Delta a$  is mesh size and  $\Delta t$  is the time step,
- $\Delta a = a^*/N_a$ , where  $N_a$  is a maximum number of age nodes given by  $a_i = i\Delta a$ ,  $0 \leq i \leq N_a$ ,
- time is discretized into  $N_t$  steps with equidistant interval  $\Delta t = t^{k+1} - t^k$ .

The basic principle in finite volume method is to divide the domain into a number of control volumes and approximate the integral conservation law on each control volume. The one-dimensional property space along the horizontal axis has been partitioned into  $N_a$  control volumes. The flux  $\mathcal{F}$  is computed at each grid point using a central upwind scheme. An illustration of our numerical scheme is shown in the Figure 5.3. Highlighted light green box represents a control volume and we approximate the integral conservation law on each of the control volume in given domains. The green arrows are pointing the flux through the boundary of the control volume where the flux  $\mathcal{F}$  is computed at each grid point using central upwind scheme as schematically depicted with magenta boxes for  $k = 2$  at  $i = 2, 3$  with the red arrows.

In the sequel, we describe the discretized model and fluxes. The discretized cell densities of proliferating and quiescent cells associated with the  $i^{th}$  spatial interval at time  $k$  reads

$$p_i^k = \frac{1}{\Delta a} \int_{a_{i-\frac{1}{2}}}^{a_{i+\frac{1}{2}}} p(a, t^k) da, \quad q_i^k = \frac{1}{\Delta a} \int_{a_{i-\frac{1}{2}}}^{a_{i+\frac{1}{2}}} q(a, t^k) da.$$

The necessary Courant-Friedrichs-Lewy (CFL) condition for convergence of the solution requires

$$\left. \begin{aligned} & \Delta t [\gamma^k + \max(\mu_q(a_i))] \\ & \Delta t \left[ \frac{\max(g(a_i))}{\Delta a} + \max(\alpha(x_{1,i}^k, a_i) + \beta(a_i)) \right] \end{aligned} \right\} \leq 1.$$

The initial conditions for  $q_i^0$  and  $p_i^0$  are defined below

$$q_i^0 = \frac{1}{\Delta a} \int_{a_{i-\frac{1}{2}}}^{a_{i+\frac{1}{2}}} (a, t^0) da, \quad p_i^0 = \frac{1}{\Delta a} \int_{a_{i-\frac{1}{2}}}^{a_{i+\frac{1}{2}}} p(a, t^0) da.$$

Next, the discretized form of the PDEs (5.1) are given as

$$\begin{aligned} q_i^{k+1} - q_i^k &= \Delta t \alpha(x_{1,i}^k, a_i) p_i^k - \Delta t (\gamma^k + \mu_q(a_i)) q_i^k, \\ p_i^{k+1} - p_i^k - \frac{\Delta t}{\Delta a} (\mathcal{F}_{i+1/2}^k - \mathcal{F}_{i-1/2}^k) &= \Delta t \gamma^k q_i^k - \Delta t (\alpha(x_{1,i}^k, a_i) + \beta(a_i) + \mu_p(a_i)), \end{aligned}$$



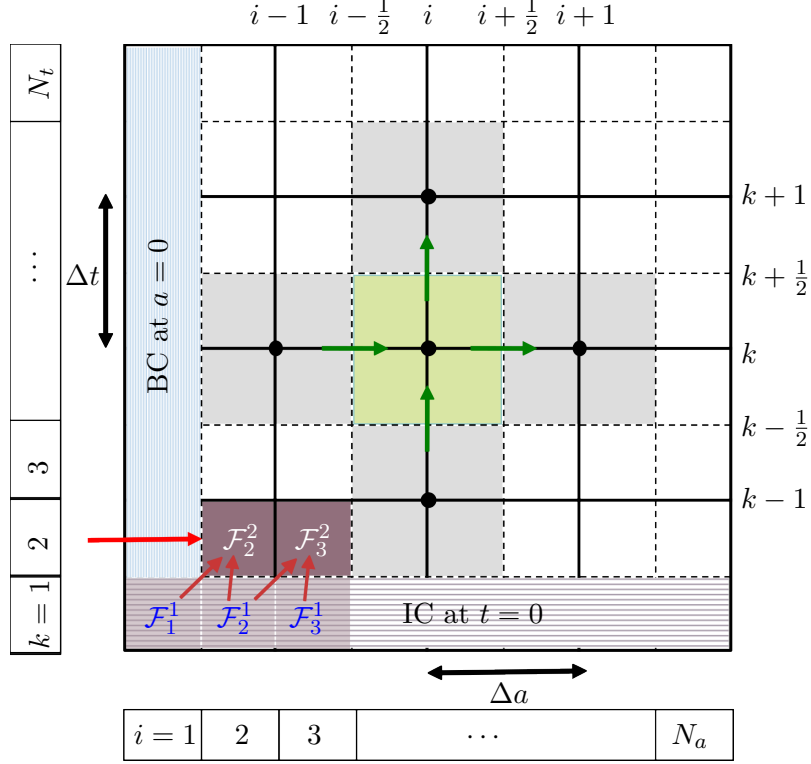


Figure 5.3: Computational mesh illustrating finite volume scheme with central upwind discretization.

where  $\gamma^k = \gamma(N^k)$  and  $N^k = \Delta a \sum_i [q_i^k + p_i^k]$ . The fluxes represented by  $\mathcal{F}$  are defined using central upwind scheme as follows

$$\mathcal{F}_{i+1/2}^k = g(a_{i+1/2})p_{i-1}^k.$$

The cell division boundary condition at age  $a = 0$  reads

$$g(a_0)p_0^{k+1} = 2\Delta a \sum_{i=1}^{a^*} \beta(a_i)p_i^k.$$

Then, we define the growth factors as

$$g_f = 1/(1 + k_t N^k)$$

and the discretized form of the cell cycle model (5.10a)-(5.10d) is

$$\begin{aligned} x_{1,i+1}^k &= x_{1,i}^k + \Delta t \left( k_{1s} \left( \frac{g_f}{k_{gf} + g_f} \right) - k_{14} x_{4,i}^k x_{1,i}^k - k_{1d} \left( \frac{x_{1,i}^k}{k_1 + x_{1,i}^k} \right) \right), \\ x_{2,i+1}^k &= x_{2,i}^k + \Delta t \left( k_{21} \left( \frac{x_{2t} - x_{2,i}^k}{k_2 + (x_{2t} - x_{2,i}^k)} \right) x_{1,i}^k - k_{32} x_{2,i}^k x_{3,i}^k - k_{2d} x_{2,i}^k \right), \\ x_{3,i+1}^k &= x_{3,i}^k + \Delta t \left( k_{3s} - k_{32} x_{2,i}^k x_{3,i}^k - k_{31} \left( \frac{x_{3,i}^k}{k_3 + x_{3,i}^k} \right) x_{1,i}^k - k_{3d} x_{3,i}^k \right), \\ x_{4,i+1}^k &= x_{4,i}^k + \Delta t \left( k_{4s} + k_{42} \left( \frac{k_{34}}{k_{34} + x_{3,i}^k} \right) x_{2,i}^k - k_{41} \left( \frac{x_{4,i}^k}{k_4 + x_{4,i}^k} \right) x_{1,i}^k - k_{4d} x_{4,i}^k \right), \end{aligned}$$

with the following initial conditions

$$x_{1,i} = x_{10}, \quad x_{2,i} = x_{20}, \quad x_{3,i} = x_{30}, \quad x_{4,i} = x_{40}.$$

We have used ode45 function of MATLAB to solve cell cycle model at each time step  $k$ . The resulting outcome of Cyclin D – CDK4/6 complex  $x_{1,i}^k$  is then used in the macroscale model by updated total number of cell population influenced by the growth factors. The implementation of the numerical algorithm is described using pseudocode given in Algorithm 1. The main loop is with respect to time evolution, and on each time step  $k$ , concentration of growth factors is updated based on updated total population of cells. These growth factors influence the cell cycle dynamics and this represents the feedback from macro- to microscale. The concentration of D – CDK4/6 complex entirely depends on growth factors and consequently influences the transition rates in macroscale and it closes the feedback loop.

---

**Algorithm 1:** Numerical method
 

---

```

initialization;
forall time step  $k = 1, 2, \dots, N_t$  do
    Compute  $N^k, g_f^k$ ;
    Compute  $x_1^k, x_2^k, x_3^k, x_4^k$  using ode45;
    forall age step  $i = 1, 2, \dots, N_a$  do
        Compute  $\beta(a_i)$ ;
        Compute  $\alpha(a_i, x_{1,i}^k)$ ;
        Compute  $\Gamma(N^k)$ ;
        Compute  $q_i^{k+1}$  and  $p_i^{k+1}$ ;
    end
    Compute CFL condition;
    if  $CFL < 1$  then
        continue;
    else
        break;
        disp('CFL is not satisfied')
    end
end
    
```

---

### 5.3.1 Simulation results

In this section, we present the numerical results of the model proposed in (5.1)-(5.2) and (5.10a)-(5.10d) for illustration purposes. The behavioral patterns of the model are investigated hereby with the objective to observe the evolution of both sub-populations coupled with cell cycle dynamics. The initial states and the used parameters are given in Table 5.3 and 5.2. In all the simulations, we used the spatial step size  $\Delta a = 0.5$  with maximum age of cells  $a^* = 50$  and the time step  $\Delta t = 0.02$ . Moreover, for sake of simplicity, we use unit speed, i.e.,  $g(a) = 1$ . In the sequel, we will discuss the following three case studies.

*Local stability of the non-trivial steady-state solution:*

First, we investigate the local stability of the non-trivial steady-state. The parameter values used are  $\mu_p = \mu_q = 0.0014$ . We take  $\gamma(N) = 6.8964 \times 10^{-6}$  and  $\rho_1 = 1.0$ . The initial conditions are assumed as  $p(a, 0) = q(a, 0) = \frac{k_0}{\sqrt{2\pi\sigma^2}} \exp\left(-\frac{(a-\mu)^2}{2\sigma^2}\right)$ , where  $k_0 = 10^6$ ,  $\mu = 2$  and  $\sigma^2 = 200$ . Figure 5.4 (a) and (b) represents the cell density distribution of proliferating  $p(a, t)$  and quiescent  $q(a, t)$  cells, respectively. Both subpopulations show the trends of achieving a steady-state with time. Figure 5.4 (c) represents the evolution of microscale state  $x_1$  concerning age  $a$  and, additionally, with respect to time due to a continuous change in the growth factors. In Figure 5.5 (a), we plot the total cell population  $N(t)$  comprised of proliferating, and quiescent cells exhibit an exponential increase in cell number and ultimately achieve a steady-state. On the other hand, Figure 5.5 (b) shows the the growth factors, which are influenced by total cell population, are maximum initially due to low cell count and gradually start declining until achieving an

Param.	Description	Value	Unit
$\nu$	Maximum transition rate from quiescent to proliferation phase	0.6 [147]	day <sup>-1</sup>
$\theta$	Total cell population beyond which $\Gamma$ is zero	$0.095 \times 10^6$ [147]	-
$\kappa$	Hill coefficient	1 [147]	-
$\rho_1$	Maximum effect of Cyclin D/CDK 4-6 complex on cell division	0.7	-
$\rho_2$	Value of Cyclin D/CDK 4-6 complex to achieve half maximum effect	0.35	-
$\gamma_1$	Hill coefficient	8	-
$\sigma_1$	Maximum rate of switching cells from proliferating to quiescent phase	0.01	-
$\sigma_2$	Switching Cyclin D/CDK 4-6 complex value beyond which $\alpha$ is close to zero	0.35	-
$\sigma_3$	Switching age value beyond which $\alpha$ is close to zero	14	h
$\gamma_2$	Hill coefficient	7	-
$\gamma_3$	Hill coefficient	7	-
$k_t$	Rate constant which measures the effect of total population on growth factors	$1.80 \times 10^{-9}$	-

Table 5.2: Parameters used in the simulations of multiscale model of proliferating and quiescent cell populations.

equilibrium. The transition rate  $\gamma(N)$  from quiescent to proliferating phase is depicted in Figure 5.5 (c). When the overall cell population increases, cell transition rate from quiescent to proliferating phase declines due to low count of growth factors.

The growth factors influence the behavior of Cyclin D – CDK4/6 complex as depicted in Figure 5.4. The total cell count is initially low (see Figure 5.5 (a)) and growth factors are at their maximum (see Figure 5.5 (b)) which results in the proper activation and degradation of Cyclin D – CDK4/6 complex along the age. The latter depicts a complete cell cycle or successful division of cells on average. However, as the growth factors decline to a point where no (or fewer) new cells are required, the average behavior of Cyclin D – CDK4/6 complex in proliferating cells also exhibit non-oscillatory dynamics and it throughout remains at a lower concentration, which is a depiction of no cell divisions. Here, a question may arise that how the behavior of a single cell can stand for the dynamics of whole population level. Indeed, the cell cell variability aspect and spatial variance are dominating factors in this mechanism and predictions of our proposed model in Figure 5.4 are only representing an averaged behavior of all the cells in a population. The feedback signal itself in Eq. (7.12) which depends on total cell population is an ideal representation of growth factors which entirely relies on total number of cells and ignores various other possible scenarios, for instance, availability of nutrients, PH level, oxygen concentration etc. Furthermore, the gamma function  $\gamma(N)$  which determines the cell transitions from quiescent to proliferating cells, is depicted in Figure 5.5 (c). It represents an inverse relation to total cell population and declines to a very low number when the respective cell populations attain a steady-state. In terms of feedback from cell cycle to population level, only concentration of Cyclin D – CDK4/6 complex is taken into account. It mainly influences the transition rate  $\alpha(x_1, a)$  from proliferating to quiescent cells.

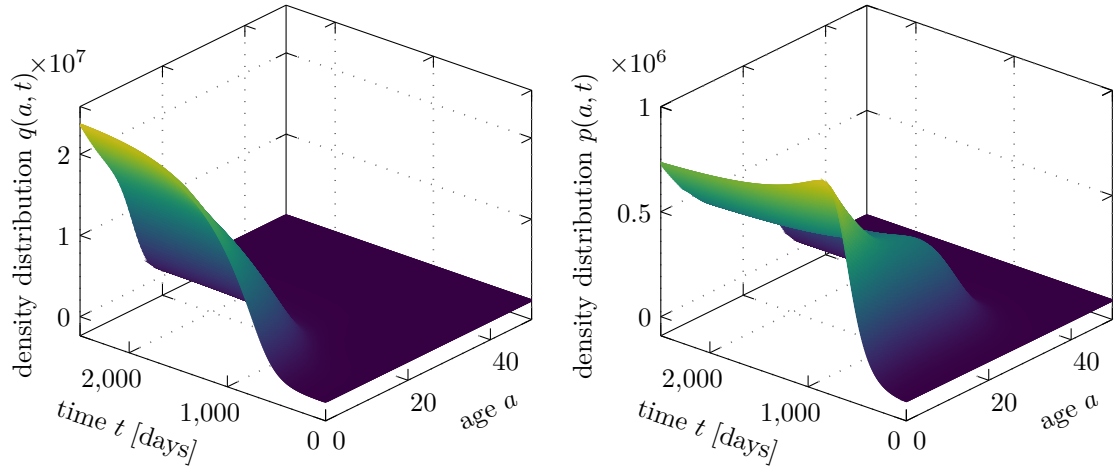


Figure 5.4: Cell density distribution quiescent and proliferating cell populations are shown with respect to age  $a$  and time  $t$ .

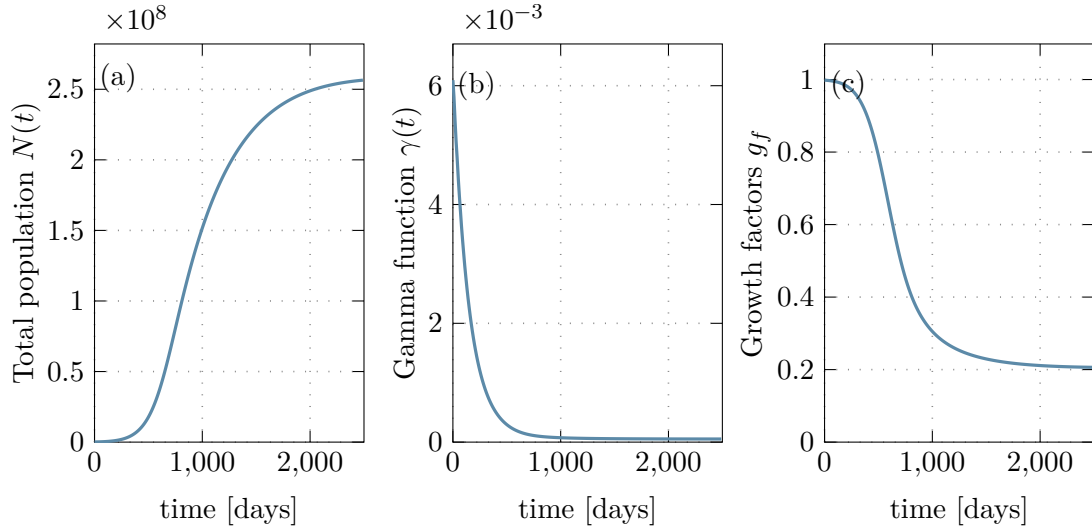


Figure 5.5: (a)  $N(t)$  achieves steady state. (b) Gamma function  $\gamma$  declines as the total cell population achieves steady state. (c) Growth-factors  $g_f$  decreasing with increase in cell population.

It is evident from the distribution of proliferating cells in Figure 5.4 that new cells are entering proliferating phase at age  $a = 0$  and after 20 hours of aging, cells start leaving the proliferating phase depending on their cycle length and concentration of Cyclin D – CDK4/6 complex. However, quiescent cells  $q(a, t)$  are accumulating with the proliferating cells which do not achieve certain level of Cyclin D – CDK4/6 concentration to pass a restriction point from  $G_1 - S$  phase of cell cycle.

Local stability of the trivial steady-state:

Next, we investigate the local stability of the trivial steady-state. Thereby, we choose the death rates to be constants and  $\mu_p = \mu_q = 0.0184$ . Moreover, we take  $\rho_1 = 0.20$  and  $\nu = 0.1$ . The initial conditions are taken as  $p(a, 0) = q(a, 0) = \frac{k_0}{\sqrt{2\pi\sigma^2}} \exp\left(-\frac{(a-\mu)^2}{2\sigma^2}\right)$ ,

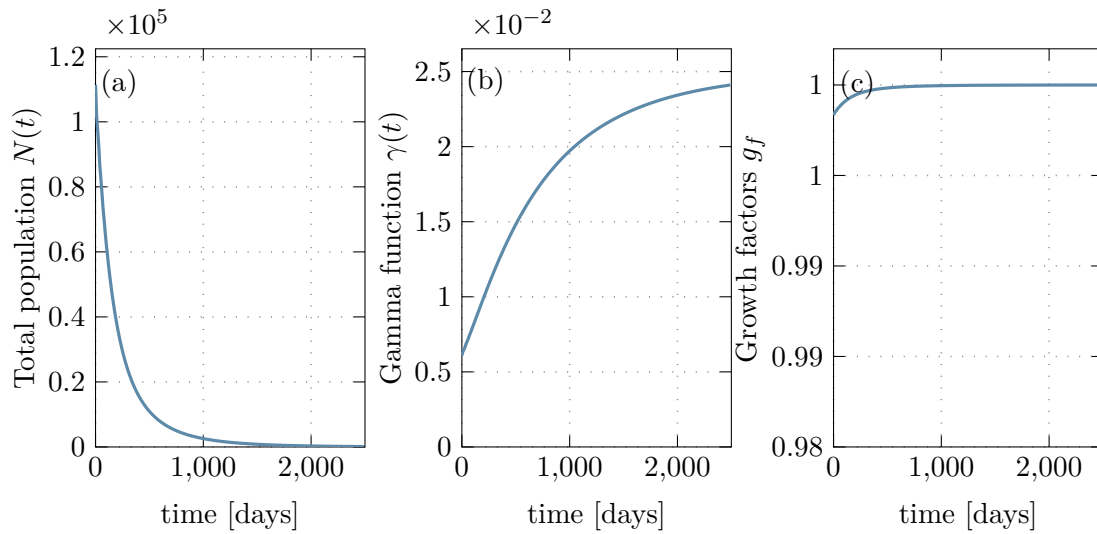


Figure 5.6: (a) Total population of cells  $N(t)$  decays to zero. (b) Gamma function  $\gamma$  increasing to its maximum value due to less number of cells. (c) Growth-factors  $g_f$  remain maximum due to decline in cell count.

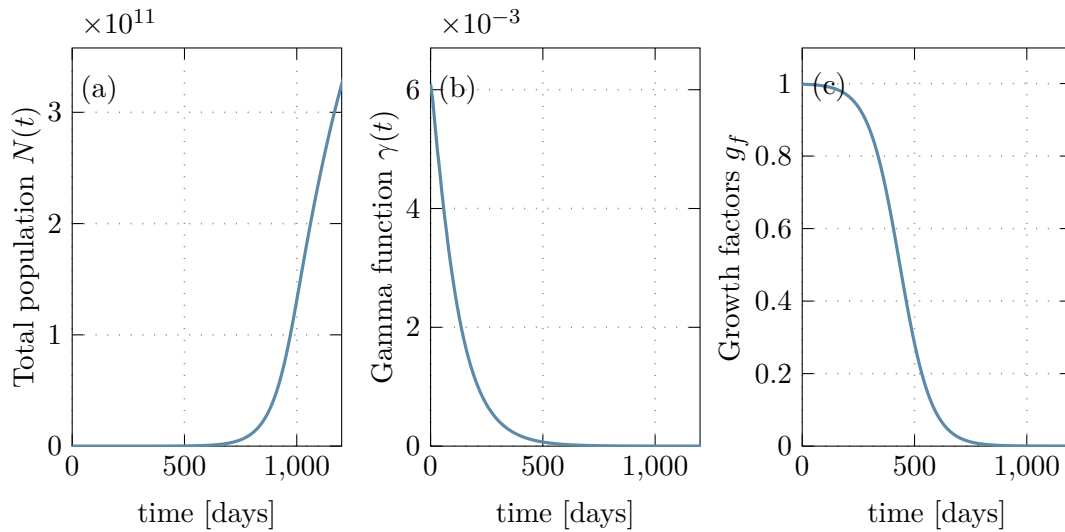


Figure 5.7: (a) Total cell population  $N(t)$  which is the sum of proliferating and quiescent cells of all ages. It grows exponentially with time thus depicting an unstable behavior. (b) Gamma function, representing the rate at which the cells move back to proliferation phase from quiescent phase, is also declining. (c) Growth factors increasing with the increase in total cell population. However, as the change in  $N(t)$  larger and larger, the change in growth factors is negligible.

where  $k_0 = 10^6$ ,  $\mu = 2$  and  $\sigma^2 = 200$ . The trivial steady-state is locally stable as shown in Figure 5.6. The parameters used in Figure 5.6 are same as mentioned above. The total cell population  $N(t)$  is plotted in Figure 5.6(a). The trivial steady-state is achieved until 2500 hours and cell population declines to zero. The growth factors, on the other hand, reach to their maximum value 1 and retain that value throughout due to very low

cell number. The gamma function also attains its maximum with time.

Param.	Description	Value	Unit
$k_{1s}$	Rate constant for synthesis of Cyclin D – CDK4/6 induced by $g_f$	0.155	$h^{-1}$
$k_{gf}$	Michaelis constant for synthesis of the Cyclin D – CDK4/6 induced by $g_f$	0.1	$\mu M$
$k_{14}$	Bimolecular rate constant for binding of Cyclin D – CDK4/6 to p21	0.15	$\mu M^{-1}h^{-1}$
$k_{1d}$	Maximum degradation rate of Cyclin D – CDK4/6 complex	0.255	$\mu M h^{-1}$
$k_1$	Michaelis constant for the degradation of Cyclin D – CDK4/6 complex	0.1	$\mu M$
$k_{21}$	Rate constant for activation of E2F by Cyclin D – CDK4/6 complex	0.805	$h^{-1}$
$k_2$	Michaelis constant for E2F activation by Cyclin D – CDK4/6 complex	0.01	$\mu M$
$x_{2t}$	Total concentration of the transcription factor E2F	2	$\mu M$
$k_{32}$	Bimolecular rate constant for binding of Rb to E2F	0.01	$\mu M^{-1}h^{-1}$
$k_{2d}$	Apparent first-order rate constant for non-specific E2F degradation	0.02	$h^{-1}$
$k_{3s}$	Basal rate of synthesis of Rb	0.8	$h^{-1}$
$k_{31}$	Rate constant for phosphorylation of Rb by Cyclin D – CDK4/6 complex	2.2	$h^{-1}$
$k_3$	Michaelis constant for Rb phosphorylation by Cyclin D – CDK4/6 complex	0.1	$\mu M$
$k_{3d}$	Apparent first-order rate constant for Rb degradation	0.01	$h^{-1}$
$k_{4s}$	Basal, E2F-independent rate of synthesis of p21	0.8	$\mu M h^{-1}$
$k_{42}$	Rate constant for synthesis of p21 induced by E2F	0.1	$h^{-1}$
$k_{34}$	Constant of inhibition by Rb of p21 synthesis	0.1	$\mu M$
$k_{41}$	Rate constant for p21 inactivation via phosphorylation by Cyclin D – CDK4/6 complex	50	$h^{-1}$
$k_4$	Michaelis constant for p21 phosphorylation by Cyclin D – CDK4/6	0.5	$\mu M$
$k_{4d}$	Apparent first-order rate constant for non-specific p21 degradation	0.06	$h^{-1}$

Table 5.3: Parameters of the cell-cycle model, [126]. Here  $\mu M$  and  $h$  represents micromolar and hour, respectively.

*Instability in the solution:*

Finally, we investigate the instability of the solution in Figure 5.7. The dynamics of the proposed model is very robust in general due to the feedback loops. However, the transition function  $\alpha(a, x_1)$  is very sensitive with respect to a noise in the cell cycle states. Here, to analyse a situation in which cell cycle behaves abnormally, we changed a parameter  $k_{gf} = 0.0001$  which means that the influence of the growth factors on production of Cyclin D – CDK4/6 complex is somehow compromised. More precisely, by changing this

value, we are inducing delays in the completing an oscillation of Cyclin D – CDK4/6 complex. Resultantly, the cell number grows exponentially. All other parameters used in this case study are similar to the case study of non-trivial steady-states. The total cell number is plotted in Figure 5.7 (a). It grows exponentially in the presence of larger amount of growth factors, as shown in Figure 5.7 (b). However, the transition function  $\gamma(N)$  is reducing over time.

## 5.4 Discussion and conclusion

The proposed model does have some limitations also. The model, for example, excludes cell-to-cell variability, which is an important aspect to capture noise and heterogeneity from the cellular level. The feedback model, which includes growth factors, is relatively simple, and activation of the Cyclin D – CDK4/6 complex can only be characterized by taking into account all signaling pathways. Furthermore, at the microscale, the cell cycle model is confined to Cyclin D and the proteins in direct interaction with it; nevertheless, multiple additional proteins can control this network in various situations/scenarios. Finally, while the Cyclin D complex and its inhibitor CDK4/6 play an important role in the  $G_1 - S$  transition, the other restriction point in the S phase for detecting DNA damage has been overlooked.

In a nutshell, we proposed a non-linear, multiscale modeling of physiologically-structured quiescent and proliferating cells in relation to cell-cycle dynamics, which play an essential part in committing a cell to irreversible cell-division process. The non-dividing quiescent cell population is also modeled, and there exists a bi-directional transition between the two sets of populations. A closed feedback loop not only couples the two scales but further aids in keeping the overall growth of the cells in homeostasis. Finally, numerical simulations were conducted with three scenarios of some variations in the parameters. The first scenario explains the steady-state behavior of the model in a healthy person under normal conditions. The second scenario relates to a trivial steady-state where, hypothetically, the decline in cell number density is more than the rise due to newborn cells. Finally, in the third case study, we investigate the impact of Cyclin D – CDK4/6 complex on the transition between two sub-populations. It turns out that any fluctuations in synthesis and degradation of Cyclin D – CDK4/6 complex can result in an abnormal growth in cell number, thus leading to cancer.





---

**Mathematical analysis: Wellposedness and stability properties of multiscale model**

---

In this chapter, we demonstrate the uniqueness and existence of non-negative solutions using semigroup and spectral theory from functional analysis. The main objective is to rigorously determine the well-posed nature of the model equations introduced in Chapter 5. We also derive steady-state solutions and then obtain spectral criteria for local stability for steady-state solutions in the sense that if the growth bound of the linearised semigroup is negative, the steady-state solution is the locally asymptotically stable, and if growth bound is positive, the steady-state solution is unstable. In the sequel, a brief introduction to semigroup theory is provided. Following that, we will derive wellposedness and stability conditions for our model from Chapter 5.

**6.1 Semigroup theory: A brief overview**

Semigroup theory is a powerful mathematical framework that plays a pivotal role in the analysis of evolution equations arising in various fields of science and engineering. This theory provides a systematic approach to understanding the behavior of dynamical systems governed by ordinary and partial differential equations (ODEs and PDEs) in both deterministic and stochastic settings. In this introductory discussion, we will explore the fundamental concepts of semigroup theory and its application in proving the existence, uniqueness, and stability of coupled ODE-PDE models.

Let  $X$  be a Banach space (a complete normed vector space) and let  $B(X)$  be the set of all bounded linear operators from  $X$  to itself. A *semigroup* of operators on  $X$  is a family of operators  $T(t) : 0 \leq t \leq \infty$  such that, [148]:

- For each  $t \geq 0$ ,  $T(t)$  is a bounded linear operator from  $X$  to itself, i.e.,  $T(t) \in B(X)$ .
- The family  $\{T(t) : t \geq 0\}$  satisfies the semigroup property: For all  $s, t \geq 0$ , the composition of operators  $T(s)$  and  $T(t)$  is equivalent to applying  $T(s + t)$ :

$$T(s + t) = T(s) \circ T(t),$$

where  $\circ$  represents the composition of operators.

A semigroup of bounded linear operators,  $T(t)$ , is *uniformly continuous* if

$$\lim_{t \rightarrow 0} \|T(t) - I\| = 0.$$

A linear operator  $A$  defined by

$$D(A) = \{x \in: \lim_{t \rightarrow 0} \frac{T(t)x - x}{t} \text{ exists}\}$$

and

$$Ax = \lim_{t \rightarrow 0} \frac{T(t)x - x}{t} = \frac{d^+T(t)x}{dt} \Big|_{t=0} \text{ for } x \in D(A)$$

is the *infinitesimal generator of the semigroup*  $T(t)$ ,  $D(A)$  is the domain of  $A$ .

In essence, a semigroup of operators defines a continuous transformation of elements in the Banach space  $X$  as time progresses. It is a powerful mathematical tool commonly used to study time-dependent linear evolution equations and dynamical systems in functional analysis and partial differential equations.

Coupled ODE-PDE models are frequently encountered in scientific and engineering disciplines which describe the interplay between ODEs that govern localized phenomena and PDEs that describe spatial distributions. Semigroup theory can be instrumental in establishing the existence and uniqueness of solutions to such coupled systems, [149]. The key idea is to represent the ODE-PDE system as an abstract Cauchy problem, often in the form:

$$\begin{aligned} \frac{d}{dt}u(t) &= Au(t) + F(u(t)), \\ \frac{d}{dt}v(t, x) &= Bv(t, x) + G(v(t, x)). \end{aligned}$$

Here,  $u$  and  $v$  represent the ODE and PDE components, respectively, while  $A$ ,  $B$ ,  $F$ , and  $G$  are linear or nonlinear operators. Semigroup theory provides conditions under which this abstract problem admits a unique solution for all initial conditions, ensuring the wellposedness of the coupled model.

Stability analysis is another essential aspect of understanding the behavior of coupled differential equation models over time and yet again semigroup theory provides a rigorous framework for analyzing the stability of solutions to such systems. Stability in this context refers to the behavior of solutions with respect to perturbations in initial conditions or model parameters. By investigating the spectral properties of the generators associated with the semigroups corresponding to the ODE and PDE components, we can determine conditions under which the coupled system exhibits stability, asymptotic behavior, or chaotic dynamics, which are crucial for predicting the long-term behavior of complex dynamical systems.

## 6.2 Existence and uniqueness of non-negative solution

This section shows that the initial-boundary value problem (5.1)-(5.2), (5.10a)-(5.10d) has a unique solution. For simplicity, we will use the cell-cycle model for the whole time  $t$  and not just with respect to age  $a$ . First, we define the Banach spaces,  $X = L^1(0, a^*) \times L^1(0, a^*)$  and  $Y = L^1(0, a^*) \times L^1(0, a^*) \times L^1(0, a^*) \times L^1(0, a^*)$  with the norm  $\|\phi\| = \sum_{i=1}^2 \|\phi_i\|_1$  for  $\phi(a) = (\phi_1(a), \phi_2(a))^T \in X$  and  $\|\varphi\| = \sum_{i=1}^4 \|\varphi_i\|_1$  for  $\varphi(a) = (\varphi_1(a), \varphi_2(a), \varphi_3(a), \varphi_4(a))^T \in Y$ , where  $\|\cdot\|_1$  is ordinary norm of  $L^1(0, a^*)$ . First, we take the initial-boundary value problem of the system (5.1)-(5.2) as an abstract Cauchy problem on the Banach space  $X$ . Further, assume that  $g_a, g_{aa} \in L^\infty((0, a^*) \times \mathbb{R}^+)$ , and death rates are non-negative, i.e.,  $\mu_p(\cdot) = \mu_q(\cdot) \geq 0$ , locally integrable on  $[0, a^*)$ .

The transition rate  $\alpha(a, x_1) \in L^\infty((0, a^*) \times (0, a^*))$ , and  $\beta(a) \in L^1(0, a^*)$ . Now, first we define a linear operator  $A_1$ :

$$(A_1\phi)(a) = \begin{pmatrix} -\mu_q(a)\phi_1(a) \\ -\frac{\partial(g(a)\phi_2(a))}{\partial a} - (\beta(a) + \mu_p(a))\phi_2(a) \end{pmatrix}, \quad \phi(a) = (\phi_1(a), \phi_2(a))^T \in D(A_1),$$

where  $T$  depicts the vector's transpose and the domain  $D(A_1)$  is defined below

$$D(A_1) = \left\{ (\phi_1, \phi_2) \mid \phi_i \text{ is absolute continuous on } [0, a^*), \phi(0) = \left( 0, 2 \int_0^{a^*} \beta(a)\phi_2(a)da \right)^T \right\}.$$

The nonlinear operator  $F_1 : X \times Y \rightarrow X$  is given by

$$(F_1(\phi, \varphi))(a) = \begin{pmatrix} \frac{-\nu\theta^\kappa\phi_1(a)}{\theta^\kappa + (N\phi)^\kappa} + \alpha(\varphi_1, a)\phi_2(a) \\ \frac{\nu\theta^\kappa\phi_1(a)}{\theta^\kappa + (N\phi)^\kappa} - \alpha(\varphi_1, a)\phi_2(a) \end{pmatrix}, \quad \phi \in X, \quad \varphi \in Y,$$

where the linear operator  $N$  on  $L^1(0, a^*) \times L^1(0, a^*)$  is given by

$$N\phi = \int_0^{a^*} (\phi_1(a) + \phi_2(a)) da.$$

Let  $v(t) = (q(\cdot, t), p(\cdot, t))^T \in X$ . We can define an initial-boundary value problem (5.1)-(5.2) in the form of an abstract semilinear IVP in  $X$ :

$$\frac{d}{dt}v(t) = A_1v(t) + F_1(v(t), u(t)), \quad v(0) = v_0 \in X, \quad (6.1)$$

where  $v_0(a) = (q_0(a), p_0(a))$ .

Next, we define initial value problem (5.10a)-(5.10d) as Cauchy problem on the Banach space  $Y$ . Let  $A_2$  be a linear operator written as follows

$$(A_2\varphi)(a) = \begin{pmatrix} 0 \\ -k_{2d}\varphi_2(a) \\ k_{3s} - k_{3d}\varphi_3(a) \\ k_{4s} - k_{4d}\varphi_4(a) \end{pmatrix}, \quad \varphi(a) = (\varphi_1(a), \varphi_2(a), \varphi_3(a), \varphi_4(a))^T \in D(A_2),$$

where the domain  $D(A_2)$  is

$$D(A_2) = \{ \varphi \in Y \mid \varphi_i \text{ is absolute continuous on } [0, a^*), \varphi(0) = (0, 0, 0, 0)^T \}.$$

We define the nonlinear operator  $F_2 : X \times Y \rightarrow Y$  by

$$(F_2(\phi, \varphi))(a) = \begin{pmatrix} k_{1s} \left( \frac{g_f(N\phi)}{k_{gf} + g_f(N\phi)} \right) - k_{14}\varphi_4(a)\varphi_1(a) - k_{1d} \left( \frac{\varphi_1(a)}{k_1 + \varphi_1(a)} \right), \\ k_{21} \left( \frac{x_{2t} - \varphi_2(a)}{k_2 + (x_{2t} - \varphi_2(a))} \right) \varphi_1(a) - k_{32}\varphi_2(a)\varphi_3(a) \\ - k_{32}\varphi_2(a)\varphi_3(a) - k_{31} \left( \frac{\varphi_3(a)}{k_3 + \varphi_3(a)} \right) \varphi_1(a) \\ k_{42} \left( \frac{k_{34}}{k_{34} + \varphi_3(a)} \right) \varphi_2(a) - k_{41} \left( \frac{\varphi_4(a)}{k_4 + \varphi_4(a)} \right) \varphi_1(a) \end{pmatrix},$$

where  $\phi \in X$ ,  $\varphi \in Y$ . Let  $u(t) = (x_1(t), x_2(t), x_3(t), x_4(t))^T \in Y$ . Then the initial-boundary value problem (5.10a)-(5.10d) can be defined as an abstract semilinear IVP in  $Y$ :

$$\frac{d}{dt}u(t) = \mathbf{A}_2 v(t) + \mathbf{F}_2(v(t), u(t)), \quad u(0) = u_0 \in Y, \quad (6.2)$$

where  $u_0(t) = (x_1^0, x_2^0, x_3^0, x_4^0)$ . Now, we can define a combine Cauchy problem for (6.1) and (6.2) as follows:

$$\frac{d}{dt} \begin{pmatrix} v \\ u \end{pmatrix} = \begin{pmatrix} \mathbf{A}_1 & 0 \\ 0 & \mathbf{A}_2 \end{pmatrix} \begin{pmatrix} v \\ u \end{pmatrix} + \begin{pmatrix} \mathbf{F}_1(v, u) \\ \mathbf{F}_2(v, u) \end{pmatrix}, \quad \begin{pmatrix} v(0) \\ u(0) \end{pmatrix} = \begin{pmatrix} v_0 \\ u_0 \end{pmatrix} \in Z,$$

$$\frac{d}{dt}\zeta(t) = \mathbf{A}\zeta(t) + \mathbf{F}(\zeta(t)), \quad \zeta(0) = \zeta_0 \in Z, \quad (6.3)$$

where  $\zeta = (v, u)$ ,  $\zeta_0 = (v_0, u_0)$ ,  $\mathbf{A} = \begin{pmatrix} \mathbf{A}_1 & 0 \\ 0 & \mathbf{A}_2 \end{pmatrix}$ ,  $\mathbf{F} = \begin{pmatrix} \mathbf{F}_1 \\ \mathbf{F}_2 \end{pmatrix}$  and  $Z = \{X, Y\}$  is a Banach space.  $T(t)$  is  $C_0$ -semigroup which is generated by  $\mathbf{A}$ , for all  $t \geq 0$  and operator  $\mathbf{F}$  exhibits continuous Frechet differentiability on  $Z$  (in other words,  $\mathbf{F}_1$  and  $\mathbf{F}_2$  are Frechet differentiable on both  $X$  and  $Y$ , see Lemma 3 in the appendix, where we show Frechet differentiability of  $\mathbf{F}_1$  from  $X \rightarrow X$ ). Then there exists a maximum interval  $[0, t_1)$  for existence and uniqueness of continuous mild solution  $t \rightarrow \zeta(t, \zeta_0)$  from  $[0, t_1)$  to  $Z$  for each  $\zeta_0 \in Z$ , so that

$$\zeta(t, \zeta_0) = T(t)\zeta_0 + \int_0^t T(t-s)\mathbf{F}(\zeta(s, \zeta_0))ds, \quad \forall t \in [0, t_1) \quad (6.4)$$

and  $t_1 = +\infty$  or  $\lim_{t \rightarrow t_1^-} \|\zeta(t, \zeta_0)\| = \infty$ . Additionally, when  $\zeta_0 \in D(\mathbf{A})$ , then  $\zeta(t, \zeta_0) \in D(\mathbf{A})$  for  $0 \leq t < t_1$  and the function  $\zeta \rightarrow \zeta(t, \zeta_0)$  is continuously differentiable which also satisfies (6.3) on  $[0, t_1)$ , see Proposition 4.16 [150] and [151].

**Remark 6.2.1.** We denote the maximum value of the solution variables as  $p_{\max}$ ,  $q_{\max}$ ,  $x_{1,\max}$ ,  $x_{2,\max}$ ,  $x_{3,\max}$  and  $x_{4,\max}$ . If we normalise the governing equations using  $N(a) = p(a, t) + q(a, t) + x_1(a) + x_2(a) + x_3(a) + x_4(a)$ , then an a-priori estimate on these would lead to  $p(a, t) + q(a, t) + x_1(a) + x_2(a) + x_3(a) + x_4(a) = 1$ .

**Lemma 6.2.1.** Let  $\Omega = \{(p, q, x_1, x_2, x_3, x_4) \in Z | p \geq 0, q \geq 0, x_1 \geq 0, x_2 \geq 0, x_3 \geq 0, x_4 \geq 0\}$  and let  $\Omega_0 = \{(p, q, x_1, x_2, x_3, x_4) \in Z | 0 \leq p \leq p_{\max}, 0 \leq q \leq q_{\max}, 0 \leq x_1 \leq x_{1,\max}, 0 \leq x_2 \leq x_{2,\max}, 0 \leq x_3 \leq x_{3,\max}, 0 \leq x_4 \leq x_{4,\max}\}$ . Then, the mild solution  $\zeta(t, \zeta_0)$ ,  $\zeta_0 \in \Omega$  of (6.3), after a finite time, enters  $\Omega_0$  which is positively invariant.

*Proof.* First, we derive the solution expression from (5.2) as follows:

$$q(a, t) := \exp\left(-\int_0^t \mu_q(a) + \gamma(N(t))dt\right) \left\{ \int_0^t \exp\left(-\int_0^\xi \mu_q(a) + \gamma(N(\pi))d\pi\right) \alpha(x_1(a), a)p(a, \xi)d\xi + q_0(a) \right\}. \quad (6.5)$$

and, immediately, it follows that  $q(a, t) \geq 0$  when  $q_0(a) \geq 0$  and  $p(a, t)$  is positive. Next, to derive the solution of Eq. (5.1), we first use transformations  $\tilde{p}(a, t) = g(a)p(a, t)$  and

$\tilde{q}(a, t) = g(a)q(a, t)$  for  $t \in [0, t_1]$  and  $a \in [a_0, a^*]$ . Then for all  $t \in (0, t_1)$  and  $a \in (a_0, a^*)$ , we have from Eq. (5.1):

$$\frac{\partial \tilde{p}(a, t)}{\partial t} + g(a) \frac{\partial \tilde{p}(a, t)}{\partial a} = \gamma(N(t))\tilde{q}(a, t) - (\beta(a) + \alpha(x_1(a), a) + \mu_p(a))\tilde{p}(a, t). \quad (6.6)$$

Following that, we utilize the parameter transform given in Lemma 3.1 [140] in order to eliminate the term  $g(a)$  and introduce  $\eta$  as a new age variable for both  $p$  and  $q$ . We obtain

$$\frac{\partial}{\partial \eta} \tilde{p}(a(\eta), t) = \frac{da}{d\eta} \frac{\partial}{\partial a} \tilde{p}(a, t) = g(a) \frac{\partial}{\partial a} \tilde{p}(a, t), \quad \text{where } \frac{da}{d\eta} = g(a).$$

Therefore, from Eq. (6.6), it follows that

$$\begin{aligned} \frac{\partial \tilde{p}(a(\eta), t)}{\partial t} + \frac{\partial \tilde{p}(a(\eta), t)}{\partial \eta} &= \gamma(N(t))\tilde{q}(a(\eta), t) - (\beta(a(\eta)) + \alpha(x_1(a(\eta)), a(\eta)) \\ &\quad + \mu_p(a(\eta)))\tilde{p}(a(\eta), t). \end{aligned} \quad (6.7)$$

To determine the explicit relation of  $\tilde{p}(a(\eta), t)$ , employ the method of characteristics (MOC). We suppose that  $\tilde{p}(a(\eta), t)$  is characterized by an ordinary differential equation along the curve  $(a(\psi_1(y)), \psi_2(y)) = \psi(y)$ , then

$$\dot{\psi}_1(y) := 1 \Rightarrow \psi_1(y) = y + c_1, \quad \dot{\psi}_2(y) := 1 \Rightarrow \psi_2(y) = y + c_2, \quad z(y) := \tilde{p}(a(\psi_1(y)), \psi_2(y)),$$

where  $c_1, c_2 \in \mathbb{R}$  are constants. Then, it follows

$$\begin{aligned} \frac{dz}{dy} &= \frac{d\tilde{p}(a(\psi_1(y)), \psi_2(y))}{dy} \\ &= \frac{\partial \tilde{p}(a(\psi_1(y)), \psi_2(y))}{\partial a} \frac{da(\psi_1(y))}{d\psi_1} \frac{d\psi_1(y)}{dy} + \frac{\partial \tilde{p}(a(\psi_1(y)), \psi_2(y))}{\partial \psi_2} \frac{d\psi_2(y)}{dy} \\ &= \gamma(N(\psi_2(y)))\tilde{q}(a(\psi_1(y)), \psi_2(y)) - (\beta(a(\psi_1(y))) + \alpha(x_1(a(\psi_1(y))), a(\psi_1(y))) \\ &\quad + \mu_p(a(\psi_1(y))))\tilde{p}(a(\psi_1(y)), \psi_2(y)) \\ &= \gamma(N(\psi_2(y)))\tilde{q}(a(\psi_1(y)), \psi_2(y)) - (\beta(a(\psi_1(y))) + \alpha(x_1(a(\psi_1(y))), a(\psi_1(y))) \\ &\quad + \mu_p(a(\psi_1(y))))z(y). \end{aligned} \quad (6.8)$$

We can now write  $\tilde{p}$  using an ODE (6.8) so that

$$\begin{aligned} \tilde{p}(a(y+c_1), y+c_2) &= \tilde{p}(a(\psi_1(y)), \psi_2(y)) = z(y) \\ &= \exp\left(-\int_0^y (\beta(a(\psi_1(\xi))) + \alpha(x_1(a(\psi_1(\xi))), a(\psi_1(\xi))) + \mu_p(a(\psi_1(\xi))))d\xi\right) \\ &\quad \left[ \int_0^y \exp\left(\int_0^\zeta (\beta(a(\psi_1(\xi))) + \alpha(x_1(a(\psi_1(\xi))), a(\psi_1(\xi))) + \mu_p(a(\psi_1(\xi))))d\xi\right) \right. \\ &\quad \left. \gamma(N(\psi_2(\zeta)))\tilde{q}(a(\psi_1(\zeta)), \psi_2(\zeta))d\zeta + \tilde{p}(a(\psi_1(0)), \psi_2(0)) \right] \\ &= \exp\left(-\int_0^y (\beta(a(\xi+c_1)) + \alpha(x_1(a(\psi_1(\xi+c_1))), a(\xi+c_1)) + \mu_p(a(\xi+c_1))))d\xi\right) \\ &\quad \left[ \int_0^y \exp\left(\int_0^\zeta (\beta(a(\xi+c_1)) + \alpha(x_1(a(\psi_1(\xi+c_1))), a(\xi+c_1)) + \mu_p(a(\xi+c_1))))d\xi\right) \right. \\ &\quad \left. \gamma(N(\zeta+c_2))\tilde{q}(a(\zeta+c_1), \zeta+c_2)d\zeta + \tilde{p}(a(c_1), c_2) \right]. \end{aligned}$$

Following that, we establish the boundary set  $\Gamma := \{[a_0, a^*] \times \{0\}\} \cup \{\{0\} \times [0, t_1]\}$  in such a way that if a curve  $(a(\psi_1(y)), \psi_2(y))$  begins in  $\Gamma$ , we may utilize the boundary condition to determine  $\tilde{p}(a(c_1), c_2)$ . If we want  $(a(y + c_1), y + c_2)$  to be in  $\Gamma$ , then either  $c_1 = 0$  or  $c_2 = 0$ . This results in the two situations below. In the first scenario,  $c_1 = 0$  and  $c_2 \in [0, t_1)$  can be chosen randomly. Then, in this case,

$$\begin{aligned} \tilde{p}(a(y), y + c_2) = & \exp\left(-\int_0^y (\beta(a(\xi)) + \alpha(x_1(a(\xi)), a(\xi)) + \mu_p(a(\xi)))d\xi\right) \\ & \left[\int_0^y \exp\left(\int_0^\zeta (\beta(a(\xi)) + \alpha(x_1(a(\xi)), a(\xi)) + \mu_p(a(\xi)))d\xi\right)\gamma(N(\zeta + c_2))\right. \\ & \left.\tilde{q}(a(\zeta), \zeta + c_2)d\zeta + \tilde{p}(a(0), c_2)\right]. \end{aligned}$$

We may now utilize the characteristic solution to achieve the solution in  $\{(a(\eta), t) | t \in [0, t_1], \eta \in [0, \min(\eta^*, t))\}$ :

$$\eta \stackrel{!}{=} \psi_1(y) = y + c_1 = y \Rightarrow y = \eta \text{ and } t \stackrel{!}{=} \psi_2(y) = y + c_2 \Rightarrow c_2 = t - y,$$

which implies

$$\begin{aligned} \tilde{p}(a(\eta), t) = & \exp\left(-\int_0^\eta (\beta(a(\xi)) + \alpha(x_1(a(\xi)), a(\xi)) + \mu_p(a(\xi)))d\xi\right) \\ & \left[\int_0^\eta \exp\left(\int_0^\zeta (\beta(a(\xi)) + \alpha(x_1(a(\xi)), a(\xi)) + \mu_p(a(\xi)))d\xi\right)\gamma(N(\zeta + t - \eta))\right. \\ & \left.\tilde{q}(a(\zeta), \zeta + t - \eta)d\zeta + \tilde{p}(a(0), t - \eta)\right]. \end{aligned}$$

This establishes the equation for  $g(a(\eta))p(a(\eta), t)$  in case of  $\eta < t$ . Then, we take  $c_1 \in [0, \eta^*)$  is arbitrary and  $c_2 = 0$ . Then we achieve,

$$\begin{aligned} \tilde{p}(a(y + c_1), u) = & \exp\left(-\int_0^y (\beta(a(\xi + c_1)) + \alpha(x_1(a(\xi + c_1)), a(\xi + c_1)) + \mu_p(a(\xi + c_1)))\right. \\ & \left.d\xi\right) \left[\int_0^y \exp\left(\int_0^\zeta (\beta(a(\xi + c_1)) + \alpha(x_1(a(\xi + c_1)), a(\xi + c_1))\right.\right. \\ & \left.\left.+ \mu_p(a(\xi + c_1)))d\xi\right) + \gamma(N(\zeta))\tilde{q}(a(\zeta + c_1), \zeta)d\zeta + \tilde{p}(a(c_1), 0)\right]. \end{aligned}$$

We may now utilize the characteristic solution to achieve a solution in  $\{(a(\eta), t) | t \in [0, t_1], \eta \in [t, \eta^*)\}$ :

$$\eta \stackrel{!}{=} \psi_1(y) = y + c_1 \Rightarrow c_1 = \eta - y \text{ and } t \stackrel{!}{=} \psi_2(y) = y + c_2 \Rightarrow y = t,$$

which results into

$$\begin{aligned} \tilde{p}(a(\eta), t) = & \exp\left(-\int_0^t (\beta(a(\xi + \eta - t)) + \alpha(x_1(a(\xi + \eta - t)), a(\xi + \eta - t))\right. \\ & \left.+ \mu_p(a(\xi + \eta - t)))d\xi\right) \left[\int_0^t \exp\left(\int_0^\zeta (\beta(a(\xi + \eta - t))\right.\right. \\ & \left.\left.+ \alpha(x_1(a(\xi + \eta - t)), a(\xi + \eta - t)) + \mu_p(a(\xi + \eta - t)))d\xi\right) \\ & \left.\gamma(N(\zeta))\tilde{q}(a(\zeta + \eta - t), \zeta)d\zeta + \tilde{p}(a(\eta - t), 0)\right]. \end{aligned}$$

This establishes the equation for  $g(a(\eta))p(a(\eta), t)$  for  $\eta > t$ . Thus, the final solution for  $g(a(\eta))p(a(\eta), t)$  can be written as:

$$\tilde{p}(a(\eta), t) := \begin{cases} \exp\left(-\int_0^\eta (\beta(a(\xi)) + \alpha(x_1(a(\xi)), a(\xi)) + \mu_p(a(\xi)))d\xi\right) \left[ h(t - \eta) \right. \\ \left. \int_0^\eta \exp\left(\int_0^\zeta (\beta(a(\xi)) + \alpha(x_1(a(\xi)), a(\xi)) + \mu_p(a(\xi)))d\xi\right) \right. \\ \left. \gamma(N(\zeta + t - \eta))\tilde{q}(a(\zeta), \zeta + t - \eta)d\zeta \right], & \bar{a} < t \\ \exp\left(-\int_0^t (\beta(a(\xi + \eta - t)) + \alpha(x_1(a(\xi + \eta - t)), a(\xi + \eta - t)) + \right. \\ \left. \mu_p(a(\xi + \eta - t)))d\xi\right) \left[ p_0(a(\eta - t)) + \int_0^t \exp\left(\int_0^\zeta (\beta(a(\xi + \eta - t)) \right. \right. \\ \left. \left. + \alpha(x_1(a(\xi + \eta - t)), a(\xi + \eta - t)) + \mu_p(a(\xi + \eta - t)))d\xi\right) \gamma(N(\zeta)) \right. \\ \left. \tilde{q}(a(\zeta + \eta - t), \zeta)d\zeta \right], & \bar{a} \geq t. \end{cases}$$

where,  $h(t - \eta)$  denotes the boundary condition  $\tilde{p}(a(0), t - \eta)$ . It can be seen that above relation for  $g(a)p(a, t)$  is positive for positive initial data and when  $g(a)q(a, t) \geq 0$ .

Next, we check the positivity of coupled ODE model (5.10a)-(5.10d). Thereby, the set of ODEs are written as

$$\begin{cases} \frac{dx_1}{da} = f_1(x_1, x_4), \\ \frac{dx_2}{da} = f_2(x_1, x_2, x_3), \\ \frac{dx_3}{da} = f_3(x_1, x_2, x_3), \\ \frac{dx_4}{da} = f_4(x_1, x_2, x_3, x_4), \end{cases} \quad (6.9)$$

where  $f_1, f_2, f_3$  and  $f_4$  represent the vector fields of the corresponding microscale states  $x_1$ - $x_4$ . Note that in Eq. (6.9),  $f_1$  does not show any dependence on  $N$  (or, in other words, dependence on  $p$  and  $q$ ) because  $N$  varies with time, and at each time step, it is a fixed constant which determines growth factors for all ages. Next, in order to check the positivity of the solutions of all ODEs in this case, it is sufficient to know that the vector fields  $f_1, f_2, f_3, f_4$  are continuously differentiable and are pointing away from the negative parts in the state space. Starting with the ODE for  $x_1$  from (6.9), we substitute  $x_4 = 0$  in  $f_1(x_1, x_4)$ , which yields  $\dot{x}_1 = f_1(x_1)$ . It can be seen that  $f_1(x_1) = k_{1s} \left( \frac{g_f}{k_{gf} + g_f} \right) - k_{1d} \left( \frac{x_1}{k_1 + x_1} \right) > 0$  for all  $a > 0$ , when  $k_{1s} \left( \frac{g_f}{k_{gf} + g_f} \right) > k_{1d} \left( \frac{x_1}{k_1 + x_1} \right)$ , which means that the concentration of  $x_1$  increases more than it decreases for all ages. It is evident since growth factors are the only source of increase in the concentration of  $x_1$ . Therefore, when growth factors are at the absolute minimum,  $x_1$  is also at its lowest concentration, and the decrement (or degradation) cannot be more than the activation of complex  $x_1$ . Since the solution to the system (5.10a)-(5.10d) is unique for each given initial condition (evident from (6.3) and (6.4)), thus for any given  $x_4 > 0$ , the solution will remain in the first quadrant. This guarantees the positivity of solution for  $x_1$ . Next,

we assume  $x_1 = 0$  in  $f_2(x_1, x_2, x_3)$  which yields an ODE  $\dot{x}_2 = f_2(x_2, x_3)$ . The solution to which takes the form  $x_2(a) = x_2^0 e^{-(k_{32}x_3(a) - k_{2a})a}$ , which implies  $x_2(a) > 0$  for all  $x_2^0 > 0$  as well as for all values of  $x_3(a)$ . Thus for any given positive initial data, the solution  $x_2(a)$  is positive for all ages. In the similar fashion, we can now substitute  $x_3 = 0$  in  $f_2(x_1, x_2, x_3)$  which yields a nonlinear ODE  $\dot{x}_2 = f_2(x_1, x_2)$ . The explicit solution cannot be computed in this case. However, the phase portrait of  $(x_1, x_2)$  shows that the solution trajectories point away from the axis which separate the positive and negative space for given positive initial data. In a similar way, we can also derive sufficient conditions for the positivity of the solutions for  $x_3(a)$  and  $x_4(a)$ . With this, we attain that, if  $\zeta_0 \in \Omega$ ,  $\zeta(t, \zeta_0) \in \Omega \forall t > 0$ , .

Now, suppose  $z(t, \cdot) = q(t, \cdot) + p(t, \cdot)$  and death rates are identical, i.e.,  $\mu_p = \mu_q$ . Then, we have from Eqs. (5.1)-(5.2):

$$\frac{dz(t, \cdot)}{dt} = Bz(t, \cdot) - \left( \frac{\partial}{\partial a} + \frac{\beta(a)}{g(a)} \right) g(a)p(t, \cdot), \quad z(0) = q_0(0) + p_0(0) \in L^1(0, a^*), \quad (6.10)$$

where we define operator B as  $B = -\mu_p(a)$  and

$$D(B) = \{ \phi \in L^1(0, a^*) | \phi \text{ is absolute continuous on } [0, a^*) \text{ and } \phi(0) = 0 \}.$$

From Eq. (6.10), it leads to

$$z(t, \cdot) = W(t)z(0, \cdot) - \int_0^t U(t-s) \left( \frac{\partial}{\partial a} + \frac{\beta(a)}{g(a)} \right) g(a)p(s, \cdot) ds, \quad (6.11)$$

where operator B generates a positive  $C_0$ -semigroup  $W(t)$ . As we know,  $W(t)$  is a nilpotent translation semigroup, it leads to  $z(t)(a) \leq q_0(a-t) + p_0(a-t)$ ,  $a > t$  and  $z(t) \leq 0$  for  $t \geq a^*$ . Therefore, the mild solution  $\zeta(t, \zeta_0)$ ,  $\zeta_0 \in \Omega$  enters  $\Omega_0$  for  $t \geq \Omega$ , and in case of  $\zeta_0 \in \Omega_0$ ,  $\zeta(t, \zeta_0) \in \Omega_0$ ,  $\forall t \geq 0$ . Hence it is proved.  $\square$

We conclude from the above result that the norm of the local solution  $\zeta(t, \zeta_0)$ ,  $\zeta_0 \in D(A) \cap \Omega$ , of (6.3) is defined and is finite. As a result, we achieve the final result.

**Theorem 6.2.1.** The abstract Cauchy problem (6.3) has a unique global classical solution on  $Z$  with respect to the initial data  $z_0 \in \Omega \cap D(A)$ .

Consequently, given a positive initial data, the IVP (5.1)-(5.2) has a unique positive solution.

### 6.3 Existence and stability of steady-state solutions

Here, we establish the steady-state solution of the model and sufficient conditions for the existence of the positive steady-state. First, we introduce some notations in the sequel. Let's define  $X$  as a real/complex Banach space and  $X^*$  be its dual space, i.e., the space of all linear functionals on  $X$ . The notation  $\langle F, \psi \rangle$  represents the value of  $F \in X^*$  at  $\psi \in X$ . A close subset  $X_+$  is called cone if the following hold:

- $X_+ \neq \{0\}$ ,
- $X_+ \cap (-X_+) = \{0\}$ ,
- $\lambda X_+ \subset X_+$ ,  $\lambda \geq 0$ ,



- $X_+ + X_+ \subset X_+$ .

The dual cone  $X_+^*$  is the subset of  $X^*$  consisting of all positive linear functionals on  $X$ , i.e.,  $F \in X_+^*$  if and only if  $F \in X^*$  and  $\langle F, \psi \rangle \geq 0$  for all  $\psi \in X_+$ .

### 6.3.1 Existence of steady-state solutions

Let  $\bar{p}$ ,  $\bar{q}$ ,  $\bar{x}_1 - \bar{x}_4$  represent the steady-states of the system (5.1)-(5.2), (5.10a)-(5.10d). Then,  $\bar{p}$ ,  $\bar{q}$ ,  $\bar{x}_1 - \bar{x}_4$  must satisfy these time-invariant system of ordinary differential equations:

$$\left\{ \begin{array}{l} 0 = \alpha(a, \bar{x}_1)\bar{p}(a) - (\bar{\gamma} + \mu_q(a))\bar{q}(a), \\ \partial_a(g(a)\bar{p}(a)) = \bar{\gamma}\bar{q}(a) - (\beta(a) + \alpha(a, \bar{x}_1) + \mu_p(a))\bar{p}(a), \\ \bar{p}(0) = 2 \int_0^{a^*} \beta(a)\bar{p}(a)da, \\ \frac{d\bar{x}_1}{da} = k_{1s} \left( \frac{\bar{g}_f}{k_{gf} + \bar{g}_f} \right) - k_{14}\bar{x}_4\bar{x}_1 - k_{1d} \left( \frac{\bar{x}_1}{k_1 + \bar{x}_1} \right), \\ \frac{d\bar{x}_2}{da} = k_{21} \left( \frac{x_{2t} - \bar{x}_2}{k_2 + (x_{2t} - \bar{x}_2)} \right) \bar{x}_1 - k_{32}\bar{x}_2\bar{x}_3 - k_{2d}\bar{x}_2, \\ \frac{d\bar{x}_3}{da} = k_{3s} - k_{32}\bar{x}_2\bar{x}_3 - k_{31} \left( \frac{\bar{x}_3}{k_3 + \bar{x}_3} \right) \bar{x}_2 - k_{3d}\bar{x}_3, \\ \frac{d\bar{x}_4}{da} = k_{4s} + k_{42} \left( \frac{k_{34}}{k_{34} + \bar{x}_3} \right) \bar{x}_2 - k_{41} \left( \frac{\bar{x}_4}{k_4 + \bar{x}_4} \right) \bar{x}_1 - k_{4d}\bar{x}_4, \end{array} \right. \quad (6.12)$$

where  $\bar{\gamma} = \gamma(\bar{N})$ ,  $\bar{g}_f = g_f(\bar{N})$  and  $\bar{N} = \int_0^{a^*} (\bar{q}(a) + \bar{p}(a))da$ . Since the ODEs of the cell-cycle model are age-dependent and with the input of growth factors at a steady-state, all cell-cycle states acquire a steady-state. Therefore, to investigate the steady-states of proliferating and quiescent cell populations  $\bar{p}(a)$  and  $\bar{q}(a)$ , we do not need to solve the ODEs of the cell-cycle model explicitly. Consequently, solving the system (6.12) for  $\bar{p}$  and  $\bar{q}$ , we obtain  $\bar{q}$  as

$$\bar{q}(a) = \frac{\alpha(a, \bar{x}_1)\bar{p}(a)}{\bar{\gamma} + \mu_q(a)}, \quad (6.13)$$

and after using the above relation for  $\bar{q}$  in the equation for  $\bar{p}$  yields

$$\frac{d(g(a)\bar{p}(a))}{da} + \left( \frac{\alpha(a, \bar{x}_1)\mu_q(a)}{\bar{\gamma} + \mu_q(a)} + \beta(a) + \mu_p(a) \right) \bar{p}(a) = 0. \quad (6.14)$$

Solving Eq. (6.14) for  $\bar{p}(a)$ , yields both steady-state solutions for  $\bar{p}(a)$  and  $\bar{q}(a)$  as follows

$$\left\{ \begin{array}{l} \bar{q}(a) = \frac{\alpha(a, \bar{x}_1)\bar{p}(0)}{\bar{\gamma} + \mu_q(a)} \exp \left( - \int_0^a \frac{1}{g(a)} \left( g'(a) + \frac{\alpha(\bar{x}_1, \xi)\mu_q(\xi)}{\bar{\gamma} + \mu_q(\xi)} + \beta(\xi) + \mu_p(\xi) \right) d\xi \right), \\ \bar{p}(a) = \bar{p}(0) \exp \left( - \int_0^a \frac{1}{g(a)} \left( g'(a) + \frac{\alpha(\bar{x}_1, \xi)\mu_q(\xi)}{\bar{\gamma} + \mu_q(\xi)} + \beta(\xi) + \mu_p(\xi) \right) d\xi \right). \end{array} \right.$$

It is clear that the system defined in Eqs. (5.1)-(5.2), (5.10a)-(5.10d) always admits a trivial steady-state.

### 6.3.2 Stability of steady-state solutions

Next, we want to derive the stability conditions for a positive steady-state solution. Suppose  $q(a, t) = \bar{q}$  and  $p(a, t) = \bar{p}$ ,  $\forall t \geq 0$  represent equilibrium solutions to the PDE model (5.1)-(5.2) and  $q^*(a, t)$  and  $p^*(a, t)$  represent the corresponding perturbation terms:

$$q(a, t) = \bar{q} + \epsilon q^*(a, t), \quad p(a, t) = \bar{p} + \epsilon p^*(a, t).$$

Substituting the above relations in to the PDE model (5.1)-(5.2), we have

$$\begin{cases} \epsilon \frac{\partial}{\partial t} q^*(a, t) = \alpha(a, \bar{x}_1)(\bar{p} + \epsilon p^*(a, t)) - \left( \frac{\nu \theta^\kappa}{\theta^\kappa + (\bar{N} + \epsilon n(t))^\kappa} + \mu_q(a) \right) (\bar{q} + \epsilon q^*(a, t)), \\ \epsilon \frac{\partial}{\partial t} p^*(a, t) + \frac{\partial}{\partial a} (g(a)(\bar{p} + \epsilon p^*(a, t))) = \left( \frac{\nu \theta^\kappa}{\theta^\kappa + (\bar{N} + \epsilon n(t))^\kappa} \right) (\bar{q} + \epsilon q^*(a, t)) \\ \quad - (\beta(a) + \alpha(a, \bar{x}_1) + \mu_p(a)) (\bar{p} + \epsilon p^*(a, t)), \\ (\bar{p}(0) + \epsilon p^*(0, t)) = 2 \int_0^{a^*} \beta(a) (\bar{p} + \epsilon p^*(a, t)) da. \end{cases}$$

where,  $n(t) := \int_0^{a^*} (p^*(a, t) + q^*(a, t)) da$ . Then, take the derivative wrt epsilon  $\epsilon$ , leads to:

$$\begin{cases} \frac{\partial}{\partial t} q^*(a, t) = \alpha(a, \bar{x}_1) p^*(a, t) - \left( \frac{\partial}{\partial \epsilon} \left( \frac{\nu \theta^\kappa \epsilon}{\theta^\kappa + (\bar{N} + \epsilon n(t))^\kappa} \right) - \mu_q(a) \right) q^*(a, t), \\ \frac{\partial}{\partial t} p^*(a, t) + \frac{\partial}{\partial a} (g(a) p^*(a, t)) = \frac{\partial}{\partial \epsilon} \left( \frac{\nu \theta^\kappa \epsilon}{\theta^\kappa + (\bar{N} + \epsilon n(t))^\kappa} \right) q^*(a, t) \\ \quad - (\beta(a) + \alpha(a, \bar{x}_1) + \mu_p(a)) p^*(a, t), \\ p^*(0, t) = 2 \int_0^{a^*} \beta(a) p^*(a, t) da, \end{cases}$$

which simplifies to

$$\begin{cases} \frac{\partial}{\partial t} q^*(a, t) = \alpha(a, \bar{x}_1) p^*(a, t) - \left( \nu \theta^\kappa \left( \frac{\theta^\kappa + (\bar{N} + \epsilon n(t))^\kappa - \kappa \epsilon n(t) (\bar{N} + \epsilon n(t))^{\kappa-1}}{(\theta^\kappa + (\bar{N} + \epsilon n(t))^\kappa)^2} \right) \right. \\ \quad \left. - \mu_q(a) \right) q^*(a, t), \\ \frac{\partial}{\partial t} p^*(a, t) + \frac{\partial}{\partial a} (g(a) p^*(a, t)) = \nu \theta^\kappa \left( \frac{\theta^\kappa + (\bar{N} + \epsilon n(t))^\kappa - \kappa \epsilon n(t) (\bar{N} + \epsilon n(t))^{\kappa-1}}{(\theta^\kappa + (\bar{N} + \epsilon n(t))^\kappa)^2} \right) \\ \quad q^*(a, t) - (\alpha(a, \bar{x}_1) + \beta(a) + \mu_p(a)) p^*(a, t), \\ p^*(0, t) = 2 \int_0^{a^*} \beta(a) p^*(a, t) da. \end{cases}$$

Taking the limit  $\epsilon \rightarrow 0$ , we obtain a linear system of PDEs:

$$\begin{cases} q_t^*(a, t) = \alpha(a, \bar{x}_1) p^*(a, t) - (\mu_q(a) + \gamma(\bar{N})) q^*(a, t), \\ p_t^*(a, t) + \partial_a (g(a) p^*(a, t)) = \gamma(\bar{N}) q^*(a, t) - (\alpha(a, \bar{x}_1) + \beta(a) + \mu_p(a)) p^*(a, t), \\ p^*(0, t) = 2 \int_0^{a^*} \beta(a) p^*(a, t) da, \end{cases} \quad (6.15)$$

where  $\gamma(\bar{N}) = \nu\theta^\kappa / (\theta^\kappa + \bar{N}^\kappa)$ . Next, let  $\omega(t) = (q^*(\cdot, t), p^*(\cdot, t))^T$ , we formulate (6.15) as abstract Cauchy problem:

$$\frac{d}{dt}\omega(t) = C\omega(t), \quad \omega(0) = \omega_0 \in X, \quad (6.16)$$

on the Banach space  $X$  and the generator  $C$  is defined by

$$(C\phi)(a) = \begin{pmatrix} -(\gamma(\bar{N}) + \mu_q(a))\phi_1(a) + \alpha(a, \bar{x}_1)\phi_2(a) \\ \gamma(\bar{N})\phi_1(a) - \left(\frac{\partial}{\partial a} + \frac{1}{g(a)}(\beta(a) + \alpha(a, \bar{x}_1) + \mu_p(a))\right)g(a)\phi_2(a) \end{pmatrix},$$

where

$$\phi(a) = (\phi_1(a), \phi_2(a))^T \in D(C),$$

and  $D(C)$  is defined below:

$$D(C) = \left\{ (\phi_1, \phi_2) \mid \phi_i \text{ is absolute continuous on } [0, a^*), \phi(0) = \left( 2 \int_0^{a^*} \beta(a)\phi_2(a)da, 0 \right)^T \right\}.$$

Next, the resolvent equation for operator  $C$  is considered as,

$$(\lambda I - C)\phi = \psi, \quad \phi \in D(C), \quad \psi \in X, \quad \lambda \in \mathbb{C}. \quad (6.17)$$

Which leads to

$$(\lambda + \gamma(\bar{N}) + \mu_q(a))\phi_1(a) - \alpha(a, \bar{x}_1)\phi_2(a) = \psi_1(a) \quad (6.18a)$$

$$-\gamma(\bar{N})\phi_1(a) + \frac{\partial}{\partial a}(g(a)\phi_2(a)) + (\lambda + \beta(a) + \alpha(a, \bar{x}_1) + \mu_p(a))\phi_2(a) = \psi_2(a), \quad (6.18b)$$

and

$$\phi_2(0) = 2 \int_0^{a^*} \beta(a)\phi_2(a)da.$$

By solving (6.18a), we get

$$\phi_1(a) = \frac{\psi_1(a) + \alpha(a, \bar{x}_1)\phi_2(a)}{\lambda + \gamma(\bar{N}) + \mu_q(a)}. \quad (6.19)$$

Which after substituting in Eq. (6.18b) and solving gives

$$\begin{aligned} \phi_2(a) = & \exp\left(-\int_0^a \beta(\xi) + \alpha(\bar{x}_1, \xi) + \lambda + \mu_p(\xi) - \frac{\gamma(\bar{N})\alpha(\bar{x}_1, \xi)}{g(\xi)(\lambda + \gamma(\bar{N}) + \mu_q(\xi))}d\xi\right) \\ & \left[ \int_0^a \exp\left(\int_0^\zeta \beta(\xi) + \alpha(\bar{x}_1, \xi) + \lambda + \mu_p(\xi) - \frac{\gamma(\bar{N})\alpha(\bar{x}_1, \xi)}{g(\xi)(\lambda + \gamma(\bar{N}) + \mu_q(\xi))}d\xi\right) \right. \\ & \left. \frac{1}{g(\zeta)} \left\{ \psi_2(\zeta) + \frac{\gamma(\bar{N})\psi_1(\zeta)}{\lambda + \gamma(\bar{N}) + \mu_q(\zeta)} \right\} d\zeta + \phi_2(0) \right]. \end{aligned}$$

Substituting  $\phi_2(a)$  back in Eq. (6.19) yields

$$\begin{aligned} \phi_1(a) = & \frac{1}{\lambda + \gamma(\bar{N}) + \mu_q(a)} \left[ \exp \left( - \int_0^a \beta(\xi) + \alpha(\bar{x}_1, \xi) + \lambda + \mu_p(\xi) \right. \right. \\ & - \frac{\gamma(\bar{N})\alpha(\bar{x}_1, \xi)}{g(\xi)(\lambda + \gamma(\bar{N}) + \mu_q(\xi))} d\xi \left. \right) \left\{ \int_0^a \exp \left( \int_0^\zeta \beta(\xi) + \alpha(\bar{x}_1, \xi) + \lambda + \mu_p(\xi) \right. \right. \\ & - \frac{\gamma(\bar{N})\alpha(\bar{x}_1, \xi)}{g(\xi)(\lambda + \gamma(\bar{N}) + \mu_q(\xi))} d\xi \left. \right) \frac{1}{g(\zeta)} \left\{ \psi_2(\zeta) + \frac{\gamma(\bar{N})\psi_1(\zeta)}{\lambda + \gamma(\bar{N}) + \mu_q(\zeta)} \right\} d\zeta \\ & \left. \left. + \phi_2(0) \right\} \alpha(a, \bar{x}_1) + \psi_1(a) \right]. \end{aligned}$$

**Lemma 6.3.1.** The operator  $C$  has a compact resolvent and

$$\sigma(C) = \sigma_P(C) = \{\lambda \in \mathbb{C} \mid -\mu_q - \gamma(\bar{N}) \in \sigma_P(U_\lambda)\}, \quad (6.20)$$

where  $\sigma(C)$  is the spectrum and  $\sigma_P(C)$  represents the point spectrum of operator  $C$ .

*Proof.* Let's rewrite  $\phi_1(a)$  as

$$\phi_1(a) = (U_\lambda \psi_2)(a) + (V_\lambda \psi_1)(a),$$

where  $U_\lambda$  and  $V_\lambda$  are the linear operators on Banach space, given as

$$(U_\lambda \psi)(a) = \int_0^{a^*} \mathcal{G}_\lambda(\zeta, a) \psi(\zeta) d\zeta, \quad (V_\lambda \psi)(a) = \int_0^{a^*} \mathcal{H}_\lambda(\zeta, a) \psi(\zeta) d\zeta, \quad (6.21)$$

where

$$\begin{aligned} \mathcal{G}_\lambda(\zeta, a) = & \frac{\alpha(a, \bar{x}_1)}{g(\zeta)(\lambda + \gamma(\bar{N}) + \mu_q(a))} \exp \left( - \int_0^a \beta(\xi) + \alpha(\bar{x}_1, \xi) + \lambda + \mu_p(\xi) \right. \\ & - \frac{\gamma(\bar{N})\alpha(\bar{x}_1, \xi)}{g(\xi)(\lambda + \gamma(\bar{N}) + \mu_q(\xi))} d\xi \left. \right) \exp \left( \int_0^\zeta \beta(\xi) + \alpha(\bar{x}_1, \xi) + \lambda + \mu_p(\xi) \right. \\ & \left. - \frac{\gamma(\bar{N})\alpha(\bar{x}_1, \xi)}{g(\xi)(\lambda + \gamma(\bar{N}) + \mu_q(\xi))} d\xi \right), \end{aligned} \quad (6.22)$$

and

$$\mathcal{H}_\lambda(\zeta, a) = \frac{1}{g(\zeta)(\lambda + \gamma(\bar{N}) + \mu_q(\zeta))} \left( \gamma(\bar{N}) \mathcal{G}_\lambda(\zeta, a) + \frac{g(\zeta)}{a^*} \right).$$

Similarly, we rewrite  $\phi_2(a)$  as

$$\phi_2(a) = \frac{1}{\alpha(a, \bar{x}_1)} \{ (\lambda + \gamma(\bar{N}) + \mu_q)(U_\lambda \psi_2)(a) + \gamma(\bar{N})(U_\lambda \psi_1)(a) \}.$$

Let  $\Lambda = \{\lambda \in \mathbb{C} \mid -\mu_q(\cdot) - \gamma(\bar{N}) \in \sigma(U_\lambda)\}$ , then we can say that if  $\lambda \in \mathbb{C} \setminus \Lambda$ , operators  $U_\lambda$  and  $V_\lambda$  are compact operators from  $X$  to  $L^1(0, a^*)$ . This implies  $\phi_1(a)$  is represented by a compact operator. In a similar fashion,  $\phi_2(a)$  is also represented by a compact operator. Resultantly, we get that operator  $C$  has a compact resolvent which further implies that  $\sigma(C)$  comprises entirely of isolated eigenvalues, i.e.,  $\sigma(C) = \sigma_P(C)$  (see p.187, Theorem 6.29 in [152]). From latter, we know that  $\mathbb{C} \setminus \Lambda \subset \rho(C)$ , where  $\rho(C)$  is the resolvent of  $C$ . This implies  $\sigma_P(C) = \sigma(C) \subset \Lambda$ . Since  $U_\lambda$  is a compact operator, then it leads to  $\sigma(U_\lambda) \setminus \{0\} = \sigma_P(U_\lambda) \setminus \{0\}$ . Now if  $\lambda \in \Lambda$ , there exists an eigenfunction  $\psi_\lambda$  such that  $U_\lambda \psi_\lambda = \psi_\lambda$ . Then, it is trivial to see that  $(\phi_1(a), \phi_2(a))^T$  provides an eigenvector of  $C$  for an eigenvalue  $\lambda$ . Then  $\Lambda \subset \sigma_P(C)$ , and finally, we can say that (6.20) satisfies.  $\square$

**Lemma 6.3.2.** Let  $\mathbf{T}(t)$  be the  $C_0$ -semigroup generated by the operator  $C$ ,  $t \geq 0$ . Then,  $\mathbf{T}(t)$  is eventually norm continuous (ENC) and

$$\omega_0(C) = s(C) = \sup\{\operatorname{Re}\lambda \mid \lambda \in \sigma(C)\}, \quad (6.23)$$

where  $\omega_0(C)$  represents the growth bound of semigroup  $\mathbf{T}(t)$  and  $s(C)$  denotes the spectral bound of the operator  $C$ .

*Proof.* First, we write the bounded operator  $C$  as:

$$C\phi = \begin{pmatrix} -(\gamma(\bar{N}) + \mu_q(a)) & \alpha(a, \bar{x}_1) \\ \gamma(\bar{N}) & -\left(\frac{\partial}{\partial a} + \frac{1}{g(a)}(\beta(a) + \alpha(a, \bar{x}_1) + \mu_p(a))\right)g(a) \end{pmatrix} \begin{pmatrix} \phi_1(a) \\ \phi_2(a) \end{pmatrix},$$

for  $\phi \in X$ . To prove the compactness of  $C$ , we show that for any bounded sequence  $(\phi^n)_{n \in \mathbb{N}}$  in  $X$ , the sequence  $(C\phi^n)_{n \in \mathbb{N}}$  has a uniformly convergent subsequence. For this we use the Arzelà-Ascoli Theorem. Thereby, we need to check that  $(C\phi^n)_{n \in \mathbb{N}}$  is uniformly bounded and uniformly equicontinuous. For the boundedness, note that since we assumed that  $(\phi^n)_{n \in \mathbb{N}}$  is bounded, we have

$$\|C\phi^n\|_1 \leq \|C\| \|\phi^n\|_1 \leq \|C\| \sup_{n \in \mathbb{N}} \|\phi^n\|_1,$$

proving that  $(C\phi^n)_{n \in \mathbb{N}}$  is also bounded. Next, for the uniform equicontinuity, consider

$$\begin{aligned} \int_R |(C\phi)(a+h) - (C\phi)(a)| da &= \int_R |C(a+h) - C(a)| |\phi(a)| da \\ &\leq \int_R \left| \begin{pmatrix} -\gamma(\bar{N}) - \mu_q(a+h) & \alpha(a+h, \bar{x}_1) \\ \gamma(\bar{N}) & -\frac{\partial}{\partial a+h}g(a+h) - \beta(a+h) - \alpha(a+h, \bar{x}_1) - \mu_p(a+h) \end{pmatrix} \right. \\ &\quad \left. - \begin{pmatrix} -\gamma(\bar{N}) - \mu_q(a) & \alpha(a, \bar{x}_1) \\ \gamma(\bar{N}) & -\frac{\partial}{\partial a}g(a) - \beta(a) - \alpha(a, \bar{x}_1) - \mu_p(a) \end{pmatrix} \right| \begin{vmatrix} \phi_1(a) \\ \phi_2(a) \end{vmatrix} da \\ &= \int_R \left| \begin{pmatrix} -\mu_q(a+h) + \mu_q(a) & \alpha(\bar{x}_1, a+h) - \alpha(a, \bar{x}_1) \\ 0 & k(a+h) - k(a) \end{pmatrix} \right| \begin{vmatrix} \phi_1(a) \\ \phi_2(a) \end{vmatrix} da \\ &\leq \|\phi\| \int_R \left| \begin{pmatrix} -\mu_q(a+h) + \mu_q(a) & \alpha(\bar{x}_1, a+h) - \alpha(a, \bar{x}_1) \\ 0 & k(a+h) - k(a) \end{pmatrix} \right| da, \end{aligned}$$

where  $k(a) = -\frac{\partial}{\partial a}g(a) - \beta(a) - \alpha(a, \bar{x}_1) - \mu_p(a)$ . It follows that  $(C\phi^n)_{n \in \mathbb{N}}$  is equicontinuous. Thus, by the Arzelà-Ascoli Theorem, the sequence  $(C\phi^n)_{n \in \mathbb{N}}$  has a uniformly convergent subsequence, and therefore,  $C$  is compact which implies  $\mathbf{T}$  is ENC semigroup. As we know that the spectral mapping theorem applies to ENC semigroup, we get the spectral determined growth condition, i.e.,  $\omega_0(C) = s(C)$ , thus we obtain (6.23).  $\square$

If  $\omega_0(C) < 0$ , the steady-state solution  $\omega = 0$  of (6.16) is locally exponentially asymptotically stable in a way that there exists  $\epsilon > 0$ ,  $M \geq 1$  and  $\gamma < 0$ , such that when  $x \in X$  and  $\|x\| \leq \epsilon$ , then the solution  $\omega(t, x)$  of (6.16) exists globally and  $\|\omega(t, x)\| \leq M \exp(\gamma t) \|x\|, \forall t > 0$ .

Next, to study the stability of equilibrium states, we need to find that dominant singular point, i.e., the element of set  $\Lambda$  which has the largest real part. Then utilizing (6.20) and (6.23), we can find the growth bound of semigroup  $\mathbf{T}$ .

**Lemma 6.3.3.** The operator  $U_\lambda$ ,  $\lambda \in \mathbb{R}$  is nonsupporting with respect to  $X_+$  and

$$\lim_{\lambda \rightarrow +\infty} r(U_\lambda) = 0, \quad (6.24)$$

holds.

*Proof.* It can be seen from (6.21) and (6.22) that the operator  $U_\lambda$ ,  $\lambda \in \mathbb{R}$  is strictly positive. Now, in order to show non-supporting property of  $U_\lambda$ ,  $\lambda \in \mathbb{R}$ , we can easily verify the inequality

$$U_\lambda \psi \geq \langle f_\lambda, \psi \rangle c, \quad c = 1 \in X_+, \quad \psi \in X_+, \quad (6.25)$$

where the linear function  $f_\lambda$ , is given as

$$\begin{aligned} \langle f_\lambda, \psi \rangle = & \int_0^{a^*} \left[ \frac{s(\zeta)}{g(\zeta)(\lambda + \gamma(\bar{N}) + \mu_q(a))} \exp \left( - \int_0^a \beta(\xi) + \alpha(\bar{x}_1, \xi) + \lambda + \mu_p(\xi) \right. \right. \\ & \left. \left. - \frac{\gamma(\bar{N})\alpha(\bar{x}_1, \xi)}{g(\xi)(\lambda + \gamma(\bar{N}) + \mu_q(\xi))} d\xi \right) \exp \left( \int_0^\zeta \beta(\xi) + \alpha(\bar{x}_1, \xi) + \lambda + \mu_p(\xi) \right. \right. \\ & \left. \left. - \frac{\gamma(\bar{N})\alpha(\bar{x}_1, \xi)}{g(\xi)(\lambda + \gamma(\bar{N}) + \mu_q(\xi))} d\xi \right) \right] \psi(\zeta) d\zeta. \end{aligned} \quad (6.26)$$

Thereby, it leads us to  $U_\lambda^{n+1} \psi \geq \langle f_\lambda, \psi \rangle \langle f_\lambda, c \rangle^n c$ ,  $\forall n$ . Since  $f_\lambda$  is strictly positive and the constant function  $c = 1$  is a quasi-interior point of  $L^1(0, a^*)$ , it leads to  $\langle F, U_\lambda^n \rangle > 0$  for every pair  $\psi \in X_+ \setminus \{0\}$ ,  $F \in X_+^* \setminus \{0\}$ . Then  $U_\lambda$ ,  $\lambda \in \mathbb{R}$  is nonsupporting. Following that, we utilise (6.25) and take duality pairing with the eigenfunctional  $F_\lambda$  of  $U_\lambda$  which corresponds to  $r(U_\lambda)$ , then we get

$$r(U_\lambda) \langle F_\lambda, \psi \rangle \geq \langle F_\lambda, c \rangle \langle f_\lambda, \psi \rangle.$$

Suppose  $\psi = c$ , we obtain an inequality  $r(U_\lambda) \geq \langle f_\lambda, c \rangle$ , where

$$\begin{aligned} \langle f_\lambda, c \rangle = & \int_0^{a^*} \frac{s(\zeta)}{g(\zeta)(\lambda + \gamma(\bar{N}) + \mu_q(\zeta))} \exp \left( - \int_0^a \beta(\xi) + \alpha(\bar{x}_1, \xi) + \lambda + \mu_p(\xi) \right. \\ & \left. - \frac{\gamma(\bar{N})\alpha(\bar{x}_1, \xi)}{g(\xi)(\lambda + \gamma(\bar{N}) + \mu_q(\xi))} d\xi \right) \exp \left( \int_0^\zeta \beta(\xi) + \alpha(\bar{x}_1, \xi) + \lambda + \mu_p(\xi) \right. \\ & \left. - \frac{\gamma(\bar{N})\alpha(\bar{x}_1, \xi)}{\lambda + \gamma(\bar{N}) + \mu_q(\xi)} d\xi \right) d\zeta. \end{aligned} \quad (6.27)$$

It follows that

$$\begin{aligned} \langle f_\lambda, c \rangle \geq & \epsilon \int_0^{a^*} \frac{1}{g(\zeta)(\lambda + \gamma(\bar{N}) + \mu_q(\zeta))} \exp \left( - \int_0^a \beta(\xi) + \alpha(\bar{x}_1, \xi) + \lambda + \mu_p(\xi) \right. \\ & \left. - \frac{\gamma(\bar{N})\alpha(\bar{x}_1, \xi)}{\lambda + \gamma(\bar{N}) + \mu_q(\xi)} d\xi \right) \exp \left( \int_0^\zeta \beta(\xi) + \alpha(\bar{x}_1, \xi) + \lambda + \mu_p(\xi) \right. \\ & \left. - \frac{\gamma(\bar{N})\alpha(\bar{x}_1, \xi)}{\lambda + \gamma(\bar{N}) + \mu_q(\xi)} d\xi \right) d\zeta. \end{aligned} \quad (6.28)$$

By using the positivity of  $\gamma(\bar{N})$ ,  $\mu_p$ ,  $\mu_q$ ,  $\alpha$  and  $\beta$ , we conclude the following

$$\lim_{\lambda \rightarrow +\infty} r(U_\lambda) = 0.$$

Hence, it is proven.  $\square$

Preceding Lemma concludes that  $\lambda \rightarrow r(U_\lambda)$  is a decreasing function of  $\lambda \in \mathbb{R}$ . Furthermore, if  $\lambda \in \mathbb{R}$  so that  $r(U_\lambda) = 1$ , then  $\lambda \in \Lambda$  since  $r(U_\lambda) \in \sigma_P(U_\lambda)$ . From the monotonicity of  $r(U_\lambda)$  and (6.24), the following holds.

**Lemma 6.3.4.** There exists a unique  $\lambda_0 \in \mathbb{R} \cap \Lambda$  such that  $r(U_{\lambda_0}) = 1$ , and  $\lambda_0 > 0$  if  $r(U_0) > 1$ ;  $\lambda_0 = 0$  if  $r(U_0) = 1$ ;  $\lambda_0 < 0$  if  $r(U_0) < 1$ .

Now, we will show, using Theorem 6.13 in [153], that  $\lambda_0$  is a dominant singular point.

**Lemma 6.3.5.** If there exists a  $\lambda \in \Lambda, \lambda \neq \lambda_0$ , then  $\text{Re}\lambda < \lambda_0$ .

*Proof.* Suppose that  $\lambda \in \Lambda$  and  $U_\lambda \psi = \psi$ , then  $|U_\lambda \psi| = |\psi|$ , where  $|\psi|(a) = |\psi(a)|$ . This yields  $U_{\text{Re}\lambda} \psi \geq \psi$ . Considering the duality pairing with  $F_{\text{Re}\lambda} \in X_+^*$ , we get  $r(U_{\text{Re}\lambda}) \langle F_{\text{Re}\lambda}, |\psi| \rangle \geq \langle F_{\text{Re}\lambda}, |\psi| \rangle$ , which results into the fact that  $r(U_{\text{Re}\lambda}) \geq 1$  since  $F_{\text{Re}\lambda}$  is strictly positive. As shown that  $r(U_\lambda), \lambda \in \mathbb{R}$  is declining function, it concludes that  $\text{Re}\lambda \leq \lambda_0$ . If we suppose that  $\text{Re}\lambda = \lambda_0$ , then  $U_{\lambda_0} |\psi| = |\psi|$ . In fact, if we assume  $U_{\lambda_0} |\psi| > |\psi|$  and take duality pairing with the eigenfunctional  $F_0$  corresponding to  $r(U_{\lambda_0}) = 1$  on both sides results into  $\langle F_0, |\psi| \rangle > \langle F_0, |\psi| \rangle$ , which is a contradiction. As a consequence  $U_{\lambda_0} |\psi| = |\psi|$ , from which we deduce that  $|\psi| = c\psi_0$ , where  $c$  is a constant which we may assume 1 and  $\psi_0$  is the eigenfunction corresponding to  $r(U_{\lambda_0}) = 1$ . Therefore,  $\psi(a) = \psi_0(a) \exp(iv(a))$  for, say, a real-valued function  $v(a)$ . Substituting which into  $U_{\lambda_0} \psi_0 = |U_\lambda \psi|$ , leads us to

$$\begin{aligned} & \frac{\alpha(a, \bar{x}_1)}{g(a)(\lambda_0 + \gamma(\bar{N}) + \mu_q(a))} \int_0^{a^*} \exp\left(\int_a^\zeta \beta(\xi) + \alpha(\bar{x}_1, \xi) + \lambda_0 + \mu_p(\xi) \right. \\ & \left. - \frac{\gamma(\bar{N})\alpha(\bar{x}_1, \xi)}{\lambda_0 + \gamma(\bar{N}) + \mu_q(\xi)} d\xi\right) \psi_0(\zeta) d\zeta \\ = & \left| \frac{\alpha(a, \bar{x}_1)}{g(a)(\lambda_0 + i\text{Im}\lambda + \gamma(\bar{N}) + \mu_q(a))} \int_0^{a^*} \exp\left(\int_a^\zeta \beta(\xi) + \alpha(\bar{x}_1, \xi) + \lambda_0 + i\text{Im}\lambda \right. \right. \\ & \left. \left. + \mu_p(\xi) - \frac{\gamma(\bar{N})\alpha(\bar{x}_1, \xi)}{\lambda_0 + i\text{Im}\lambda + \gamma(\bar{N}) + \mu_q(\xi)} d\xi\right) \exp(iv(\zeta)) \psi_0(\zeta) d\zeta \right|. \end{aligned}$$

From Lemma 6.12 [153], it leads us to  $\text{Im}\lambda + v(\zeta) = \Theta$ , where  $\Theta$  is a constant. Utilizing  $U_\lambda \psi = \psi$ , we get

$$\exp(i\Theta) U_{\lambda_0} \psi_{\lambda_0} = \psi_{\lambda_0} \exp(iv(\zeta)),$$

so  $\Theta = v(\zeta)$ , leads to  $\text{Im}\lambda = 0$ . Hence, the result is proven.  $\square$

**Theorem 6.3.1.** The equilibrium state  $(\bar{q}(a), \bar{p}(a))^T$ , for (5.1)-(5.2) is locally asymptotically stable if  $r(U_0) < 1$  and locally unstable if  $r(U_0) > 1$ .

*Proof.* Lemma 6.3.4 and 6.3.5 concludes that  $\sup\{\text{Re}\lambda : -\mu_q - \gamma(\bar{N}) \in \sigma_P(U_\lambda)\} = \lambda_0$ . Therefore, it results into  $s(C) = \sup\{\text{Re}\lambda : -\mu_q - \gamma(\bar{N}) \in \sigma_P(U_\lambda)\} < 0$  if  $r(U_0) < 1$  and  $s(C) > 0$  if  $r(U_0) > 1$ . Hence proved.  $\square$





---

## Multiscale mathematical model: Healthy and cancerous proliferating and quiescent cell populations

---

This chapter proposes an extension of our physiologically structured PDE model that incorporates multiscale and nonlinear features. The model accounts for both mutated and healthy populations of quiescent and proliferating cells at the macroscale, as well as the microscale dynamics of cell cycle proteins. A reversible transition between quiescent and proliferating cell populations is assumed. The growth factors generated from the total cell population of proliferating and quiescent cells influence cell cycle dynamics. As feedback from the microscale, Cyclin D – CDK4/6 protein concentration determines the transition rates between quiescent and proliferating cell populations. In the end, we executed numerical simulations to observe the impact of the parameters on the model's nonlinear dynamics.

### 7.1 Biological problem formulation

Cell populations are dynamic, with cells continuously dividing, differentiating, and sometimes accumulating mutations, [154]. Mammalian cell division patterns are critical to understanding human tumor progression. Age-structured mathematical models provide a valuable tool to simulate and analyze these intricate processes. These models categorize cells into age groups, capturing how cell properties change. By incorporating mutations and quiescence into these models, a wide range of questions related to cancer progression, tissue homeostasis, and therapeutic interventions can be explored. As already stated in Chapter 5, several research works utilize age-structured frameworks to investigate the cell population dynamics. Some examples of age-structured growth models include epidemic [102–104], microscopic virus [105, 106] and cell population [107–110] models. On the other hand, the concealed molecular complexity of a tissue demands a more thorough modelling framework that includes special cellular and molecular interactions. Age-structured models help elucidate the growth patterns of cancerous tumors, considering factors such as mutation acquisition, clonal expansion, and the role of cancer stem cells. Additionally, they can help us understand the emergence of drug resistance in cancer populations, enabling the development of more effective treatment strategies.

Cells can be in different states, including actively proliferating, quiescent (dormant), or undergoing differentiation. Modeling these transitions is crucial for understanding cell population dynamics. The proliferating cells go through different phases in the cell cycle ( $G_1$ ,  $S$ ,  $G_2$ ,  $M$ ) while dividing. Quiescent cells do not grow or divide but move to the  $G_0$

phase, remaining until they differentiate or undergo apoptosis. The transition between proliferating and quiescent populations of cells is a critical aspect of cell biology and has several important implications for the health and function of tissues and organisms. First and foremost, maintaining a balance between proliferating and quiescent cells is essential for tissue homeostasis. Proliferating cells replace damaged or dying cells, ensuring the tissue's proper functioning and structural integrity. Quiescent cells act as a reservoir, ready to proliferate when needed. Furthermore, maintaining quiescence is a protective mechanism against cancer. Typically, cells with damaged DNA or those at risk of becoming cancerous can enter a quiescent state, preventing them from dividing and potentially developing into tumors. Loss of this control can increase the risk of cancer. These transitions are essential for maintaining tissue function, conserving energy, responding to injuries, preventing cancer, regulating stem cell behaviour, and ensuring overall health and longevity. This dynamic balance is tightly regulated and contributes to the proper functioning of tissues and organisms. Growth factors play a pivotal role in regulating the transition between proliferating and quiescent populations of cells. These signalling molecules are essential for orchestrating various cellular processes, including cell proliferation, cell cycle progression, and the maintenance of quiescence, [111].

Mutations are changes in the DNA sequence of a cell, and they can affect various aspects of cell behavior, including cell cycle regulation, response to growth factors, and the decision to enter or exit quiescence. Mutations in genes that regulate cell growth and division can disturb the finely-tuned equilibrium that governs cell proliferation, which in turn can result in the emergence of cancer. Although other factors like environmental exposures and lifestyle choices may also play a role in cancer development, mutations in genes are a major contributor to this disease. Mutations can be of several types, those that are particularly significant for cancer involve increased potential for proliferation, decreased apoptosis, genetic instability, and reduced tumor suppression [1]. The exact number of mutations needed for cancer initiation varies widely, and it is influenced by factors such as the type of cancer, the specific genetic and environmental context, and the presence of other genetic alterations. Some cancers may develop from a single critical mutation, while others may require multiple mutations, [155, 156]. Furthermore, studies have shown that the transformation of a normal cell into a cancerous one usually requires the accumulation of one to ten mutations [1, 49]. In cancerous tissues, mutated cells can coexist with healthy cells (non-cancerous or normal cells). Cancer arises from genetic mutations in a subset of cells within a tissue, and these mutated cells continue to proliferate alongside the surrounding normal cells. This coexistence is a hallmark of cancer, and the interactions between cancer and normal cells within the tumor microenvironment can influence disease progression.

This research focuses on the model development of the cell population in all healthy and mutated cell populations. We investigate the coupling dynamics of tissue cell density and cell cycle proteins. Previous studies have used age-structured models to investigate cell populations in quiescent phase [110] only, the proliferating phase [112, 113] only, or both phases together [109, 114–118]. Despite this, the impact of molecular interactions on the interplay between proliferative and quiescent phases at the subcellular level has yet to be examined. Thus, the primary aim of this paper is to develop a multiscale model utilizing mathematical techniques that can capture the intricacies of a complex system existing at the sub-cellular level. Schematics in Figure 7.1 depicts multiscale-modeling framework used in this chapter.

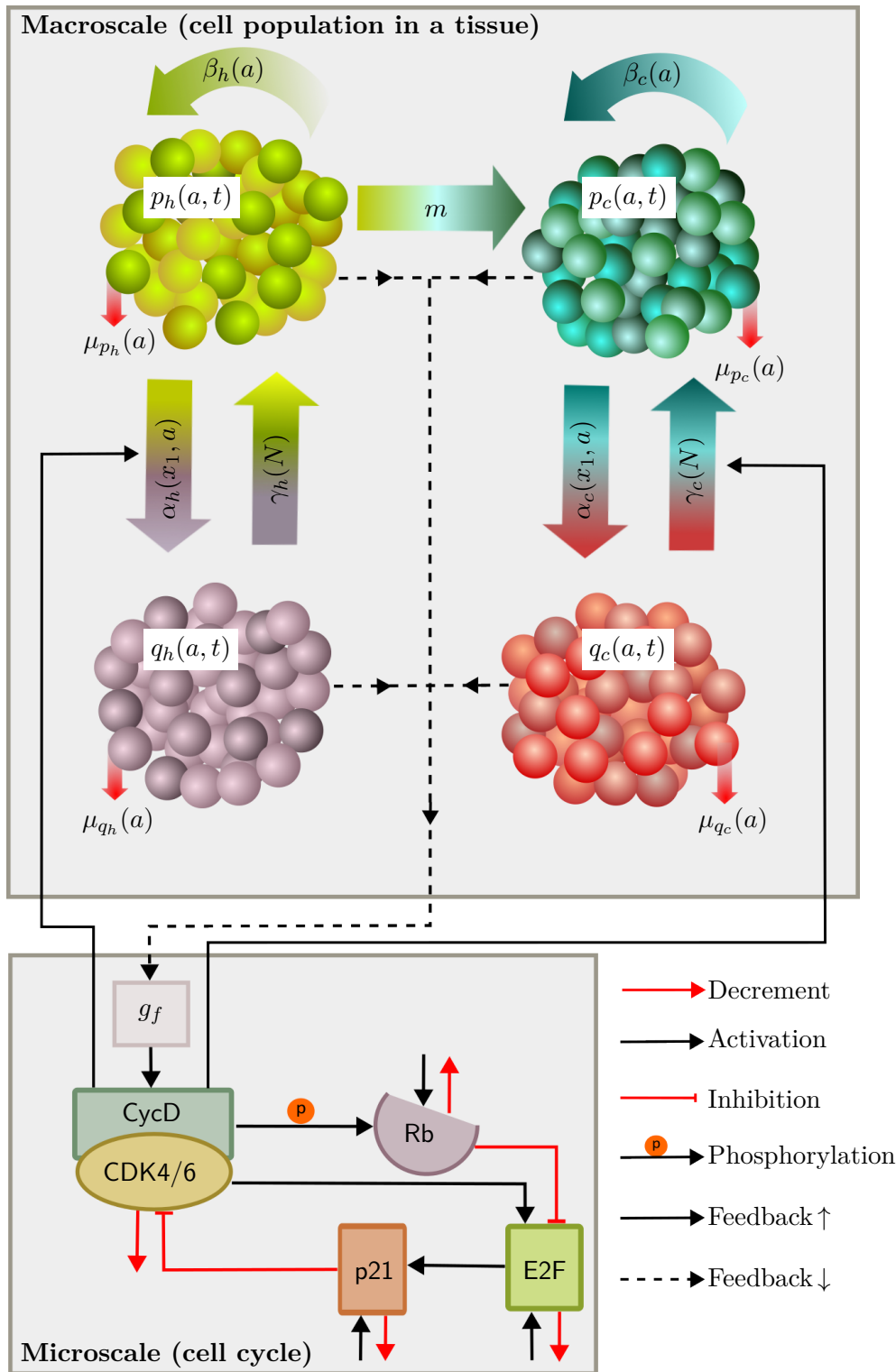


Figure 7.1: Both healthy and mutated subpopulations of proliferating and quiescent cells are depicted with possible transition effects. Healthy proliferating cells can transition to cancer proliferating cells upon mutation with rate  $m$ . Microscale (or cell cycle) dynamics with predominant protein states along with their interactions are shown, indicated by the legend in the bottom right corner. The growth factors  $g_f$  from the macroscale influences the cell-cycle.

To model the behaviour of cell populations in both healthy and mutated proliferative and quiescent compartments at the macroscale, we use partial differential equations (PDEs). For predicting sub-cellular protein interactions related to cell cycle dynamics, we employ ordinary differential equations (ODEs). The two scales are connected via the feedback incorporated in both directions. Within a cycle of cell division ( $G_1, S, G_2, M$ ), cells in the early proliferating phase ( $G_1$ ) can move to the quiescent-phase until the restriction point (R). When cells receive external signals or growth factors that promote cell cycle entry, the complex Cyclin D – CDK4/6 is activated. This activation is a key trigger for cells to exit quiescence and enter the cell cycle's proliferative  $G_1$  phase. This mechanism of bi-directional transition is captured in our model for both healthy and mutated cell lines. Moreover, our mathematical model includes mechanisms for cell proliferation (division) and mutation rate.

In summary, we are extending our multiscale model that describes the coupling between two predominant scales in Chapter 5, to a framework where healthy and mutated cell lines co-exist and we model the proliferating and quiescent cell populations for both healthy and mutated cell lineages. The main goal is to study the conditions under which cell transitioning between proliferating and quiescent states, leads to uncontrolled tumor growth. Specifically, we investigate whether Cyclin D – CDK4/6 complex is one of the important cause in creating a deregulation in cell transitioning between proliferating and quiescent cells. In the sequel, we delve into the details of multiscale mathematical modeling of proliferating and quiescent cells with regards to the dynamics of cell cycle. After which, model behavior and impact of the parameters is investigated using numerical simulations.

## 7.2 Mathematical modeling

### 7.2.1 Age-structured model

The cell densities of healthy and mutated cells in the proliferative and quiescent compartments are described by nonlinear hyperbolic transport PDEs that relate the cell density distribution to both physiological age  $a$  and time  $t$ . Specifically, the densities of healthy cells in the proliferative and quiescent phases are expressed as follows:

$$\frac{\partial}{\partial t} p_h(a, t) + \frac{\partial}{\partial a} (g_h(a) p_h(a, t)) = \gamma_h(N) q_h(a, t) - (\beta_h(a) + \alpha_h(a, x_1) + \mu_{p_h}(a)) p_h(a, t), \quad (7.1)$$

$$\frac{\partial}{\partial t} q_h(a, t) = \alpha_h(a, x_1) p_h(a, t) - (\gamma_h(N) + \mu_{q_h}(a)) q_h(a, t), \quad (7.2)$$

where the rate evolution of a cell cycle is denoted by  $g_h(a)$  in the equation. The first term on the right side,  $\gamma_h(N) q_h(a, t)$ , represents the transition to proliferating from quiescent cells, while the term  $\beta_h(a) p_h(a, t)$  represents the cell densities for completing cell division in some age of the proliferating phase. Cells which move to the quiescent phase without undergoing division are represented by  $\alpha_h(a, x_1) p_h(a, t)$ . The loss in the proliferating cells due to apoptosis/necrosis is represented by the death rate  $\mu_{p_h}(a)$ . The inflow from healthy proliferating cells, regulated by the microscale variable of Cyclin D – CDK4/6, complex concentration  $x_1$  for each age, is denoted by the first term in Eq (7.2):  $\alpha_h(a, x_1) p_h(a, t)$ . The next term depicts a loss in the quiescent cells due

to either by returning to proliferating phase at the rate  $\gamma_h(N)$  or by cell death due to apoptosis (or necrosis), as represented by the death rate  $\mu_{q_h}(a)$ .

Next, the cell density of mutated cells in mutated proliferating ( $p_c$ ) and quiescent ( $q_c$ ) phases, respectively, is presented:

$$\frac{\partial}{\partial t} p_c(a, t) + \frac{\partial}{\partial a} (g_c(a) p_c(a, t)) = \gamma_c(N) q_c(a, t) - (\beta_c(a) + \alpha_c(a, x_1) + \mu_{p_c}(a)) p_c(a, t), \quad (7.3)$$

$$\frac{\partial}{\partial t} q_c(a, t) = \alpha_c(a, x_1) p_c(a, t) - (\gamma_c(N) + \mu_{q_c}(a)) q_c(a, t), \quad (7.4)$$

where the terms used are similar to those in the case of healthier cells, as shown in Eqs (7.1) and (7.2). The total cell number in both healthy and mutated populations of cells in quiescent and proliferating phases is denoted by  $N(t)$  and is defined in Eq (7.5). In the case of quiescent cells, aging does not occur (i.e., the cells stop aging), so the convection term related to physiological age  $a$  is absent in Eqs (7.2) and (7.4). The total number of cells, represented by  $N(t)$ , represents the sum of all cells in the proliferating and quiescent phases throughout all ages, and can be expressed as

$$N(t) = \int_0^{a^*} (p_h(a, t) + q_h(a, t) + p_c(a, t) + q_c(a, t)) da, \quad (7.5)$$

where maximum age of the cells is given by  $a^*$ . The initial conditions are given below:

$$p_h(a, 0) = p_{h,0}(a), \quad q_h(a, 0) = q_{h,0}(a), \quad p_c(a, 0) = p_{c,0}(a), \quad q_c(a, 0) = q_{c,0}(a), \quad \forall a \geq 0. \quad (7.6)$$

The boundary conditions are given as follows:

$$g_h(0) p_h(0, t) = 2(1 - m) \int_0^{a^*} \beta_h(a) p_h(a, t) da, \quad (7.7)$$

$$g_c(0) p_c(0, t) = 2 \int_0^{a^*} \beta_c(a) p_c(a, t) da + 2m \int_0^{a^*} \beta_h(a) p_h(a, t) da, \quad (7.8)$$

for  $t > 0$ , where the number 2 shows the two newborn cells initializing in the proliferating phase, and the parameter  $m$  represents the mutation rate. Since healthy cell can acquire a mutation only during a division process, therefore, new born mutated cells start will start at age 0.

The function  $\beta_i(a)$  represents the cell number that finish dividing at a particular age in both healthy and mutated proliferating phases. Here, the index  $i$  indicates whether the compartment is healthy or cancerous, denoted by  $h$  and  $c$ , respectively. The function  $\beta_i(a)$  is regulated by the age of the cell, denoted by  $a$ , and is almost zero until a minimum cell age. Afterward, the function increases until it reaches the age of  $a^*$ .

$$\beta_i(a) = \frac{\rho_{1,i} a^{\gamma_{1,i}}}{\rho_{2,i}^{\gamma_{1,i}} + a^{\gamma_{1,i}}}, \quad (7.9)$$

The maximum proliferation rate is represented by  $\rho_{1,i}$ , while  $\rho_{2,i}$  is the age  $t$  achieve half-maximum. The Hill coefficient is represented by the exponent  $\gamma_{1,i}$ .

Next, we establish the rate at which cells transition to the quiescent phase from the proliferating compartments, which depends on both the age of the cell ( $a$ ) and the quantity of the Cyclin D – CDK4/6, complex ( $x_1$ ).

$$\alpha_i(a, x_1) = \sigma_{1,i} \frac{\sigma_{2,i}^{\gamma_{2,i}}}{(\sigma_{2,i}^{\gamma_{2,i}} + x_1^{\gamma_{2,i}})} \frac{\sigma_{3,i}^{\gamma_{3,i}}}{(\sigma_{3,i}^{\gamma_{3,i}} + a^{\gamma_{3,i}})}. \quad (7.10)$$

The function  $\alpha_i(a, x_1)$  depicts the number non-dividing cells due to anti-growth factors. The age-dependence of  $\alpha_i$  is motivated by the fact that cells transition to the quiescent phase from the proliferating phase only until they reach a specific age that marks a restriction point (R) in the cell cycle (which is also  $G_1 - S$  phase transition). However, before the restriction point, the Cyclin, complex's concentration  $x_1$  must be below a certain value to enable cells to exit the proliferating phase. In Eq (7.10), the Hill coefficients are represented by  $\gamma_{2,i}$  and  $\gamma_{3,i}$ , while  $\sigma_{2,i}$  and  $\sigma_{3,i}$  denote the concentration of the Cyclin D – CDK4/6, complex  $x_1$  and the age  $a$ , respectively. After  $\gamma_{2,i}$  and  $\gamma_{3,i}$ , the rate function  $\alpha$  decreases asymptotically to zero, preventing cells from transitioning to the quiescent phase. This implies that at age  $\sigma_{3,i}$ , cells are inevitably committed to entering the proliferation phase. Finally,  $\sigma_{3,i}$  represents the threshold concentration of the Cyclin, complex to determine the restriction point R.

The function  $\gamma_i(N)$ , which determines the number of cells transitioning to the proliferating phase from the quiescent phase, is represented by a Hill function of  $N$  that decreases monotonically:

$$\gamma_i(N) = \frac{\nu_i \theta_i^{\kappa_i}}{\theta_i^{\kappa_i} + N^{\kappa_i}}, \quad (7.11)$$

where the Hill function are defined as follows:  $\nu_i$  specifies the maximum rate at which cells transition to proliferating from quiescent population, when there are no cells, i.e.,  $N = 0$ ;  $\kappa_i$  is the Hill coefficient, and  $\theta_i$  represents the proportion of the total cell population that reaches half the maximum value of  $\nu_i$ . This implies that the number of quiescent cells transitioning to the proliferative compartment decreases to zero as the cell population increases, illustrating density inhibition.

Cell growth is controlled by proteins such as cytokines and other factors that regulate proliferation [137]. Cytokines bind to specific receptors, activating signaling pathways [138]. The cytokine signals that regulate cell numbers are reliant on the total population of cells, as demonstrated by various studies [139]. For a detailed explanation of cytokine signal dynamics, refer to [140, 141]. Using the quasi-steady-state approximation, we can express the quantity of growth factors ( $g_f$ ) produced by the entire cell population ( $N$ ) as

$$g_f = \frac{1}{1 + k_t N}. \quad (7.12)$$

### 7.2.2 Cell cycle model

In this framework, we will consider the same cell cycle model as in Chapter 5 because those four microscale proteins in our cell cycle model, as mentioned earlier, that are sufficient to account for the reversible transitions between the quiescent and proliferating phases. Please refer to Section 5.2.2 for more elaboration. Thereby, we consider four proteins which are described in Table 7.1. Hereby, we assume a homogeneous cell population, where all cells behave similarly, and therefore, we model the behavior of a single cell to represent the dynamics of all cells within a population. Under the fundamental assumption of uniform behavior among all constituent cells, we use an ordinary differential

Description	State
Cyclin D – CDK4/6	$x_1$
E2F	$x_2$
Rb	$x_3$
p21	$x_4$

Table 7.1: Description of the cell states at the microscale.

equation (ODE) model characterized by uniform parameters to encapsulate the intrinsic cell cycle dynamics at a microscopic level. Additionally, we account for cells with abbreviated cell cycles at a macroscopic scale, incorporating the function  $\beta_i(a)$  to accommodate this variability. Notably, our model introduces a specific chronological age denoted as  $a^*$  at which the representative cell successfully completes its division. Following Michaelis-Menten kinetics, the temporal evolution of the cell cycle dynamics, i.e., the chemical reactions occurring between enzymes and substrates during the cell cycle are presented below:

$$\frac{dx_1}{da} = k_{1s} \left( \frac{g_f}{k_{gf} + g_f} \right) - k_{14}x_4x_1 - k_{1d} \left( \frac{x_1}{k_1 + x_1} \right), \quad (7.13)$$

$$\frac{dx_2}{da} = k_{21} \left( \frac{x_{2t} - x_2}{k_2 + (x_{2t} - x_2)} \right) x_1 - k_{32}x_2x_3 - k_{2d}x_2, \quad (7.14)$$

$$\frac{dx_3}{da} = k_{3s} - k_{32}x_2x_3 - k_{31} \left( \frac{x_3}{k_3 + x_3} \right) x_1 - k_{3d}x_3, \quad (7.15)$$

$$\frac{dx_4}{da} = k_{4s} + k_{42} \left( \frac{k_{34}}{k_{34} + x_3} \right) x_2 - k_{41} \left( \frac{x_4}{k_4 + x_4} \right) x_1 - k_{4d}x_4. \quad (7.16)$$

A detailed description of all the terms involved in the model equations (7.13)-(7.16) can be found in Section 5.2.2, [157]. Although we will not delve into the full derivation of these equations here, inquisitive readers can refer to [143] for a comprehensive explanation. To aid in understanding, we have included simulations of the four microscale states mentioned earlier in Figure 7.2.

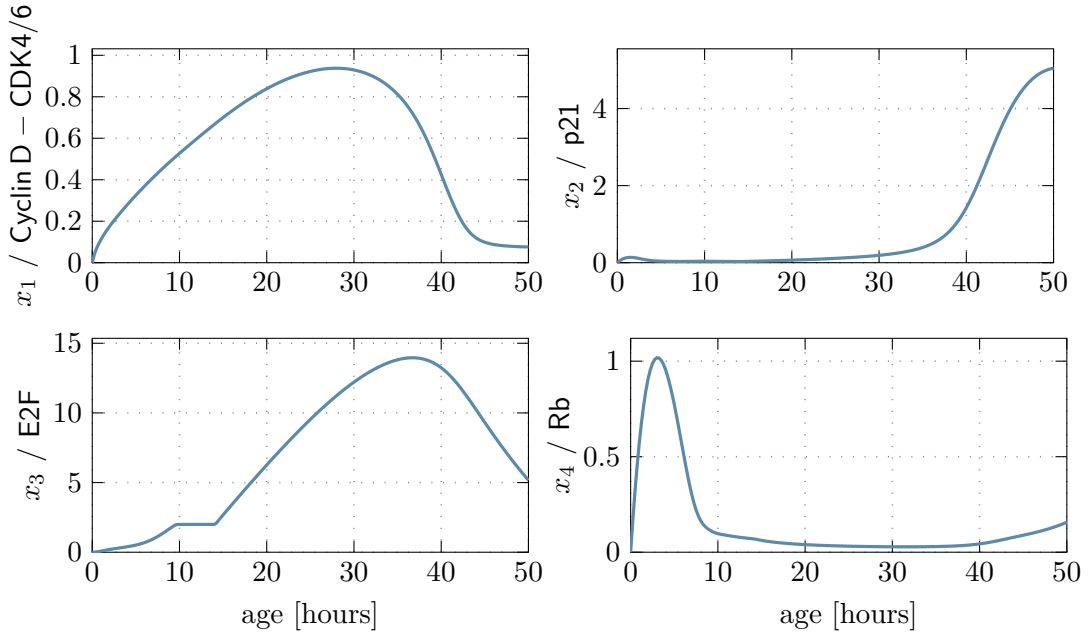


Figure 7.2: Evolution of microscale proteins from the cell-cycle. Cyclin D – CDK4/6 shows a complete activation and degradation within a full cycle. The concentration of transcription factor E2F is elevated since Retinoblastoma protein Rb is inactivated with the rise in Cyclin D – CDK4/6 complex. Similarly, protein p21 elevates near the end of the cell-cycle to help in the degradation of the Cyclin’ complex.

### 7.3 Numerical solution and simulation results

In this section, we present simulations of our model aimed at better understanding the evolution of healthy and mutated sub-populations of quiescent and proliferative cells. Simulations are performed in the computational environment of Matlab, utilizing the finite volume method with a discretization scheme based on the central upwind approach. For clarity, we provide a detailed account of the model parameters employed throughout these simulations, which is briefly summarized in Table 7.2. For cell age, we have imposed a maximum threshold of 50. Furthermore, we have set the temporal ( $\Delta t$ ) and spatial ( $\Delta a$ ) step size to values of 0.02 and 0.5, respectively, to strike an optimal balance between computational accuracy and efficiency. Notably, a unit speed is employed in our simulations, implying that both the healthy ( $g_h(a)$ ) and mutated ( $g_c(a)$ ) sub-populations advance through the cell cycle at the same pace, represented as 1 for both. In the following subsections, we present two case studies that illustrate the scenarios of steady and exponential growth in mutated cell populations, which ultimately result in a significant reduction or near absence of healthy cells within the tissue.

Param.	Description	Healthy	Mutated	Unit
$m$	Mutation rate	0.2	-	day <sup>-1</sup>
$\nu_i$	Maximum transition rate from quiescent to proliferation phase	0.6 [147]	0.6	day <sup>-1</sup>
$\theta_i$	Total cell population beyond which $\Gamma$ is zero	$0.095 \times 10^6$ [147]	$0.095 \times 10^6$	-
$\kappa_i$	Hill coefficient	1 [147]	1	-
$\rho_{1,i}$	Maximal effect of Cyclin D – CDK4/6, complex on the division of cell	0.7	0.7	-
$\rho_{2,i}$	Value of Cyclin D – CDK4/6, complex to achieve half maximum effect	0.35	0.35	-
$\gamma_{1,i}$	Hill coefficient	8	8	-
$\sigma_{1,i}$	Maximum rate of switching cells from proliferating to quiescent phase	0.01	0.01	-
$\sigma_{2,i}$	Switching Cyclin D – CDK4/6, complex value, after that $\alpha$ is close to zero	0.5[157]	0.45	
$\sigma_{3,i}$	Switching age value beyond which $\alpha$ is close to zero	14	15	h
$\gamma_{2,i}$	Hill coefficient	7	7	-
$\gamma_{3,i}$	Hill coefficient	7	7	-
$k_t$	Rate constant which measures the effect of total population on growth factors	$1.80 \times 10^{-9}$ [158]	$1.80 \times 10^{-9}$	-

Table 7.2: Parameters used in the simulations of multiscale model of healthy and mutated proliferating and quiescent cell populations.

#### *Steady-state dynamics of healthy and mutated cell populations:*

This case study aims to investigate the steady-state dynamics of both healthy and mutated cell populations, with specified death rates:  $\mu_{p_h} = \mu_{q_h} = 0.0014$  and  $\mu_{p_c} = \mu_{q_c} = 0.0014$ . To initiate the study, we define the initial conditions for all cell populations



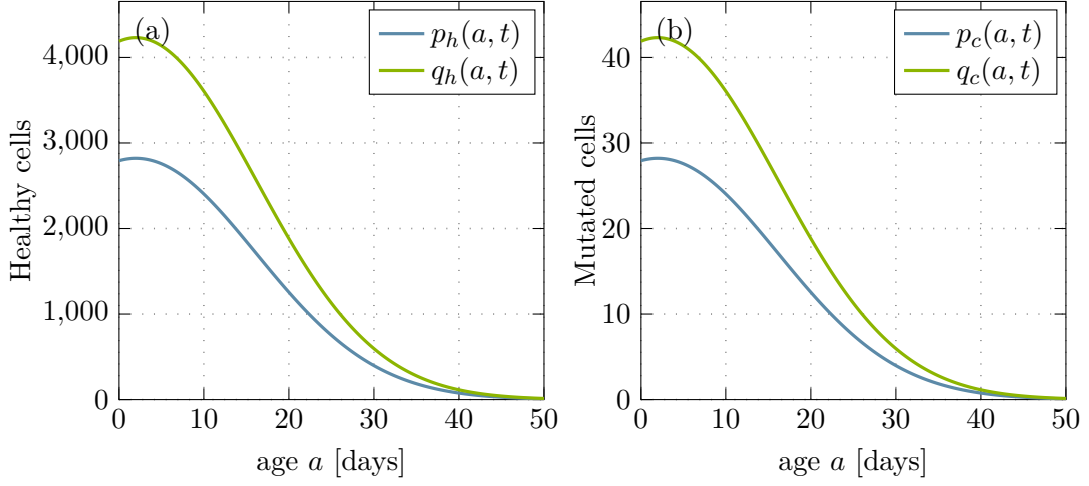


Figure 7.3: Initial conditions as normal distributions, represented as  $\frac{k_{0,i}}{\sqrt{2\pi\sigma^2}} \exp\left(-\frac{(a-\mu)^2}{2\sigma^2}\right)$  for healthy and mutated cells in proliferating and quiescent phases ( $p_h(a, t), q_h(a, t), p_c(a, t), q_c(a, t)$ ).

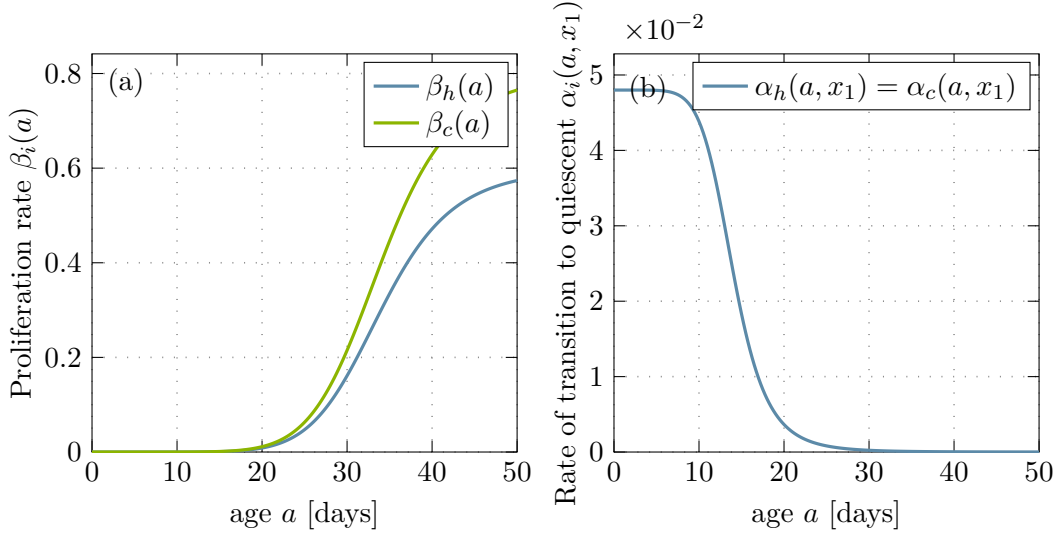


Figure 7.4: Behavior of (a) proliferation rate  $\beta_i(a)$  and (b) transition rate  $\alpha_i(a)$  of cells from proliferating to quiescent phase. Here  $i = \{h, c\}$  representing healthy and cancerous cell populations.

$(p_h(a, t), q_h(a, t), p_c(a, t), q_c(a, t))$  as normal distributions, expressed as  $\frac{k_{0,i}}{\sqrt{2\pi\sigma^2}} \exp\left(-\frac{(a-\mu)^2}{2\sigma^2}\right)$ . In this equation, we use  $\mu = 2$  and  $\sigma^2 = 200$ . The specific values assigned to  $k_{0,hq}, k_{0,hp}, k_{0,cq}$ , and  $k_{0,cp}$  are as follows:  $1.5 \times 10^5$ ,  $10^6$ ,  $1.5 \times 10^3$ , and  $10^3$ , respectively, for healthy quiescent, healthy proliferating, mutated quiescent, and mutated proliferative cell populations, see Figure 7.3. The utilization of a normal distribution is motivated by its ability to provide a suitable approximation of cell distribution within a population. This distribution effectively captures the inherent heterogeneity with respect to cell age within a given population.

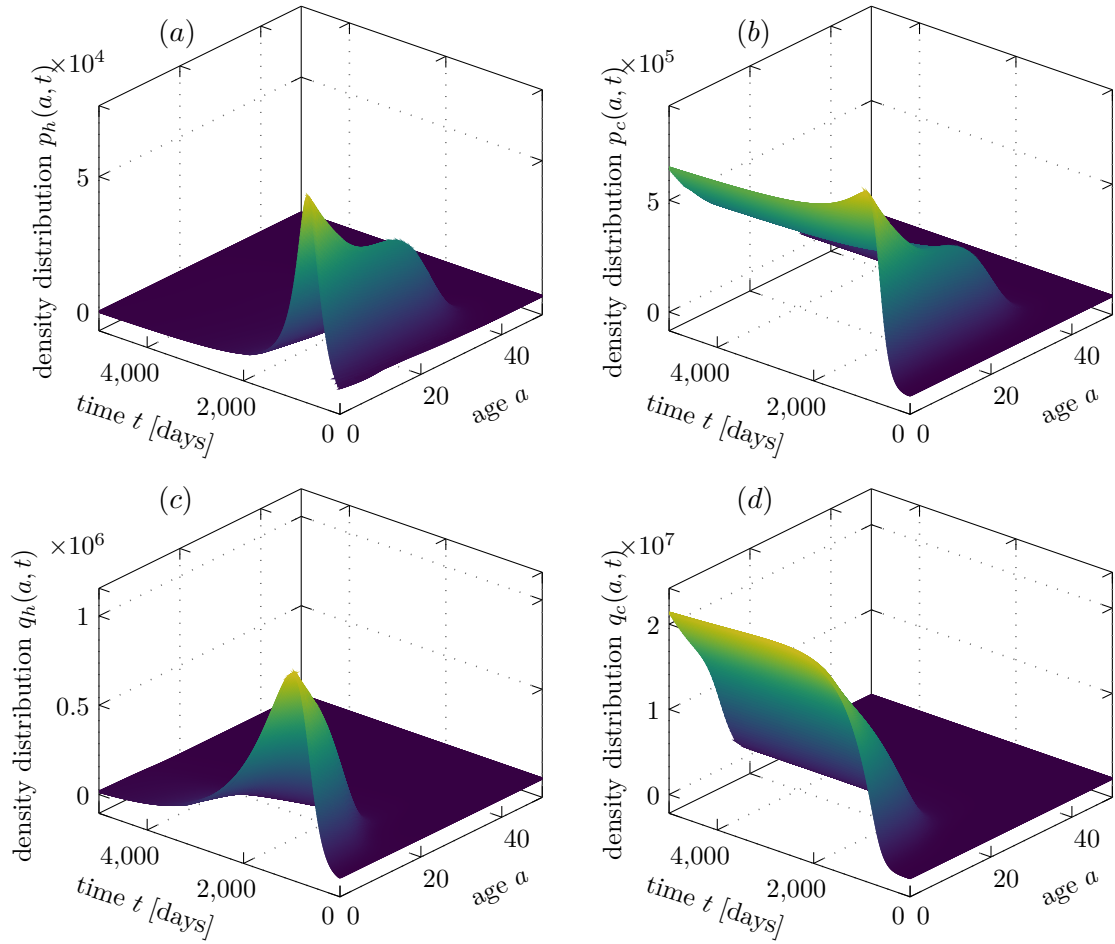


Figure 7.5: Steady state scenario of cell density distribution of different cell populations (a) healthy proliferating cells, (b) mutated proliferating cells, (c) healthy quiescent cells and (d) mutated quiescent cells.

Figure 7.5 illustrates the evolving number density distribution of various cell populations: (a) healthy proliferating cells, (b) mutated proliferating cells, (c) healthy quiescent cells and (d) mutated quiescent cells. These cell populations are tracked over time, with cell age measured in units of time and cell density quantified as cells per cubic millimeter. The mutation rate is held constant at  $m = 0.1$ . As time progresses, the populations of healthy proliferating  $p_h(a, t)$  and quiescent  $q_h(a, t)$  cells gradually diminish, while mutated proliferating  $p_c(a, t)$  and quiescent  $q_c(a, t)$  cells grow more rapidly and eventually saturate the tissue space. Simultaneously, the total cell population, encompassing both healthy and mutated proliferating and quiescent cells, represented as  $N(t)$ , undergoes a rapid initial increase, as depicted in Figure 7.6(a), before ultimately reaching a steady state. The transition from proliferating to quiescent phase is assumed to be similar for both healthy and mutated cell populations as shown by function  $\alpha$  in Figure 7.4 (b). The proliferation rate of mutated cells, however, is assumed to be slightly higher than in the healthy cells, see Figure 7.4 (a). Furthermore, Figure 7.6(c) illustrates the behavior of growth factors, which are influenced by the cell population  $N(t)$ . Initially, they surge due to the low cell count and subsequently recede until achieving an equilibrium state.

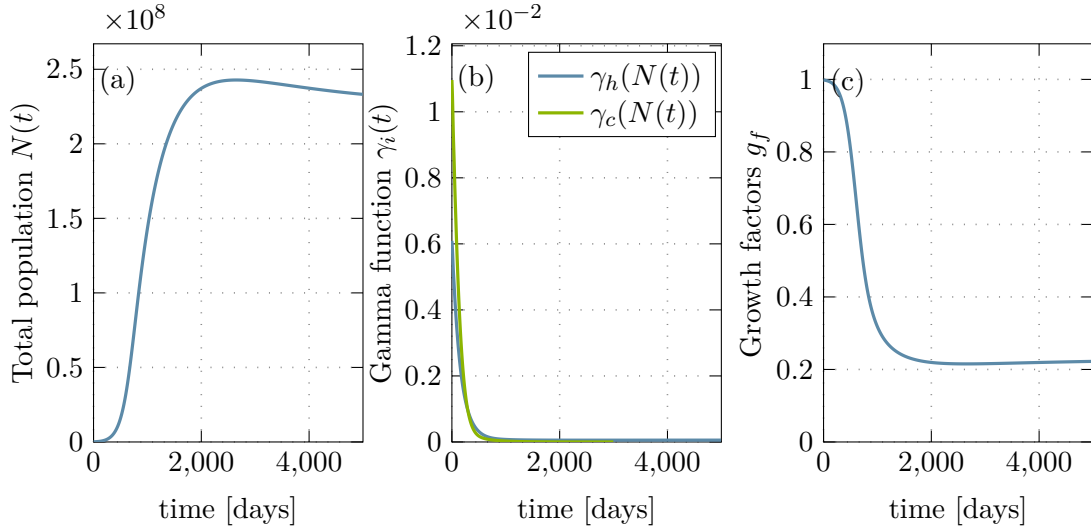


Figure 7.6: Dynamics of the combined cell population, growth factors, and transition function  $\gamma$ : (a) the total cell population  $N(t)$  reaches a steady-state, (b) both gamma functions,  $\gamma_h$  and  $\gamma_c$ , decrease as the total cell population reaches a steady-state, and (c) the growth factors  $g_f$  decrease as the cell population increases.

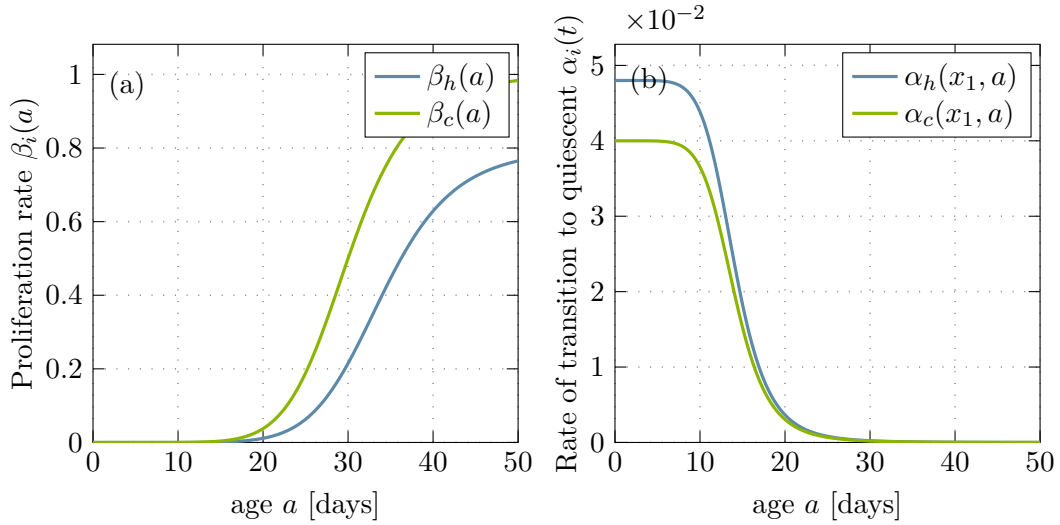


Figure 7.7: Behavior of (a) proliferation rate  $\beta_i(a)$  and (b) transition rate  $\alpha_i(a)$  of cells from proliferating to quiescent phase, Here  $i = \{h, c\}$  representing healthy and cancerous cell populations.

Lastly, Figure 7.6(b) illustrates the transition rate of cells shifting from the quiescent phase to the proliferating phase, represented as  $\gamma_i(N)$ , for both the healthy and mutated cell populations. As time progresses, this transition rate decreases owing to the growing proliferating population. Maintaining a balance between proliferating and quiescent cells is essential for tissue homeostasis. Quiescent cells conserve energy by reducing their metabolic activity. This allows the organism to allocate resources efficiently. In case of any damage to the tissue, these quiescent cells will be activated to replace damaged

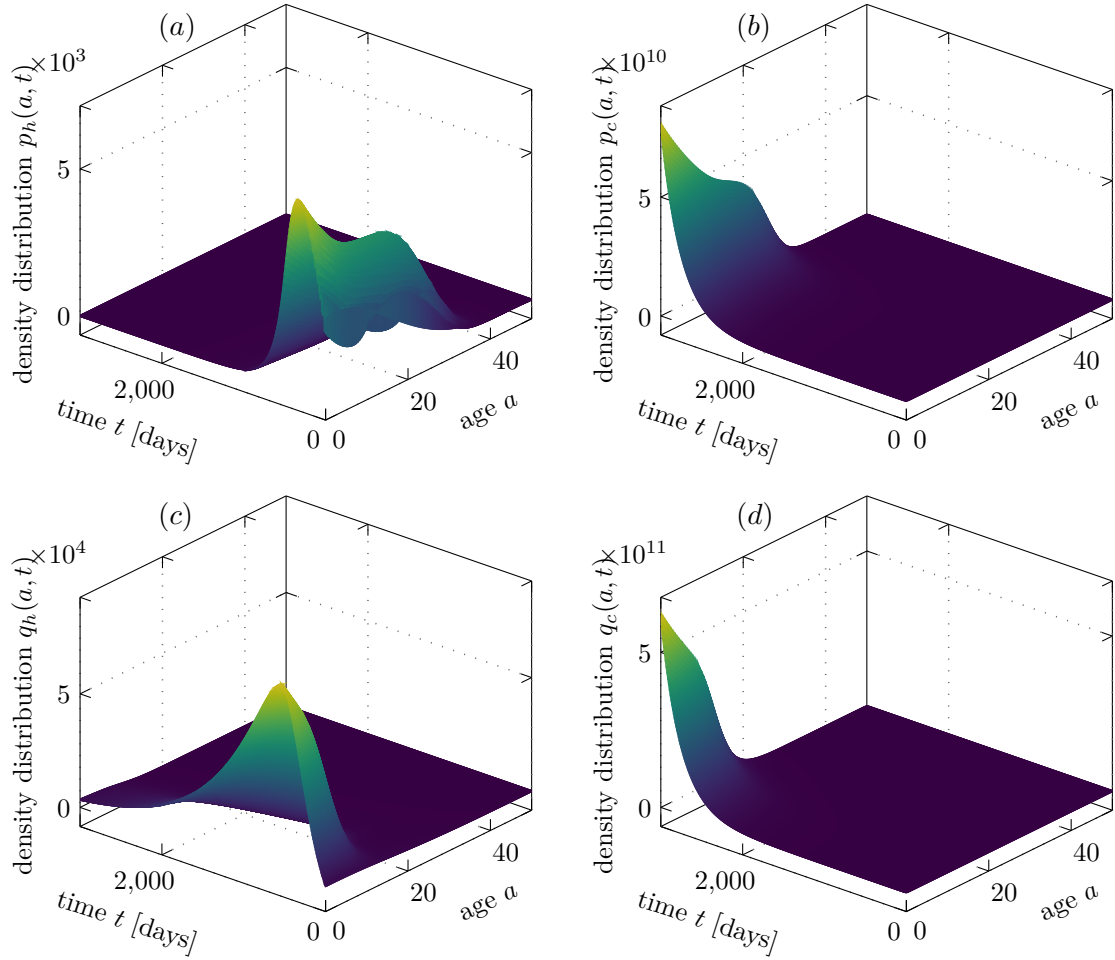


Figure 7.8: Exponential tumor growth: Cell density distribution of different cell populations (a) healthy proliferating cells, (b) mutated proliferating cells, (c) healthy quiescent cells and (d) mutated quiescent cells.

tissue and promote healing.

Exponential growth of mutated cell populations:

For this specific case study, we opted for a mutation rate of  $m = 0.2$  and applied death rates of  $\mu_{p_h} = \mu_{q_h} = 0.0014$  and  $\mu_{p_c} = \mu_{q_c} = 0.0010$ . Furthermore, we made adjustments to several other parameters, including  $\nu_{1,c} = 0.045$ ,  $\rho_{1,c} = 1.0$ ,  $\rho_{2,c} = 30$ ,  $\sigma_{1,c} = 0.040$ , and  $\sigma_{2,c} = 0.45$ . Figure 7.8 shows the cell density distribution of healthy and mutated proliferating and quiescent cells, respectively. Both healthy subpopulations exhibit trends that lead to a negligible steady state as time progresses. However, the mutated cell populations ( $p_c(a, t)$  and  $q_c(a, t)$ ) demonstrate exponential growth, emulating the behavior typically associated with cancer.

Mutated cells exhibit an elevated proliferation rate compared to their healthy counterparts, signifying that they divide and replicate at a faster pace. This heightened proliferation rate is a hallmark of the aberrant behavior often associated with mutated or cancerous cells. Therefore, the proliferation rate of mutated cells is assumed to be slightly higher than that of healthy cells, as illustrated in Figure 7.7(a). Additionally, the transition from the proliferating phase to the quiescent phase represents a critical

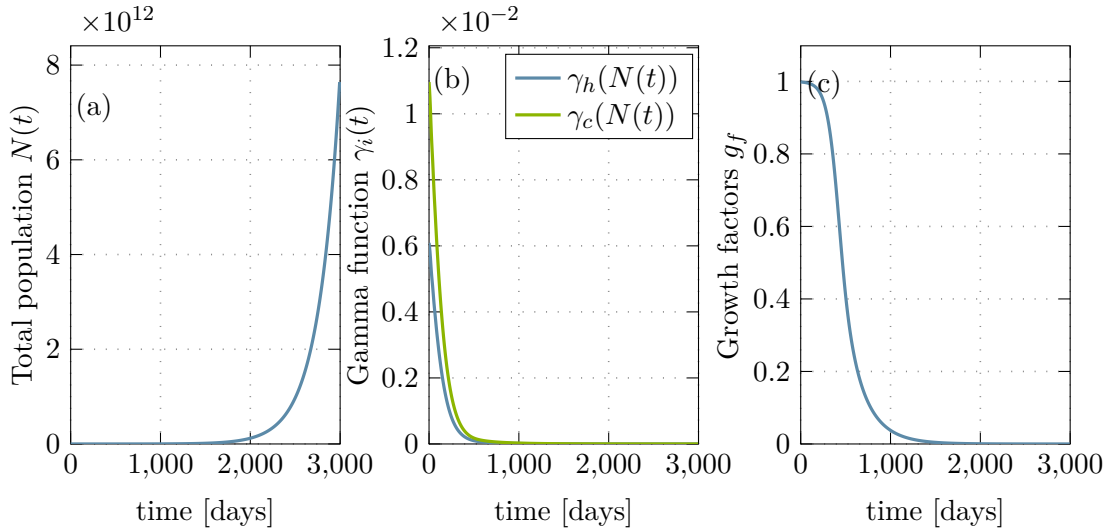


Figure 7.9: Dynamics of entire cell population, growth factors, and  $\gamma$  transitions: (a) The total cell population  $N(t)$  exhibits exponential growth. (b) Both gamma functions,  $\gamma_h$  and  $\gamma_c$ , decrease as the total cell population increases. (c) As the cell population increases, the growth factors  $g_f$  decrease.

mechanism by which cells can temporarily halt their division and conserve energy and resources, helping to maintain tissue stability and prevent uncontrolled growth. However in mutated cells, this transition can be impaired or delayed, causing mutated cells to continue dividing rapidly without entering quiescence as they should. This dysregulation contributes to the uncontrolled growth characteristic of many cancer cells. Therefore, it is assumed to be less frequent in mutated cell populations compared to healthy cells, as indicated by the function  $\alpha$  depicted in Figure 7.7(b).

Figure 7.9 provides insights into the total cell count, growth factors, and the transition function from quiescent to proliferating phases,  $\gamma_i(N)$ . The total cell population, comprising both healthy and mutated proliferating and quiescent cell populations, undergoes exponential growth in cell numbers over time. Initially, the growth factors reach their maximum values due to the low cell count and then gradually decrease to extremely low levels. Finally, the transition functions  $\gamma_h$  and  $\gamma_c$  also decrease as the cell population expands.

## 7.4 Discussion and conclusion

This study proposes a non-linear, multiscale mathematical model of physiologically-structured healthy and mutated quiescent and proliferating cells coupled to cell cycle dynamics. We incorporated reversible transitioning from quiescent to proliferating cells and vice versa. The proposed model allow us to explore the effects of different parameters, including mutation rates, proliferation rates, and transition rates, on cell population dynamics. We also performed numerical simulations to study the impact of Cyclin D – CDK4/6, complex on the transition between two sub-populations. One notable finding of this study, is the pivotal role played by the Cyclin' complex in the reversible transition, with any irregularity in this process having the potential to lead to cancer.

The proposed model has several limitations that need to be addressed. Firstly, it

lacks the incorporation of cell heterogeneity, a crucial aspect in accounting for cellular variability and noise. Additionally, the feedback model involving growth factors is relatively simplistic, and a more comprehensive characterization of the activation of the Cyclin, D – CDK4/6 complex should encompass all relevant signaling pathways. Furthermore, at the microscale, it would have been beneficial to model cell cycle dynamics separately for healthy and mutated cell populations to explore the distinct behaviors within their respective compartments. Lastly, while the Cyclin, D – CDK4/6 complex is pivotal for the  $G_1$  to S phase transition, the model overlooks the existence of other restriction points that detect DNA damage occurring during the S phase.

---

**Mathematical analysis: Wellposedness and stability properties of multiscale model of healthy and cancer cell populations**

---

In this chapter, we investigate the wellposedness of the model, proposed in Chapter 7, derive steady-state solutions, and find sufficient conditions of stability for derived solutions by utilizing semigroup and spectral theory.

**8.1 Existence and uniqueness of non-negative solution**

This section presents the uniqueness of the solution to the initial-boundary value problem (7.1)–(7.7) and (7.13)–(7.16), which we will simplify by using the microscale model for the entire time  $t$ , instead only until age  $a$ . We introduce Banach spaces,  $X = L^1(0, a^*) \times L^1(0, a^*) \times L^1(0, a^*) \times L^1(0, a^*)$  and  $Y = L^1(0, a^*) \times L^1(0, a^*) \times L^1(0, a^*) \times L^1(0, a^*)$ , with the norm  $|\phi| = \sum_{i=1}^4 |\phi_i|$  for  $\phi(a) = (\phi_1(a), \phi_2(a), \phi_3(a), \phi_4(a))^T \in X$  and  $|\varphi| = \sum_{i=1}^4 |\varphi_i|$  for  $\varphi(a) = (\varphi_1(a), \varphi_2(a), \varphi_3(a), \varphi_4(a))^T \in Y$ , where  $|\cdot|$  is the standard norm of  $L^1(0, a^*)$ . We first treat the initial-boundary value problem of system (7.1)–(7.7) as an abstract Cauchy problem on Banach space  $X$ . We assume that  $gh_a, gh_{aa}, g_{c_a}, g_{c_{aa}} \in L^\infty((0, a^*) \times \mathbb{R}^+)$ , and non-negative death rates, that is,  $\mu_{p_h}(\cdot) = \mu_{q_h}(\cdot) \geq 0$  and  $\mu_{p_c}(\cdot) = \mu_{q_c}(\cdot) \geq 0$ , and are locally integrable on  $[0, a^*)$ . The transition rate  $\alpha_i(a, x_1) \in L^\infty((0, a^*) \times (0, a^*))$ , and  $\beta_i(a) \in L^1(0, a^*)$ . We start by defining a linear operator  $A_1$  as follows:

$$(A_1\phi)(a) = \begin{pmatrix} -\frac{\partial(g_h(a)\phi_1(a))}{\partial a} - (\beta_h(a) + \mu_{p_h}(a))\phi_1(a) \\ -\mu_{q_h}(a)\phi_2(a) \\ -\frac{\partial(g_c(a)\phi_3(a))}{\partial a} - (\beta_c(a) + \mu_{p_c}(a))\phi_3(a) \\ -\mu_{q_c}(a)\phi_4(a) \end{pmatrix},$$

where

$$\phi(a) = (\phi_1(a), \phi_2(a), \phi_3(a), \phi_4(a))^T \in D(A_1).$$

The symbol T denotes the transpose of the vector, and the domain  $D(A_1)$  is given by the following:

$$D(A_1) = \left\{ (\phi_1, \phi_2, \phi_3, \phi_4) \mid \phi_i \text{ is absolute continuous on } [0, a^*), \right. \\ \left. \phi(0) = \left( 2(1-m) \int_0^{a^*} \beta_h(a)\phi_1(a)da, 0, 2 \int_0^{a^*} \beta_c(a)\phi_3(a)da + 2m \int_0^{a^*} \beta_h(a)\phi_1(a)da, 0 \right)^T \right\}.$$

The nonlinear operator  $F_1 : X \times Y \rightarrow X$  is given by

$$(F_1(\phi, \varphi))(a) = \begin{pmatrix} \frac{\nu_h \theta_h^{\kappa_h} \phi_2(a)}{\theta_h^{\kappa_h} + (N\phi)^{\kappa_h}} - \alpha_h(\varphi_1, a) \phi_1(a) \\ \frac{-\nu_h \theta_h^{\kappa_h} \phi_2(a)}{\theta_h^{\kappa_h} + (N\phi)^{\kappa_h}} + \alpha_h(\varphi_1, a) \phi_1(a) \\ \frac{\nu_c \theta_c^{\kappa_c} \phi_3(a)}{\theta_c^{\kappa_c} + (N\phi)^{\kappa_c}} - \alpha_c(\varphi_1, a) \phi_4(a) \\ \frac{-\nu_c \theta_c^{\kappa_c} \phi_3(a)}{\theta_c^{\kappa_c} + (N\phi)^{\kappa_c}} + \alpha_c(\varphi_1, a) \phi_4(a) \end{pmatrix}, \quad \phi \in X, \varphi \in Y,$$

where the linear operator  $N$  on  $L^1(0, a^*) \times L^1(0, a^*) \times L^1(0, a^*) \times L^1(0, a^*)$  is given by

$$N\phi = \int_0^{a^*} (\phi_1(a) + \phi_2(a) + \phi_3(a) + \phi_4(a)) da.$$

Consider  $v(t) = (p_h(\cdot, t), q_h(\cdot, t), p_c(\cdot, t), q_c(\cdot, t))^T \in X$ . We can define the initial-boundary value problem (7.1)–(7.7) as an abstract semilinear initial value problem (IVP) in  $X$ , as shown below:

$$\frac{d}{dt}v(t) = A_1v(t) + F_1(v(t), v(t)), \quad v(0) = v_0 \in X, \quad (8.1)$$

where  $v_0(a) = (p_{h_0}(a), q_{h_0}(a), p_{c_0}(a), q_{c_0}(a))$ .

Next, we define IVP (7.13) as a Cauchy problem on the Banach space  $Y$ . Suppose  $A_2$  is a linear operator which reads

$$(A_2\varphi)(a) = \begin{pmatrix} 0 \\ -k_{2d}\varphi_2(a) \\ k_{3s} - k_{3d}\varphi_3(a) \\ k_{4s} - k_{4d}\varphi_4(a) \end{pmatrix}, \quad \varphi(a) = (\varphi_1(a), \varphi_2(a), \varphi_3(a), \varphi_4(a))^T \in D(A_2),$$

where the domain  $D(A_2)$  is

$$D(A_2) = \{\varphi \in Y \mid \varphi_i \text{ is absolute continuous on } [0, a^*), \varphi(0) = (0, 0, 0, 0)^T\}.$$

We define the nonlinear operator  $F_2 : X \times Y \rightarrow Y$  by

$$(F_2(\phi, \varphi))(a) = \begin{pmatrix} k_{1s} \left( \frac{g_f(N\phi)}{k_{gf} + g_f(N\phi)} \right) - k_{14}\varphi_4(a)\varphi_1(a) - k_{1d} \left( \frac{\varphi_1(a)}{k_1 + \varphi_1(a)} \right), \\ k_{21} \left( \frac{x_{2t} - \varphi_2(a)}{k_2 + (x_{2t} - \varphi_2(a))} \right) \varphi_1(a) - k_{32}\varphi_2(a)\varphi_3(a) \\ - k_{32}\varphi_2(a)\varphi_3(a) - k_{31} \left( \frac{\varphi_3(a)}{k_3 + \varphi_3(a)} \right) \varphi_1(a) \\ k_{42} \left( \frac{k_{34}}{k_{34} + \varphi_3(a)} \right) \varphi_2(a) - k_{41} \left( \frac{\varphi_4(a)}{k_4 + \varphi_4(a)} \right) \varphi_1(a) \end{pmatrix},$$

where  $\phi \in X, \varphi \in Y$ . Take  $v(t) = (x_1(t), x_2(t), x_3(t), x_4(t))^T \in Y$ . Then (7.13)–(7.16) can be expressed as an abstract semilinear IVP in  $Y$ :

$$\frac{d}{dt}v(t) = A_2v(t) + F_2(v(t), v(t)), \quad v(0) = v_0 \in Y, \quad (8.2)$$



where  $v_0(t) = (x_1^0, x_2^0, x_3^0, x_4^0)$ , we can now establish a joint Cauchy problem for (8.1) and (8.2) as shown below:

$$\frac{d}{dt} \begin{pmatrix} v \\ v \end{pmatrix} = \begin{pmatrix} A_1 & 0 \\ 0 & A_2 \end{pmatrix} \begin{pmatrix} v \\ v \end{pmatrix} + \begin{pmatrix} F_1(v, v) \\ F_2(v, v) \end{pmatrix}, \quad \begin{pmatrix} v(0) \\ v(0) \end{pmatrix} = \begin{pmatrix} v_0 \\ v_0 \end{pmatrix} \in Z,$$

$$\frac{d}{dt} \zeta(t) = A\zeta(t) + F(\zeta(t)), \quad \zeta(0) = \zeta_0 \in Z, \quad (8.3)$$

where  $\zeta = (v, v)$ ,  $\zeta_0 = (v_0, v_0)$ ,  $A = \begin{pmatrix} A_1 & 0 \\ 0 & A_2 \end{pmatrix}$ ,  $F = \begin{pmatrix} F_1 \\ F_2 \end{pmatrix}$  and the Banach space is  $Z = \{X, Y\}$ . Assuming that  $T(t)$  is a  $C_0$ -semigroup generated by  $A$  for  $t \geq 0$ , and the operator  $F$  is continuously Fréchet differentiable on  $Z$  (specifically, both  $F_1$  and  $F_2$  are Fréchet differentiable on  $X$  and  $Y$ ), a continuous mild solution  $t \rightarrow \zeta(t, \zeta_0)$  exists and is unique for each  $\zeta_0 \in Z$  on a maximal interval  $[0, t_1)$  in  $Z$ .

$$\zeta(t, \zeta_0) = T(t)\zeta_0 + \int_0^t T(t-s)F(\zeta(s, \zeta_0))ds, \quad \forall t \in [0, t_1), \quad (8.4)$$

where  $t_1$  can be either  $+\infty$  or  $\lim_{t \rightarrow t_1^-} |\zeta(t, \zeta_0)| = \infty$ . Moreover, if  $\zeta_0 \in D(A)$ , then  $\zeta(t, \zeta_0) \in D(A)$  for  $0 \leq t < t_1$ , and the function  $\zeta \rightarrow \zeta(t, \zeta_0)$  is continuously differentiable and satisfies (8.3) on  $[0, t_1)$ . This has been established in Proposition 4.16 [150, 151].

**Remark 8.1.1.** Let's take  $p_{h,\max}$ ,  $q_{h,\max}$ ,  $p_{c,\max}$ ,  $q_{c,\max}$ ,  $x_{1,\max}$ ,  $x_{2,\max}$ ,  $x_{3,\max}$  and  $x_{4,\max}$  to represent the maximum values of the solution variables. If we normalise the governing equations using  $N(a) = p_h(a, t) + q_h(a, t) + p_c(a, t) + q_c(a, t) + x_1(a) + x_2(a) + x_3(a) + x_4(a)$ , then an a-priori estimate on these would lead to  $p_h(a, t) + q_h(a, t) + p_c(a, t) + q_c(a, t) + x_1(a) + x_2(a) + x_3(a) + x_4(a) = 1$ .

**Lemma 8.1.1.** Let  $\Omega = \{(p_h, q_h, p_c, q_c, x_1, x_2, x_3, x_4) \in Z | p_h \geq 0, q_h \geq 0, p_c \geq 0, q_c \geq 0, x_1 \geq 0, x_2 \geq 0, x_3 \geq 0, x_4 \geq 0\}$  and let  $\Omega_0 = \{(p_h, q_h, p_c, q_c, x_1, x_2, x_3, x_4) \in Z | 0 \leq p_h \leq p_{h,\max}, 0 \leq q_h \leq q_{h,\max}, 0 \leq p_c \leq p_{c,\max}, 0 \leq q_c \leq q_{c,\max}, 0 \leq x_1 \leq x_{1,\max}, 0 \leq x_2 \leq x_{2,\max}, 0 \leq x_3 \leq x_{3,\max}, 0 \leq x_4 \leq x_{4,\max}\}$ . Then after a finite time, the mild solution  $\zeta(t, \zeta_0)$  of (8.3), where  $\zeta_0 \in \Omega$ , enters a positively invariant set  $\Omega_0$ .

*Proof.* To obtain the solution of Eq (7.1), we will begin by utilizing transformations  $\tilde{p}_h(a, t) = g_h(a)p_h(a, t)$  and  $\tilde{q}_h(a, t) = g_h(a)q_h(a, t)$  for  $t \in [0, t_1]$  and  $a \in [a_0, a^*]$ . Then, for  $t \in (0, t_1)$  and  $a \in (a_0, a^*)$ , we have from Eq (7.1)

$$\frac{\partial \tilde{p}_h(a, t)}{\partial t} + g_h(a) \frac{\partial \tilde{p}_h(a, t)}{\partial a} = \gamma_h(N(t))\tilde{q}_h(a, t) - (\beta_h(a) + \alpha_h(x_1(a), a) + \mu_{p_h}(a))\tilde{p}_h(a, t), \quad (8.5)$$

Next, we apply the parameter transform to remove the term  $g_h(a)$  and define a new age variable  $\eta$  for both  $p_h$  and  $q_h$ , Lemma 3.1 [140]. This yields the expression:

$$\frac{\partial}{\partial \eta} \tilde{p}_h(a(\eta), t) = \frac{da}{d\eta} \frac{\partial}{\partial a} \tilde{p}_h(a, t) = g_h(a) \frac{\partial}{\partial a} \tilde{p}_h(a, t), \quad \text{where } \frac{da}{d\eta} = g_h(a).$$

Therefore, from Eq (8.5), it follows that

$$\begin{aligned} \frac{\partial \tilde{p}_h(a(\eta), t)}{\partial t} + \frac{\partial \tilde{p}_h(a(\eta), t)}{\partial \eta} &= \gamma_h(N(t))\tilde{q}_h(a(\eta), t) - (\beta_h(a(\eta)) + \alpha_h(x_1(a(\eta)), a(\eta))) \\ &\quad + \mu_{p_h}(a(\eta))\tilde{p}_h(a(\eta), t). \end{aligned} \quad (8.6)$$

To obtain the explicit relation of  $\tilde{p}_h(a(\eta), t)$ , we will utilize the method of characteristics (MOC). Specifically, we assume that  $\tilde{p}_h(a(\eta), t)$  is governed by an ODE along the curve  $(a(\psi_1(y)), \psi_2(y)) = \psi(y)$ , and therefore, we have

$$\dot{\psi}_1(y) := 1 \Rightarrow \psi_1(y) = y + c_1, \quad \dot{\psi}_2(y) := 1 \Rightarrow \psi_2(y) = y + c_2, \quad z(y) := \tilde{p}_h(a(\psi_1(y)), \psi_2(y)),$$

where  $c_1, c_2 \in \mathbb{R}$  are constants. Then, it follows

$$\begin{aligned} \frac{dz}{dy} &= \frac{d\tilde{p}_h(a(\psi_1(y)), \psi_2(y))}{dy} \\ &= \frac{\partial \tilde{p}_h(a(\psi_1(y)), \psi_2(y))}{\partial a} \frac{da(\psi_1(y))}{d\psi_1} \frac{d\psi_1(y)}{dy} + \frac{\partial \tilde{p}_h(a(\psi_1(y)), \psi_2(y))}{\partial \psi_2} \frac{d\psi_2(y)}{dy} \\ &= \gamma_h(N(\psi_2(y))) \tilde{q}_h(a(\psi_1(y)), \psi_2(y)) - (\beta_h(a(\psi_1(y))) + \alpha_h(x_1(a(\psi_1(y))), a(\psi_1(y))) \\ &\quad + \mu_{p_h}(a(\psi_1(y)))) \tilde{p}_h(a(\psi_1(y)), \psi_2(y)) \\ &= \gamma_h(N(\psi_2(y))) \tilde{q}_h(a(\psi_1(y)), \psi_2(y)) - (\beta_h(a(\psi_1(y))) + \alpha_h(x_1(a(\psi_1(y))), a(\psi_1(y))) \\ &\quad + \mu_{p_h}(a(\psi_1(y)))) z(y). \end{aligned} \tag{8.7}$$

We can now write  $\tilde{p}_h$  using an ODE (8.7) so that

$$\begin{aligned} \tilde{p}_h(a(y + c_1), y + c_2) &= \tilde{p}_h(a(\psi_1(y)), \psi_2(y)) = z(y) \\ &= \exp \left( - \int_0^y (\beta_h(a(\psi_1(\xi))) + \alpha_h(x_1(a(\psi_1(\xi))), a(\psi_1(\xi))) + \mu_{p_h}(a(\psi_1(\xi)))) d\xi \right) \\ &\quad \left[ \int_0^y \exp \left( \int_0^\zeta (\beta_h(a(\psi_1(\xi))) + \alpha_h(x_1(a(\psi_1(\xi))), a(\psi_1(\xi))) + \mu_{p_h}(a(\psi_1(\xi)))) d\xi \right) \right. \\ &\quad \left. \gamma_h(N(\psi_2(\zeta))) \tilde{q}_h(a(\psi_1(\zeta)), \psi_2(\zeta)) d\zeta + \tilde{p}_h(a(\psi_1(0)), \psi_2(0)) \right] \\ &= \exp \left( - \int_0^y (\beta_h(a(\xi + c_1)) + \alpha_h(x_1(a(\psi_1(\xi + c_1))), a(\xi + c_1)) + \mu_{p_h}(a(\xi + c_1))) d\xi \right) \\ &\quad \left[ \int_0^y \exp \left( \int_0^\zeta (\beta_h(a(\xi + c_1)) + \alpha_h(x_1(a(\psi_1(\xi + c_1))), a(\xi + c_1)) + \mu_{p_h}(a(\xi + c_1))) d\xi \right) \right. \\ &\quad \left. \gamma_h(N(\zeta + c_2)) \tilde{q}_h(a(\zeta + c_1), \zeta + c_2) d\zeta + \tilde{p}_h(a(c_1), c_2) \right]. \end{aligned}$$

Now, we define the boundary set  $\Gamma$  as  $[a_0, a^*) \times 0 \cup 0 \times [0, t_1]$ , which enables us to use the boundary condition to determine  $\tilde{p}_h(a(c_1), c_2)$  if a curve  $(a(\psi_1(y)), \psi_2(y))$  begins in  $\Gamma$ . In order for  $(a(y + c_1), y + c_2)$  to lie on  $\Gamma$ , either  $c_1 = 0$  or  $c_2 = 0$ . Therefore, we have the following two scenarios:

In the first scenario, we can randomly choose  $c_1 = 0$  and  $c_2 \in [0, t_1]$ . In this case, we have

$$\begin{aligned} \tilde{p}_h(a(y), y + c_2) &= \exp \left( - \int_0^y (\beta_h(a(\xi)) + \alpha_h(x_1(a(\xi))), a(\xi)) + \mu_{p_h}(a(\xi))) d\xi \right) \\ &\quad \left[ \int_0^y \exp \left( \int_0^\zeta (\beta_h(a(\xi)) + \alpha_h(x_1(a(\xi))), a(\xi)) + \mu_{p_h}(a(\xi))) d\xi \right) \right. \\ &\quad \left. \gamma_h(N(\zeta + c_2)) \tilde{q}_h(a(\zeta), \zeta + c_2) d\zeta + \tilde{p}_h(a(0), c_2) \right]. \end{aligned}$$

The solution in  $(a(\eta), t) | t \in [0, t_1], \eta \in [0, \min(\eta^*, t))$  can be obtained using the characteristic solution as follows:

$$\eta \stackrel{!}{=} \psi_1(y) = y + c_1 = y \Rightarrow y = \eta \text{ and } t \stackrel{!}{=} \psi_2(y) = y + c_2 \Rightarrow c_2 = t - y,$$

which implies

$$\begin{aligned} \tilde{p}_h(a(\eta), t) = & \exp \left( - \int_0^\eta (\beta_h(a(\xi)) + \alpha_h(x_1(a(\xi)), a(\xi)) + \mu_{p_h}(a(\xi))) d\xi \right) \\ & \left[ \int_0^\eta \exp \left( \int_0^\zeta (\beta_h(a(\xi)) + \alpha_h(x_1(a(\xi)), a(\xi)) + \mu_{p_h}(a(\xi))) d\xi \right) \right. \\ & \left. \gamma_h(N(\zeta + t - \eta)) \tilde{q}_h(a(\zeta), \zeta + t - \eta) d\zeta + \tilde{p}_h(a(0), t - \eta) \right]. \end{aligned}$$

Using the above equation, we can obtain the expression for  $g_h(a(\eta))p_h(a(\eta), t)$  when  $\eta < t$ . By choosing an arbitrary  $c_1 \in [0, \eta^*)$  and setting  $c_2 = 0$ , we obtain

$$\begin{aligned} \tilde{p}_h(a(y + c_1), u) = & \exp \left( - \int_0^y (\beta_h(a(\xi + c_1)) + \alpha_h(x_1(a(\xi + c_1)), a(\xi + c_1)) \right. \\ & \left. + \mu_{p_h}(a(\xi + c_1))) d\xi \right) \left[ \int_0^y \exp \left( \int_0^\zeta (\beta_h(a(\xi + c_1)) + \alpha_h(x_1(a(\xi + c_1)), a(\xi + c_1)) \right. \right. \\ & \left. \left. + \mu_{p_h}(a(\xi + c_1))) d\xi \right) + \gamma_h(N(\zeta)) \tilde{q}_h(a(\zeta + c_1), \zeta) d\zeta + \tilde{p}_h(a(c_1), 0) \right]. \end{aligned}$$

Using the characteristic solution, we can obtain a solution in the set  $(a(\eta), t) | t \in [0, t_1], \eta \in [t, \eta^*)$  as follows:

$$\eta \stackrel{!}{=} \psi_1(y) = y + c_1 \Rightarrow c_1 = \eta - y \text{ and } t \stackrel{!}{=} \psi_2(y) = y + c_2 \Rightarrow y = t,$$

which results into

$$\begin{aligned} \tilde{p}_h(a(\eta), t) = & \exp \left( - \int_0^t (\beta_h(a(\xi + \eta - t)) + \alpha_h(x_1(a(\xi + \eta - t)), a(\xi + \eta - t)) \right. \\ & \left. + \mu_{p_h}(a(\xi + \eta - t))) d\xi \right) \left[ \int_0^t \exp \left( \int_0^\zeta (\beta_h(a(\xi + \eta - t)) \right. \right. \\ & \left. \left. + \alpha_h(x_1(a(\xi + \eta - t)), a(\xi + \eta - t)) + \mu_{p_h}(a(\xi + \eta - t))) d\xi \right) \right. \\ & \left. \gamma_h(N(\zeta)) \tilde{q}_h(a(\zeta + \eta - t), \zeta) d\zeta + \tilde{p}_h(a(\eta - t), 0) \right]. \end{aligned}$$

Hence, the relation for  $g_h(a(\eta))p_h(a(\eta), t)$  is now established for  $\eta > t$ . As a result, the

ultimate solution for  $g_h(a(\eta))p_h(a(\eta), t)$  can be expressed as

$$\tilde{p}_h(a(\eta), t) := \begin{cases} \exp\left(-\int_0^\eta (\beta_h(a(\xi)) + \alpha_h(x_1(a(\xi)), a(\xi)) + \mu_{p_h}(a(\xi)))d\xi\right) \left[ h(t-\eta) \right. \\ \left. \int_0^\eta \exp\left(\int_0^\zeta (\beta_h(a(\xi)) + \alpha_h(x_1(a(\xi)), a(\xi)) + \mu_{p_h}(a(\xi)))d\xi\right) \right. \\ \left. \gamma_h(N(\zeta+t-\eta))\tilde{q}_h(a(\zeta), \zeta+t-\eta)d\zeta \right], & \bar{a} < t, \\ \exp\left(-\int_0^t (\beta_h(a(\xi+\eta-t)) + \alpha_h(x_1(a(\xi+\eta-t)), a(\xi+\eta-t)) + \right. \\ \left. \mu_{p_h}(a(\xi+\eta-t)))d\xi\right) \left[ p_0(a(\eta-t)) + \int_0^t \exp\left(\int_0^\zeta (\beta_h(a(\xi+\eta-t)) \right. \right. \\ \left. \left. + \alpha_h(x_1(a(\xi+\eta-t)), a(\xi+\eta-t)) + \mu_{p_h}(a(\xi+\eta-t)))d\xi\right) \gamma_h(N(\zeta)) \right. \\ \left. \tilde{q}_h(a(\zeta+\eta-t), \zeta)d\zeta \right], & \bar{a} \geq t, \end{cases}$$

where the boundary condition  $\tilde{p}_h(a(0), t-\eta)$  is denoted as  $h(t-\eta)$ . Note that for positive initial data, the above expression is positive and for  $g_h(a)q_h(a, t) \geq 0$ .

We then derive the solution expression from (7.2) as shown below:

$$q_h(a, t) := \exp\left(-\int_0^t \mu_{q_h}(a) + \gamma_h(N(t))dt\right) \left\{ \int_0^t \exp\left(-\int_0^\xi \mu_{q_h}(a) + \gamma_h(N(\pi))d\pi\right) \right. \\ \left. \alpha_h(x_1(a), a)p_h(a, \xi)d\xi + q_{h,0}(a) \right\}. \quad (8.8)$$

As a direct consequence, we observe that  $q_h(a, t)$  is non-negative for positive initial data and whenever  $g_h(a)q_h(a, t) \geq 0$ . Similarly, we can obtain the solution expression for  $p_c$  and  $q_c$ .

Next, to ensure the positivity of the coupled ODE model (7.13), we express the system of ODEs as follows:

$$\begin{cases} \frac{dx_1}{da} = F_1(x_1, x_4), \\ \frac{dx_2}{da} = F_2(x_1, x_2, x_3), \\ \frac{dx_3}{da} = F_3(x_1, x_2, x_3), \\ \frac{dx_4}{da} = F_4(x_1, x_2, x_3, x_4), \end{cases} \quad (8.9)$$

where  $F_1, F_2, F_3$  and  $F_4$  correspond to the vector fields of the microscale states  $x_1-x_4$ . It is worth noting that in (8.9),  $F_1$  does not depend on  $N$  (i.e.,  $p_h, q_h, p_c$  and  $q_c$ ), as  $N$  changes with time and is a fixed constant at each time step, which determines the growth factors entire age range.

To ensure that the solutions of all ODEs is positive, it is essential to verify that the vector fields  $F_1, F_2, F_3, F_4$  are smoothly differentiable and oriented in a direction that points away from the negative regions in the state space. Starting with the ODE for  $x_1$  from (8.9), we set  $x_4 = 0$  in  $F_1(x_1, x_4)$  to obtain  $\dot{x}_1 = F_1(x_1)$ . We can observe that

$$F_1(x_1) = k_{1s} \left( \frac{g_f}{k_{gf} + g_f} \right) - k_{1d} \left( \frac{x_1}{k_1 + x_1} \right) > 0 \text{ for all } a > 0 \text{ when } k_{1s} \left( \frac{g_f}{k_{gf} + g_f} \right) > k_{1d} \left( \frac{x_1}{k_1 + x_1} \right).$$

This implies that the concentration of  $x_1$  consistently rises more than it falls over time, as the sole source of an increase in  $x_1$  concentration is from growth factors. Consequently, during periods when growth factors are at their minimum, the concentration of  $x_1$  is also at its minimum, meaning the amount of degradation or decrement cannot surpass the activation of the  $x_1$  complex. Given that the solution to system (7.13)-(7.16) is unique for each initial condition, as can be observed from (8.3) and (8.4), we can infer that the solution remains in the first quadrant for any  $x_4 > 0$ . Therefore, the positivity of the solution for  $x_1$  is guaranteed. To obtain an ODE for  $\dot{x}_2$ , we assume  $x_1 = 0$  in  $F_2(x_1, x_2, x_3)$ . This results in  $\dot{x}_2 = F_2(x_2, x_3)$ , whose solution takes the form  $x_2(a) = x_2^0 e^{-(k_{32}x_3(a) - k_{2d})a}$ . Therefore, for any positive initial data,  $x_2(a)$  remains positive for all ages and  $x_3(a)$  values. Similarly, we substitute  $x_3 = 0$  in  $F_2(x_1, x_2, x_3)$  to obtain a nonlinear ODE  $\dot{x}_2 = F_2(x_1, x_2)$  for  $x_2$ . Although an explicit solution cannot be computed, the phase portrait of  $(x_1, x_2)$  reveals that the solution trajectories move away from the axis separating the positive and negative space for positive initial data. By following a similar procedure, we can establish sufficient conditions for the positivity of solutions for  $x_3(a)$  and  $x_4(a)$ . Therefore, we conclude that if  $\zeta_0 \in \Omega$ , then  $\zeta(t, \zeta_0) \in \Omega$  for all  $t > 0$ .  $\square$

The above analysis implies that the local solution  $\zeta(t, \zeta_0)$  of (8.3) with initial conditions  $\zeta_0 \in D(\mathbf{A}) \cap \Omega$  has a well-defined and finite norm. Consequently, we obtain our final result.

**Theorem 8.1.1.** The abstract Cauchy problem (8.3) has a unique global classical solution on  $Z$  with respect to the initial data  $z_0 \in \Omega \cap D(\mathbf{A})$ .

As a result of having positive initial data, the IVP (7.1)-(7.4) possesses a singular positive solution.

## 8.2 Existence and stability of steady-state

This section aims to determine the steady-state solution of the model and to present sufficient conditions for the existence of a positive steady-state. To this end, we specify some notation. Let  $X$  be a real or complex Banach space, and let  $X^*$  denote its dual space. We denote the value of  $F \in X^*$  at  $\psi \in X$  as  $\langle F, \psi \rangle$ . Additionally, we define a cone  $X_+$  as a non-zero set that satisfies  $X_+ \cap (-X_+) = 0$ ,  $\lambda X_+ \subset X_+$  for  $\lambda \geq 0$ , and  $X_+ + X_+ \subset X_+$ . Furthermore, we define the dual cone, denoted as  $X_+^*$ , as the subset of the dual space.

### 8.2.1 Existence of steady-states

The steady-states of the system (7.1)-(7.4) and (7.13)-(7.16) are denoted by  $\bar{p}_h(a)$ ,  $\bar{q}_h(a)$ ,  $\bar{p}_c(a)$ ,  $\bar{q}_c(a)$  and  $\bar{x}_1 - \bar{x}_4$ . These steady-states must satisfy the following set of

time-invariant ordinary differential equations:

$$\left\{ \begin{array}{l}
 \frac{\partial(g_h(a)\bar{p}_h(a))}{\partial a} = \bar{\gamma}_h\bar{q}_h(a) - (\beta_h(a) + \alpha_h(a, \bar{x}_1) + \mu_{p_h}(a))\bar{p}_h(a), \\
 0 = \alpha_h(a, \bar{x}_1)\bar{p}_h(a) - (\bar{\gamma}_h + \mu_{q_h}(a))\bar{q}_h(a), \\
 \frac{\partial(g_c(a)\bar{p}_c(a))}{\partial a} = \bar{\gamma}_c\bar{q}_c(a) - (\beta_c(a) + \alpha_c(a, \bar{x}_1) + \mu_{p_c}(a))\bar{p}_c(a), \\
 0 = \alpha_c(a, \bar{x}_1)\bar{p}_c(a) - (\bar{\gamma}_c + \mu_{q_c}(a))\bar{q}_c(a), \\
 \bar{p}_h(0) = 2(1 - m) \int_0^{a^*} \beta_h(a)\bar{p}_h(a)da, \\
 \bar{p}_c(0) = 2 \int_0^{a^*} \beta_c(a)\bar{p}_c(a)da + 2 \int_0^{a^*} \beta_h(a)\bar{p}_h(a)da, \\
 \frac{d\bar{x}_1}{da} = k_{1s} \left( \frac{\bar{g}_f}{k_{gf} + \bar{g}_f} \right) - k_{14}\bar{x}_4\bar{x}_1 - k_{1d} \left( \frac{\bar{x}_1}{k_1 + \bar{x}_1} \right), \\
 \frac{d\bar{x}_2}{da} = k_{21} \left( \frac{x_{2t} - \bar{x}_2}{k_2 + (x_{2t} - \bar{x}_2)} \right) \bar{x}_1 - k_{32}\bar{x}_2\bar{x}_3 - k_{2d}\bar{x}_2, \\
 \frac{d\bar{x}_3}{da} = k_{3s} - k_{32}\bar{x}_2\bar{x}_3 - k_{31} \left( \frac{\bar{x}_3}{k_3 + \bar{x}_3} \right) \bar{x}_2 - k_{3d}\bar{x}_3, \\
 \frac{d\bar{x}_4}{da} = k_{4s} + k_{42} \left( \frac{k_{34}}{k_{34} + \bar{x}_3} \right) \bar{x}_2 - k_{41} \left( \frac{\bar{x}_4}{k_4 + \bar{x}_4} \right) \bar{x}_1 - k_{4d}\bar{x}_4,
 \end{array} \right. \quad (8.10)$$

where  $\bar{\gamma}_i = \gamma_i(\bar{N})$ ,  $\bar{g}_f = g_f(\bar{N})$  and  $\bar{N} = \int_0^{a^*} (\bar{p}_h(a) + \bar{q}_h(a) + \bar{p}_c(a) + \bar{q}_c(a))da$ . Since the cell cycle model's ODEs are age-dependent and the system is in a steady-state due to the input of growth factors, all cell cycle states attain a steady-state. As a result, we can determine the steady-states of the quiescent and proliferating cell populations, represented by  $\bar{p}_h(a)$ ,  $\bar{q}_h(a)$ ,  $\bar{p}_c(a)$  and  $\bar{q}_c(a)$ , without explicitly solving the equations of microscale model. Solving the system (8.10) for  $\bar{p}_h$ ,  $\bar{q}_h$ ,  $\bar{p}_c$  and  $\bar{q}_c$  allows us to obtain the values of  $\bar{q}_h$  and  $\bar{q}_c$ :

$$\bar{q}_h(a) = \frac{\alpha_h(a, \bar{x}_1)\bar{p}_h(a)}{\bar{\gamma}_h + \mu_{q_h}(a)}, \quad \bar{q}_c(a) = \frac{\alpha_c(a, \bar{x}_1)\bar{p}_c(a)}{\bar{\gamma}_c + \mu_{q_c}(a)}, \quad (8.11)$$

and substituting the aforementioned expressions for  $\bar{q}_h$  and  $\bar{q}_c$  into the equations for  $\bar{p}_h$  and  $\bar{p}_c$ , respectively, results in the following expressions:

$$\frac{d(g_h(a)\bar{p}_h(a))}{da} + \left( \frac{\alpha_h(a, \bar{x}_1)\mu_{q_h}(a)}{\bar{\gamma}_h + \mu_{q_h}(a)} + \beta_h(a) + \mu_{p_h}(a) \right) \bar{p}_h(a) = 0, \quad (8.12)$$

$$\frac{d(g_c(a)\bar{p}_c(a))}{da} + \left( \frac{\alpha_c(a, \bar{x}_1)\mu_{q_c}(a)}{\bar{\gamma}_c + \mu_{q_c}(a)} + \beta_c(a) + \mu_{p_c}(a) \right) \bar{p}_c(a) = 0. \quad (8.13)$$

Solving Eq (8.12) for  $\bar{p}_h(a)$  and  $\bar{p}_c(a)$ , yields steady-state solutions for  $\bar{p}_h(a)$ ,  $\bar{q}_h(a)$ ,  $\bar{p}_c(a)$  and  $\bar{q}_c(a)$  as follows:

$$\begin{aligned}\bar{p}_h(a) &= \bar{p}_h(0) \exp\left(-\int_0^a \frac{1}{g_h(a)} \left(g'_h(a) + \frac{\alpha_h(\bar{x}_1, \xi)\mu_{q_h}(\xi)}{\bar{\gamma}_h + \mu_{q_h}(\xi)} + \beta_h(\xi) + \mu_{p_h}(\xi)\right) d\xi\right), \\ \bar{q}_h(a) &= \frac{\alpha_h(a, \bar{x}_1)\bar{p}_h(0)}{\bar{\gamma}_h + \mu_{q_h}(a)} \exp\left(-\int_0^a \frac{1}{g_h(a)} \left(g'_h(a) + \frac{\alpha_h(\bar{x}_1, \xi)\mu_{q,h}(\xi)}{\bar{\gamma}_h + \mu_{q_h}(\xi)} + \beta_h(\xi) + \mu_{p_h}(\xi)\right) d\xi\right), \\ \bar{p}_c(a) &= \bar{p}_c(0) \exp\left(-\int_0^a \frac{1}{g_c(a)} \left(g'_c(a) + \frac{\alpha_c(\bar{x}_1, \xi)\mu_{q_c}(\xi)}{\bar{\gamma}_c + \mu_{q_c}(\xi)} + \beta_c(\xi) + \mu_{p_c}(\xi)\right) d\xi\right), \\ \bar{q}_c(a) &= \frac{\alpha_c(a, \bar{x}_1)\bar{p}_c(0)}{\bar{\gamma}_c + \mu_{q_c}(a)} \exp\left(-\int_0^a \frac{1}{g_c(a)} \left(g'_c(a) + \frac{\alpha_c(\bar{x}_1, \xi)\mu_{q,c}(\xi)}{\bar{\gamma}_c + \mu_{q_c}(\xi)} + \beta_c(\xi) + \mu_{p_c}(\xi)\right) d\xi\right).\end{aligned}$$

It is evident that the system described in Eqs (7.1)–(7.4), (7.13) always has a trivial steady-state.

### 8.2.2 Stability analysis of steady-state solutions

Our next objective is to obtain the stability criteria for a positive steady-state solution. Suppose  $p_h(a, t) = \bar{p}_h$ ,  $q_h(a, t) = \bar{q}_h$ ,  $p_c(a, t) = \bar{p}_c$ ,  $q_c(a, t) = \bar{q}_c$ ,  $\forall t \geq 0$  represent equilibrium solutions to the PDE model (7.1)–(7.4) and  $p_h^*(a, t)$ ,  $q_h^*(a, t)$ ,  $p_c^*(a, t)$  and  $q_c^*(a, t)$  represent the corresponding perturbation terms:

$$p_h(a, t) = \bar{p}_h + \epsilon p_h^*(a, t), \quad q_h(a, t) = \bar{q}_h + \epsilon q_h^*(a, t),$$

$$p_c(a, t) = \bar{p}_c + \epsilon p_c^*(a, t), \quad q_c(a, t) = \bar{q}_c + \epsilon q_c^*(a, t).$$

After substituting the aforementioned expressions into the PDE model (7.1)–(7.4), we obtain

$$\begin{aligned}\epsilon \frac{\partial}{\partial t} p_h^*(a, t) + \frac{\partial}{\partial a} (g_h(a)(\bar{p}_h + \epsilon p_h^*(a, t))) &= \left( \frac{\nu_h \theta_h^{\kappa_h}}{\theta_h^{\kappa_h} + (\bar{N} + \epsilon n(t))^{\kappa_h}} \right) (\bar{p}_h + \epsilon q_h^*(a, t)) \\ &\quad - (\beta_h(a) + \alpha_h(a, \bar{x}_1) + \mu_{p_h}(a)) (\bar{p}_h + \epsilon p_h^*(a, t)), \\ \epsilon \frac{\partial}{\partial t} q_h^*(a, t) &= \alpha_h(a, \bar{x}_1) (\bar{p}_h + \epsilon p_h^*(a, t)) - \left( \frac{\nu_h \theta_h^{\kappa_h}}{\theta_h^{\kappa_h} + (\bar{N} + \epsilon n(t))^{\kappa_h}} + \mu_{q_h}(a) \right) (\bar{p}_h + \epsilon q_h^*(a, t)), \\ \epsilon \frac{\partial}{\partial t} p_c^*(a, t) + \frac{\partial}{\partial a} (g_c(a)(\bar{p}_c + \epsilon p_c^*(a, t))) &= \left( \frac{\nu_c \theta_c^{\kappa_c}}{\theta_c^{\kappa_c} + (\bar{N} + \epsilon n(t))^{\kappa_c}} \right) (\bar{p}_c + \epsilon q_c^*(a, t)) \\ &\quad - (\beta_c(a) + \alpha_c(a, \bar{x}_1) + \mu_{p_c}(a)) (\bar{p}_c + \epsilon p_c^*(a, t)), \\ \epsilon \frac{\partial}{\partial t} q_c^*(a, t) &= \alpha_c(a, \bar{x}_1) (\bar{p}_c + \epsilon p_c^*(a, t)) - \left( \frac{\nu_c \theta_c^{\kappa_c}}{\theta_c^{\kappa_c} + (\bar{N} + \epsilon n(t))^{\kappa_c}} + \mu_{q_c}(a) \right) (\bar{p}_c + \epsilon q_c^*(a, t)), \\ (\bar{p}_h(0) + \epsilon p_h^*(0, t)) &= 2(1 - m) \int_0^{a^*} \beta_h(a) (\bar{p}_h + \epsilon p_h^*(a, t)) da, \\ (\bar{p}_c(0) + \epsilon p_c^*(0, t)) &= 2 \int_0^{a^*} \beta_c(a) (\bar{p}_c + \epsilon p_c^*(a, t)) da + 2m \int_0^{a^*} \beta_h(a) (\bar{p}_h + \epsilon p_h^*(a, t)) da,\end{aligned}$$

where  $n(t) := \int_0^{a^*} (p_h^*(a, t) + q_h^*(a, t) + p_c^*(a, t) + q_c^*(a, t)) da$ . Then, take the derivative with respect to epsilon  $\epsilon$ , leads to

$$\begin{aligned} \frac{\partial}{\partial t} p_h^*(a, t) + \frac{\partial}{\partial a} (g_h(a) p_h^*(a, t)) &= \frac{\partial}{\partial \epsilon} \left( \frac{\nu_h \theta_h^{\kappa_h} \epsilon}{\theta_h^{\kappa_h} + (\bar{N} + \epsilon n(t))^{\kappa_h}} \right) q_h^*(a, t) \\ &\quad - (\beta_h(a) + \alpha_h(a, \bar{x}_1) + \mu_{p_h}(a)) p_h^*(a, t), \\ \frac{\partial}{\partial t} q_h^*(a, t) &= \alpha_h(a, \bar{x}_1) p_h^*(a, t) - \left( \frac{\partial}{\partial \epsilon} \left( \frac{\nu_h \theta_h^{\kappa_h} \epsilon}{\theta_h^{\kappa_h} + (\bar{N} + \epsilon n(t))^{\kappa_h}} \right) - \mu_{q_h}(a) \right) q_h^*(a, t), \\ \frac{\partial}{\partial t} p_c^*(a, t) + \frac{\partial}{\partial a} (g_c(a) p_c^*(a, t)) &= \frac{\partial}{\partial \epsilon} \left( \frac{\nu_c \theta_c^{\kappa_c} \epsilon}{\theta_c^{\kappa_c} + (\bar{N} + \epsilon n(t))^{\kappa_c}} \right) q_c^*(a, t) \\ &\quad - (\beta_c(a) + \alpha_c(a, \bar{x}_1) + \mu_{p_c}(a)) p_c^*(a, t), \\ \frac{\partial}{\partial t} q_c^*(a, t) &= \alpha_c(a, \bar{x}_1) p_c^*(a, t) - \left( \frac{\partial}{\partial \epsilon} \left( \frac{\nu_c \theta_c^{\kappa_c} \epsilon}{\theta_c^{\kappa_c} + (\bar{N} + \epsilon n(t))^{\kappa_c}} \right) - \mu_{q_c}(a) \right) q_c^*(a, t), \\ p_h^*(0, t) &= 2(1 - m) \int_0^{a^*} \beta_h(a) p_h^*(a, t) da, \\ p_c^*(0, t) &= 2 \int_0^{a^*} \beta_c(a) p_c^*(a, t) da + 2m \int_0^{a^*} \beta_h(a) p_h^*(a, t) da, \end{aligned}$$

which simplifies to

$$\begin{aligned} \frac{\partial}{\partial t} p_h^*(a, t) + \frac{\partial}{\partial a} (g_h(a) p_h^*(a, t)) &= \nu_h \theta_h^{\kappa_h} \left( \frac{(\theta_h^{\kappa_h} + (\bar{N} + \epsilon n(t))^{\kappa_h}) - \kappa_h \epsilon n(t) (\bar{N} + \epsilon n(t))^{\kappa_h - 1}}{(\theta_h^{\kappa_h} + (\bar{N} + \epsilon n(t))^{\kappa_h})^2} \right) \\ &\quad q_h^*(a, t) - (\alpha_h(a, \bar{x}_1) + \beta_h(a) + \mu_{p_h}(a)) p_h^*(a, t), \\ \frac{\partial}{\partial t} q_h^*(a, t) &= \alpha_h(a, \bar{x}_1) p_h^*(a, t) - \left( \left( \frac{(\theta_h^{\kappa_h} + (\bar{N} + \epsilon n(t))^{\kappa_h}) - \kappa_h \epsilon n(t) (\bar{N} + \epsilon n(t))^{\kappa_h - 1}}{(\theta_h^{\kappa_h} + (\bar{N} + \epsilon n(t))^{\kappa_h})^2} \right) \right. \\ &\quad \left. \nu_h \theta_h^{\kappa_h} - \mu_{q_h}(a) \right) q_h^*(a, t), \\ \frac{\partial}{\partial t} p_c^*(a, t) + \frac{\partial}{\partial a} (g_c(a) p_c^*(a, t)) &= \nu_c \theta_c^{\kappa_c} \left( \frac{(\theta_c^{\kappa_c} + (\bar{N} + \epsilon n(t))^{\kappa_c}) - \kappa_c \epsilon n(t) (\bar{N} + \epsilon n(t))^{\kappa_c - 1}}{(\theta_c^{\kappa_c} + (\bar{N} + \epsilon n(t))^{\kappa_c})^2} \right) \\ &\quad q_c^*(a, t) - (\alpha_c(a, \bar{x}_1) + \beta_c(a) + \mu_{p_c}(a)) p_c^*(a, t), \\ \frac{\partial}{\partial t} q_c^*(a, t) &= \alpha_c(a, \bar{x}_1) p_c^*(a, t) - \left( \left( \frac{(\theta_c^{\kappa_c} + (\bar{N} + \epsilon n(t))^{\kappa_c}) - \kappa_c \epsilon n(t) (\bar{N} + \epsilon n(t))^{\kappa_c - 1}}{(\theta_c^{\kappa_c} + (\bar{N} + \epsilon n(t))^{\kappa_c})^2} \right) \right. \\ &\quad \left. \nu_c \theta_c^{\kappa_c} - \mu_{q_c}(a) \right) q_c^*(a, t), \\ p_h^*(0, t) &= 2(1 - m) \int_0^{a^*} \beta_h(a) p_h^*(a, t) da, \\ p_c^*(0, t) &= 2 \int_0^{a^*} \beta_c(a) p_c^*(a, t) da + 2m \int_0^{a^*} \beta_h(a) p_h^*(a, t) da. \end{aligned}$$



In the limit as  $\epsilon$  approaches zero, we arrive at a linear system of partial differential equations:

$$\left\{ \begin{array}{l} \frac{\partial}{\partial t} p_h^*(a, t) + \frac{\partial}{\partial a} (g_h(a) p_h^*(a, t)) = \gamma_h(\bar{N}) q_h^*(a, t) - (\alpha_h(a, \bar{x}_1) + \beta_h(a) + \mu_{p_h}(a)) p_h^*(a, t), \\ \frac{\partial}{\partial t} q_h^*(a, t) = \alpha_h(a, \bar{x}_1) p_h^*(a, t) - (\mu_{q_h}(a) + \gamma_h(\bar{N})) q_h^*(a, t), \\ \frac{\partial}{\partial t} p_c^*(a, t) + \frac{\partial}{\partial a} (g_c(a) p_c^*(a, t)) = \gamma_c(\bar{N}) q_c^*(a, t) - (\alpha_c(a, \bar{x}_1) + \beta_c(a) + \mu_{p_c}(a)) p_c^*(a, t), \\ \frac{\partial}{\partial t} q_c^*(a, t) = \alpha_c(a, \bar{x}_1) p_c^*(a, t) - (\mu_{q_c}(a) + \gamma_c(\bar{N})) q_c^*(a, t), \\ p_h^*(0, t) = 2(1 - m) \int_0^{a^*} \beta_h(a) p_h^*(a, t) da, \\ p_c^*(0, t) = 2 \int_0^{a^*} \beta_c(a) p_c^*(a, t) da + 2m \int_0^{a^*} \beta_h(a) p_h^*(a, t) da, \end{array} \right. \quad (8.14)$$

where  $\gamma_i(\bar{N}) = \nu_i \theta_i^{\kappa_i} / (\theta_i^{\kappa_i} + \bar{N}^{\kappa_i})$ , where  $i = \{h, c\}$ . Next, we formulate (8.14) as semilinear problem:

$$\frac{d}{dt} \omega(t) = C\omega(t), \quad \omega(0) = \omega_0 \in X, \quad (8.15)$$

where the generator  $C$  is defined on the Banach space  $X$  as follows:

$$(C\phi)(a) = \begin{pmatrix} -\left(\frac{\partial}{\partial a} + \frac{1}{g_h(a)}(\beta_h(a) + \alpha_h(a, \bar{x}_1) + \mu_{p_h}(a))\right) g_h(a) \phi_1(a) + \gamma_h(\bar{N}) \phi_2(a) \\ \alpha_h(a, \bar{x}_1) \phi_1(a) - (\gamma_h(\bar{N}) + \mu_{q_h}(a)) \phi_2(a) \\ -\left(\frac{\partial}{\partial a} + \frac{1}{g_c(a)}(\beta_c(a) + \alpha_c(a, \bar{x}_1) + \mu_{p_c}(a))\right) g_c(a) \phi_1(a) + \gamma_c(\bar{N}) \phi_2(a) \\ \alpha_c(a, \bar{x}_1) \phi_1(a) - (\gamma_c(\bar{N}) + \mu_{q_c}(a)) \phi_2(a) \end{pmatrix},$$

where

$$\phi(a) = (\phi_1(a), \phi_2(a), \phi_3(a), \phi_4(a))^T \in D(C),$$

where  $D(C)$  is defined below:

$$D(C) = \left\{ (\phi_1, \phi_2) \mid \phi_i \text{ is absolute continuous on } [0, a^*], \right. \\ \left. \phi(0) = \left( 2(1 - m) \int_0^{a^*} \beta_h(a) \phi_1(a) da, 0, 2 \int_0^{a^*} \beta_c(a) \phi_2(a) da + 2m \int_0^{a^*} \beta_h(a) \phi_1(a) da, 0 \right)^T \right\}.$$

Next, we take the resolvent equation for the operator  $C$ :

$$(\lambda I - C)\phi = \psi, \quad \phi \in D(C), \quad \psi \in X, \quad \lambda \in \mathbb{C}, \quad (8.16)$$

which leads to

$$-\gamma_h(\bar{N}) \phi_2(a) + \frac{\partial}{\partial a} (g_h(a) \phi_1(a)) + (\lambda + \beta_h(a) + \alpha_h(a, \bar{x}_1) + \mu_{p_h}(a)) \phi_1(a) = \psi_1(a), \quad (8.17)$$

$$(\lambda + \gamma_h(\bar{N}) + \mu_{q_h}(a)) \phi_2(a) - \alpha_h(a, \bar{x}_1) \phi_1(a) = \psi_2(a), \quad (8.18)$$

$$-\gamma_c(\bar{N}) \phi_4(a) + \frac{\partial}{\partial a} (g_c(a) \phi_3(a)) + (\lambda + \beta_c(a) + \alpha_c(a, \bar{x}_1) + \mu_{p_c}(a)) \phi_3(a) = \psi_3(a), \quad (8.19)$$

$$(\lambda + \gamma_c(\bar{N}) + \mu_{q_c}(a)) \phi_4(a) - \alpha_c(a, \bar{x}_1) \phi_3(a) = \psi_4(a), \quad (8.20)$$

and

$$\phi_1(0) = 2(1-m) \int_0^{a^*} \beta_h(a) \phi_1(a) da, \quad \phi_3(0) = 2 \int_0^{a^*} \beta_c(a) \phi_3(a) da + 2m \int_0^{a^*} \beta_h(a) \phi_1(a) da.$$

By solving (8.18) and (8.20), we get

$$\phi_2(a) = \frac{\psi_2(a) + \alpha_h(a, \bar{x}_1) \phi_1(a)}{\lambda + \gamma_h(\bar{N}) + \mu_{q_h}(a)}, \quad \phi_4(a) = \frac{\psi_4(a) + \alpha_c(a, \bar{x}_1) \phi_3(a)}{\lambda + \gamma_c(\bar{N}) + \mu_{q_c}(a)}, \quad (8.21)$$

which after substituting in Eqs. (8.17) and (8.19) gives

$$\begin{aligned} \phi_1(a) &= \exp \left( - \int_0^a \beta_h(\xi) + \alpha_h(\bar{x}_1, \xi) + \lambda + \mu_{p_h}(\xi) - \frac{\gamma_h(\bar{N}) \alpha_h(\bar{x}_1, \xi)}{g_h(\xi)(\lambda + \gamma_h(\bar{N}) + \mu_{q_h}(\xi))} d\xi \right) \\ &\quad \left[ \int_0^a \exp \left( \int_0^\zeta \beta_h(\xi) + \alpha_h(\bar{x}_1, \xi) + \lambda + \mu_{p_h}(\xi) - \frac{\gamma_h(\bar{N}) \alpha_h(\bar{x}_1, \xi)}{g_h(\xi)(\lambda + \gamma_h(\bar{N}) + \mu_{q_h}(\xi))} d\xi \right) \right. \\ &\quad \left. \frac{1}{g_h(\zeta)} \left\{ \psi_1(\zeta) + \frac{\gamma_h(\bar{N}) \psi_2(\zeta)}{\lambda + \gamma_h(\bar{N}) + \mu_{q_h}(\zeta)} \right\} d\zeta + \phi_1(0) \right], \\ \phi_3(a) &= \exp \left( - \int_0^a \beta_c(\xi) + \alpha_c(\bar{x}_1, \xi) + \lambda + \mu_{p_c}(\xi) - \frac{\gamma_c(\bar{N}) \alpha_c(\bar{x}_1, \xi)}{g_c(\xi)(\lambda + \gamma_c(\bar{N}) + \mu_{q_c}(\xi))} d\xi \right) \\ &\quad \left[ \int_0^a \exp \left( \int_0^\zeta \beta_c(\xi) + \alpha_c(\bar{x}_1, \xi) + \lambda + \mu_{p_c}(\xi) - \frac{\gamma_c(\bar{N}) \alpha_c(\bar{x}_1, \xi)}{g_c(\xi)(\lambda + \gamma_c(\bar{N}) + \mu_{q_c}(\xi))} d\xi \right) \right. \\ &\quad \left. \frac{1}{g_c(\zeta)} \left\{ \psi_3(\zeta) + \frac{\gamma_c(\bar{N}) \psi_4(\zeta)}{\lambda + \gamma_c(\bar{N}) + \mu_{q_c}(\zeta)} \right\} d\zeta + \phi_3(0) \right]. \end{aligned}$$

Substituting  $\phi_1(a)$  and  $\phi_3(a)$  back in Eq (8.21) yields

$$\begin{aligned} \phi_2(a) &= \frac{1}{\lambda + \gamma_h(\bar{N}) + \mu_{q_h}(a)} \left[ \exp \left( - \int_0^a \beta_h(\xi) + \alpha_h(\bar{x}_1, \xi) + \lambda + \mu_{p_h}(\xi) \right. \right. \\ &\quad \left. \left. - \frac{\gamma_h(\bar{N}) \alpha_h(\bar{x}_1, \xi)}{g_h(\xi)(\lambda + \gamma_h(\bar{N}) + \mu_{q_h}(\xi))} d\xi \right) \left\{ \int_0^a \exp \left( \int_0^\zeta \beta_h(\xi) + \alpha_h(\bar{x}_1, \xi) + \lambda + \mu_{p_h}(\xi) \right) \right. \right. \\ &\quad \left. \left. - \frac{\gamma_h(\bar{N}) \alpha_h(\bar{x}_1, \xi)}{g_h(\xi)(\lambda + \gamma_h(\bar{N}) + \mu_{q_h}(\xi))} d\xi \right) \frac{1}{g_h(\zeta)} \left\{ \psi_1(\zeta) + \frac{\gamma_h(\bar{N}) \psi_2(\zeta)}{\lambda + \gamma_h(\bar{N}) + \mu_{q_h}(\zeta)} \right\} d\zeta \right. \\ &\quad \left. + \phi_1(0) \right\} \alpha_h(a, \bar{x}_1) + \psi_2(a) \Big], \\ \phi_4(a) &= \frac{1}{\lambda + \gamma_c(\bar{N}) + \mu_{q_c}(a)} \left[ \exp \left( - \int_0^a \beta_c(\xi) + \alpha_c(\bar{x}_1, \xi) + \lambda + \mu_{p_c}(\xi) \right. \right. \\ &\quad \left. \left. - \frac{\gamma_c(\bar{N}) \alpha_c(\bar{x}_1, \xi)}{g_c(\xi)(\lambda + \gamma_c(\bar{N}) + \mu_{q_c}(\xi))} d\xi \right) \left\{ \int_0^a \exp \left( \int_0^\zeta \beta_c(\xi) + \alpha_c(\bar{x}_1, \xi) + \lambda + \mu_{p_c}(\xi) \right) \right. \right. \\ &\quad \left. \left. - \frac{\gamma_c(\bar{N}) \alpha_c(\bar{x}_1, \xi)}{g_c(\xi)(\lambda + \gamma_c(\bar{N}) + \mu_{q_c}(\xi))} d\xi \right) \frac{1}{g_c(\zeta)} \left\{ \psi_3(\zeta) + \frac{\gamma_c(\bar{N}) \psi_4(\zeta)}{\lambda + \gamma_c(\bar{N}) + \mu_{q_c}(\zeta)} \right\} d\zeta \right. \\ &\quad \left. + \phi_3(0) \right\} \alpha_c(a, \bar{x}_1) + \psi_4(a) \Big]. \end{aligned}$$

**Lemma 8.2.1.** The resolvent of operator  $C$  is compact and its spectrum, denoted by  $\sigma(C)$ , satisfies the condition:

$$\sigma(C) = \sigma_P(C) = \{\lambda \in \mathbb{C} \mid 1 \in \sigma_p(U_\lambda)\}. \quad (8.22)$$

Here,  $\sigma_P(\mathbf{C})$  refers to the point spectrum of  $\mathbf{C}$ , and  $U_\lambda$  is an operator dependent on  $\lambda$ .

*Proof.* The expression of  $\phi_1(a)$  and  $\phi_3(a)$  can be re-written as

$$\begin{aligned}\phi_1(a) &= \frac{1}{\alpha_h(a, \bar{x}_1)} \{(\lambda + \gamma_h(\bar{N}) + \mu_{q_h})(U_{h,\lambda}\psi_2)(a) + \gamma_h(\bar{N})(U_{h,\lambda}\psi_1)(a)\}, \\ \phi_3(a) &= \frac{1}{\alpha_c(a, \bar{x}_1)} \{(\lambda + \gamma_c(\bar{N}) + \mu_{q_c})(U_{c,\lambda}\psi_4)(a) + \gamma_c(\bar{N})(U_{c,\lambda}\psi_3)(a)\},\end{aligned}$$

where the linear operator on Banach space,  $U_{i,\lambda}$  is given as

$$(U_{i,\lambda}\psi)(a) = \int_0^{a^*} \mathcal{H}_{i,\lambda}(\zeta, a)\psi(\zeta)d\zeta, \quad i = \{h, c\}, \quad (8.23)$$

where

$$\begin{aligned}\mathcal{H}_\lambda(\zeta, a) &= \frac{\alpha_i(a, \bar{x}_1)}{g_i(\zeta)(\lambda + \gamma_i(\bar{N}) + \mu_{q_i}(a))} \exp\left(-\int_0^a \beta_i(\xi) + \alpha_i(\bar{x}_1, \xi) + \lambda + \mu_{p_i}(\xi)\right. \\ &\quad \left.- \frac{\gamma_i(\bar{N})\alpha_i(\bar{x}_1, \xi)}{g_i(\xi)(\lambda + \gamma_i(\bar{N}) + \mu_{q_i}(\xi))}d\xi\right) \exp\left(\int_0^\zeta \beta_i(\xi) + \alpha_i(\bar{x}_1, \xi) + \lambda + \mu_{p_i}(\xi)\right. \\ &\quad \left.- \frac{\gamma_i(\bar{N})\alpha_i(\bar{x}_1, \xi)}{g_i(\xi)(\lambda + \gamma_i(\bar{N}) + \mu_{q_i}(\xi))}d\xi\right).\end{aligned} \quad (8.24)$$

Similarly, we rewrite  $\phi_2(a)$  and  $\phi_4(a)$  as

$$\phi_2(a) = (U_{i,\lambda}\psi_2)(a) + (V_{i,\lambda}\psi_1)(a), \quad \phi_4(a) = (U_{i,\lambda}\psi_4)(a) + (V_{i,\lambda}\psi_3)(a),$$

where the linear operator on Banach space,  $V_{i,\lambda}$  is given as

$$\begin{aligned}(V_{i,\lambda}\psi)(a) &= \int_0^{a^*} \mathcal{G}_{i,\lambda}(\zeta, a)\psi(\zeta)d\zeta, \\ \text{where } \mathcal{G}_{i,\lambda}(\zeta, a) &= \frac{1}{g_i(\zeta)(\lambda + \gamma_i(\bar{N}) + \mu_{q_i}(\xi))} \left( \gamma_i(\bar{N})\mathcal{H}_{i,\lambda}(\zeta, a) + \frac{g_i(\zeta)}{a^*} \right).\end{aligned}$$

Let  $\Lambda = \lambda \in \mathbb{C}, |1 \in \sigma(U_\lambda)$ . For  $\lambda \in \mathbb{C} \setminus \Lambda$ , the operators  $U_{i,\lambda}$  and  $V_{i,\lambda}$  are compact operators from  $X$  to  $L^1(0, a^*)$ , implying that  $\phi_1(a)$  and  $\phi_3(a)$  are represented by compact operators, and similarly,  $\phi_2(a)$  and  $\phi_4(a)$  are also represented by compact operators. As a result, the operator  $\mathbf{C}$  has a compact resolvent, which confirms that its spectrum  $\sigma(\mathbf{C})$  constitutes only isolated eigenvalues, i.e.,  $\sigma(\mathbf{C}) = \sigma_P(\mathbf{C})$  (see Theorem 6.29 on page 187 in [152]). Hence,  $\mathbb{C} \setminus \Lambda \subset \rho(\mathbf{C})$ , where  $\rho(\mathbf{C})$  is the resolvent of operator  $\mathbf{C}$ . Therefore,  $\sigma_P(\mathbf{C}) = \sigma(\mathbf{C}) \subset \Lambda$ . Since  $U_\lambda$  is a compact operator, we have  $\sigma(U_\lambda) \setminus 0 = \sigma_P(U_\lambda) \setminus 0$ . If  $\lambda \in \Lambda$ , there exists an eigenfunction  $\psi_\lambda$  such that  $U_\lambda\psi_\lambda = \psi_\lambda$ . It is easy to see that  $(\phi_1(a), \phi_2(a), \phi_3(a), \phi_4(a))^T$  provides an eigenvector of  $\mathbf{C}$  for the eigenvalue  $\lambda$ . Thus, we have  $\Lambda \subset \sigma_P(\mathbf{C})$ , and we can conclude that (8.22) is satisfied.  $\square$

**Lemma 8.2.2.** Consider the operator  $\mathbf{C}$  which generates  $C_0$ -semigroup for  $t \geq 0$ . Then,  $\mathbf{T}(t)$  is eventually norm continuous (ENC), and we have

$$\omega_0(\mathbf{C}) = s(\mathbf{C}) = \sup \operatorname{Re} \lambda, |\lambda \in \sigma(\mathbf{C})}, \quad (8.25)$$

where  $s(\mathbf{C})$  represents the spectral bound of the operator  $\mathbf{C}$ , and  $\omega_0(\mathbf{C})$  denotes the growth bound of the semigroup  $\mathbf{T}(t)$ .

*Proof.* To begin, we express the bounded operator  $C$  as

$$C\phi = \begin{pmatrix} k_h(a) & \gamma_h(\bar{N}) & 0 & 0 \\ \alpha_h(a, \bar{x}_1) & -\gamma_h(\bar{N}) - \mu_{q_h}(a) & 0 & 0 \\ 0 & 0 & k_c(a) & \gamma_c(\bar{N}) \\ 0 & 0 & \alpha_c(a, \bar{x}_1) & -\gamma_c(\bar{N}) - \mu_{q_c}(a) \end{pmatrix} \begin{pmatrix} \phi_1(a) \\ \phi_2(a) \\ \phi_3(a) \\ \phi_4(a) \end{pmatrix},$$

for  $\phi \in X$ ,  $k_h(a) = -\frac{\partial g_h(a)}{\partial a} - \beta_h(a) - \alpha_h(a, \bar{x}_1) - \mu_{p_h}(a)$  and  $k_c(a) = -\frac{\partial g_c(a)}{\partial a} - \beta_c(a) - \alpha_c(a, \bar{x}_1) - \mu_{p_c}(a)$ . To establish the compactness of  $C$ , our strategy is to demonstrate that for any bounded sequence  $(\phi^n)_{n \in \mathbb{N}}$  in  $X$ , the sequence  $(C\phi^n)_{n \in \mathbb{N}}$  contains a subsequence that converges uniformly. To accomplish this, we invoke the Arzelà-Ascoli Theorem, which requires us to verify that  $(C\phi^n)_{n \in \mathbb{N}}$  is uniformly bounded and uniformly equicontinuous. To prove boundedness, since we assume  $(\phi^n)_{n \in \mathbb{N}}$  to be bounded, we get

$$\|C\phi^n\|_1 \leq \|C\| \|\phi^n\|_1 \leq \|C\| \sup_{n \in \mathbb{N}} \|\phi^n\|_1,$$

which determines that  $(C\phi^n)_{n \in \mathbb{N}}$  is also bounded. For uniform equicontinuity, we consider

$$\begin{aligned} & \int_R |(C\phi)(a+h) - (C\phi)(a)| da = \int_R |C(a+h) - C(a)| |\phi(a)| da \\ & \leq \int_R \left| \begin{pmatrix} k_h(a+h) & \gamma_h(\bar{N}) & 0 & 0 \\ \alpha_h(a+h, \bar{x}_1) & -\gamma_h(\bar{N}) - \mu_{q_h}(a+h) & 0 & 0 \\ 0 & 0 & k_c(a+h) & \gamma_c(\bar{N}) \\ 0 & 0 & \alpha_c(a+h, \bar{x}_1) & -\gamma_c(\bar{N}) - \mu_{q_c}(a+h) \end{pmatrix} \right. \\ & \quad \left. - \begin{pmatrix} k_h(a) & \gamma_h(\bar{N}) & 0 & 0 \\ \alpha_h(a, \bar{x}_1) & -\gamma_h(\bar{N}) - \mu_{q_h}(a) & 0 & 0 \\ 0 & 0 & k_c(a) & \gamma_c(\bar{N}) \\ 0 & 0 & \alpha_c(a, \bar{x}_1) & -\gamma_c(\bar{N}) - \mu_{q_c}(a) \end{pmatrix} \right| \begin{vmatrix} \phi_1(a) \\ \phi_2(a) \\ \phi_3(a) \\ \phi_4(a) \end{vmatrix} da \\ & = \int_R \begin{vmatrix} m_1 & 0 & 0 & 0 \\ m_2 & m_3 & 0 & 0 \\ 0 & 0 & k_c(a+h) - k_c(a) & 0 \\ 0 & 0 & \alpha_c(a+h, \bar{x}_1) - \alpha_c(a, \bar{x}_1) & -\mu_{q_c}(a+h) - \mu_{q_c}(a) \end{vmatrix} \begin{vmatrix} \phi_1(a) \\ \phi_2(a) \\ \phi_3(a) \\ \phi_4(a) \end{vmatrix} da \\ & \leq \|\phi\| \int_R \begin{vmatrix} m_1 & 0 & 0 & 0 \\ m_2 & m_3 & 0 & 0 \\ 0 & 0 & k_c(a+h) - k_c(a) & 0 \\ 0 & 0 & \alpha_c(a+h, \bar{x}_1) - \alpha_c(a, \bar{x}_1) & -\mu_{q_c}(a+h) - \mu_{q_c}(a) \end{vmatrix} da. \end{aligned}$$

where  $m_1 = k_h(a+h) - k_h(a)$ ,  $m_2 = \alpha_h(a+h, \bar{x}_1) - \alpha_h(a, \bar{x}_1)$ , and  $m_3 = -\mu_{q_h}(a+h) - \mu_{q_h}(a)$ . Hence, we have shown that  $(C\phi^n)_{n \in \mathbb{N}}$  is equicontinuous, and by the Arzelà-Ascoli Theorem, we can conclude that there exists a uniformly convergent subsequence of  $(C\phi^n)_{n \in \mathbb{N}}$ . Consequently,  $C$  is compact, which in turn implies that  $\mathbf{T}$  is an ENC semigroup. Since the spectral mapping theorem can be applied to ENC semigroups, we have the spectral determined growth condition given by  $\omega_0(C) = s(C)$ . Thus, we obtain (8.25).  $\square$

The local exponential asymptotic stability of the steady-state solution  $\omega = 0$  of (8.15) is established when  $\omega_0(C) < 0$ . Specifically, there exist constants  $\epsilon > 0$ ,  $M \geq 1$ , and

$\gamma < 0$  such that if  $x \in X$  and  $|x| \leq \epsilon$ , then the solution  $\omega(t, x)$  of (8.15) exists globally and satisfies  $|\omega(t, x)| \leq M \exp(\gamma t)|x|$  for all  $t > 0$ . In order to examine the stability of steady states, it is necessary to identify the dominant singular point within the set  $\Lambda$ , which corresponds to the element with the highest real value. By utilizing (8.22) and (8.25), we can then determine the growth bound of the semigroup  $\mathbf{T}$ .

**Lemma 8.2.3.** For any  $\lambda \in \mathbb{R}$ , the operator  $U_{i,\lambda}$  is nonsupporting with respect to  $X_+$  and

$$\lim_{\lambda \rightarrow +\infty} r(U_{i,\lambda}) = 0 \quad (8.26)$$

holds.

*Proof.* By Eqs. (8.23) and (8.24), we can conclude that the operator  $U_{i,\lambda}$ ,  $\lambda \in \mathbb{R}$  is strictly positive. To prove that  $U_\lambda$ ,  $\lambda \in \mathbb{R}$  is non-supporting, we can easily demonstrate the inequality

$$U_{i,\lambda}\psi \geq \langle f_{i,\lambda}, \psi \rangle c, \quad c = 1 \in X_+, \quad \psi \in X_+, \quad (8.27)$$

where the linear function  $f_{i,\lambda}$ , is

$$\begin{aligned} \langle f_{i,\lambda}, \psi \rangle = & \int_0^{a^*} \left[ \frac{s_i(\zeta)}{g_i(\zeta)(\lambda + \gamma_i(\bar{N}) + \mu_{q_i}(a))} \exp\left(-\int_0^a \beta_i(\xi) + \alpha_i(\bar{x}_1, \xi) + \lambda + \mu_{p_i}(\xi) - \right. \right. \\ & \left. \left. \frac{\gamma_i(\bar{N})\alpha_i(\bar{x}_1, \xi)}{g(\xi)(\lambda + \gamma_i(\bar{N}) + \mu_{q_i}(\xi))} d\xi\right) \exp\left(\int_0^\zeta \beta_i(\xi) + \alpha_i(\bar{x}_1, \xi) + \lambda + \mu_{p_i}(\xi) \right. \right. \\ & \left. \left. - \frac{\gamma_i(\bar{N})\alpha_i(\bar{x}_1, \xi)}{g_i(\xi)(\lambda + \gamma_i(\bar{N}) + \mu_{q_i}(\xi))} d\xi\right) \right] \psi(\zeta) d\zeta. \end{aligned} \quad (8.28)$$

Thereby, it leads us to  $U_{i,\lambda}^{n+1}\psi \geq \langle f_{i,\lambda}, \psi \rangle \langle f_{i,\lambda}, c \rangle^n c$ ,  $\forall n$ . which holds for all  $\psi \in X_+$ , where  $f_{i,\lambda}$  is strictly positive and the constant function  $c = 1$  is a quasi-interior point of  $L^1(0, a^*)$ . This implies that  $\langle F, U_{i,\lambda}^n \rangle > 0$  for every pair  $\psi \in X_+ \setminus \{0\}$ ,  $F \in X_+^* \setminus \{0\}$ , and therefore  $U_{i,\lambda}$ ,  $\lambda \in \mathbb{R}$  is non-supporting. We then use inequality (8.27) and take the duality pairing with the eigenfunctional  $F_{i,\lambda}$  of  $U_{i,\lambda}$  corresponding to  $r(U_{i,\lambda})$ , yielding

$$r(U_{i,\lambda}) \langle F_\lambda, \psi \rangle \geq \langle F_\lambda, c \rangle \langle f_{i,\lambda}, \psi \rangle.$$

Assuming  $\psi = c$ , we obtain the inequality:

$$r(U_{i,\lambda}) \geq \langle f_{i,\lambda}, c \rangle,$$

where

$$\begin{aligned} \langle f_{i,\lambda}, c \rangle = & \int_0^{a^*} \frac{s_i(\zeta)}{g_i(\zeta)(\lambda + \gamma_i(\bar{N}) + \mu_{q_i}(\zeta))} \exp\left(-\int_0^a \beta_i(\xi) + \alpha_i(\bar{x}_1, \xi) + \lambda + \mu_{p_i}(\xi) \right. \\ & \left. - \frac{\gamma_i(\bar{N})\alpha_i(\bar{x}_1, \xi)}{g(\xi)(\lambda + \gamma_i(\bar{N}) + \mu_{q_i}(\xi))} d\xi\right) \exp\left(\int_0^\zeta \beta_i(\xi) + \alpha_i(\bar{x}_1, \xi) + \lambda + \mu_{p_i}(\xi) \right. \\ & \left. - \frac{\gamma_i(\bar{N})\alpha_i(\bar{x}_1, \xi)}{g_i(\xi)(\lambda + \gamma_i(\bar{N}) + \mu_{q_i}(\xi))} d\xi\right) d\zeta. \end{aligned} \quad (8.29)$$

It follows that

$$\begin{aligned}
 \langle f_\lambda, c \rangle \geq & \epsilon \int_0^{a^*} \frac{1}{g_i(\zeta)(\lambda + \gamma_i(\bar{N}) + \mu_{q_i}(\zeta))} \exp\left(-\int_0^a \beta_i(\xi) + \alpha_i(\bar{x}_1, \xi) + \lambda + \mu_{p_i}(\xi) \right. \\
 & \left. - \frac{\gamma_i(\bar{N})\alpha_i(\bar{x}_1, \xi)}{g(\xi)(\lambda + \gamma_i(\bar{N}) + \mu_{q_i}(\xi))} d\xi\right) \exp\left(\int_0^\zeta \beta_i(\xi) + \alpha_i(\bar{x}_1, \xi) + \lambda + \mu_{p_i}(\xi) \right. \\
 & \left. - \frac{\gamma_i(\bar{N})\alpha_i(\bar{x}_1, \xi)}{g_i(\xi)(\lambda + \gamma_i(\bar{N}) + \mu_{q_i}(\xi))} d\xi\right) d\zeta. \tag{8.30}
 \end{aligned}$$

By using the positivity of  $\gamma_i(\bar{N})$ ,  $\mu_{p_i}$ ,  $\mu_{q_i}$ ,  $\alpha_i$  and  $\beta_i$ , we conclude the following:

$$\lim_{\lambda \rightarrow +\infty} r(U_{i,\lambda}) = 0.$$

Hence, it is proven.  $\square$

The previous lemma implies that the function  $\lambda \rightarrow r(U_{i,\lambda})$  is decreasing for all  $\lambda \in \mathbb{R}$ . Moreover, if there exists a  $\lambda \in \mathbb{R}$  such that  $r(U_{i,\lambda}) = 1$ , then it follows that  $\lambda \in \Lambda$ , as  $r(U_{i,\lambda}) \in \sigma_P(U_{i,\lambda})$ . Combining this with the monotonicity property of  $r(U_{i,\lambda})$  and inequality (8.26), we obtain the following result.

**Lemma 8.2.4.** There exists a unique  $\lambda_0 \in \mathbb{R} \cap \Lambda$  such that  $r(U_{i,\lambda_0}) = 1$ , and  $\lambda_0 > 0$  if  $r(U_0) > 1$ ;  $\lambda_0 = 0$  if  $r(U_0) = 1$ ;  $\lambda_0 < 0$  if  $r(U_0) < 1$ .

We will demonstrate that  $\lambda_0$  is a dominant singular point, utilizing Theorem 6.13 in [153].

**Lemma 8.2.5.** If there exists a  $\lambda \in \Lambda$ ,  $\lambda \neq \lambda_0$ , then  $\operatorname{Re}\lambda < \lambda_0$ .

*Proof.* Let  $\lambda \in \Lambda$  and  $U_{i,\lambda}\psi = \psi$ . Then  $|\psi|(a) = |\psi(a)|$ , and we have  $|U_{i,\lambda}\psi| = |\psi|$ . Therefore, we obtain  $U_{i,\operatorname{Re}\lambda}\psi \geq \psi$ . By taking the duality pairing with  $F_{\operatorname{Re}\lambda} \in X_+^*$ , we get  $r(U_{i,\operatorname{Re}\lambda})\langle F_{\operatorname{Re}\lambda}, |\psi| \rangle \geq \langle F_{\operatorname{Re}\lambda}, |\psi| \rangle$ . We have  $r(U_{i,\operatorname{Re}\lambda}) \geq 1$ , as  $F_{\operatorname{Re}\lambda}$  is strictly positive. Since  $r(U_{i,\lambda})$ ,  $\lambda \in \mathbb{R}$  is a declining function, we conclude that  $\operatorname{Re}\lambda \leq \lambda_0$ . Suppose  $\operatorname{Re}\lambda = \lambda_0$ . Then  $U_{i,\lambda_0}|\psi| = |\psi|$ . If we assume  $U_{i,\lambda_0}|\psi| > |\psi|$ , then taking the duality pairing with the eigenfunctional  $F_0$  corresponding to  $r(U_{i,\lambda_0}) = 1$  results in  $\langle F_0, |\psi| \rangle > \langle F_0, |\psi| \rangle$ , which is a contradiction. Therefore, we have  $U_{i,\lambda_0}|\psi| = |\psi|$ , and we can deduce that  $|\psi| = c\psi_0$ , where constant  $c$  is assumed to be 1, and  $\psi_0$  is the eigenfunction relating to  $r(U_{i,\lambda_0}) = 1$ . Therefore, we have  $\psi(a) = \psi_0(a) \exp(iv(a))$  for a real-valued function  $v(a)$ . Substituting this into  $U_{i,\lambda_0}\psi_0 = |U_{i,\lambda}\psi|$  yields

$$\begin{aligned}
 & \frac{\alpha_i(a, \bar{x}_1)}{g_i(a)(\lambda_0 + \gamma_i(\bar{N}) + \mu_{q_i}(a))} \int_0^{a^*} \exp\left(\int_a^\zeta \beta_i(\xi) + \alpha_i(\bar{x}_1, \xi) + \lambda_0 + \mu_{p_i}(\xi) \right. \\
 & \left. - \frac{\gamma_i(\bar{N})\alpha_i(\bar{x}_1, \xi)}{\lambda_0 + \gamma_i(\bar{N}) + \mu_{q_i}(\xi)} d\xi\right) \psi_0(\zeta) d\zeta = \left| \frac{\alpha_i(a, \bar{x}_1)}{g_i(a)(\lambda_0 + i\operatorname{Im}\lambda + \gamma_i(\bar{N}) + \mu_{q_i}(a))} \right. \\
 & \left. \int_0^{a^*} \exp\left(\int_a^\zeta \beta_i(\xi) + \alpha_i(\bar{x}_1, \xi) + \lambda_0 + i\operatorname{Im}\lambda + \mu_{p_i}(\xi) - \frac{\gamma_i(\bar{N})\alpha_i(\bar{x}_1, \xi)}{\lambda_0 + i\operatorname{Im}\lambda + \gamma_i(\bar{N}) + \mu_{q_i}(\xi)} d\xi\right) \right. \\
 & \left. \exp(iv(\zeta))\psi_0(\zeta) d\zeta \right|.
 \end{aligned}$$

Lemma 6.12 [153] implies that  $\operatorname{Im}\lambda + v(\zeta)$  equals a constant  $\Theta$ . Using the fact that  $U_{i,\lambda}\psi = \psi$ , we obtain the equation  $\exp(i\Theta)U_{i,\lambda_0}\psi_{\lambda_0} = \psi_{\lambda_0} \exp(iv(\zeta))$ . This equation shows that if  $\Theta = v(\zeta)$ , then  $\operatorname{Im}\lambda = 0$ . Therefore, the proof is complete.  $\square$

**Theorem 8.2.1.** The equilibrium state  $(\bar{p}_h(a), \bar{q}_h(a), \bar{p}_c(a), \bar{q}_c(a))^T$ , for (7.1)–(7.4), is locally asymptotically stable if  $r(U_0) < 1$  and locally unstable if  $r(U_0) > 1$ .

*Proof.* Lemmas 8.2.4 and 8.2.5 suggests that  $\sup \operatorname{Re} \lambda : 1 \in \sigma_P(U_{i,\lambda}) = \lambda_0$ . This implies that if  $r(U_0) < 1$ , then  $s(C) = \sup \operatorname{Re} \lambda : 1 \in \sigma_P(U_{i,\lambda}) < 0$ . Conversely, if  $r(U_0) > 1$ , then  $s(C) = \sup \operatorname{Re} \lambda : 1 \in \sigma_P(U_{i,\lambda}) > 0$ . Therefore, the proof is complete.  $\square$

We checked the wellposedness of the model, derive non-trivial equilibrium solutions and find spectral criteria for local stability.





---

### Conclusion and future outlooks

---

The process of cancer genesis is complex and involves a delicate balance between proliferation and quiescence and the impact of genetic mutations. In this thesis, we have delved into multiscale modeling and stability analysis to understand cancer genesis better in various modeling frameworks in our pursuit of unraveling the complexities of cancer genesis. We have presented and analyzed a series of mathematical models that capture the complexities of cell cycle dynamics, the evolution of cancer stem cell lineages, mutation acquisitions, and the interplay between quiescent and proliferating cell populations. The culmination of this research represents a significant step forward in understanding the underlying mechanisms driving the initiation and progression of cancer.

The cell cycle phases dictate the orderly progression of cells, and any disruptions can lead to aberrant growth, a hallmark of cancer. In Chapter 2, we introduced a mathematical model of cell cycle dynamics comprising nine core proteins that maintain the temporal oscillatory dynamics. Next, we explored the evolution of cancer stem cell lineages, incorporating feedback regulation mechanisms in Chapter 3. Our findings revealed how feedback loops can drive the expansion of cancer stem cells, highlighting their pivotal role in cancer progression. Understanding the dynamics of cancer stem cells is essential for designing therapies that can effectively target these elusive and resilient cell populations. In Chapter 4, we addressed the well-posedness of a coupled PDE-ODE model of stem cell lineage introduced in Chapter 3. This research underscores the importance of mathematical rigor in modeling biological systems and ensures the reliability of our models as tools for understanding cancer genesis.

Furthermore, we extended our modeling framework to consider the interplay between quiescent and proliferating cell populations in Chapter 5. This chapter sheds light on the importance of understanding the balance between these two populations in the context of cancer. We proposed nonlinear, multiscale modeling of physiologically structured quiescent and proliferating cell densities coupled with cell-cycle dynamics, essential in committing a cell to an irreversible cell-division process. The insights gained from our models can aid in developing targeted therapies that specifically target proliferating or quiescent cells, offering a promising avenue for future cancer treatment strategies. In Chapter 6, we also checked the wellposedness of the model, derived non-trivial equilibrium solutions, and found spectral criteria for local stability in the sense that if the growth bound of the linearised semigroup is negative, the steady-state solution is the locally asymptotically stable, and if the growth bound is positive, the steady-state solution is unstable. Finally, in Chapter 7 and 8, we extended our multiscale model of proliferating and quiescent cell populations with mutation acquisitions. We also performed stability

analysis of a multiscale model incorporating cell cycle dynamics. Similar to Chapter 8, using semigroup and spectral theory, we investigated the well-posedness of the model, derived steady-state solutions, and found sufficient stability conditions. In the end, we executed numerical simulations to observe the impact of the parameters on the model's nonlinear dynamics. These findings contribute to the growing body of knowledge aimed at elucidating the dynamics of cancer cells within the context of the cell cycle.

The apex of this research represents a significant step forward in the underlying mechanisms driving the initiation and progression of cancer. While we have achieved significant milestones, it is crucial to acknowledge the limitations of our work and propose future directions. In the sequel, we highlight some of the limitations of this work and potential avenues for future research:

A primary limitation of this work is that the mathematical models presented in this thesis involve simplifications and assumptions to make them tractable. While these simplifications are necessary for analysis, they may not fully capture the intricacies of real biological systems. For instance, the cell cycle model consists of nine essential proteins that are important for temporal oscillatory dynamics. However, it is important to acknowledge that the cell cycle is an intricate biological process governed by a vast array of proteins and complex regulatory mechanisms. These simplifications were chosen to facilitate a more manageable analysis and gain initial insights into the cell cycle dynamics. Future work should strive for more detailed and realistic models, which means that to enhance the comprehensiveness and accuracy of our model, we can consider extending it by incorporating additional proteins and elements that are known to play critical roles in the cell cycle.

Another limitation is that the mathematical models we have put forth in this thesis have primarily been deterministic, assuming a perfect, predictable environment for biological systems. Nevertheless, biological systems are inherently stochastic in reality, and there is significant randomness and variability in various cellular processes. For instance, in population dynamics, stochasticity refers to random variability or uncertainty that affects the growth, interactions, and behaviors of individuals within a population. This noise can arise from various sources and processes, including genetic mutations, environmental fluctuations, demographic events, or stochastic birth and death rates. Such systems often exhibit fluctuations and diverse outcomes in response to the same initial conditions. Consequently, to address this limitation and improve the models' predictability, future research should pivot toward the incorporation of stochastic elements. Therefore, the possible extension of this work would be the utilization of stochastic differential equations or the implementation of agent-based modeling, which can effectively account for the intrinsic variability and unpredictability observed in biological systems.

Furthermore, integrating approaches from control theory into the development of personalized treatment strategies is a crucial step in the advancement of healthcare. In the course of this work, our primary focus has been to develop simple yet complex models that capture the complexity of sub-cellular and population dynamics in cancer genesis. We have dedicated considerable effort to analyzing the model's well-posedness and stability, laying a strong foundation for understanding these dynamics. Now is the right time to build upon this foundation and extend these models with optimization approaches from control theory, and the goal is to tailor treatment approaches to cancer. One promising avenue could be dynamically adjusting drug dosages or treatment schedules in chemotherapy. Implementing such an approach recognizes the ever-evolving nature

of the disease and the distinctive responses of individual patients. The incorporation of control theory principles will eventually benefit us in developing treatment strategies that are adaptable and patient-specific, thereby optimizing therapeutic outcomes while minimizing adverse effects.

Finally, experimental validation is indispensable to affirm the predictions and hypotheses derived from our mathematical models. It is not uncommon to encounter challenges in finding empirical data that aligns precisely with the settings and assumptions of a mathematical model, as we have experienced in Chapter 3, where we validated our model against experimental data of breast, prostate, colon, and TUBO cancer cell lines. Collaborations between mathematicians, biologists, and clinicians are crucial for bridging the gap between theoretical modeling and real-world clinical applications. Such collaborations will enable us to acquire empirical data that validates and refines our mathematical models, ensuring their accuracy and relevance to actual biological systems.

In conclusion, our work represents a significant contribution to the field of mathematical modeling in cancer research. We have investigated several aspects of cancer genesis, but there is still much to explore and refine. As we address the limitations and pursue these future directions, we move closer to improving our understanding of cancer dynamics and, ultimately, developing better models for effective treatments of this complex disease.



---

## Appendix

---

**Lemma 1.** Let  $p$  and  $g$  be real-valued functions such that  $p, g \in L^1([0, T])$  and  $y_0 \in \mathbb{R}$ . Then, there exists a uniquely determined  $y : [0, T] \rightarrow \mathbb{R}$  that solves the IVP

$$\frac{dy}{dt} + p(t)y = g(t), \quad y(0) = y_0. \quad (.1)$$

Moreover, it holds that

$$y(t) = \exp\left(-\int_0^t p(\epsilon)d\epsilon\right) \left(\int_0^t \exp\left(\int_0^\lambda p(\epsilon)d\epsilon\right)g(\lambda)d\lambda + y_0\right) \quad (.2)$$

*Proof.* See the proof in [159]. □

**Lemma 2.** Let  $\theta^a \in \Theta$ ,  $\eta > 0$ ,  $p$  and  $g$  be non-negative functions on  $[0, T'] \times X_{T'} \times \Theta$  and  $z_0$  be a function defined on  $\Theta$ . Furthermore, for  $t \in [0, T']$ ,  $x \in X_{T'}$  and  $\theta \in \Theta$  define

$$z(t, x, \theta) := \exp\left(-\int_0^t p(\lambda, x, \theta)d\lambda\right) \left(\int_0^t \exp\left(\int_0^\lambda p(\epsilon, x, \theta)d\epsilon\right)g(\lambda, x, \theta)d\lambda + z_0(\theta)\right).$$

If it holds that

$$p(t, y^a, \theta^a), p(t, y^b, \theta^b), g(t, y^a, \theta^a), g(t, y^b, \theta^b) \leq \text{const.}(\theta^a, \eta) \quad \text{and} \quad (.3)$$

$$|p(t, y^a, \theta^a) - p(t, y^b, \theta^b)|, |g(t, y^a, \theta^a) - g(t, y^b, \theta^b)| \leq \text{const.}(\theta^a, \eta)\|y^a - y^b\|_t \quad (.4)$$

for all  $\theta^b \in \Theta$  with  $\|\theta^a - \theta^b\| < \eta$  and  $y^a \in Y_{T'}^\theta$ , then for all  $\theta^b \in \Theta$  and  $y^a \in Y_{T'}^\theta$ , we also have

$$|z(t, y^a, \theta^a) - z(t, y^b, \theta^b)| \leq \text{const.}(\theta^a, \eta) \left(\int_0^t \|y^a - y^b\|_\lambda d\lambda + |z_0(\theta^a) - z_0(\theta^b)|\right).$$

*Proof.* See the proof in [97]. □

**Lemma 3** (Fréchet differentiability).  $F_1 : X \rightarrow X$  is Fréchet differentiable at  $\phi \in X$ , where  $X$  is a Banach space.

*Proof.* For  $F_1$  to be Fréchet differentiable, we need to show that

$$\lim_{\|h\| \rightarrow 0} \frac{\|F_1(\phi + h, \varphi) - F_1(\phi, \varphi) - Ah\|}{\|h\|} = 0, \quad (.5)$$

where  $A = DF_1(\phi)$  and  $\|\cdot\|$  is a norm in  $X$ . Consider

$$\begin{aligned}
 & \frac{\|F_1(\phi + h, \varphi) - F_1(\phi, \varphi) - Ah\|}{\|h\|} \\
 &= \frac{1}{\|h\|} \left\| \left( \frac{-\nu\theta^\kappa(\phi_1(a) + h)}{\theta^\kappa + (N\phi + 2a^*h)^\kappa} + \alpha(\varphi_1, a)(\phi_2(a) + h) \right) - \left( \frac{-\nu\theta^\kappa\phi_1(a)}{\theta^\kappa + (N\phi)^\kappa} + \alpha(\varphi_1, a)\phi_2(a) \right) \right. \\
 & \quad \left. - \left( \frac{\nu\theta^\kappa(\phi_1(a) + h)}{\theta^\kappa + (N\phi + 2a^*h)^\kappa} - \alpha(\varphi_1, a)(\phi_2(a) + h) \right) - \left( \frac{\nu\theta^\kappa\phi_1(a)}{\theta^\kappa + (N\phi)^\kappa} - \alpha(\varphi_1, a)\phi_2(a) \right) \right\| \\
 & \quad - \left( \frac{\partial}{\partial\phi_1} \left( \frac{-\nu\theta^\kappa\phi_1(a)}{\theta^\kappa + (N\phi)^\kappa} + \alpha(\varphi_1, a)\phi_2(a) \right) + \frac{\partial}{\partial\phi_2} \left( \frac{-\nu\theta^\kappa\phi_1(a)}{\theta^\kappa + (N\phi)^\kappa} + \alpha(\varphi_1, a)\phi_2(a) \right) \right) \\
 & \quad - \left( \frac{\partial}{\partial\phi_1} \left( \frac{\nu\theta^\kappa\phi_1(a)}{\theta^\kappa + (N\phi)^\kappa} - \alpha(\varphi_1, a)\phi_2(a) \right) + \frac{\partial}{\partial\phi_2} \left( \frac{\nu\theta^\kappa\phi_1(a)}{\theta^\kappa + (N\phi)^\kappa} - \alpha(\varphi_1, a)\phi_2(a) \right) \right) \Big\| h \\
 &= \frac{1}{\|h\|} \left\| \left( \begin{aligned} & -\nu\theta^\kappa\phi_1(a) \left( \frac{1}{\theta^\kappa + (N\phi + 2a^*h)^\kappa} - \frac{1}{\theta^\kappa + (N\phi)^\kappa} \right) \\ & \nu\theta^\kappa\phi_1(a) \left( \frac{1}{\theta^\kappa + (N\phi + 2a^*h)^\kappa} - \frac{1}{\theta^\kappa + (N\phi)^\kappa} \right) \end{aligned} \right) + \left( \begin{aligned} & \frac{-\nu\theta^\kappa}{\theta^\kappa + (N\phi + 2a^*h)^\kappa} + \alpha(\varphi_1, a) \\ & \frac{\nu\theta^\kappa}{\theta^\kappa + (N\phi + 2a^*h)^\kappa} - \alpha(\varphi_1, a) \end{aligned} \right) h \right. \\
 & \quad - \left( \begin{aligned} & \frac{-(\theta^\kappa + (N\phi)^\kappa)\nu\theta^\kappa + \nu\theta^\kappa\phi_1(a)ka^*(N\phi)^{k-1}}{(\theta^\kappa + (N\phi)^\kappa)^2} + \frac{\nu\theta^\kappa\phi_1(a)ka^*(N\phi)^{k-1}}{(\theta^\kappa + (N\phi)^\kappa)^2} + \alpha(\varphi_1, a) \\ & \frac{(\theta^\kappa + (N\phi)^\kappa)\nu\theta^\kappa - \nu\theta^\kappa\phi_1(a)ka^*(N\phi)^{k-1}}{(\theta^\kappa + (N\phi)^\kappa)^2} - \frac{\nu\theta^\kappa\phi_1(a)ka^*(N\phi)^{k-1}}{(\theta^\kappa + (N\phi)^\kappa)^2} - \alpha(\varphi_1, a) \end{aligned} \right) h \Big\| \\
 &= \frac{1}{\|h\|} \left\| \left( \begin{aligned} & -\nu\theta^\kappa\phi_1(a) \left( \frac{(N\phi)^\kappa - (N\phi + 2a^*h)^\kappa}{\{\theta^\kappa + (N\phi + 2a^*h)^\kappa\}\{\theta^\kappa + (N\phi)^\kappa\}} \right) \\ & \nu\theta^\kappa\phi_1(a) \left( \frac{(N\phi)^\kappa - (N\phi + 2a^*h)^\kappa}{\{\theta^\kappa + (N\phi + 2a^*h)^\kappa\}\{\theta^\kappa + (N\phi)^\kappa\}} \right) \end{aligned} \right) + \left( \begin{aligned} & \frac{-\nu\theta^\kappa}{\theta^\kappa + (N\phi + 2a^*h)^\kappa} + \alpha(\varphi_1, a) \\ & \frac{\nu\theta^\kappa}{\theta^\kappa + (N\phi + 2a^*h)^\kappa} - \alpha(\varphi_1, a) \end{aligned} \right) h \right. \\
 & \quad - \left( \begin{aligned} & \frac{-(\theta^\kappa + (N\phi)^\kappa) + (N\phi)^{k-1}ka^*\phi_1(a)}{(\theta^\kappa + (N\phi)^\kappa)^2} + \frac{\phi_1(a)ka^*(N\phi)^{k-1}}{(\theta^\kappa + (N\phi)^\kappa)^2} + \frac{\alpha(\varphi_1, a)}{\nu\theta^\kappa} \\ & \frac{(\theta^\kappa + (N\phi)^\kappa) - (N\phi)^{k-1}ka^*\phi_1(a)}{(\theta^\kappa + (N\phi)^\kappa)^2} - \frac{\phi_1(a)ka^*(N\phi)^{k-1}}{(\theta^\kappa + (N\phi)^\kappa)^2} - \frac{\alpha(\varphi_1, a)}{\nu\theta^\kappa} \end{aligned} \right) \nu\theta^\kappa h \Big\| \\
 &= \left\| \left( \begin{aligned} & \frac{-1}{h} \left( \frac{(N\phi)^\kappa - (N\phi + 2a^*h)^\kappa}{\{\theta^\kappa + (N\phi + 2a^*h)^\kappa\}\{\theta^\kappa + (N\phi)^\kappa\}} \right) \\ & \frac{1}{h} \left( \frac{(N\phi)^\kappa - (N\phi + 2a^*h)^\kappa}{\{\theta^\kappa + (N\phi + 2a^*h)^\kappa\}\{\theta^\kappa + (N\phi)^\kappa\}} \right) \end{aligned} \right) \nu\theta^\kappa\phi_1(a) + \left( \begin{aligned} & \frac{-\nu\theta^\kappa}{\theta^\kappa + (N\phi + 2a^*h)^\kappa} + \alpha(\varphi_1, a) \\ & \frac{\nu\theta^\kappa}{\theta^\kappa + (N\phi + 2a^*h)^\kappa} - \alpha(\varphi_1, a) \end{aligned} \right) \right. \\
 & \quad \left. - \left( \begin{aligned} & \frac{-\nu\theta^\kappa}{\theta^\kappa + (N\phi)^\kappa} + \alpha(\varphi_1, a) \\ & \frac{\nu\theta^\kappa}{\theta^\kappa + (N\phi)^\kappa} - \alpha(\varphi_1, a) \end{aligned} \right) \right\|. \tag{.6}
 \end{aligned}$$

Further by taking the limit  $h \rightarrow 0$ , we achieve

$$\lim_{\|h\| \rightarrow 0} \frac{\|F_1(\phi + h, \varphi) - F_1(\phi, \varphi) - Ah\|}{\|h\|} = \left\| \left( \begin{aligned} & \frac{-\nu\theta^\kappa}{\theta^\kappa + (N\phi)^\kappa} + \alpha(\varphi_1, a) \\ & \frac{\nu\theta^\kappa}{\theta^\kappa + (N\phi)^\kappa} - \alpha(\varphi_1, a) \end{aligned} \right) - \left( \begin{aligned} & \frac{-\nu\theta^\kappa}{\theta^\kappa + (N\phi)^\kappa} + \alpha(\varphi_1, a) \\ & \frac{\nu\theta^\kappa}{\theta^\kappa + (N\phi)^\kappa} - \alpha(\varphi_1, a) \end{aligned} \right) \right\| = 0. \tag{.7}$$

Thus, we show that  $F_1$  is Fréchet differentiable in  $X$ .  $\square$

In the similar fashion,  $F_1$  and  $F_2$  can be shown Fréchet differentiable in both  $X$  and  $Y$ .

---

## Bibliography

---

- [1] D. Hanahan and R. A. Weinberg, “The hallmarks of cancer,” *Cell*, vol. 100, no. 1, pp. 57–70, 2000.
- [2] D. Hanahan and R. A. Weinberg, “Hallmarks of cancer: The next generation,” *cell*, vol. 144, no. 5, pp. 646–674, 2011.
- [3] D. Hanahan, “Hallmarks of cancer: New dimensions,” *Cancer discovery*, vol. 12, no. 1, pp. 31–46, 2022.
- [4] D. Hanahan and J. Folkman, “Patterns and emerging mechanisms of the angiogenic switch during tumorigenesis,” *cell*, vol. 86, no. 3, pp. 353–364, 1996.
- [5] M. R. Junttila and G. I. Evan, “P53—a jack of all trades but master of none,” *Nature reviews cancer*, vol. 9, no. 11, pp. 821–829, 2009.
- [6] D. L. Burkhardt and J. Sage, “Cellular mechanisms of tumour suppression by the retinoblastoma gene,” *Nature Reviews Cancer*, vol. 8, no. 9, pp. 671–682, 2008.
- [7] C. J. Sherr and F. McCormick, “The rb and p53 pathways in cancer,” *Cancer cell*, vol. 2, no. 2, pp. 103–112, 2002.
- [8] J. Folkman, “Tumor angiogenesis: Therapeutic implications,” *New england journal of medicine*, vol. 285, no. 21, pp. 1182–1186, 1971.
- [9] M. A. Blasco, “Telomeres and human disease: Ageing, cancer and beyond,” *Nature Reviews Genetics*, vol. 6, no. 8, pp. 611–622, 2005.
- [10] J. W. Shay and W. E. Wright, “Hayflick, his limit, and cellular ageing,” *Nature reviews Molecular cell biology*, vol. 1, no. 1, pp. 72–76, 2000.
- [11] I. J. Fidler, “The pathogenesis of cancer metastasis: The ‘seed and soil’ hypothesis revisited,” *Nature reviews cancer*, vol. 3, no. 6, pp. 453–458, 2003.
- [12] J. E. Talmadge and I. J. Fidler, “Aacr centennial series: The biology of cancer metastasis: Historical perspective,” *Cancer research*, vol. 70, no. 14, pp. 5649–5669, 2010.
- [13] F. Roth-Walter, E. Jensen-Jarolim, and H. Stockinger, “Principles and comparative aspects of adaptive immunity,” *comparative medicine: anatomy and physiology. Jensen-Jarolim E (Ed), Springer, Berlin, Germany*, 2013.
- [14] B. Albert, A. Johnson, J. Lewis, M. Raff, K. Roberts, and P. Walter, *Molecular biology of the cell*, 2002.
- [15] C. Darwin and W. F. Bynum, *The origin of species by means of natural selection: or, the preservation of favored races in the struggle for life*. AL Burt New York, 2009.

- 
- [16] M. Lynch, “Rate, molecular spectrum, and consequences of human mutation,” *Proceedings of the National Academy of Sciences*, vol. 107, no. 3, pp. 961–968, 2010.
- [17] *Yourgenome*, <https://www.yourgenome.org/copyright/>, Accessed on 2017-01-19.
- [18] D. N. Cooper, E. V. Ball, and M. Krawczak, “The human gene mutation database,” *Nucleic acids research*, vol. 26, no. 1, pp. 285–287, 1998.
- [19] B. Di Ventura, C. Lemerle, K. Michalodimitrakis, and L. Serrano, “From in vivo to in silico biology and back,” *Nature*, vol. 443, no. 7111, pp. 527–533, 2006.
- [20] B. B. Aldridge, J. M. Burke, D. A. Lauffenburger, and P. K. Sorger, “Physico-chemical modelling of cell signalling pathways,” *Nature cell biology*, vol. 8, no. 11, pp. 1195–1203, 2006.
- [21] D. C. Walker and J. Southgate, “The virtual cell—a candidate co-ordinator for ‘middle-out’ modelling of biological systems,” *Briefings in bioinformatics*, vol. 10, no. 4, pp. 450–461, 2009.
- [22] S. Sanga, H. B. Frieboes, X. Zheng, R. Gatenby, E. L. Bearer, and V. Cristini, “Predictive oncology: A review of multidisciplinary, multiscale in silico modeling linking phenotype, morphology and growth,” *Neuroimage*, vol. 37, S120–S134, 2007.
- [23] G. An, “Introduction of an agent-based multi-scale modular architecture for dynamic knowledge representation of acute inflammation,” *Theoretical Biology and Medical Modelling*, vol. 5, pp. 1–20, 2008.
- [24] G. Schaller and M. Meyer-Hermann, “Continuum versus discrete model: A comparison for multicellular tumour spheroids,” *Philosophical Transactions of the Royal Society A: Mathematical, Physical and Engineering Sciences*, vol. 364, no. 1843, pp. 1443–1464, 2006.
- [25] J. S. Lowengrub *et al.*, “Nonlinear modelling of cancer: Bridging the gap between cells and tumours,” *Nonlinearity*, vol. 23, no. 1, R1, 2009.
- [26] Z. Wang and T. S. Deisboeck, “Computational modeling of brain tumors: Discrete, continuum or hybrid?” *Scientific modeling and simulations*, pp. 381–393, 2009.
- [27] J. Monod, “The growth of bacterial cultures,” *Annual review of microbiology*, vol. 3, no. 1, pp. 371–394, 1949.
- [28] K. S. Korolev, J. B. Xavier, and J. Gore, “Turning ecology and evolution against cancer,” *Nature Reviews Cancer*, vol. 14, no. 5, pp. 371–380, 2014.
- [29] Z. Neufeld, W. von Witt, D. Lakatos, J. Wang, B. Hegedus, and A. Czirok, “The role of allee effect in modelling post resection recurrence of glioblastoma,” *PLoS computational biology*, vol. 13, no. 11, e1005818, 2017.
- [30] J. Baranyi, T. Roberts, and P. McClure, “A non-autonomous differential equation to model bacterial growth,” *Food microbiology*, vol. 10, no. 1, pp. 43–59, 1993.
- [31] D.-Q. Jiang, Y. Wang, and D. Zhou, “Phenotypic equilibrium as probabilistic convergence in multi-phenotype cell population dynamics,” *Plos one*, vol. 12, no. 2, e0170916, 2017.



- [32] F. R. Sharpe and A. J. Lotka, "L. a problem in age-distribution," *The London, Edinburgh, and Dublin Philosophical Magazine and Journal of Science*, vol. 21, no. 124, pp. 435–438, 1911.
- [33] A. M'kendrick, "Applications of mathematics to medical problems," *Proceedings of the Edinburgh Mathematical Society*, vol. 44, pp. 98–130, 1925.
- [34] M. E. Gurtin and R. C. MacCamy, "Non-linear age-dependent population dynamics," *Archive for Rational Mechanics and Analysis*, vol. 54, pp. 281–300, 1974.
- [35] G. Webb, "Random transitions, size control, and inheritance in cell population dynamics," *Mathematical biosciences*, vol. 85, no. 1, pp. 71–91, 1987.
- [36] D. O. Morgan, *The cell cycle: principles of control*. New science press, 2007.
- [37] B. Alberts, *Molecular biology of the cell*. Garland science, 2017.
- [38] N. Liu, T. Chen, X. Wang, D. Yang, B. Xue, and H. Zhu, "Msi1 confers resistance to trail by activating erk in liver cancer cells," *FEBS letters*, vol. 589, no. 8, pp. 897–903, 2015.
- [39] C. Joseph *et al.*, "Cell cycle deficits in neurodegenerative disorders: Uncovering molecular mechanisms to drive innovative therapeutic development," *Aging and disease*, vol. 11, no. 4, p. 946, 2020.
- [40] S. J. Morrison and J. Kimble, "Asymmetric and symmetric stem-cell divisions in development and cancer," *nature*, vol. 441, no. 7097, pp. 1068–1074, 2006.
- [41] A. J. Levine and M. Oren, "The first 30 years of p53: Growing ever more complex," *Nature reviews cancer*, vol. 9, no. 10, pp. 749–758, 2009.
- [42] M. Al-Hajj and M. F. Clarke, "Self-renewal and solid tumor stem cells," *Oncogene*, vol. 23, no. 43, p. 7274, 2004.
- [43] E. Fuchs and T. Chen, "A matter of life and death: Self-renewal in stem cells," *EMBO reports*, vol. 14, no. 1, pp. 39–48, 2013.
- [44] S. Elmore, "Apoptosis: A review of programmed cell death," *Toxicologic pathology*, vol. 35, no. 4, pp. 495–516, 2007.
- [45] T. Reya, S. J. Morrison, M. F. Clarke, and I. L. Weissman, "Stem cells, cancer, and cancer stem cells," *Nature*, vol. 414, no. 6859, p. 105, 2001.
- [46] C. T. Jordan, M. L. Guzman, and M. Noble, "Cancer stem cells," *New England Journal of Medicine*, vol. 355, no. 12, pp. 1253–1261, 2006.
- [47] W. R. Taylor *et al.*, "Small-molecule ferroptotic agents with potential to selectively target cancer stem cells," *Scientific reports*, vol. 9, no. 1, p. 5926, 2019.
- [48] L. A. Loeb, K. R. Loeb, and J. P. Anderson, "Multiple mutations and cancer," *Proceedings of the National Academy of Sciences*, vol. 100, no. 3, pp. 776–781, 2003.
- [49] I. Martincorena *et al.*, "Universal patterns of selection in cancer and somatic tissues," *Cell*, vol. 171, no. 5, pp. 1029–1041, 2017.
- [50] J. C. Barrett, "Mechanisms of multistep carcinogenesis and carcinogen risk assessment.," *Environmental Health Perspectives*, vol. 100, pp. 9–20, 1993.

- [51] A. D. Lander, K. K. Gokoffski, F. Y. Wan, Q. Nie, and A. L. Calof, “Cell lineages and the logic of proliferative control,” *PLoS Biology*, vol. 7, no. 1, e1000015, 2009.
- [52] M. D. Johnston, C. M. Edwards, W. F. Bodmer, P. K. Maini, and S. J. Chapman, “Mathematical modeling of cell population dynamics in the colonic crypt and in colorectal cancer,” *Proceedings of the National Academy of Sciences*, vol. 104, no. 10, pp. 4008–4013, 2007.
- [53] G. Bocharov *et al.*, “Feedback regulation of proliferation vs. differentiation rates explains the dependence of cd4 t-cell expansion on precursor number,” *Proceedings of the National Academy of Sciences*, vol. 108, no. 8, pp. 3318–3323, 2011.
- [54] S. J. Morrison, N. Uchida, and I. L. Weissman, “The biology of hematopoietic stem cells,” *Annual review of cell and developmental biology*, vol. 11, no. 1, pp. 35–71, 1995.
- [55] N. Uchida, W. H. Fleming, E. J. Alpern, and I. L. Weissman, “Heterogeneity of hematopoietic stem cells,” *Current opinion in immunology*, vol. 5, no. 2, pp. 177–184, 1993.
- [56] S. Bernard, J. Bélair, and M. C. Mackey, “Oscillations in cyclical neutropenia: New evidence based on mathematical modeling,” *Journal of Theoretical Biology*, vol. 223, no. 3, pp. 283–298, 2003.
- [57] R. Ashkenazi, S. N. Gentry, and T. L. Jackson, “Pathways to tumorigenesis—modeling mutation acquisition in stem cells and their progeny,” *Neoplasia*, vol. 10, no. 11, 1170–IN6, 2008.
- [58] C. Colijn and M. C. Mackey, “A mathematical model of hematopoiesis—i. periodic chronic myelogenous leukemia,” *Journal of Theoretical Biology*, vol. 237, no. 2, pp. 117–132, 2005.
- [59] F. Michor *et al.*, “Dynamics of chronic myeloid leukaemia,” *Nature*, vol. 435, no. 7046, p. 1267, 2005.
- [60] S. N. Gentry, “Mathematical modeling of mutation acquisition in hierarchical tissues: Quantification of the cancer stem cell hypothesis,” 2008.
- [61] S. N. Gentry and T. L. Jackson, “A mathematical model of cancer stem cell driven tumor initiation: Implications of niche size and loss of homeostatic regulatory mechanisms,” *PloS one*, vol. 8, no. 8, e71128, 2013.
- [62] S. L. Weekes *et al.*, “A multicompartiment mathematical model of cancer stem cell-driven tumor growth dynamics,” *Bulletin of Mathematical Biology*, vol. 76, no. 7, pp. 1762–1782, 2014.
- [63] I. Østby, H. B. Benestad, and P. Grøttum, “Mathematical modeling of human granulopoiesis: The possible importance of regulated apoptosis,” *Mathematical Biosciences*, vol. 186, no. 1, pp. 1–27, 2003.
- [64] S. Gentry, R. Ashkenazi, and T. Jackson, “A maturity-structured mathematical model of mutation, acquisition in the absence of homeostatic regulation,” *Mathematical Modelling of Natural Phenomena*, vol. 4, no. 3, pp. 156–182, 2009.
- [65] S. H. Cheshier, S. J. Morrison, X. Liao, and I. L. Weissman, “In vivo proliferation and cell cycle kinetics of long-term self-renewing hematopoietic stem cells,” *Proceedings of the National Academy of Sciences*, vol. 96, no. 6, pp. 3120–3125, 1999.

- [66] A. O'Neill and D. V. Schaffer, "The biology and engineering of stem-cell control," *Biotechnology and Applied Biochemistry*, vol. 40, no. 1, pp. 5–16, 2004.
- [67] M. Alison and S. Islam, "Attributes of adult stem cells," *The Journal of Pathology: A Journal of the Pathological Society of Great Britain and Ireland*, vol. 217, no. 2, pp. 144–160, 2009.
- [68] P. Gabriel, S. P. Garbett, V. Quaranta, D. R. Tyson, and G. F. Webb, "The contribution of age structure to cell population responses to targeted therapeutics," *Journal of Theoretical Biology*, vol. 311, pp. 19–27, 2012.
- [69] D. R. Barreda, P. C. Hanington, and M. Belosevic, "Regulation of myeloid development and function by colony stimulating factors," *Developmental & Comparative Immunology*, vol. 28, no. 5, pp. 509–554, 2004.
- [70] S. Bernard, J. Bélair, and M. C. Mackey, "Oscillations in cyclical neutropenia: New evidence based on mathematical modeling," *Journal of theoretical biology*, vol. 223, no. 3, pp. 283–298, 2003.
- [71] S. Rubinow, "A maturity-time representation for cell populations," *Biophysical journal*, vol. 8, no. 10, pp. 1055–1073, 1968.
- [72] M. Ullah *et al.*, "Differentiation of cancer cells upregulates hla-g and pd-l1," *Oncology Reports*, vol. 43, no. 6, pp. 1797–1804, 2020.
- [73] R. Lakshmanaswamy, *Approaches to understanding breast cancer*. Academic Press, 2017.
- [74] M. B. Goldring and S. Goldring, "Cytokines and cell growth control," *Critical reviews in eukaryotic gene expression*, vol. 1, no. 4, pp. 301–326, 1991.
- [75] D. Metcalf, "Hematopoietic cytokines," *Blood*, vol. 111, no. 2, pp. 485–491, 2008.
- [76] J. E. Layton, H. Hockman, W. P. Sheridan, and G. Morstyn, "Evidence for a novel in vivo control mechanism of granulopoiesis: Mature cell-related control of a regulatory growth factor," *Blood*, vol. 74, no. 4, pp. 1303–1307, 1989.
- [77] J. L. Abkowitz, S. N. Catlin, M. T. McCallie, and P. Gutterp, "Evidence that the number of hematopoietic stem cells per animal is conserved in mammals," *Blood*, vol. 100, no. 7, pp. 2665–2667, 2002.
- [78] M. Wu *et al.*, "Imaging hematopoietic precursor division in real time," *Cell Stem Cell*, vol. 1, no. 5, pp. 541–554, 2007.
- [79] D. J. Araten *et al.*, "A quantitative measurement of the human somatic mutation rate," *Cancer Research*, vol. 65, no. 18, pp. 8111–8117, 2005.
- [80] A. L. Jackson and L. A. Loeb, "The mutation rate and cancer," *Genetics*, vol. 148, no. 4, pp. 1483–1490, 1998.
- [81] D. L. Rimoin, J. M. Connor, R. E. Pyeritz, and B. R. Korf, *Emery and Rimoin's principles and practice of medical genetics*. Churchill Livingstone Elsevier, 2007.
- [82] P. Reizenstein, "Growth of normal and malignant bone marrow cells," *Leukemia research*, vol. 14, no. 8, pp. 679–681, 1990.
- [83] M. Aglietta *et al.*, "Kinetics of human hemopoietic cells after in vivo administration of granulocyte-macrophage colony-stimulating factor.," *The Journal of Clinical Investigation*, vol. 83, no. 2, pp. 551–557, 1989.

- [84] W.-C. Lo *et al.*, “Feedback regulation in multistage cell lineages,” *Mathematical Biosciences and Engineering*, vol. 6, no. 1, p. 59, 2009.
- [85] C. Ginestier *et al.*, “Aldh1 is a marker of normal and malignant human mammary stem cells and a predictor of poor clinical outcome,” *Cell stem cell*, vol. 1, no. 5, pp. 555–567, 2007.
- [86] W. J. Ellis *et al.*, “Characterization of a novel androgen-sensitive, prostate-specific antigen-producing prostatic carcinoma xenograft: Lucap 23,” *Clinical Cancer Research*, vol. 2, no. 6, pp. 1039–1048, 1996.
- [87] L. Ricci-Vitiani *et al.*, “Identification and expansion of human colon-cancer-initiating cells,” *Nature*, vol. 445, no. 7123, pp. 111–115, 2007.
- [88] J. Darnell, H. Lodish, and D. Baltimore, *Molecular cell biology*. 1990.
- [89] R. Molina-Peña and M. M. Álvarez, “A simple mathematical model based on the cancer stem cell hypothesis suggests kinetic commonalities in solid tumor growth,” *PloS one*, vol. 7, no. 2, e26233, 2012.
- [90] G. Chivassa, C. Fornari, R. Sirovich, M. Pennisi, M. Beccuti, and F. Cordero, “A mathematical model to study breast cancer growth,” in *2017 IEEE International Conference on Bioinformatics and Biomedicine (BIBM)*, IEEE, 2017, pp. 1438–1445.
- [91] I. A. Rodriguez-Brenes *et al.*, “Cellular hierarchy as a determinant of tumor sensitivity to chemotherapy,” *Cancer research*, vol. 77, no. 9, pp. 2231–2241, 2017.
- [92] K. H. Vining and D. J. Mooney, “Mechanical forces direct stem cell behaviour in development and regeneration,” *Nature reviews Molecular cell biology*, vol. 18, no. 12, pp. 728–742, 2017.
- [93] J. Hadamard, *Lectures on Cauchy’s problem in linear partial differential equations*. Courier Corporation, 2003.
- [94] G. Avalos, P. G. Geredeli, and J. T. Webster, “Semigroup well-posedness of a linearized, compressible fluid with an elastic boundary,” *arXiv preprint arXiv:1703.10855*, 2017.
- [95] F. Rothe, *Global solutions of reaction-diffusion systems*. Springer, 2006, vol. 1072.
- [96] S. Eisenhofer, “A coupled system of ordinary and partial differential equations modeling the swelling of mitochondria,” Ph.D. dissertation, Technische Universität München, 2013.
- [97] P. Blandfort, “Mathematical modeling of synaptic transmission at chemical synapses,” 2015.
- [98] G. Peralta and G. Propst, “Local well-posedness of a class of hyperbolic pde-ode systems on a bounded interval,” *Journal of Hyperbolic Differential Equations*, vol. 11, no. 04, pp. 705–747, 2014.
- [99] J. Kelkel and C. Surulescu, “A weak solution approach to a reaction–diffusion system modeling pattern formation on seashells,” *Mathematical methods in the applied sciences*, vol. 32, no. 17, pp. 2267–2286, 2009.

- [100] A. Marciniak-Czochra, T. Stiehl, A. D. Ho, W. Jäger, and W. Wagner, “Modeling of asymmetric cell division in hematopoietic stem cells—regulation of self-renewal is essential for efficient repopulation,” *Stem Cells and Development*, vol. 18, no. 3, pp. 377–386, 2009.
- [101] L. C. Evans, *Partial differential equations*. American Mathematical Soc., 2010, vol. 19.
- [102] L. Zou, S. Ruan, and W. Zhang, “An age-structured model for the transmission dynamics of hepatitis b,” *SIAM Journal on Applied Mathematics*, vol. 70, no. 8, pp. 3121–3139, 2010.
- [103] H. Inaba, “Age-structured homogeneous epidemic systems with application to the mseir epidemic model,” *Journal of mathematical biology*, vol. 54, no. 1, pp. 101–146, 2007.
- [104] S. N. Busenberg, M. Iannelli, and H. R. Thieme, “Global behavior of an age-structured epidemic model,” *SIAM Journal on Mathematical Analysis*, vol. 22, no. 4, pp. 1065–1080, 1991.
- [105] C. J. Browne and S. S. Pilyugin, “Global analysis of age-structured within-host virus model,” *Discrete & Continuous Dynamical Systems-B*, vol. 18, no. 8, p. 1999, 2013.
- [106] Y. Yang, S. Ruan, and D. Xiao, “Global stability of an age-structured virus dynamics model with beddington-deangelis infection function,” *Mathematical Biosciences & Engineering*, vol. 12, no. 4, p. 859, 2015.
- [107] O. Arino, E. Sánchez, and G. F. Webb, “Necessary and sufficient conditions for asynchronous exponential growth in age structured cell populations with quiescence,” *Journal of Mathematical Analysis and Applications*, vol. 215, no. 2, pp. 499–513, 1997.
- [108] B. P. Ayati, G. F. Webb, and A. R. A. Anderson, “Computational methods and results for structured multiscale models of tumor invasion,” *Multiscale Modeling & Simulation*, vol. 5, no. 1, pp. 1–20, 2006.
- [109] J. Dyson, R. Villella-Bressan, and G. F. Webb, “Asynchronous exponential growth in an age structured population of proliferating and quiescent cells,” *Mathematical biosciences*, vol. 177, pp. 73–83, 2002.
- [110] M. Gyllenberg and G. F. Webb, “Age-size structure in populations with quiescence,” *Mathematical biosciences*, vol. 86, no. 1, pp. 67–95, 1987.
- [111] F. S. Heldt, A. R. Barr, S. Cooper, C. Bakal, and B. Novák, “A comprehensive model for the proliferation–quiescence decision in response to endogenous dna damage in human cells,” *Proceedings of the National Academy of Sciences*, vol. 115, no. 10, pp. 2532–2537, 2018.
- [112] B. Basse *et al.*, “A mathematical model for analysis of the cell cycle in human tumors,” *J. Mathematical Biology*, vol. 47(4), pp. 295–312, 2003.
- [113] F. Billy, J. Clairambault, F. Delaunay, C. Feillet, and N. Robert, “Age-structured cell population model to study the influence of growth factors on cell cycle dynamics,” *Mathematical Biosciences and Engineering*, vol. 10(1), pp. 1–17, 2013.

- [114] V. Akimenko and R. Anguelov, “Steady states and outbreaks of two-phase nonlinear age-structured model of population dynamics with discrete time delay,” *Journal of biological dynamics*, vol. 11, no. 1, pp. 75–101, 2017.
- [115] E. O. Alzahrani, A. Asiri, M. M. El-Dessoky, and Y. Kuang, “Quiescence as an explanation of gompertzian tumor growth revisited,” *Mathematical biosciences*, vol. 254, pp. 76–82, 2014.
- [116] P. Gabriel, S. P. Garbett, V. Quaranta, D. R. Tyson, and G. F. Webb, “The contribution of age structure to cell population responses to targeted therapeutics,” *Journal of theoretical biology*, vol. 311, pp. 19–27, 2012.
- [117] Z. Liu, J. Chen, J. Pang, P. Bi, and S. Ruan, “Modeling and analysis of a nonlinear age-structured model for tumor cell populations with quiescence,” *Journal of Nonlinear Science*, vol. 28, no. 5, pp. 1763–1791, 2018.
- [118] Z. Liu, C. Guo, J. Yang, and H. Li, “Steady states analysis of a nonlinear age-structured tumor cell population model with quiescence and bidirectional transition,” *Acta Applicandae Mathematicae*, pp. 1–20, 2020.
- [119] B. Basse and U. Paolo, “A generalised age-and phase-structured model of human tumour cell populations both unperturbed and exposed to a range of cancer therapies,” *Bulletin of mathematical biology*, vol. 69, pp. 1673–1690, 2007.
- [120] S. Cooper, “On the proposal of a go phase and the restriction point,” *The FASEB journal*, vol. 12, no. 3, pp. 367–373, 1998.
- [121] A. Zetterberg and O. Larsson, “Cell cycle progression and cell growth in mammalian cells: Kinetic aspects of transition events,” *Cell cycle control*, pp. 206–227, 1995.
- [122] C. T. J. van Velthoven and T. A. Rando, “Stem cell quiescence: Dynamism, restraint, and cellular idling,” *Cell stem cell*, vol. 24, no. 2, pp. 213–225, 2019.
- [123] L. H. Hartwell and M. B. Kastan, “Cell cycle control and cancer,” *Science*, vol. 266, no. 5192, pp. 1821–1828, 1994.
- [124] A. Csikász-Nagy, D. Battogtokh, K. C. Chen, B. Novák, and J. J. Tyson, “Analysis of a generic model of eukaryotic cell-cycle regulation,” *Biophysical journal*, vol. 90, no. 12, pp. 4361–4379, 2006.
- [125] J. E. Ferrell Jr, T. Y.-C. Tsai, and Q. Yang, “Modeling the cell cycle: Why do certain circuits oscillate?” *Cell*, vol. 144, no. 6, pp. 874–885, 2011.
- [126] C. Gérard and A. Goldbeter, “A skeleton model for the network of cyclin-dependent kinases driving the mammalian cell cycle,” *Interface Focus*, vol. 1, no. 1, pp. 24–35, 2011.
- [127] M. N. Obeyesekere, S. O. Zimmerman, E. S. Tecarro, and G. Auchmuty, “A model of cell cycle behavior dominated by kinetics of a pathway stimulated by growth factors,” *Bulletin of mathematical biology*, vol. 61, no. 5, pp. 917–934, 1999.
- [128] J. C. Sible and J. J. Tyson, “Mathematical modeling as a tool for investigating cell cycle control networks,” *Methods*, vol. 41, no. 2, pp. 238–247, 2007.
- [129] R. Singhanian, R. M. Sramkoski, J. W. Jacobberger, and J. J. Tyson, “A hybrid model of mammalian cell cycle regulation,” *PLoS Comput Biol*, vol. 7, no. 2, e1001077, 2011.

- [130] D. W. Stacey, “Cyclin d1 serves as a cell cycle regulatory switch in actively proliferating cells,” *Current opinion in cell biology*, vol. 15, no. 2, pp. 158–163, 2003.
- [131] R. M. Zwijsen, R. Klompmaker, E. B. Wientjens, P. M. Kristel, B. van der Burg, and R. J. Michalides, “Cyclin d1 triggers autonomous growth of breast cancer cells by governing cell cycle exit,” *Molecular and Cellular Biology*, vol. 16, no. 6, pp. 2554–2560, 1996.
- [132] M. Hitomi and D. W. Stacey, “Cellular ras and cyclin d1 are required during different cell cycle periods in cycling nih 3t3 cells,” *Molecular and Cellular Biology*, vol. 19, no. 7, pp. 4623–4632, 1999.
- [133] M. V. Blagosklonny and A. B. Pardee, “The restriction point of the cell cycle,” *Cell cycle*, vol. 1, no. 2, pp. 102–109, 2002.
- [134] C. P. Bagowski, J. Besser, C. R. Frey, and J. E. Ferrell Jr, “The jnk cascade as a biochemical switch in mammalian cells: Ultrasensitive and all-or-none responses,” *Current Biology*, vol. 13, no. 4, pp. 315–320, 2003.
- [135] C. J. Sherr, “D-type cyclins,” *Trends in biochemical sciences*, vol. 20, no. 5, pp. 187–190, 1995.
- [136] F. R. Goutelle Sylvain Michel Maurin and P. Maire, “The hill equation: A review of its capabilities in pharmacological modelling,” *Fundamental & clinical pharmacolog*, vol. 22, pp. 633–648, 2008.
- [137] A. D. Lander, K. K. Gokoffski, F. Y. M. Wan, Q. Nie, and A. L. Calof, “Cell lineages and the logic of proliferative control,” *PLoS Biology*, vol. 7, no. 1, e1000015, 2009.
- [138] M. B. Goldring and Goldring, “Cytokines and cell growth control,” *Critical reviews in eukaryotic gene expression*, vol. 1, no. 4, pp. 301–326, 1991.
- [139] D. Metcalf, “Hematopoietic cytokines,” *Blood*, vol. 111, no. 2, pp. 485–491, 2008.
- [140] I. Batool and N. Bajcinca, “Evolution of cancer stem cell lineage involving feedback regulation,” *PLoS ONE*, vol. 16(5), e0251481, 2021.
- [141] I. Batool and N. Bajcinca, “Well-posedness of a coupled pde–ode model of stem cell lineage involving homeostatic regulation,” *Results in Applied Mathematics*, vol. 9, p. 100 135, 2021.
- [142] C. J. Sherr and J. M. Roberts, “Cdk inhibitors: Positive and negative regulators of g1-phase progression,” *Genes & development*, vol. 13, no. 12, pp. 1501–1512, 1999.
- [143] C. Gérard and A. Goldbeter, “The cell cycle is a limit cycle,” *Mathematical Modelling of Natural Phenomena*, vol. 7, no. 6, pp. 126–166, 2012.
- [144] D. Kuzmin, “A guide to numerical methods for transport equations,” *Friedrich–Alexander university, Germany*, 2010.
- [145] F. Bouchut, *Nonlinear stability of finite Volume Methods for hyperbolic conservation laws: And Well-Balanced schemes for sources*. Springer Science & Business Media, 2004.
- [146] E. Godlewski and P.-A. Raviart, *Hyperbolic systems of conservation laws*. Ellipses, 1991.

- 
- [147] C. Foley, S. Bernard, and M. C. Mackey, “Cost-effective g-csf therapy strategies for cyclical neutropenia: Mathematical modelling based hypotheses,” *Journal of theoretical biology*, vol. 238, no. 4, pp. 754–763, 2006.
- [148] A. Pazy, *Semigroups of linear operators and applications to partial differential equations*. Springer Science & Business Media, 2012, vol. 44.
- [149] A. Lunardi, *Analytic semigroups and optimal regularity in parabolic problems*. Springer Science & Business Media, 2012.
- [150] G. F. Webb *et al.*, *Theory of nonlinear age-dependent population dynamics*. CRC Press, 1985.
- [151] S. Zheng, *Nonlinear evolution equations*. CRC Press, 2004.
- [152] T. Kato, *Perturbation theory for linear operators*. Springer Science & Business Media, 2013, vol. 132.
- [153] H. J. Heijmans, “The dynamical behaviour of the age-size-distribution of a cell population,” in *The dynamics of physiologically structured populations*, Springer, 1986, pp. 185–202.
- [154] M. A. Nowak, *Evolutionary dynamics: exploring the equations of life*. Harvard university press, 2006.
- [155] B. Vogelstein and K. W. Kinzler, “Cancer genes and the pathways they control,” *Nature medicine*, vol. 10, no. 8, pp. 789–799, 2004.
- [156] C. Kandath *et al.*, “Mutational landscape and significance across 12 major cancer types,” *Nature*, vol. 502, no. 7471, pp. 333–339, 2013.
- [157] I. Batool and N. Bajcinca, “A multiscale model of proliferating and quiescent cell populations coupled with cell cycle dynamics,” in *Computer Aided Chemical Engineering*, vol. 51, Elsevier, 2022, pp. 481–486.
- [158] I. Batool and N. Bajcinca, “Stability analysis of a multiscale model of cell cycle dynamics coupled with quiescent and proliferating cell populations,” *PLoS one*, vol. 18, no. 1, e0280621, 2023.
- [159] W. E. Boyce, R. C. DiPrima, and D. B. Meade, *Elementary differential equations*. John Wiley & Sons, 2017.



---

## Lebenslauf

---

M.Sc. Iqra Batool



### Ausbildung

---

- 2017 – 2023    **Ph.D. Rheinland-Pfälzische Technische Universität**  
Fachbereich Maschinenbau und Verfahrenstechnik  
Disertation: *Mathematical Multiscale Modeling and Stability Analysis of Cancer Genesis*
- 2014 – 2016    **M.Sc. COMSATS Institute of Information Technology, Islamabad, Pakistan**  
Masterstudium, Fachbereich Mathematik, Fakultät für Naturwissenschaften  
Masterarbeit: *Study of Dynamics in Non-Isothermal Liquid Chromatographic Columns*
- 2010 – 2014    **B.Sc. International Islamic University, Islamabad, Pakistan**  
Bachelorstudium, Fachbereich Mathematik, Fakultät für Naturwissenschaften
- 2008 – 2010    **F.Sc. Government College, Pind Dadan Khan, Jhelum, Pakistan**  
Hauptfächer: Mathematik, Physik, Chemie

### Berufserfahrung

---

#### Wissenschaftlicher Mitarbeiter

- 2017 – 2024    **Rheinland-Pfälzische Technische Universität (RPTU)**  
Fachbereich Maschinenbau und Verfahrenstechnik  
Lehrstuhl für Mechatronik in Maschinenbau und Fahrzeugtechnik

#### Lehre

- 2017 – 2024    **Betreuung von Veranstaltungen an der RPTU**
- Übung Regelungstheorie
  - Übung Hybride und diskrete dynamische Systeme